Developing a Framework for Minimization of Structural Steel Use and ECI Costs

Deniz Yümlü
TECHNISCHE UNIVERSITEIT DELFT 5612772

Developing a Framework for Minimization of Structural Steel Use and ECI Costs

Developing a structural design framework by testing design choices on multistorey steel office structure with a parametric study in order to understand effects of each selection on steel weight and total ECI cost

By

Deniz Yümlü

in partial fulfilment of the requirements for the degree of

Master of Science

in Structural Engineering

at the Delft University of Technology.

Colophon

Graduation Student

Name: Deniz Yümlü

Student Number: 5612772

Graduation Committee

Chairperson: Prof. Dr. H.M. (Henk) Jonkers TU Delft

Supervisor: Dr. Ir. F. (Florentia) Kavoura TU Delft

Supervisor: Ir. H. (Hagar) El Bamby TU Delft

TU Delft

Acknowledgements

Words cannot express my gratitude to my professor and chair of my committee Prof. Dr. Henk Jonkers for his invaluable patience and feedback. I also could not have undertaken this journey without my defence committee, Dr. Ir. Florentia Kavoura and Ir. Hagar El Bamby who generously provided knowledge and expertise. Additionally, this endeavour would not have been possible without the one-on-one meetings with and feedback from Ir. Hagar El Bamby, who actively helped improvement of the thesis.

I am also grateful Begüm Kavrazlı, who supported me through every difficulty and motivated for the thesis. Special thanks to Kerem Er for his editing help and proof reading. Thanks should also go to the librarians, research assistants, and study participants from the university, who impacted and inspired me. Rukiye Eryaşar has provided an architectural output for the project, giving insight to production of a realistic interior design.

Lastly, I would be remiss in not mentioning my family, especially my parents, Simge and Erol Yümlü, and brother, Ege Yümlü. Their belief in me has kept my spirits and motivation high during this process.

Deniz Yümlü

Executive Summary

Introduction

Sustainability is increasingly important in the construction industry and other sectors. Buildings account for 39% of global energy-related carbon emissions, with 28% from operational emissions (energy for heating, cooling, and power) and 11% from materials and construction (Embodied Carbon, 2022). This thesis focuses on steel structures, emphasizing material use and structural design.

The environmental impact of structures is primarily assessed using two criteria: material use and the Environmental Cost Indicator (ECI) value. Numerous decisions in steel structural design influence these criteria, including material weight, production energy, building use, transportation, construction, and end-of-life processes. This thesis does not investigate construction and transportation as they are case-specific and time-dependent. Future research in project management could address these areas. Instead, this thesis conducts a parametric study to test structural variables and their effects on structures.

The high vacancy rate of offices in European countries has become a significant problem in large towns. For example, the average vacancy rate in 125 of the largest German towns has risen from approximately 1% in 1990 to 7.5% (Hauke et al., 2016). A multistorey steel office structure is designed as a parametric study to address this issue. Minimizing and reusing steel may help mitigate this problem.

The thesis analyses several decisions to optimize material use, including connection design allowing for disassembly and reuse of structural members, cross-section design, and member spacing. Additionally, it considers the reuse of steel for cross-section production and the design of structural (stability) systems for optimal material usage. A framework that helps designers produce more optimized steel designs with less time compared to modelling 50-60 alternatives would make the choice to design for optimal material use more straightforward.

A research gap exists in the analysis of short structures, as most studies focus on tall structures due to their greater potential for material and ECI cost savings. However, 80% of structures are short, and even minimal savings in one could result in significant total ECI Cost and material savings.

This thesis investigates optimizing steel use and ECI costs by addressing the following research question:

'How can a step-by-step structural design framework for multistorey steel offices be developed to optimize structural steel use, reuse potential, and resulting ECI costs in comparison to conventional steel structures, by conducting a parametric study on a 5-storey 30x30m office building?'

A parametric study is conducted on a 5-storey (22.5-meter) steel office building to examine the effects of various design choices. Different spacings for columns, beams, and composite beams, as well as different stability systems, are tested. Additionally, the effects of cross-section selection and steel-to-steel and composite connections are investigated. The results provide insights into the structural behaviour for each case, contributing to the development of a comprehensive design framework. The framework distinguishes between tall and short structures based on second-order effects rather than height or total stories.

Research Approach and Gap

This thesis aims to leverage earlier research in developing a comprehensive framework for optimizing steel use and ECI Cost in multistorey steel office structures. Well-researched areas, such as composite demountable connections and stability systems for tall structures, are integrated into the framework. The study investigates various spacings, including composite spacings, and emphasizes the importance of connection design and demountability principles, particularly for flooring systems and beams.

Existing research often overlooks the specific advantages of different spacings for material use and ECI Cost. Common practice typically selects 6-meter column spacings based on produced cross-section spans, with recommendations given in broad intervals (e.g., 3-9 meters). However, the literature lacks clarity on which end of these intervals is most effective. Only one identified source addresses this issue but includes concrete and excludes composite beams. This thesis includes composite beams as concrete remains a constant variable, and smaller frames do not meet functional requirements.

A significant research gap is identified in the analysis of short structures. Current studies primarily focus on specific structure types (e.g., skyscrapers) or programs, and stability system research predominantly addresses tall structures. Tall structures experience significant lateral loading and second-order effects, leading to more critically loaded exterior sections. In contrast, short structures are primarily loaded due to occupation, with interior columns bearing the brunt of the load. Therefore, stability systems for tall structures cannot be directly applied to short structures without further testing.

The study finds that cross-sections significantly impact material use and ECI Cost. Different cross-sections for the same system can lead to varying material use, affecting overall efficiency. In practice, IPE, HEA, and HEB sections are typically used for beams and columns, while CHS, RHS, and SHS sections are used for diagrid designs. However, the literature lacks comprehensive analysis on the most optimal sections for each member and the effects of substituting one type with another.

Developing a harmonious framework requires considering the interdependencies of column spacing, beam spacing, and composite spacings. Despite the growing body of academic work on optimization techniques in structural design, expert knowledge is needed to translate these findings into practical methods for engineers. This framework addresses the research gap by providing a practical tool for engineers to design structures with minimal steel use and ECI Cost. Further research in this field will aid structural engineers and architects in understanding how to reduce embodied carbon, contributing to the literature on sustainable design.

Results & Conclusions

A parametric study was conducted on a 5-storey, 30x30m office structure to optimize steel use and minimize ECI costs. The structure was designed to withstand snow, wind, live, and dead loads. The design choices examined included:

- Column Spacing
- Beam and Composite Beam Spacings
- Cross-Section Types
- Stability Systems and their Reuse Potential
- Slab Type
- Connection Design

Over 50 models were developed to test various alternatives and combinations. Key findings from the parametric study are as follows:

Column Spacings

Column spacings of 3, 5, 6, and 10 meters were tested in the parametric study. The 3-meter spacing was found to be slightly more optimal than the 5-meter spacing. However, the 5.6% reduction in steel use for a 40% decrease in column spacing was deemed infeasible due to functional requirements and insufficient material savings. The optimal column spacings are ranked as follows: 3m, 5m, 6m, and 10m. This is because increased beam and composite beam spans necessitate larger cross-sections. Since beams outnumber columns significantly, smaller beam sections are selected for larger columns. Table S I shows the total steel weight for each tested column spacing.

Table S I: Steel use with different Column Spacings

	Model	Column (kN)	Beam (kN)	Braces (kN)	Total Steel (kN)
Column Spacing 3m	Regular System	8.32E+02	3.50E+02	3.92E+00	1.19E+03
Column Spacing 5m	Regular System (2.5m)	5.81E+02	6.69E+02	2.87E+00	1.25E+03
Column Spacing 6m	Regular System (2m)	5.79E+02	8.11E+02	2.41E+00	1.39E+03
	Regular System (3m)	5.84E+02	7.79E+02	4.49E+00	1.37E+03
Column Spacing 10m	Regular System (2.5m)	6.86E+02	2.29E+03	2.87E+00	2.98E+03

Beam and Composite Beam Spacings

Beam spacings follow column spacings, as frames work together with beams placed at column locations. Thus, beam and column spacings are interdependent and inseparable design variables. Composite beam spacings, in turn, follow beam and column spacings. Various models with different column and composite spacings were tested to determine the optimal spacings for steel use. Since concrete is not a variable in this thesis, the highest composite beam spacings were found to be the most advantageous for steel use. Spacings of 2-3 meters were most beneficial for 6-meter beam spacing, and 2.5 meters for 5-meter beam spacing. Spacings over 3.5 meters are not recommended in the design guidelines. Table S I also includes composite spacings, except for 1-meter composite spacings, as they resulted in higher steel use. Composite beams are primarily IPE140, and reducing the spacing did not significantly affect the beams.

Cross-Section Types

The selection of cross-section types is straightforward yet critical. Recommended cross-sections for each member include IPE, HEB, and HEA for columns and beams, and RHS, SHS, and CHS for diagrid braces due to torsional effects. Each member's optimal cross-section was tested by selecting those closest to a 1.0 Unity Check. Steel use for each member was then compared, leading to the selection of the most optimal cross-sections: IPE for beams, HEA for columns, and CHS for diagrid braces. Thinner cross-sections generally perform better for steel weight, with larger but thinner sections outperforming smaller, thicker ones. However, IPE sections are less effective for columns, indicating that thinness is not always advantageous.

Cross-sections also vary in their ECI cost coefficients. CHS sections have a lower ECI cost per kg compared to IPE/HE sections, while steel rods for braced frames have the highest ECI cost. These differences stem from the manufacturing process. IPE/HE sections require two heating cycles—one to shape the steel into a rectangle and another to cut and form the I/H shape. In contrast, CHS sections are produced by heating and rolling steel around a cylinder, requiring only one heating cycle, which results in a lower ECI cost. Table S II presents the steel weight for different cross-sections, and Table S III shows the ECI cost differences per kg for each cross-section type.

Table S II: Steel weight with different cross sections

System	Column	Beam	Brace	Total Steel
Diagrid 60	3.55E+02	6.06E+02	1.85E+02	1.15E+03
Diagrid HEA to HEB	4.16E+02	6.06E+02	1.85E+02	1.21E+03
Diagrid IPE to HEA	3.55E+02	6.79E+02	1.85E+02	1.22E+03
Diagrid to RHS	3.55E+02	6.06E+02	3.02E+02	1.26E+03
Diagrid All Different Cross Sections	4.16E+02	6.79E+02	3.02E+02	1.40E+03

Table S III: ECI Cost per kg for different types of cross sections

IPE/HE/UPE			CHS tube			Steel Rod Bracing		
	Total ECI	Demountable		Total ECI	Demountable		Total ECI	Demountable
Total and demountable ECI	1.57E+00	1.48E+00	Total ECI	1.07E+00	9.88E-01	Total ECI	2.12E+00	2.01E+00

Stability Systems

The selection of an optimal stability system is crucial for minimizing material use and ECI costs, as it directly influences the efficiency of cross-sections. This thesis focuses on steel stability systems, including X- and V-braced frames, conservative frames, and diagrid designs. Various configurations of X- and V-braced frames and different diagrid angles were tested. Conventional systems were designed with beams, columns, and a steel core for stability. The most optimal conventional structure was identified with 5 m column-beam spacing and 2.5 m composite beam spacing. The optimal diagrid angle for the current design is 60 degrees. However, the optimal diagrid angle can vary with structural dimensions, generally falling within the 60–70-degree range.

Stability systems were first compared based on steel usage under identical loading conditions. Performance depends significantly on the structure's height due to second-order effects. A structure with significant second-order effects is considered tall. While extensive research exists on stability systems for tall structures, short structures, which comprise over 80% of buildings, are less studied despite their potential for significant cumulative ECI savings.

Short structures are critically loaded due to occupational rather than lateral loads, making the interior columns the most loaded. Stability systems, typically designed to resist lateral loads, have not been extensively studied for short structures due to the perceived lower potential for material and ECI savings. This thesis addresses this gap by analysing short structures through a parametric study.

For short structures, conventional systems perform well, but diagrid designs outperform them. This is due to the division of building sections in diagrid designs, allowing exterior and interior columns to be optimized separately. Diagrid systems eliminate the need for exterior columns to match the interior ones, resulting in more optimized cross-sections and reduced steel use and ECI costs. Braces are not effective for short structures as they do not optimize cross-sections efficiently.

Stability systems for short structures were ranked, with Diagrid 60 and 65 designs performing the best. Conservative designs performed better than several diagrids and similarly to braced systems in terms of steel use. ECI cost does not directly correlate with steel use due to different ECI coefficients for cross-sections. Diagrid designs, particularly Diagrid 70 (5 m), performed better in ECI costs despite slightly higher steel use compared to the optimal conservative design (5 m; 2.5 m).

Table S IV and Figure S I present the resulting material use and ECI costs for the final selected designs. Diagrid 70 showed superior ECI performance due to the use of CHS sections compared to IPE/HE sections, illustrating the importance of cross-section selection on overall ECI efficiency.

Table S IV: Steel weight for final designs for column spacing of 5 and 6 meters

Column Spacing 5 m				
Model	Column (kN)	Beam (kN)	Braces (kN)	Total Steel (kN)
Regular System 2.5 m	5.81E+02	6.69E+02	2.87E+00	1.25E+03
X Bracing Sides	5.72E+02	6.69E+02	3.25E+00	1.24E+03
X Bracing Sides Middle	5.72E+02	6.69E+02	3.25E+00	1.24E+03
V Bracing Middle	5.72E+02	6.69E+02	2.49E+00	1.24E+03
Diagrid 60	3.55E+02	6.06E+02	1.85E+02	1.15E+03
Diagrid 65	3.55E+02	6.37E+02	1.94E+02	1.19E+03
Diagrid 70	3.55E+02	5.75E+02	3.91E+02	1.32E+03
Diagrid 75	3.55E+02	7.78E+02	2.51E+02	1.38E+03
G+D60	4.18E+02	6.05E+02	1.42E+02	1.17E+03

Column Spacing 6 m				
Model	Column (kN)	Beam (kN)	Braces (kN)	Total Steel (kN)
Regular System 2 m	5.79E+02	8.11E+02	2.41E+00	1.39E+03
Regular System 3 m	5.84E+02	7.79E+02	4.49E+00	1.37E+03
Diagrid 60	3.73E+02	7.65E+02	1.85E+02	1.32E+03
Diagrid 65	3.04E+02	7.13E+02	2.12E+02	1.23E+03
Diagrid 70	3.08E+02	7.03E+02	2.26E+02	1.24E+03
Diagrid 75 small	3.10E+02	6.94E+02	2.67E+02	1.27E+03

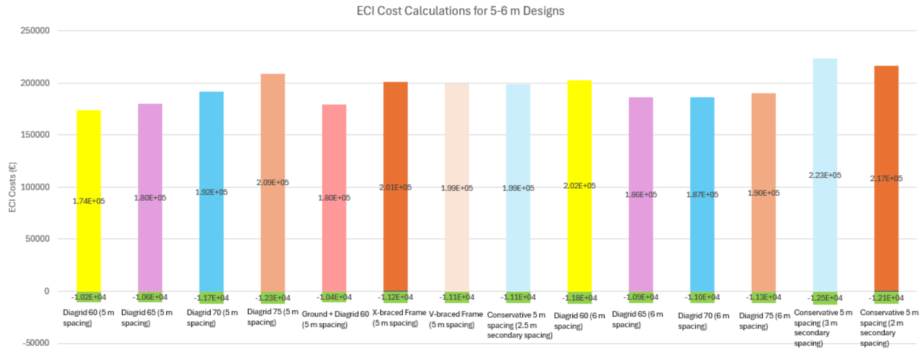

Figure S I: All resulting ECI Costs for tested designs

Demountability

Demountability is a critical design choice for optimizing ECI costs. While demountability initially increases steel use due to the need for elastic design, the end-of-life ECI cost can be subtracted from the total ECI cost for the initial design. For secondary structures reusing disassembled members, the production ECI cost can be assumed to be zero, which constitutes the most significant portion of the ECI cost in structural design. If members are designed to be demounted again after the second structure, the end-of-life ECI cost can also be assumed zero. Therefore, demountability is essential for achieving minimal ECI cost in structural designs.

Demountability begins with the composite slab. To ensure demountability, 22 mm oversized bolt holes filled with resin must be designed for the initial settlement of the slab and safe disassembly. These oversized holes ensure 95% demountability in composite slabs. Bolted connectors are preferred over welded headed stud connectors as they require fewer bolts, reducing the number of demounting locations. Additionally, construction loading on the beams should be avoided by supporting the slabs during the concrete hardening phase or, ideally, using prefabricated slabs.

Demountability must also be achieved in connections between steel members. Welding between members should be avoided, and the use of welds minimized. Three demountable connection designs have been selected from the diagrid design, as diagrid structures have the most unconventional connections among the compared designs. These designs provide guidance on the principles and requirements for steel-to-steel demountable connections.

Table S V presents the ECI cost calculations for the Diagrid 60 design, with end-of-life stages subtracted due to demountability. Although the significance of this subtraction is less compared to production costs, it remains a key point. For secondary structures, production costs are assumed to be zero. Thus, if a structure can be designed with reused sections and designed for demountability, zero ECI costs can be achieved for stages A and C.

Table S V: Example of ECI Cost Calculations for Diagrid 60 Design

Diagrid 60 Final Design					
Production Stage			End of Life Stage		
Beam	Braces (Diagrid)	Column	Beam	Braces (Diagrid)	Column
A1-A3	A1-A3	A1-A3	C1-C4	C1-C4	C1-C4
5.91E+03	1.41E+03	3.46E+03	2.79E+02	8.54E+01	1.63E+02
5.85E+03	1.35E+03	3.42E+03	2.89E+02	8.87E+01	1.69E+02
4.94E+01	4.70E+01	2.89E+01	-1.10E+01	-3.35E+00	-6.42E+00
6.65E+00	1.05E+01	3.89E+00	2.46E-01	7.52E-02	1.44E-01
1.61E-01	4.41E-02	9.42E-02	1.13E-02	3.45E-03	6.60E-03
1.80E+03	1.92E+02	1.05E+03	1.72E+02	5.13E+01	1.00E+02
4.15E+01	3.08E+00	2.43E+01	1.74E+00	5.31E-01	1.02E+00
1.01E+03	1.08E+02	5.90E+02	1.15E+02	3.36E+01	6.73E+01
1.80E+04	1.86E+03	1.05E+04	2.04E+03	5.96E+02	1.19E+03
3.12E+02	3.62E+01	1.82E+02	2.80E+01	8.24E+00	1.64E+01
1.75E-01	3.96E-02	1.03E-01	2.02E-01	6.17E-02	1.18E-01
1.21E+04	3.58E+03	7.09E+03	5.26E+02	1.61E+02	3.08E+02
5.18E+03	2.08E+02	3.03E+03	2.18E+01	6.68E+00	1.28E+01
9.16E+04	1.87E+04	5.36E+04	5.41E+03	1.63E+03	3.17E+03
Total ECI Cost (A+C)		1.74E+05	Total Demountable ECI Cost		1.64E+05

Additionally, demountability was examined across different stability systems. Four main types of stability systems were analysed, assuming 100% demountability of all members, and the possibility of reuse between the members was examined. Diagrid variants are more tailor-made and CHS members with angles are not as commonly used as IPE/HE members and bracings. Figure S II shows the results of the demountability analysis, indicating that braced and conservative designs have a higher potential for reuse compared to diagrid designs. Consequently, braced and conservative designs are rated as yellow in the structural framework.

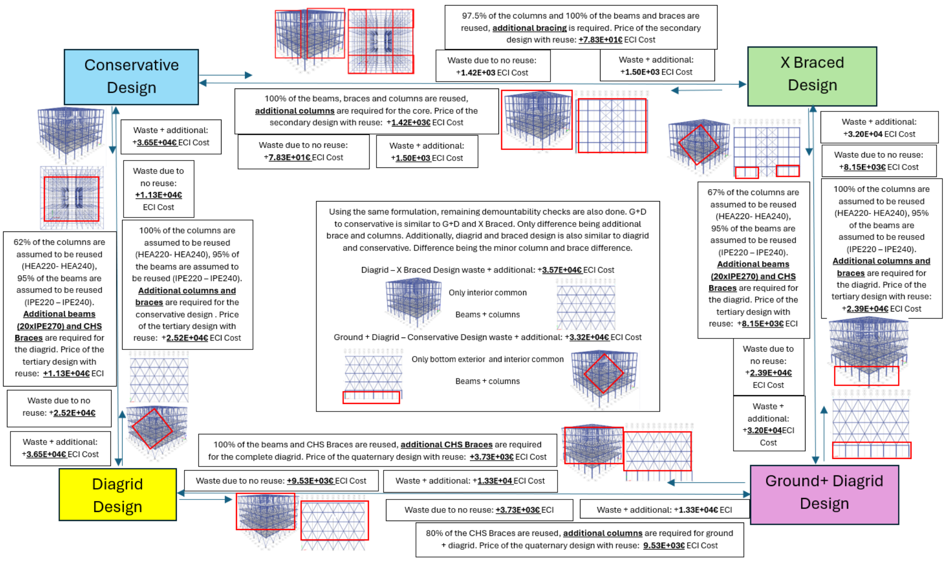

Figure S II: Demountability within the Stability Systems

Tall Structures

In developing a comprehensive structural framework, it is essential to account for stability systems in both tall and short structures. Although stability systems in tall buildings are extensively researched, a new model with a consistent grid has been developed to compare all selected systems under identical conditions. The optimal spacings, cross-sections, and diagrid angles identified for shorter structures remain applicable due to their height-independent principles. However, diagrid angle optimization is influenced by building width rather than height, with both literature and parametric studies indicating an optimal angle range of 60 to 70 degrees.

To evaluate the stability systems for tall structures, a 15-storey, 67.5-meter-tall steel office building was designed, preserving the optimal 5-meter beam and column spacing and 2.5-meter composite beam spacing from conservative and diagrid structures. However, second-order effects required re-evaluation due to the increased height. The analysis showed that the lowest α_{cr} value was significantly below 10, indicating that second-order effects must be incorporated into the design. These effects, including significant deflections and additional moments from axial load eccentricity, were critical in determining member performance.

The study identified the most effective stability systems as Diagrid, Ground + Diagrid, V-Braced, X-Braced, and Conservative. Except for the Diagrid, optimal models included a core addition, which significantly enhanced lateral stability and strengthen all exterior vertical columns. Braced structures without a core required substantial external bracing, optimally bracing 4 out of 6 column-beam frames. Testing various bracing configurations revealed that fewer braced locations led to critical stress concentrations, necessitating thicker cross-sections. The inclusion of a braced core effectively shifted the structure's centre of mass, improved lateral bracing, and reduced lateral displacement and second-order effects, leading to more efficient cross-section designs.

Beam cross-sections also played a significant role in storey displacement. Smaller optimized beams increased storey displacement and second-order effects due to reduced self-weight, necessitating larger column sections. Therefore, stronger beams performed better in the optimized designs, leading to a more efficient use of steel. Table S VI and Figure S III present the resulting steel weight and ECI cost for the stability systems of the tall structure.

Table S VI: Resulting Steel Weight for Stability Systems of Tall Structural Design

Column Spacing 5 m				
Model	Column (kN)	Beam (kN)	Braces (kN)	Total Steel (kN)
Conservative with Core	4.90E+03	3.75E+03	4.85E+02	9.14E+03
X Bracing and middle	4.90E+03	3.75E+03	4.88E+02	9.14E+03
X Bracing Sides + Core	4.39E+03	3.30E+03	4.13E+02	8.11E+03
V Bracing and middle	4.39E+03	3.77E+03	5.38E+02	8.70E+03
V Bracing Sides + Core	4.39E+03	3.30E+03	4.84E+02	8.18E+03
Diagrid 60	2.19E+03	1.80E+03	1.55E+03	5.54E+03
Diagrid 60 + core	2.37E+03	1.80E+03	1.60E+03	5.77E+03
Ground +Diagrid 60	2.60E+03	2.69E+03	1.25E+03	6.54E+03
Ground +Diagrid 60 + cor	2.50E+03	1.79E+03	1.67E+03	5.97E+03

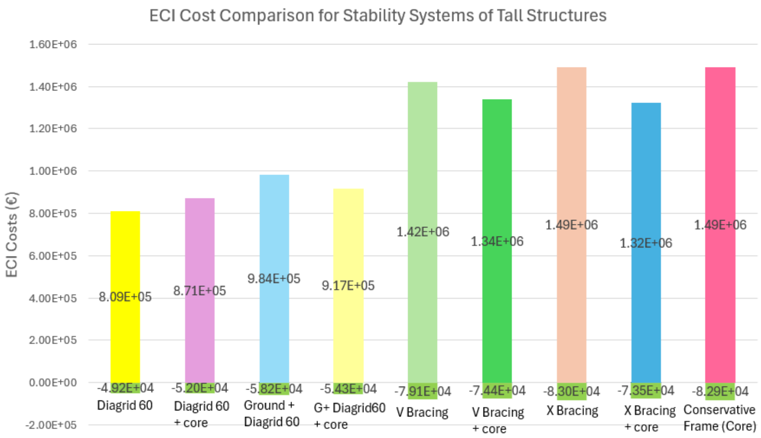

Figure S III: Resulting ECI Costs for Stability Systems of Tall Structural Design

Resulting Framework

Figure S IV presents the resulting frameworks based on all conducted tests, comparing ECI costs for various design choices. A more general version of the framework, without specific ECI percentages, applicable to other structures, is provided in Section 5.6.2.

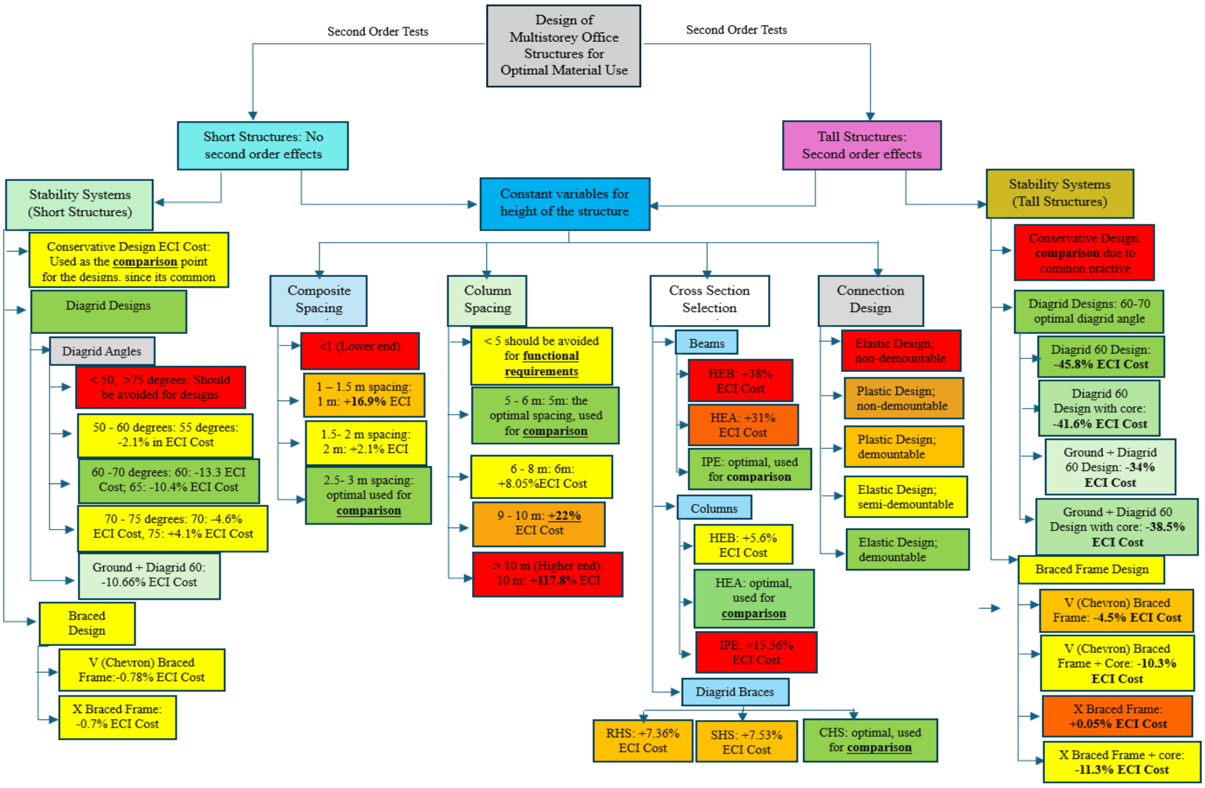

Figure S IV: Resulting Framework with ECI Cost for study

Recommendations

Future improvements to this thesis could include several new additions. For slabs and stability systems, concrete considerations can be integrated into the framework, although this thesis focused primarily on steel. Future work could explore composite structures for stability systems and slabs, with a greater emphasis on concrete thickness.

Additionally, construction, transportation, and use (occupation) are critical ECI cost contributors in the construction industry. Addressing occupation has significant potential to lower ECI costs, as buildings contribute 39% of global carbon emissions, with 28% from operational emissions. Developing a framework for the occupation phase could further reduce ECI costs.

Transportation and construction aspects can be combined in future project management research. Optimizing routes and suppliers can significantly reduce transportation ECI costs by minimizing fuel consumption. Similarly, effective project planning and site management can reduce the need for construction machinery, further lowering fuel usage. These areas could benefit from a similar guiding tool or framework to enhance sustainability in construction.

Abstract

This thesis investigates the optimization of steel weight and the Environmental Cost Indicator (ECI) in steel structures, addressing the significant contribution of materials and construction to global carbon emissions. Focusing on European office structures, which face high vacancy rates and substantial environmental impact, a parametric study is conducted on a 5-storey, 30x30m steel office building. The study evaluates design choices, including column, beam, and composite beam spacings, cross-section selection, connection design, and stability systems.

A preliminary building is designed under consistent load conditions, followed by over 50 variants incorporating different stability systems, frame designs, and composite beam spacings. Analysis indicates that smaller column and beam spacings, along with larger composite beam spacings, optimize steel use and ECI costs. HEA sections for columns, IPE sections for beams, and CHS sections for diagrid braces and angled columns are identified as the most efficient.

The study also highlights that material use does not always correlate with ECI costs. Designs incorporating demountability initially increase steel use due to elastic design requirements but result in lower ECI costs over multiple lifecycles by enabling reuse of materials. Several diagrid designs, benefiting from lower ECI costs per kilogram of CHS sections, perform better than conventional and braced structures despite higher initial material use.

Demountability was a key focus, with bolted connections identified as essential for achieving demountability standards. The reuse potential of stability members varies significantly; unlike conventional designs, diagrid structures are tailor-made, making their reuse challenging for subsequent applications.

The findings are consolidated into a final design framework to guide engineers in optimizing steel use and ECI costs, providing a practical tool that reduces the need for extensive modelling. This research fills gaps in the literature by focusing on short structures and offering insights into efficient structural design practices.

1 Table of Contents

List of Figures

List of Tables

1 Introduction and Scope

1.1 Introduction

Sustainability has become a critical focus in the construction industry, particularly following the 2015 Paris Agreement, due to the sector's substantial environmental impact. The need to improve construction practices to reduce their detrimental effects on the environment has become increasingly urgent (Cole, 1999; Holmes and Hudson, 2000). Buildings account for 39% of global energy-related carbon emissions: 28% from operational emissions (energy for heating, cooling, and power) and 11% from materials and construction (Embodied Carbon, 2022).

In modern construction, designs have traditionally been driven by cost and scope considerations, but there is an increasing shift towards sustainability. The environmental impact of construction, green building practices, design for recycling, and eco-labelling of materials have garnered significant attention from building professionals globally (Crawley and Aho, 1999). Building performance, particularly in terms of environmental impact, has become a primary concern within the industry (Crawley and Aho, 1999), with environmental performance assessment emerging as a critical issue in sustainable construction (Holmes and Hudson, 2000). In steel structural design, numerous decisions influence the ECI of a structure, including its lifetime ECI. These decisions encompass variables such as material quantity, energy used in material production, structure utilization, transportation, construction, and end-of-life processes. Properly addressing these variables can optimize the environmental footprint of steel structures. This thesis conducts a parametric study to examine how different structural engineering designs affect the ECI cost.

High office vacancy rates are a significant issue in European cities, with the vacancy rate in 125 of Germany's largest towns rising from approximately 1% in 1990 to 7.5% (Hauke et al., 2016). Consequently, a multistorey steel office structure was designed for the parametric study, incorporating various design choices and variables. These variables were analysed by examining decisions such as connection design, potential for disassembly and reuse of structural members, cross-section design, member spacing for material optimization, reuse of steel in cross-section production, and optimizing the structural system design.

In several studies, it has been established that operational energy is the predominant contributor to the life cycle impacts of conventional buildings. However, for new and low-energy buildings, the significance of different life cycle phases is evolving (Blengini & Di Carlo, 2010). Although 72% of carbon emissions in the building industry stem from operational emissions (Embodied Carbon, 2022), this thesis does not address operational and construction phase precautions, as they warrant separate studies. The primary objective of this thesis is to develop a structural design framework for steel structures that minimizes ECI costs associated with steel usage. Comparisons between different buildings are inconclusive due to varying structural dimensions and design conditions. Therefore, the thesis identifies effective material minimization strategies through the comparative analysis of several distinctive designs on the same structure.

Current literature includes ECI cost calculations based on the mass (kg) of materials used in construction, applying impact category factors to these materials. Smarter design can alter these amounts. For example, disassembly of connections can reduce ECI costs by enabling the reuse of members. Optimal system design and appropriate cross-section choices for design loads can minimize structural steel usage by optimizing material strength. Additionally, using scrap material in production further reduces ECI costs. The goal of this thesis is to develop a framework for minimizing the ECI cost of steel structures.

Inspiration for this thesis arose during preliminary research, which revealed a lack of comprehensive examination of design selections for structures. Previous research often focuses on specific decisions rather than exploring their combined effects. For instance, Cho et al. (2012) examines bracing stability systems and the percentage of steel saved in tall structures, but greater material savings are possible when integrating optimal spacing designs, stability systems, demountable connections, and composite flooring systems.

Preliminary research also indicated a predominant focus on tall structures to understand stability system effects. Material use is less optimized in tall structures due to second-order effects and lateral displacement causing critical loading. However, over 80% of global structures are classified as short, meaning small reductions in material usage for these structures can result in substantial global savings.

Given that most buildings globally are not tall structures, any developed framework must also consider short buildings. Due to second-order effects, members of tall structures experience different loading compared to short structures. Additionally, the effects on tall buildings have been separately researched for stability systems; integrating this research can aid in framework development.

A parametric study was conducted on a short, 5-storey (22.5 meter) steel office building, examining the impact of various design choices. Column, beam, and composite beam spacings, as well as different stability systems, were tested. Additionally, the effects of cross-section selection and steel-to-steel and composite connections were investigated. The results provided insights into structural behaviour for the framework development. The distinction between tall and short structures in the framework is based on second-order effects rather than height or storey number. Distinction using height of a structure varies with each design due to differing floor plans. The framework includes a structural explanation of these classification differences.

Accuracy of the framework also depends on accounting for the structure's end-of-life phase. If materials are reused or recycled, ECI cost calculations must be adjusted accordingly. In cases of demountability, a slight increase in material use can lead to significant ECI cost savings. Therefore, the framework includes considerations for these scenarios.

This thesis offers valuable insights for both industry and academic literature. While industry has long pursued designs minimizing material use, these efforts are often superficial. Many design guides provide optimal spacings for columns and beams based on the span of produced industrial cross-sections, not material efficiency. Engineers typically avoid mid-span connections due to potential weak points. However, this framework focuses on determining which end of the spacing range is most effective for minimizing material use and total ECI cost. Existing guides do not address this optimization, focusing instead on common practice.

Occasionally, using more material weight can reduce the ECI cost, contrary to industry focus on minimizing material use for cost optimization. Demountable designs, while more expensive to construct due to additional material use, significantly lower total ECI cost. Demountable structures must avoid plastic deformations to ensure reuse, whereas allowing plastic deformations optimizes cross-section use by maximizing strength and deformation capacity. This leads to irreversible deformations, reduced dimensional stability, and the generation of residual stresses, rendering members lower-grade or scrap after the structure's lifetime. In contrast, elastic design maintains deformations within the elastic range, enabling member reuse post-structure lifetime, albeit with increased material use. Reuse also results in negative ECI cost. Therefore, a holistic examination of the structure is necessary, as every decision impacts ECI cost. Developing a structural design framework for steel structures requires harmonizing these decisions.

1.2 Research Question and Scope

This thesis addresses the following research questions:

- What is the optimal structural system selection, column spacing, cross-section selection and composite (secondary) beam spacing to minimize the total weight of steel and ECI cost of a structure?
- What are the design choices to make a multistorey steel structure more weight optimized?
- How to design a structure to be deconstructed at the end of life?
- What parts of the structure can be designed demountable and what are the limitations of demountability for a multistorey steel structure?
- What are the step-by-step requirements and methods to ensure the structural steel use is optimized in a multistorey steel structure?
- How does stability systems contribute to the steel weight of a 5-storey office structure?
- What percentage of the steel weight can be saved if the design strategy is to optimize the weight use rather than cost, profit or ease of construction compared to a conventional design?
- What are the reused structural members and the resulting Environmental Cost Indicator (ECI) costs for subsequent structures when different stability systems are analysed for multi-storey steel office structures?
- How can a step-by-step structural design framework for multistorey steel offices be developed to optimize structural steel use, reuse potential, and resulting ECI costs in comparison to conventional steel structures, by conducting a parametric study on a 5-storey 30x30m office building?

This thesis aims to develop a structural design framework applicable to various types of steel structures, optimizing steel weight and associated Environmental Cost. To ensure generalizability, a parametric study is conducted.

This framework does not encompass all types of steel structures, as such a scope would require extensive modelling and calculations. The focus is on steel-based stability systems, excluding composite structures and steel stability systems with concrete cores, due to the objective of minimizing steel weight. Concrete, with its distinct ECI coefficients, necessitates separate iterations to determine optimal material ratios for ECI cost calculations.

An exception is made for flooring systems, as slabs are typically made from concrete or steel-concrete composites. Secondary beams are necessary for diagrid stability systems to connect inner columns to exterior diagrids. These beams also serve as the primary load-carrying components of the flooring system; hence, composite slabs are included in the analysis.

Short and tall structures require different designs due to second-order effects. The parametric study focuses on a shorter structure with a height of 22.5 meters. Structural systems like space trusses and super frames are not applicable to short structures, and exoskeleton structures function similarly to regular bracing systems, thus they are excluded from this study. Bracing systems, diagrids, and conventional structural designs with steel cores are selected as the main stability systems for testing.

1.3 Methodology

Shown below in Figure 1 is the design flow chart for the development of the framework:

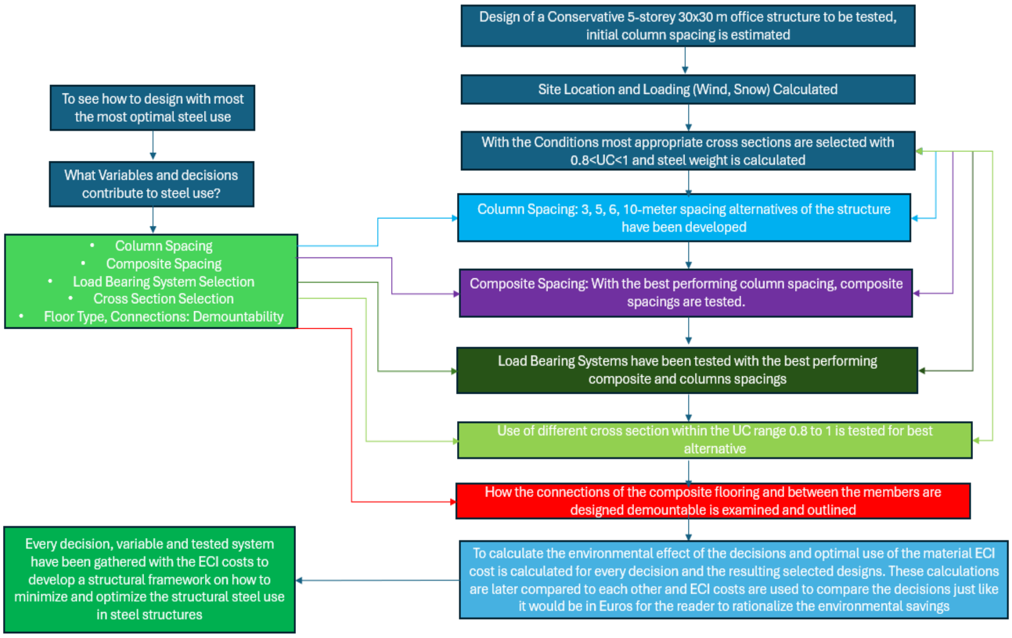

Figure 1: Design workflow for the development of structural design framework for steel structures

To develop a design framework for optimizing the ECI cost of steel structures, the following methodology was employed:

1. Design selections affecting steel usage, total steel weight, and ECI cost are identified. Demountability was recognized as a critical factor for ECI cost optimization.
2. A literature review was conducted to identify and analyse gaps in existing research essential for developing the framework.
3. Missing and non-specific (broad) parts are identified and a parametric study for a 5-storey steel office building is developed to obtain detailed insights on design selections.
4. To carry out the parametric study, a site is selected, and loads are identified to develop the structure with preliminary cross-section and design selections.
5. Parametric study is conducted to test identified design selections, examining over 50 models of the same structure to determine the impact material use.
6. For each design selection, the optimal option was determined through testing, and the reasoning and limitations were documented. Differences in design effects (e.g., short vs. tall structures) were identified and explained.
7. Combining the optimal design selections, 3-4 models were identified and compared with a conventional structural design. Comparisons focused on steel usage, analysing and contrasting each specific load-carrying system. Differences and their underlying reasons were thoroughly examined.
8. The best overall system is selected, and reasoning on why it outperforms other designs is explained.
9. To guide the reader on system connections, given the importance of demountability, examples of each connection type were developed to demonstrate methods, consequences, and limitations of demountable connections.
10. Analysis results of the parametric study are combined and discussed to develop the framework.

11. The total ECI cost associated with each decision and selected models have been compared and analysed to develop the structural design framework.
12. Reuse potential of stability systems are investigated and ECI Costs for subsequent designs are calculated.
13. Steps 7, 8, 10, and 11 are repeated to test tall structures and finalize the structural framework.
14. Framework is developed encompassing all considered structure types, guiding readers through specific selections to minimize steel weight. The aim is to provide a guide for achieving the lowest steel weight and ECI cost within the selected structure range.

2 Literature Review

The construction industry significantly consumes resources and exerts considerable pressure on the environment (de Klijn-Chevalerias and Javed, 2017). Construction and building use account for 36 to 40 percent of global energy consumption and greenhouse gas emissions (Marique and Rossi, 2018). Building-related emissions are projected to double by 2050 (Pomponi and Moncaster, 2016). Immediate action is required to control these emissions. Control mechanisms include managing life cycle emissions through solar panels, smart building systems, and greywater management systems. Additionally, optimizing project management to reduce greenhouse gas emissions from vehicles and improving design and construction practices can further mitigate emissions. This thesis focuses on structural design and the partly, construction of steel structures, emphasizing planning for deconstruction and reuse.

This thesis focuses solely on structural design, minimizing material use, and facilitating disassembly for two main reasons. First, structural components contribute significantly to building weight and carbon emissions, accounting for approximately half of material-related emissions (Webster et al., 2012). Kaethner and Burridge (2012) investigated various structures and their embodied carbon. They found that superstructures and substructures are responsible for over 50% of embodied carbon emissions of buildings. Figure 2 illustrates the breakdown of embodied carbon across different structural elements. Second, by specifying the point of interest, focus is narrower and deeper analysis can be carried out.

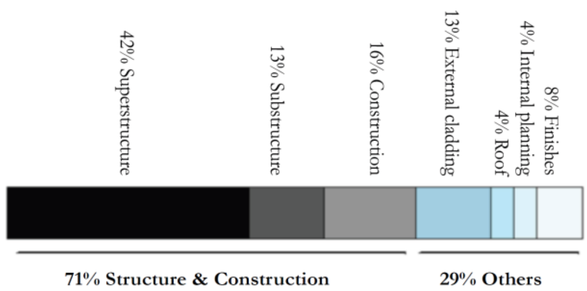

Figure 2: Average breakdown in building elements of embodied carbon (Kaethner and Burridge, 2012)

2.1 Production of Steel

The construction process starts with material selection, with this thesis focusing on steel. Energy consumption during the production phase of building materials has significantly escalated with industrialization (Huberman and Pearlmutter, 2008). The steel industry, responsible for approximately 997 kg of carbon dioxide emissions per ton of steel, contributes 4-5% of global carbon dioxide emissions (Nidheesh & Kumar, 2019). Over 60% of these emissions occur before the steelmaking process (Zhang et al., 2018). Steel can be produced using two methods: electric arc furnace (EAF) and blast furnace (BF) processes. Globally, 62% of structural steel is produced via BF, while only 29% is produced via EAF according to Global Steel Plant Tracker (GSPT). Nidheesh and Kumar (2019) and Gan et al. (2017) demonstrated that EAF steel reduces carbon dioxide emissions by 60% compared to BF steel, albeit at a significantly higher cost due to scrap metal purchase. Industry does not distinguish between primary and secondary steel hence scrap is nearly as expensive as regular steel (Gan et al., 2017). Due to the additional costs in industry, the percentage of use of EAF steel is not desirable, however, with increased use of Electric Arc Furnace Steel production, carbon emissions can be lowered by up to 75% compared to traditional blast furnace steel production (Steelmaking in EAFS produces 75% lower CO2 emissions, 2022). With increased use of EAF steel between 1998 and 2018, total iron and steel industry energy use fell by 34 percent (Sustainable steelmaking, n.d.).

Reusability of steel can significantly reduce CO2 emissions, with Kim and Kim (2020) demonstrating a reduction of up to 77%. However, similar to EAF and BF steel, there is a trade-off between sustainability and cost, limiting its widespread adoption in the industry. Reusing steel increases total costs by 40%, primarily due to the purchase of scrap metal. The article suggests optimization rather than exclusive selection, highlighting economic uncertainty as a significant factor.

2.2 Frame Design

A critical aspect of steel construction, where industry and research converge, is the design of structural systems. This begins with determining column and beam spacings.

System design is a crucial aspect of structural design. Determining the placement and spacing of columns, beams, and slabs is essential. To optimize space, middle columns or wider column spacings can be utilized. This thesis aims to identify what is most beneficial for material use and ECI cost rather than space optimization. For the first tests on developing the structural system, research has been conducted. Figure 3 and Figure 4 illustrates the tested frames and their material use.

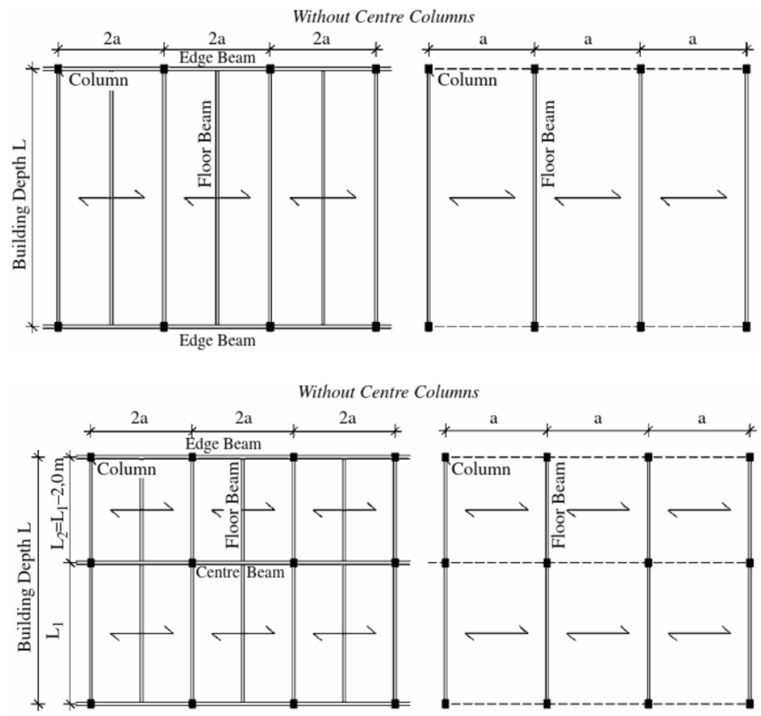

Figure 3: Variants of slabs with downstand beams with specification of the construction gird and components (Hauke et al., 2016)

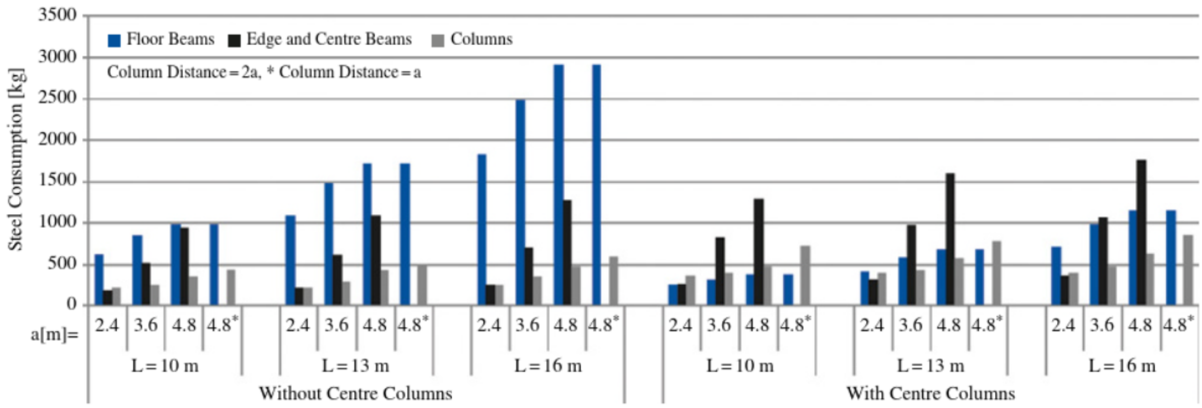

Figure 4: Steel consumption per slab for selected variants of slabs with downstand beams (Hauke et al., 2016)

Results from the tests in Figure 3 and Figure 4 reveals several optimization techniques for frame design and spacings. Firstly, the analysis indicates that centre-columns are essential to reduce material use. However, increasing the number of cross-sections significantly complicates construction and increases time (Hauke et al., 2016). The parametric study aims to develop a framework guiding minimal steel weight, necessitating middle columns. Secondly, column spacings were tested for building depths between 10-16 meters. Although higher column spacings use more steel, eliminating edge columns resulted in the best performance. Optimal results were achieved when column and beam spacing were identical and edge and centre columns were removed (Hauke et al., 2016). However, this configuration eliminates composite beams and results in a deck without composite flooring systems. The goal of the thesis is to examine combined systems and their harmonious function focusing solely on steel, so this optimal method was not adopted for the tests. Additionally, the analysis indicated that increased building depth decreases ecological benefits and raises costs (Hauke et al., 2016). This factor is not included in the framework as building depth depends on the site, and engineers aim to maximize site area utilization

2.3 Slab Design

Selection of flooring systems was discussed in Section 2.2. Composite beams are used to transfer loads using steel, maintaining concrete as a constant variable for different spacings. This section investigates the cost and material savings differences between the two systems.

Table 1 shows two different analysis results for comparison of composite and RCC slabs. All examined articles had similar savings.

	R.C.C STRUCTURE	COMPOSITE STRUCTURE	DIFFERENCE	In %
SLAB	30515095.46 Rs	22001265.2 Rs	-8513830.26 Rs	-27.9004
BEAM	7023461.66 Rs	18657333.23 Rs	11633871.34 Rs	62.35549
COLUMN	9236275.38 Rs	10488763.64 Rs	1252488.26 Rs	13.56053
FOOTING	9945576.59 Rs	5510013.64 Rs	-4435562.95 Rs	-44.5983
TOTAL	56720409.09 Rs	56657375.48 Rs	-63033.61 Rs	-0.11125

	R.C.C STRUCTURE	COMPOSITE STRUCTURE	DIFFERENCE	In %
SLAB	39990551.1 Rs	28772039.3 Rs	-11218511.8 Rs	-28.0529
BEAM	8207075.16 Rs	20863500 Rs	12656424.84 Rs	60.663
COLUMN	13701333.92 Rs	13060635.76 Rs	-640698.16 Rs	-4.67617
FOOTING	11130922.5 Rs	6701718.52 Rs	-4429203.98 Rs	-39.7919
TOTAL	73029882.68 Rs	69397893.58 Rs	-3631989.1 Rs	-5.23357

Table 1: Comparison of Composite and RCC Systems for 12 and 15 stories (Wagh & Waghe, 2014)

From the article, slab systems are the focus. A 28% reduction is observed when comparing conventional and composite slabs. Cost estimation, which depends on material usage, indicates that composite slabs are more material-efficient. The cost comparison shows that steel-concrete composite designs are more economical for high-rise buildings and facilitate faster construction (Wagh & Waghe, 2014). For the thesis, the composite slab is selected for its optimal design. This choice is based on the efficient material use shown in Table 1, the use of steel as a load-bearing material in conjunction with concrete, and the consistent concrete thickness in the design.

2.4 Stability Systems

The design of load-bearing systems, a key factor in reducing environmental impact, continues the structural system design. With significant technological advancements and rapid population growth, available urban land is becoming limited. This necessitates vertical construction in metropolises to accommodate population needs. Engineers and researchers are increasingly exploring vertical building possibilities, testing the limits of human ingenuity.

Tall buildings are subjected to distinct loading effects compared to conventional structures, including vertical forces such as occupancy, snow, and dead loads, as well as lateral forces from wind and earthquakes. As first noted by Fazlur Khan, the structural demands imposed by lateral loads increase significantly with building height, leading to a 'premium for height' that substantially raises material consumption (Moon, 2008). This underscores the critical importance of material-efficient design strategies in tall buildings. Vertical forces are generally more manageable, as they align with the strong axis of the resisting cross-sections. However, the effects of horizontal forces intensify with height, increasing the base moment. Second-order loading creates eccentricity and additional moments, making design more challenging. Researchers and engineers have developed various systems to address these challenges. Stability systems minimize second-order effects and lateral displacement while effectively withstanding both lateral and vertical loads with efficient material use. Figure 5 and Figure 6 illustrate exterior load-bearing structural systems used in high-rise structures.

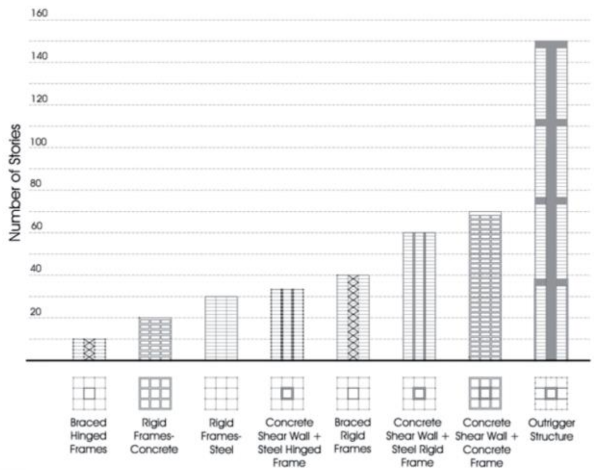

Figure 5: Interior load carrying systems for structures (Ali and Moon, 2007)

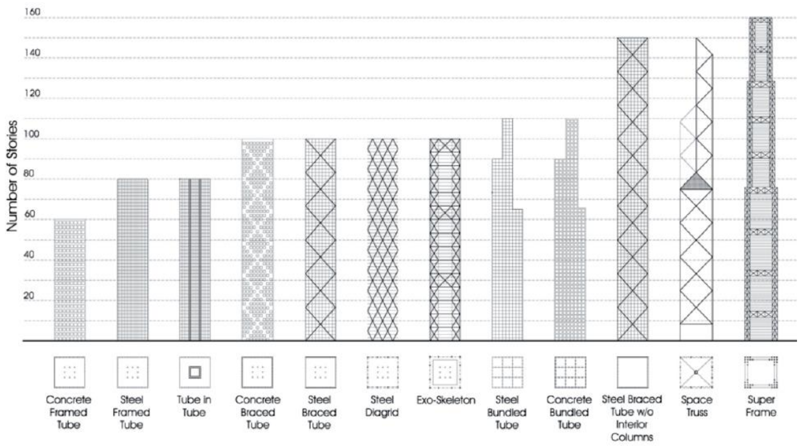

Figure 6: Exterior load carrying systems for structures (Ali and Moon, 2007)

Using these classifications, further research compared the material use of stability systems under identical loading conditions to identify the most optimal system for this thesis.

2.4.1 Conservative Design

In this thesis, the terms 'conventional' or 'conservative' structure refer to regular column-beam structural systems with a steel core for elevators and stairs. These structures are designed with uniform cross-sections for beams, columns, and secondary beams to simplify construction. Connections are typically welded due to the precision and skilled labour required for bolting. Figure 7 illustrates an example of a conventional or conservative structure used in this thesis. Conventional structures typically have a concrete core for lateral stability. However, concrete is avoided in this thesis due to ECI cost calculations and required iterations. Alternatives for core design using steel are considered. Figure 8 shows an example of a steel core from a real structure.

Figure 7: Example of conventional (conservative) structure in practice, Ethiopia

Figure 8: Example of a steel braced core in practice

2.4.2 Braced Systems

Braced structures are commonly used in high-rise buildings. Bracing acts as a glue between columns, enabling the system to move as a unit and reducing the load on overloaded columns. Bracing systems primarily withstand lateral or dynamic loads rather than dead or occupancy loads. In earthquake-prone regions like Türkiye or Chile, bracings are mandated by codes. The most popular bracing systems for steel frames are X and Chevron (V) bracings. A critical point is that braces only transfer tension and do not withstand compressive loads (Faggiano, 2016), behaving like cables under tension and 'slacking' under compression. Compressive resistance is not zero, estimated to be so in structural design.

2.4.3 Outrigger Systems

Outriggers are deep, stiff beams that connect the central core to the outermost columns, reducing sway and maintaining column positions (Kamath & Rao, 2012). These beams reduce core movement relative to the structure's free movement, resulting in decreased lateral displacement at the top. Less displacement reduces second-order effects, loading, and material use, leading to smaller cross-sections. The structural system's stiffness increases by 20 to 30 percent with outrigger beams (Taranath, 2016).

2.4.4 Comparison between Braced Systems

Optimal design selection can reduce material use by 25-30%, as shown in studies by Milana et al. (2014) and Cho et al. (2012). These studies examined various bracing systems, including X-braced frames, Chevron braced frames, outrigger frames, and basic frame designs. While percentages and cost calculations may vary between structures, the underlying principles remain consistent. Understanding and incorporating earlier research on structural systems is essential for this thesis.

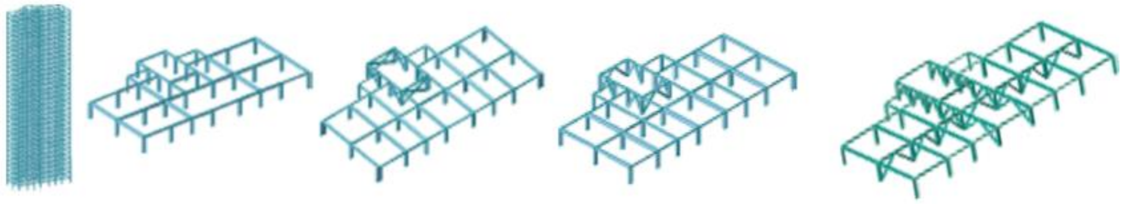

Figure 9: A) Basic System B) X Brace C) Chevron Brace D) Outrigger System (Cho et al., 2012)

Cho et al. (2012) found that Chevron braced frames are the most effective, reducing material use by 28.6% compared to basic systems and 13.8% compared to outrigger systems. Lateral stability is crucial for material savings, particularly in tall structures. Even a simple bracing system can reduce material use by nearly 30%. Milana et al. (2014) examined high-rise structures, incorporating complete structural bracing systems like diagrids, which offered new possibilities for weight savings.

2.4.5 Diagrid Structures

Diagrid structures are bracing systems designed to withstand axial loads and shear, unlike regular bracing systems that only handle tension. This design eliminates exterior vertical columns, creating a distinct system. The distinctive composition of diagrid structures offers exceptional structural efficiency for tall buildings and enhances aesthetic integration within orthogonal urban environments (Moon, 2009). Diagonal columns or braces in diagrids provide lateral load resistance and withstand vertical loading. The load is transferred to each member and divided at nodes where diagrid members meet, reducing the likelihood of overloading any single point compared to conventional structures. Figure 10 illustrates force transfer and node design in diagrids. Composite beams must connect each node for full optimization, with required beam locations changing on each floor. Critical nodes must be connected by interior secondary beams. Diagrid designs vary, with module height, diagrid angle, design area, floor height, building height, and geometry influencing the optimal angle. Prescribing the optimal diagrid design is highly dependent on geometry and thus case specific. However, understanding the geometric principles and performance criteria of diagrid designs can be applied universally to various structures.

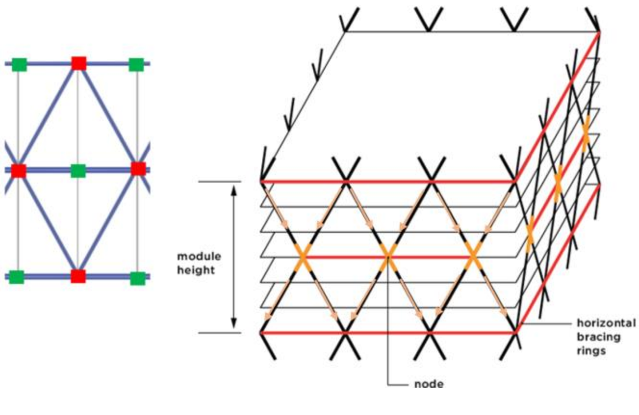

Figure 10: Diagrid design representation and understanding module detail (left), complete structural detail (right)

The diagrid structural system offers greater flexibility in interior space planning and facade design (Jani & Patel, 2013). Figure 11 resents two examples of diagrid floor plans from different designs. These examples illustrate how diagrid exterior members connect to interior columns. Composite beams meeting diagrids on each floor are placed but are insufficient for load bearing. Diagrids do not fully enclose certain floors, requiring diagonal beams to facilitate moment transfer.

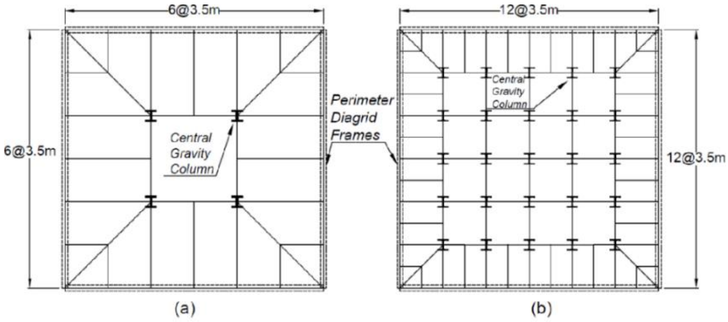

Figure 11: Diagrid Structures floor plans a) with 2x2 inner columns b) with 5x5 inner columns (Asadi et al., 2018)

Diagrids offer design flexibility with small modules, enabling new and modern shapes. Selecting the optimal diagrid module is crucial for the specific design. There are four types of diagrid modules: Small (2 to 4 stories), Midrange (6 to 8 stories), Large (10+ stories), and Irregular (for different shapes) (Boake, 2014). For short structures, only small modules are applicable, also providing shape flexibility. Larger modules are employed for taller structures, which can accommodate thicker diagrid members.

Milana et al. (2014) examined high-rise structures with various stability systems, including braced frames and diagrids. The study also compared diagrid structures with different angles, which vary by design. The angle of diagrids alters the geometry of the exterior load-carrying structure and are highly dependent on the interior beam column system. Thus, only an optimal angle range can be determined, rather than a specific 'perfect' angle.

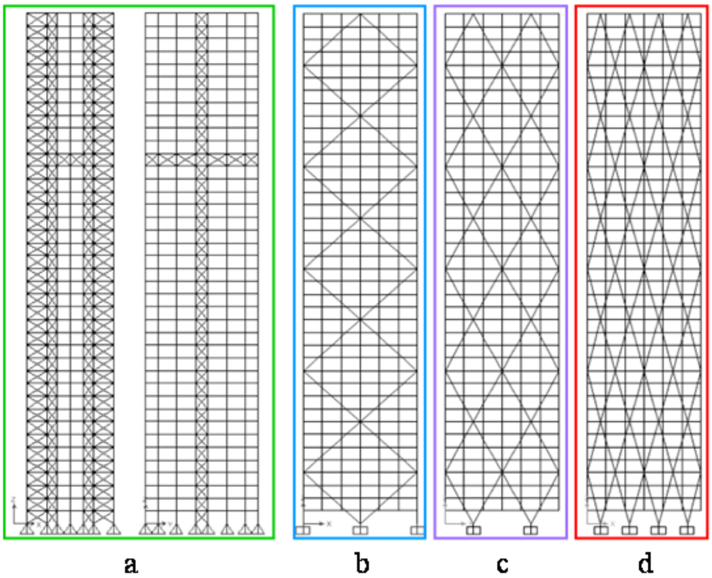

Figure 12: A) Outrigger Structure B) Diagrid Structure α=42 C) Diagrid Structure α=60 D) Diagrid Structure α=75 .(Milana et al., 2014)

The article indicates that diagrid structures with 42, 60, and 75-degree braces resulted in 19%, 26%, and 33% weight savings, respectively. In-depth tests for rigidity, robustness, serviceability, and sustainability showed that the 60-degree system is the most advantageous. For most structures, depending on shape, design, and height, the optimal diagrid angle is between 55-75 degrees (Ashtari et al., 2021). Well-engineered diagrid systems save steel weight compared to outrigger structures and potentially more than conventional or conservative structures. Both articles highlight how correct design can significantly reduce material use and enhance sustainability.

2.4.5.1 Diagrid Connections

Diagrids are complex to design and connect, with numerous members joining at various angles to the same node. This complexity makes node design challenging. Constructability poses significant challenges in diagrid structures due to the complexity and higher cost of their joints compared to conventional orthogonal structures. To mitigate these issues and reduce on-site labour, prefabrication of nodal elements is crucial (Moon, 2009). Figure 13 and Figure 14 illustrate several different diagrid connections, especially exterior connections.

Figure 13: Diagrid Connections (Boake, 2014) in a) Swiss Re-Tower 30 St Mary Axe b) Ottawa Congress Centre

Figure 14: Diagrid Connections in CCTV Beijing China (Boake, 2014)

An analysis of the nodes in the Swiss Re and Hearst buildings underscores the importance of axial force transfer through the nodes (Boake, 2014). This transfer is facilitated by a connecting plate that supports loads from each member. Due to the varying orientations of the members, the plate must be designed to resist forces from multiple directions, presenting a more complex challenge compared to conventional designs. Whether it is a hexagonal prism (Figure 13b), stiffening plates on each cross-section (Figure 13a), or a hidden stiffening plate support for the facade (Figure 14), members are connected at the nodes. Plates are essential for withstanding multidirectional loads and preventing overstress in the node members.

2.5 Cross-section Selection

Examining structures in detail reveals additional sustainability improvements, particularly in the main structural systems: beams, columns, and slabs. For beams and columns, sustainability can be enhanced through optimal design, correct cross-section selection, or scenario-specific 'tailor-made' tapered designs. These designs are case-specific and not extensively covered in the literature. However, selecting the correct cross-section can lead to substantial weight savings and directly impacts axial load capacity, moment capacity, rebar layout, structural stiffness, performance, joint design, connections, and foundation design (Anwar & Najam, 2017). Thus, cross-section selection influences nearly every aspect of structural design.

Selecting the appropriate cross-section is crucial, as it significantly impacts material weight and failure, which is influenced by the geometry and cross-sectional characteristics (Dimopoulos & Gantes, 2008). Industry practice favours the smallest cross-sections and lowest steel grades to achieve economical designs and avoid overdesign. However, different cross-sections (e.g., HEA, HEB, IPE) can be used for columns and beams. Preliminary research reveals no clear comparison of which cross-section is best for material use, but several options are provided for designers and engineers. Identifying the best option for different members can significantly reduce steel weight. This principle is particularly relevant to diagrids, a key focus of this thesis. The optimal cross-sections for diagrids are not yet fully tested, and possibilities and limitations of the structural systems are still being explored. Commonly used sections include Hollow Sections (CHS, RHS, SHS) and steel-concrete composites due to torsional effects. Even minor differences in cross-section selection can significantly impact total steel weight and ECI cost.

Although cross-section selection is well understood in the industry, research lacks guidance on which scenarios make a given cross-section most advantageous. Industry standards provide only a range of reasonable cross-sections for engineers, but both literature and industry lacks information on the best options for material use.

2.6 Demountability and Disassembly

Optimizing steel weight involves not only lowering ECI cost but also planning for reuse and disassembly. Reusing structural steel, rather than recycling, offers significant potential for cost-effective systems and environmental benefits in construction (Uy et al., 2017).

2.6.1 Steel to Steel Connections

The demountability of construction systems, particularly steel-framed buildings, is crucial as it enables the reuse of structural components without the need for recycling. Steel structures are inherently adaptable and can be easily demounted, allowing for the reuse of their components (Dai et al., 2022). Demountable beams and columns can be reused in different structures after disassembly, significantly lowering their ECI cost. Initial ECI cost calculations can exclude the end-of-life stage, except for transportation. The primary ECI cost savings benefit future structures that use the disassembled members, as they will not require fabrication again. Thus, production costs for subsequent designs can be assumed to be close to zero if all beams and columns are reused.

In steel and composite structures, preassembled building units are installed using bolted or other joints at the construction site offer benefits. Boltless techniques include plug-in, contact joints, and cleating (Hauke et al., 2016), enabling reassembly. Cabaleiro et al. (2023) examined various connection types, highlighting the importance of connections for demountability. Achieving demountable structures requires incorporating the 'Design for Deconstruction' or 'Design for Disassembly' (DfD) philosophy from the outset. Demountable connections must exclude welding, particularly between column-beam connections. Several different connection types are shown in Table 2:

Table 2: Summary table of several types of connections (Cabaleiro et al., 2023)

Type	Removable	Reconfigurable	Application	Number of References at Scopus (a)	Research Level Based on Scopus References	Sustainable (b)
Welded	No	No	All profiles type	10,695	very high	very low
Bolted	Yes	difficult	All profiles type	2139	high	low
Blind bolts	Yes	difficult	Square/rectangular tubes	151	medium	low
Storage racks	Yes	medium	Continuously perforated columns and beams equipped with quick hooks made using tabs	171	medium	medium
Scaffolding (disk locks)	Yes	medium	Round tubes	84	medium	medium
Scaffolding (quick round tube couplers)	Yes	easy	Round tubes	14	low	high
Bolted with removable brackets	Yes	medium	I-type profiles	18	low	high
I-type profiles by a collar connection	Yes	easy	I-type profiles and square/rectangular tubes	9	low	high
Clamp-based connections for I-type profiles	Yes	easy	I-type profiles	12	low	very high
Clamp-based connections for square or rectangular profiles	Yes	easy	Square/rectangular tubes	2	very low	very high

(a) All searches were performed in SCOPUS for: steel AND structures AND connection OR joint; (b) In this work, "sustainable steel structures" are defined as structures that are fully reconfigurable and reusable as many times as necessary.

Numerous failure tests and examinations of various criteria, along with the information in Table 2, show that the clamp-based system is the best solution for I-shaped profiles due to its demountability and sustainability (Cabaleiro et al., 2023). However, it has limitations, such as rigidity, cost, and applicability only to I-type cross-sections. This article focuses on I-sections, the most industrially used steel cross-section. Insufficient research exists for clamp-based bolted connections in hollow sections. Demountable and reusable materials come with additional costs (Kim & Kim, 2020). Bolted connections are common, unlike designing for demountability and end-of-life reuse. Elastic design is required for reusable cross-sections, preventing plastic deformations that degrade cross-sections and result in material waste (Nijgh et al., 2019). Consequently, thicker and larger cross-sections are needed, increasing costs. While this might add to environmental costs due to increased steel usage, it can be justified in ECI calculations by accounting for reuse at the end of the structure's life.

2.6.2 Composite Connections

Demountability can also be achieved in composite slab connections. Demountable and reusable slabs are structurally feasible, even though conventional composite connections typically involve concrete cast on steel with shear studs. Bolted shear connectors, rather than headed studs, can be used to make composite beams demountable (Uy et al., 2017). Flooring systems comprise a significant portion of structures, and their reuse can substantially reduce the total ECI cost. Brambilla et al. (2019) examined demountable shear connection systems for steel-concrete composite floor systems. The research suggests that such connections promote disassembly and reuse, potentially resulting in a circular construction economy. Flooring systems, shown in Figure 15, are compared for environmental effects.

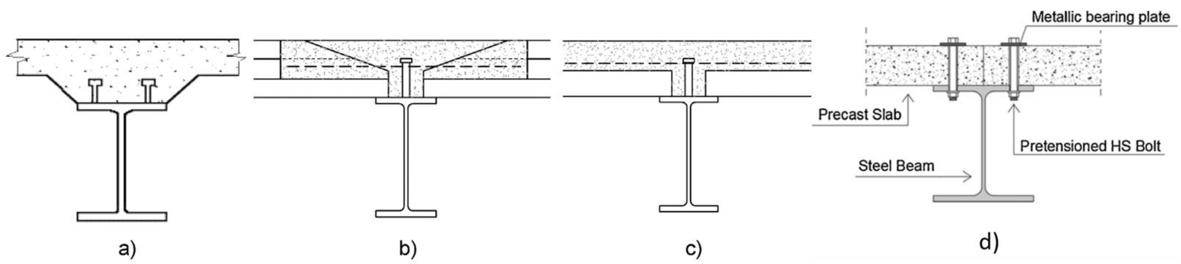

Figure 15: Types of steel-concrete composite flooring systems: A) Composite Slab B) Precast Hollow Core Sections (HCS) C) Precast Solid D) ReuseStru (Brambilla, G. et al., 2019)

The results indicate that demountable flooring systems, such as ReuseStru, provide lower values in almost all impact categories, resulting in a lower ECI cost. Since many impact categories are dominated by the production stage, ReuseStru's benefits are derived from the absence of new structural element production for the relocated building (Brambilla et al., 2019). Conventional systems like composite slabs, precast HCS, and precast solids are fully recycled after demolition. In comparison, ReuseStru is still more sustainable, making it advantageous for circular construction. Another crucial point for slab and beam demountability is the oversizing of bolt holes. Oversizing bolt holes and resin injection into the composite connection are required to meet demountability standards. A 22 mm bolt oversize is needed to achieve 95% demountability (Nijgh & Veljkovic, 2020). These principles are applied to composite slab design.

2.7 Environmental Cost Indicator (ECI) Cost

Life cycle assessment (LCA) is a systematic methodology for evaluating the environmental impacts of a product, process, or activity. It involves quantifying the energy and materials consumed, as well as the waste and emissions generated, to assess their environmental impacts and identify potential improvements (Asif et al., 2007). A critical metric within LCA is the Environmental Cost Indicator (ECI) value, which serves as a key indicator of the overall environmental burden.

The Environmental Cost Indicator (ECI) value quantifies environmental impact in Euros (€). It assesses the environmental impact of a design across all material life cycles and is crucial for Life Cycle Assessment (LCA) of a structure. The calculation principle is straightforward, encompassing 11 impact categories associated with a material:

1. Global Warming Potential (GWP): Global Warming is defined as the effect of human (anthropogenic) emissions of gasses on the heat-absorbing potential of the atmosphere (Ottelé & Jonkers, 2022). Unit of the GWP value is $kgCO_2$ equivalent.
2. Ozone layer Depletion Potential (ODP): Depletion of Ozone in the stratosphere (higher atmospheric layer) occurs because of chemical reaction with specific gasses produced and emitted by human activities (Ottelé & Jonkers, 2022). Unit of ODP is $kgCFC_{11}$ equivalent.
3. Human Toxicity Potential (HTP)
4. Freshwater Aquatic Eco-Toxicity Potential (FAETP)
5. Marine Aquatic Eco-Toxicity Potential (MAETP)
6. Terrestrial Eco-Toxicity Potential (TETP)

3, 4, 5, 6: Emitted harmful substances can end up in atmosphere, soil, or water (fresh, marine). The distribution of specific components to these different environments and its toxicity for biotic elements in these environments is measured/modelled (Ottelé & Jonkers, 2022). Different environments different impact categories hence different monetary value for each category shown at the end of Section 2.7. Unit of all toxicity potentials is kg 1,4-DichloroBenzene equivalents.

7. Photochemical Oxidation Potential (POCP): Photochemical oxidation is the oxidation of compounds driven by UV-light of specific air-pollutants in the troposphere results in formation of ‘smog’ (Ottelé & Jonkers, 2022). Unit of POCP is kgC_2H_4 (ethylene) equivalents.
8. Acidification Potential (AP): Acidic compounds are chemically active and can have both strong (detrimental) effects on 1. Soil- and water chemistry, affecting life in it, and 2. Construction materials (Ottelé & Jonkers, 2022). Unit of AP is $kgSO_2$ equivalent.
9. Eutrophication Potential (EP): Eutrophication is the process of excess deposition of nutrients in the terrestrial and aquatic environment (Ottelé & Jonkers, 2022). Might result oxygen depletion in aquatic environments and water quality. Unit of EP is $kgPO_4$ equivalent.
10. Abiotic Depletion Potential fuel compounds
11. Abiotic Depletion Potential non-fuel compounds

10, 11: Depletion of abiotic resources is defined as the consumption of finite resources and is estimated/quantified by relating yearly consumption/extraction rates to total present reserves (Ottelé & Jonkers, 2022). Unit of both ADP are $kgSb$ equivalent.

Each material and cross-section have associated values for these impact categories, provided by the material producer and available on the EPD International website (EPD library). Once obtained, the weight of each cross-section is multiplied by the manufacturer's coefficients to calculate the associated equivalent values. The final step in calculating ECI cost involves multiplying the kg of impactful materials by the monetary costs in Table 3.

Table 3: Impact Categories and Environmental Costs (Monetary values)

Impact Category	Unit	Cost (€)
GWP total	kg CO2e	0.133
GWP fossil	kg CO2e	0.133
GWP Biogenic	kg CO2e	0.133
GWP LULUC	kg CO2e	0.133
Ozone depletion pot	kg CFC11e	30
Acidification pot	mol H+e	7.65
EP-freshwater	kg Pe	16.46
EP-marine	kg Ne	20
EP-terrestrial	mol Ne	31.0554
POCP ("smog")	kg NMVOCe	1.547
ADP- minerals & metals	kg Sbe	2.132
ADP- fossil resources	MJ	0.0169
Water use	m3e depr.	0.065

Monetary values have been adjusted in the last years due to inflation in 2022 according to Eco-costs emissions 2023 and Bruyn, 2018.

2.8 State of the Current Research

Research and examination of the aforementioned articles reveal several methods to minimize steel usage. However, there is no comprehensive study showing total ECI cost savings by combining these methods or how they can be designed together. Current studies tend to focus on specific types of structures (e.g., skyscrapers) or programs (Amato and Eaton, 1998). Shorter structures, with lower second-order effects and different design scenarios, are affected significantly by occupational loads, raising uncertainty about applying the same principles.

Every solution to an environmental problem in construction comes with added costs. Therefore, industry experimentation and research focus not only on ECI cost but also on total cost and material use minimization. However, material usage does not always correlate with ECI cost. Sometimes, using more material is more sustainable, a concept missing from current literature.

Theory offers examined design choices but lacks guidelines for achieving optimal steel usage based on ECI cost calculations. Distinct benchmarks in Environmental Cost Indicator (ECI) calculations highlight the necessity for a comprehensive assessment tool that thoroughly evaluates building performance across a wide range of environmental criteria (Ding, 2008). While optimization techniques in structural design have advanced, expert knowledge remains crucial to effectively translate these findings into practical methods for engineers (D'Amico & Pomponi, 2018). This thesis aims to fill this gap. The developed framework provides step-by-step design choices and resulting ECI savings, applicable to most structures. It incorporates existing research and the parametric study. Given the extensive research on tall structures, this study focuses on stability systems and comparisons to short structures in the examination of tall structural models. Combining the parametric study with research makes the framework inclusive of most steel structures, avoiding case-specific or building-specific limitations.

The thesis results can be improved or modified in the future to account for composite structures and additional steel structural systems. A major enhancement would be to include occupational costs, the most expensive part of ECI calculations. Previous studies suggest that the ECI costs of building use could be three times higher (Embodied carbon, 2022). Improved construction planning and resource use can further reduce ECI costs. While more possibilities exist, this framework is developed for structural aspects, and other building components may be addressed in future frameworks.

3 Design Concepts

3.1 Analysis of Preliminary Designs and Loading

To develop an environmentally sustainable structure, several methods can reduce energy consumption, such as biowaste systems, solar panels, and wind turbines. However, this thesis focuses on reducing the material weight and total Environmental Cost Indicator (ECI) cost during construction through structural design optimization. A parametric study was conducted to optimize potential designs for steel structures. Composite or concrete structural designs were excluded, except for composite flooring systems, to minimize concrete use and incorporate secondary steel beams to assess their impact on slabs. All developed systems were compared with a conventional column-beam system to determine the optimal material usage.

The parametric study was conducted on a steel 5-storey (22.5 m) 30x30 meter office building designed for the site in Rotterdam, as shown in Figure 16. The site was chosen for its economic significance and proximity to office buildings and open areas. Legal site regulations were not considered to maximize the parametric study's flexibility. Each storey is 4.5 meters high, based on office structural design standards.

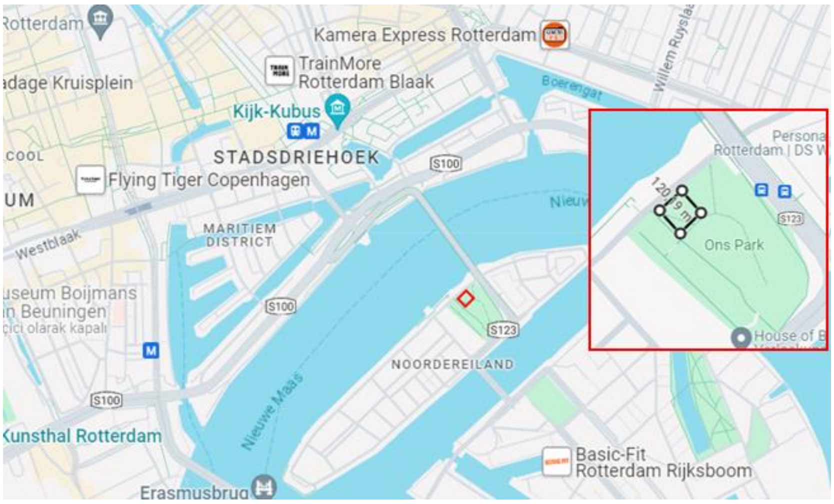

Figure 16: Selected site location for the parametric study office structure

The site is accessible via major roads. The structure was designed according to Eurocode regulations and the respective site-specific loads.

3.2 Preliminary Designs

Based on the literature review and additional research, several structural systems were selected to assess differences in steel usage, as material quantity is a critical contributor to Environmental Costs. The primary considerations for the most sustainable structural design include:

- Demountability: Maximizing demountability, ideally fully, to enable the reuse of structural members, which would significantly reduce the total ECI cost by contributing negative ECI costs. This becomes even more critical for subsequent designs, reducing production ECI Cost to nearly zero.
- Steel Production Method: Favouring steel produced via electric arc furnace (EAF) due to its potential 85% reduction in carbon dioxide emissions compared to the more commonly used, but carbon-intensive, blast furnace method.
- Structural Design: The design critically impacts material usage, encompassing cross-section selection, column and beam spacing, and stability system choice.

The systems selected for comparison include:

- A conservative structural system
- Diagrid systems with angles of 60, 65, 70, and 75 degrees
- Chevron (V)-braced structure
- X-braced structure

These systems were compared with a conventional system featuring similar beam and composite beam spacings for better analysis. Additionally, different column spacings (3, 5, 6, and 10 meters) were examined to determine the optimal spacing for material usage. Table 4 summarizes the tested variables and their effects on the structure, while Figure 17 and Figure 18 illustrate the selected designs for the parametric study and material use assessment. Detailed analysis and additional models with various spacings are presented in Section 4.

Table 4: Tested variables for the optimization of steel weight

Variables	Effect on the structure
Cross-section Selection	Correct cross-section selection significantly reduces total material weight, with larger effects at greater column spacings (Section 4.4).
Column Spacing	Column spacing, a critical initial design step, can increase material usage by ~3% per meter increases due to thickening of the beams. (Section 4.1).
Beam and Composite Beam Spacing	Beam and composite systems are crucial, as most steel weight is in beams. They follow column spacings, and composite spacings are detailed in Section 4.2.
Structural System Selection	Aims to optimize material usage through different stability systems, detailed in Section 4.3.
Connection Selection	Demountable connections facilitate disassembly and reuse, reducing environmental impact and ECI Cost but requiring more material due to elastic design (Sections 4.5 and 4.6).
Slab Type	Slab weight significantly impact self-weight of the structure. Composite spacings are calculated in Section 4.2, the slab thickness is kept thin. Concrete is a non-variable in the thesis, however, demountability of the connection is crucial for ECI Cost. Outlined in Section 4.5.

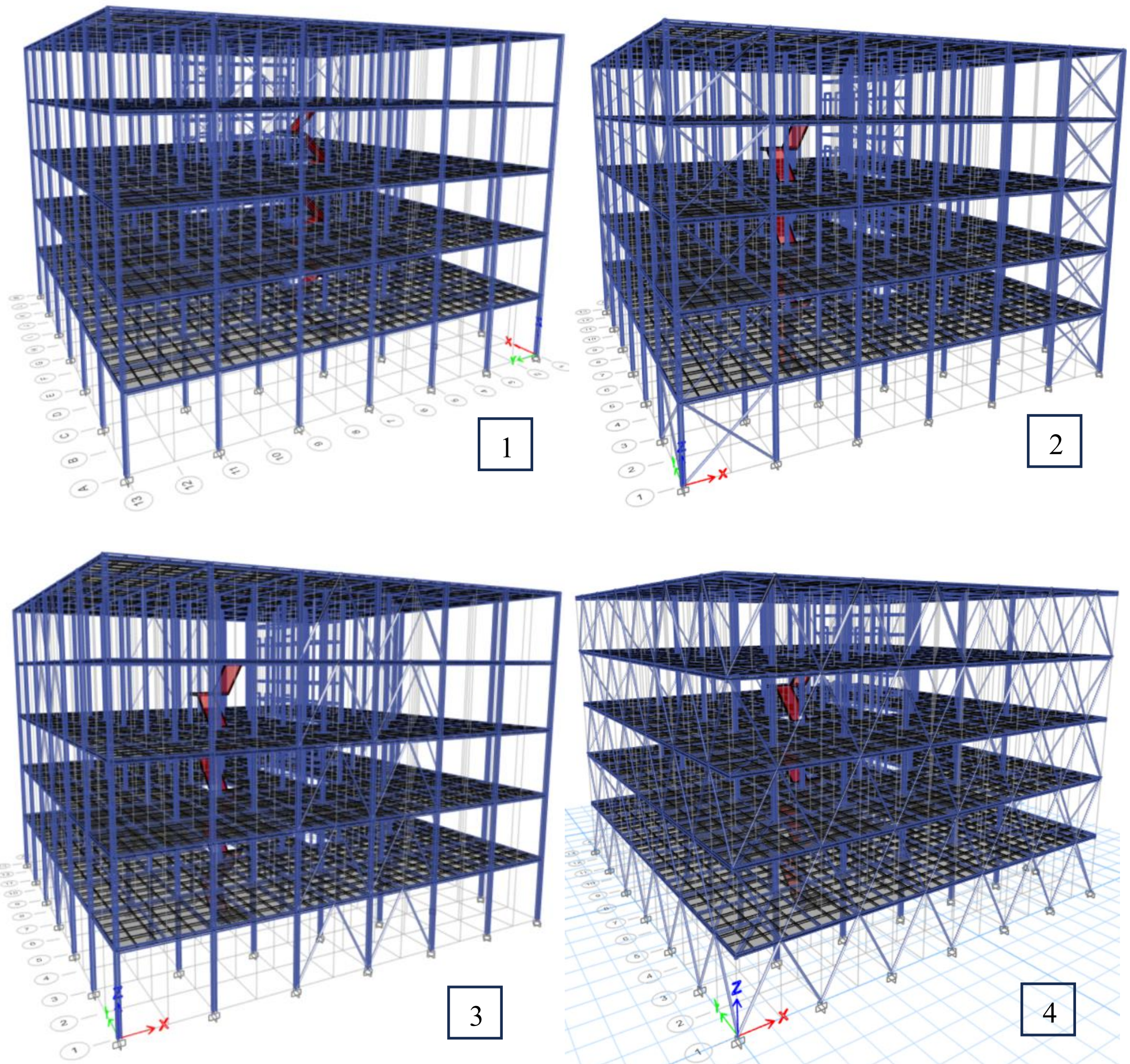

Figure 17: Examples of Types of different structural models examined for the designed structure 3D representation: 1) Conventional system 2) X-braced system 3) Chevron (V)-braced system 4) Diagrid frame system

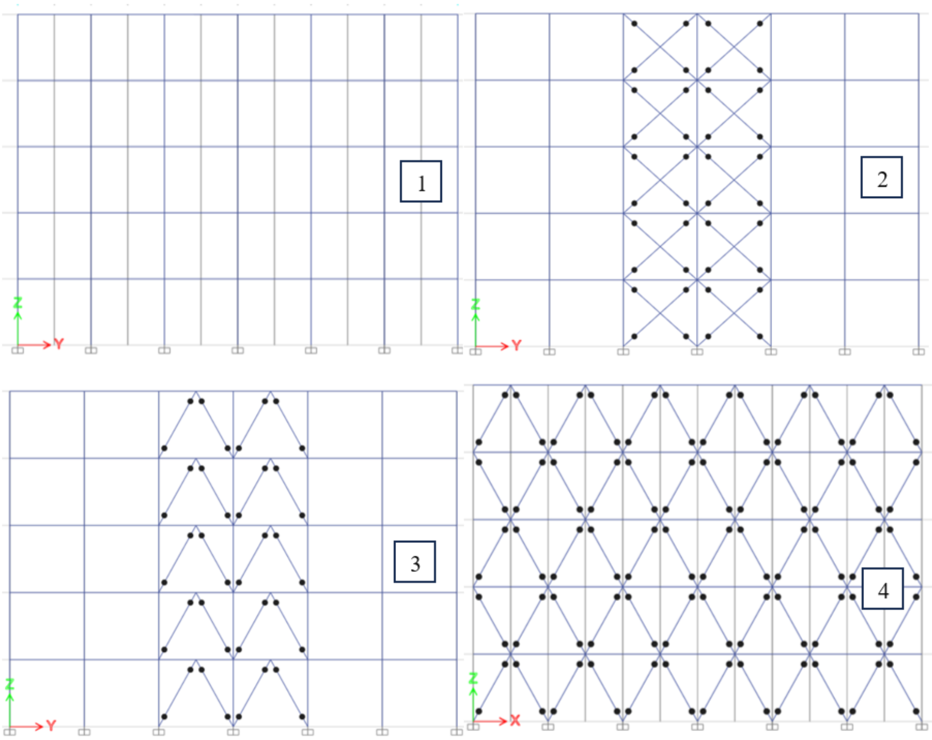

Figure 18: Examples of Types of different structural models examined for the designed structure 2D representation): 1) Conventional system 2) X-braced system 3) Chevron (V)-braced system 4) Diagrid frame system

3.3 Loads on the Structure

3.3.1 Snow Load + add model loads

The characteristic snow load in the selected site location is found to be 0.7 kN/m^2 using the Dlubal Software Eurocode Database. The following equation from NEN-EN1991-1-3 (2003) is used to find the snow load, s:

$$s = \mu_1 C_e C_t s_k \tag{3.1}$$

Where:

μ_1 is the snow load shape coefficient

C_e is the exposure coefficient

C_t is the thermal coefficient

s_k is the characteristic value of snow load on the ground (kN/m^2)

The snow load is calculated to be 0.56 kN/m^2 using a Normal Topography from Table 7.1: (NDP) Values of Ce for different wind exposure conditions from EN1991-1-3 (2023) and thermal coefficient as 1. There is no pitch in the structure hence the snow load shape coefficient μ_1 is found to be 0.8 from equation 3.2.

$$\mu_1 = 0.8\, C_{e,F} \tag{3.2}$$

The exposure coefficient for flat roofs $C_{e,F}$ is given by following formula in equation 3.3:

$$C_{e,F} = \begin{cases} C_e \, for \; L_c \leq 50\,m \\ C_e + (1.25 - C_e)\dfrac{(L_c - 50\,m)}{350\,m} \;\; for\, 50\,m < L_c < 400\,m \\ 1.25 \, for \; L_c \geq 400\,m \end{cases} \tag{3.3}$$

With the Snow load now obtained, there are 3 different wind load scenarios on the roof structure shown in Figure 19.

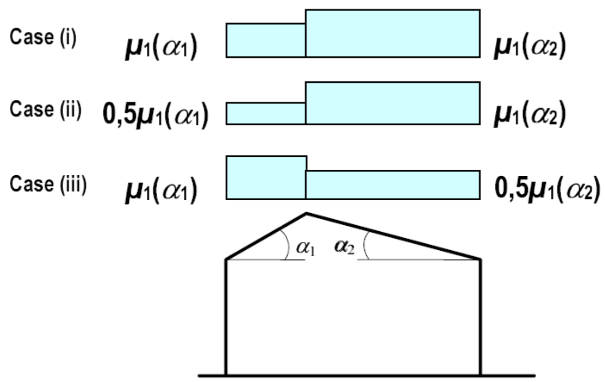

Figure 19: Different snow load cases for roof structures (EN1991-1-3(2003))

The minimum and maximum loads on sides to be $0.5s$ $0.28\ kN/m^2$ $(0.5s)$ and $0.56\ kN/m^2$ (s). All 3 cases are used for analysis and modelling; however, it is known due to the geometrical shape (square) that Case 2 and 3 do not give different results and it is suggested in the codes that only balanced combination can be used, however, both are accounted in the load combinations to fully test the structure, its sway and lateral displacements. Shown in Appendix A: Section 8.1.3 is the snow load present on the roof of the structure. The load present as calculated is $0.28\ kN/m^2$ present along the roof of the structure

3.3.2 Wind Load

The fundamental value of basic wind velocity at the site location in Rotterdam is obtained to be $27\ m/s$ using the Dlubal Software Eurocode Database. Using NEN-EN1991-1-4 (2005), equation 3.4 can be used to determine the basic wind velocity v_b:

$$v_b = c_{dir} \cdot c_{season} \cdot v_{b,0} \tag{3.4}$$

Where:

v_b is the basic wind velocity

$v_{b,0}$ is the fundamental value of basic wind velocity

c_{dir} is the directional factor

c_{season} is the season factor

Values for c_{dir} and c_{season} is recommended to be taken as 1 in NEN-EN1991-1-4 (2005) resulting in $v_b = 27\ m/s$.

Moreover, the mean wind, v_m is calculated using equations 3.5, 3.6, 3.7 and 3.8 from NEN-EN1991-1-4 (2005):

$$v_m(z) = c_r(z)\,.\,c_0(z).\,v_b \tag{3.5}$$

Where:

$c_r(z)$ is the roughness factor, given in 4.3.2 NEN-EN-1191-1-4 (2005)

$c_0(z)$ is the orography factor, taken as 1.0 unless specified otherwise in 4.3.3 NEN-EN-1191-1-4 (2005)

$$c_r(z) = k_r\,.\,ln\left(\frac{z}{z_0}\right) \quad for \quad z_{min} \leq z \leq z_{max} \tag{3.6}$$

$$c_r(z) = c_r\,(z_{min}) \quad for \quad z \leq z_{min} \tag{3.7}$$

Where:

z_0 is the roughness length

k_r terrain factor depending on the roughness length z_0 calculated using:

$$k_r = 0.19\left(\frac{z_0}{z_{0,II}}\right)^{0.07} \tag{3.8}$$

Where:

$z_{0,II} = 0.05$ (terrain category II, Table 4.1 NEN-EN1991-1-4 (2005)

z_{min} is the minimum height defined in Table 4.1 NEN-EN-1191-1-4 (2005)

z_{max} is to be taken as 200 m

Using Table 4.1 NEN-EN1991-1-4 (2005), Terrain Category III is selected and z_0 and z_{min} are obtained. Following the obtained values k_r and c_r is calculated from the equations from NEN-EN1991-1-4 (2005).

The terrain orography cannot be assessed visually in detail as the methodology from NEN-EN-1191-1-4 (2005) suggests, c_o is taken as 1. The wind pressure, q_p is calculated using the equation 3.9:

$$q_p(z) = [1 + 7.\,I_v(z)]\,.\,\frac{1}{2}.\,\rho\,.\,v_m^2(z) = c_e(z)\,.\,q_b \tag{3.9}$$

Where:

ρ is the air density (recommended value is 1.25 kg/m^3)

$c_e(z)$ is the exposure factor given as:

$$c_e(z) = \frac{q_p(z)}{q_b} \tag{3.10}$$

q_b is the basic velocity pressure given as:

$$I_v(z) = \frac{\sigma_v}{v_m(z)} = \frac{k_I}{c_0(z)\ .\ \ln{(z/z_0)}} \quad for \quad z_{min} \leq z \leq z_{max} \tag{3.11}$$

$$I_v(z) = I_v(z_{\min}) \quad for \quad z \leq z_{min} \tag{3.12}$$

Where:

k_I is the turbulence factor (recommended value is 1.0)

c_0 is the orography factor described in 4.3.3 NEN-EN-1191-1-4 (2005)

z_0 is the roughness length, given in Table 4.1 NEN-EN-1191-1-4 (2005)

$$q_b = \frac{1}{2}\ .\ \rho\ .\ v_b^2 \tag{3.13}$$

Using the procedure from equations 3.10 to 3.13, l_v and $q_p(z)$ are calculated. These results are used to obtain the wind pressures acting on the members.

3.3.3 Wind Load on Roof

Wind effects certain areas of the roof differently due to the variance in wind direction, resulting in a nonhomogeneous distribution of pressures applied on the roof. Structural design of the structure influences the areas shown in figures below. Figure 20 shows different effected areas of the roof structure for 0^o and 90^o angles consecutively. For the designed steel multistorey office structure, $h = 22.5\ m, b = 30\ m\ (for\ both\ 0^o\ and\ 90^o\ case),\ d = 30\ m\ (for\ both\ 0^o\ and\ 90^o\ case)$ and more importantly e is calculated as 30 m ($e = \min{(b, 2h)}$).

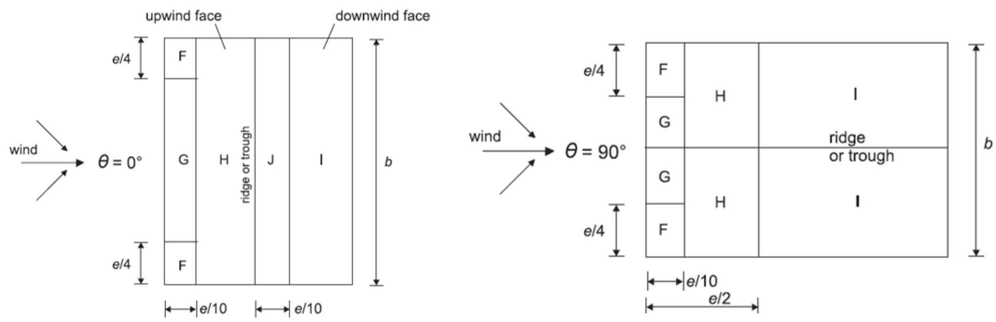

Figure 20: Differently loaded areas due to wind pressures 1) 0/180 degrees 2) 90 degrees (NEN-EN 1991-1-4:2005)

Table 7.2: Recommended values of pressure coefficients for flat roofs (NEN-EN 1991-1-4:2005) shows the external pressure coefficients c_{pe} for flat roof structures. The actual applied pressured are calculated from $c_{pe} = 0.764 * c_{pe}$ [kN/m²] (EN1991-1-4, 5.1) and applied to the structure. Both cases in 0^o wind is added to the model as different cases to be verified. For 90^o wind, even though only one pressure coefficient is given, 2 cases are labelled, also for 270^o wind. This is done due to verify and examine

every effect of the loads. The designed structure is symmetric; however, this parametric study is carried out for scientific reasons, meaning all the effects on the structure are added to the structure. This is also can be used as a guideline on how to derive these loads for similar structures even the structure is non-symmetric. The parametric study is done to be more inclusive rather than specific.

3.3.4 Wind Load on Vertical Walls

Wind also has an influence on the walls and consequently the columns when it is applied from each direction. Figure 21 shows the way vertical walls from the given direction. Table 7.1: Recommended values of external pressure coefficients for vertical walls of rectangular plan buildings (NEN-EN 1991-1-4:2005) shows the values of pressure coefficients on the vertical walls for the specified areas in Figure 21.

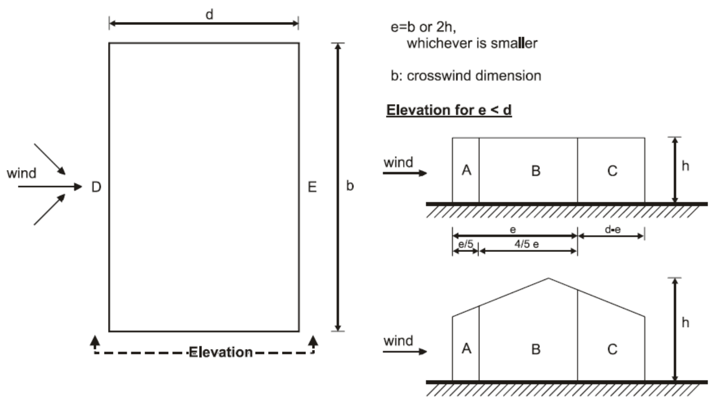

Figure 21: Distribution of wind pressures and effected zones of vertical walls (NEN-EN 1991-1-4:2005)

The zone h/d is 0.75 hence the values are extrapolated from 1 to 0.25 values (close to the zone 1). Wind pressure on the walls is calculated by using the equation $w_e = q(z) * C_{pe}$ [kN/m²] is used from NEN-EN1991-1-4, 5.1. These pressures are combined with the 0^o pressures on the roof when modelling the 0^o cases for the design checks. Same is done for the 90^o case. Resulting wind load on the structure is shown in Appendix A.

3.4 Load Combinations

Table A.1.3 and Table A.1.4 (NEN-EN-1990 (2021)) shows the factors that are used to check the ULS and Table A.1.6 (NEN-EN-1990 (2021)) design coefficients. Consequence Classes are given in Table A.1.1 (NEN-EN-1990 (2021)) and Consequence Class 2 (CC2) is selected since it is an office building. Resulting coefficients are later used in Tables A.1.7 and A.1.8 (NEN-EN-1990 (2021)) to determine the design combinations.

Using the tables above, the load combinations used for modelling are detailed in Appendix B. Initially, loads are applied separately as individual cases. Subsequently, these load cases are combined based on the combinations from the tables to identify the most critical case for each member. Due to the large number of equations, the specific combinations are not listed in this section. Although the critical load combinations could be estimated, all combinations in Appendix B were tested to ensure safety. The governing load combination was found to be $1.35G_k + 1.5Q_k$, representing the most critical dead and live load combination for design.

3.5 Functional Requirements

To design a realistic office structure, functional requirements must be defined and consistently applied across all designs. The final selected design is presented in Section 5.3, including a floor plan that adheres to these requirements.

- **Floor-to-Floor Heights**: Research (Mori Building Co. Ltd., Ceiling Height Office Specifications) indicates that typical office floor-to-floor heights range from 4 to 4.5 meters. For this study, a height of 4.5 meters was selected to provide ample open space.
- **Column Spacing**: Open space is crucial in office designs, making feasible column spacing essential. Section 4.1 discusses column spacings of 3, 4, 5, 6, and 10 meters. While the thesis aims to optimize material use and ECI cost for steel, larger column spacings are preferable if they do not significantly compromise material savings and ECI cost.
- **Natural Lighting**: Natural lighting is important for increasing office worker productivity (Bowen Interiors, 2023). Steel structures are ideal for incorporating glass facades, which enhance natural lighting. Therefore, glass facades were included in all designs.
- **Floor Planning**: Office layouts typically include individual offices along the sides, open desk areas in the centre, and necessary stairs and elevators for vertical access. These elements were designed according to appropriate load conditions and incorporated into the designs. The modelling methodology for stairs and elevator shafts is detailed in Section 3.7.

3.6 Modelling Method

This thesis focuses on investigating stability systems exclusively made of steel, excluding composite systems, except for the composite flooring system. Consequently, concrete cores, shear walls, and rigid frames are not analysed due to the differing environmental impacts and iterative calculation steps for ECI costs.

The design options include braced frames, diagrid structures, and conservative beam-and-column systems, as outlined in Section 2.4. Super frames and space trusses are not considered due to their limited applicability in short structures. Diagrid systems, offering modern approaches to stability and freedom of shape, require consideration of several variables: diagrid angles (55-75 degrees (Payam Ashtari et al., 2021)), optimal module sizes (small, midrange, large, irregular (Boake, 2014)), and secondary beam spacing.

Bracing systems, including X and V configurations, also require design decisions regarding bracing locations. While existing literature primarily addresses tall structures, this thesis focuses on short structures (5 stories), where even a 5% material optimization can result in significant savings.

Key design decisions optimize load distribution among different cross-sections. Moments, axial compression, and shear are strategically assigned to appropriate members. End releases (black dots) are applied in ETABS to ensure accurate moment distribution and load transfer, particularly in composite flooring systems, braces, and diagrids.

Figure 22 illustrates the floor plans for conventional (left) and diagrid (right) structures. Composite beams beneath the concrete slab transfer moments to the main beams, optimizing material use and design. Without end releases, secondary beams would act as primary moment carriers, necessitating larger cross-sections.

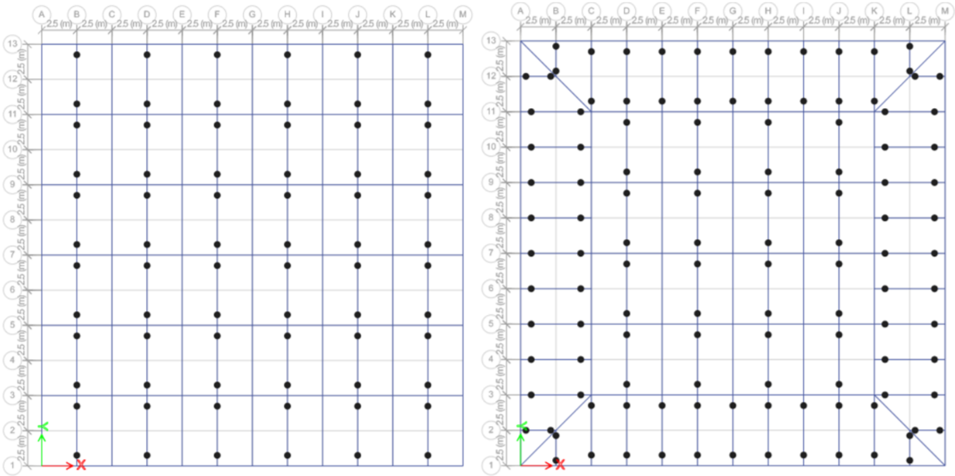

Figure 22: Floor Plan Models of a) Conventional and Braced Design b) Diagrid Design

Figure 23 shows the bracing systems: X-braced (left) and V-braced (right). Bracings provide lateral stability by connecting columns and facilitating load transfer, with end releases assigned to sections. The parametric study tests bracing systems in three locations on the structure for column spacings of 5-6 meters.

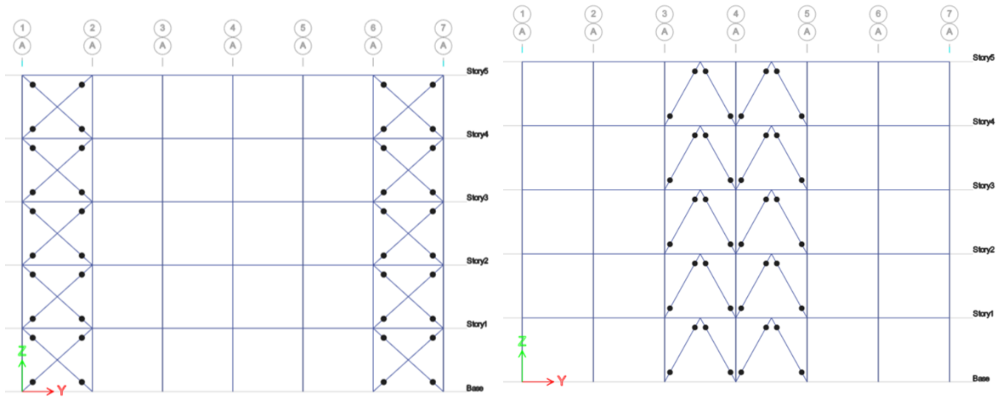

Figure 23: Braced Design Models a) X-Braced b) V-Braced

Bracings are slender stability elements designed to connect columns and provide lateral stability by facilitating load transfer between them. They are not intended to withstand main loads but to transfer them, necessitating end releases in the sections. The design of X-braced frames accounts only for the tension contribution of the braces, assuming that at collapse, compression braces have buckled and offer no load-bearing capacity. Conversely, in V-braced frames, the compression brace contributes to the system's overall stability and must therefore be included in the design model (Faggiano, 2016).

Diagrid structures, known for their structural efficiency and architectural appeal, have been widely adopted in tall buildings globally (Sun Moon, 2011). Diagrids, functioning as stronger braces that carry axial compression and shear, eliminate the need for exterior columns. Figure 24 depicts a modelling of a diagrid structure (Diagrid 60). The diagonal members are assumed to be pin-ended, and therefore resist the transverse shear and moment through axial action only (Moon, 2009). End releases at the diagrid ends ensure moment transfer to foundations, optimizing cross-sections by preventing moment resistance across the entire diagrid member. This optimization is necessitated by the shape of diagrids. The cross-sections of lateral members are optimized by ensuring that moments are transferred rather than resisted by the entire cross-section, enhancing structural efficiency.

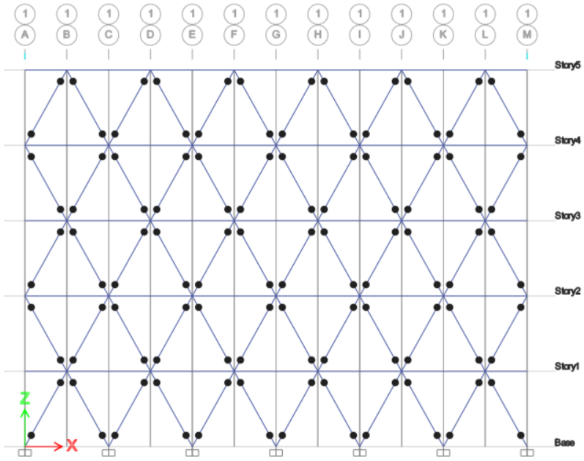

Figure 24: Diagrid Model (Diagrid 60)

Finally, all foundations are designed to resist moments and connect to the main load-bearing systems.

3.7 Modelling of the Core and Stairs

To finalize a realistic model, the stairs and elevator shaft have been designed. For conservative designs without a lateral stability system, a steel core was added at the locations of the stairs and elevator shafts. Figure 25 and Figure 26 show the stair and elevator models, and Figure 27 illustrates the core design for the conservative structures.

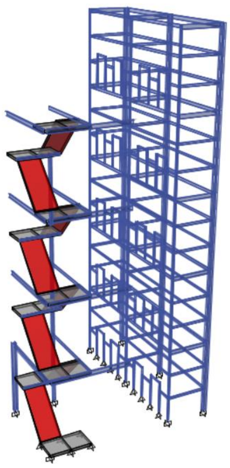

Figure 25: Extruded 3D stairs and elevator shaft model

Stairs are modelled as inclined concrete slabs with a loading of $2-4\ kN/m^2$, using $3\ kN/m^2$ for verification according to NEN-EN-1991-1-1 Table 6.2. Modern stairs can be made from thin steel sheet sections, but concrete stairs were chosen as they do not vary in stability design efficiency. Intermediate slabs ensure appropriate angles between floors. An additional column supports the stairs to prevent overturning, designed with moment releases as it is not part of the main load-carrying system. Supports are fixed on the ground slab, and end releases in the beams are designated for composite beams, not the stair design.

Elevator shaft is a completely distinctive design, no concrete at all. Elevator shafts are usually designed with concrete shear walls completely closed elevator shaft, however, for this structure, a steel cage supporting the elevators have been designed to withstand the elevator loading. Elevator shaft in structures can act as a core, resulting in contribution to structural stability of the design hence they are designed with the material of interest, steel. Additional columns are 1 m from the original location to make the cage. Furthermore, secondary beams are added each 1.5 m height to shorten the buckling length of the columns. Elevators in reality are connected to the beams of the steel cage hence increasing number of beams also contribute to safety. Secondary beams are not designed to be the main load carrying system; hence they are modelled with moment (end) releases.

The elevator shaft is designed as a steel cage, avoiding concrete to align with the steel focus of this thesis. Additional columns spaced 1 meter apart from the original columns, and secondary beams at 1.5-meter intervals are added on columns to reduce buckling length and support the elevator system. Elevators are designed for an imposed load of $10\ kN/m^2$, increased by an impact factor of 1.25 or 1.5. (Subramanian, 2013) to $15\ kN/m^2$. Each cage contains 2 elevators (1.4 x 2.4 m each). Loads are divided among the four supporting columns per cage (six in total), with point loads of 51 kN on middle columns and 25.5 kN on side columns. Only the column supports are fixed to ensure proper load transfer. Figure 26 depicts the design model for stairs (A) and the elevator shaft (B).

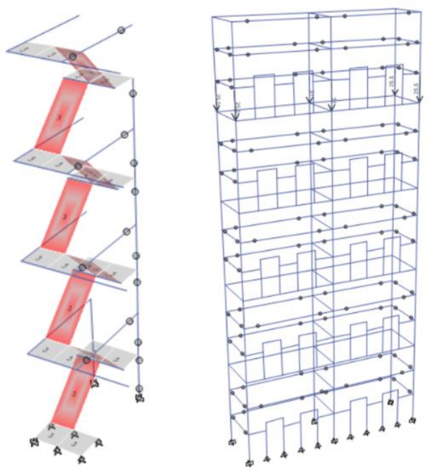

Figure 26: Design Model of the A) Stairs and B) Elevator Shaft

Typically, core design uses composite systems with concrete shear walls for lateral stability. Cores provide a stiffer centre to the structure, increasing overall rigidity and reducing susceptibility to lateral displacements. In this thesis, to avoid composite systems, X bracing is used between interior columns at locations where concrete walls would normally be. This provides similar structural properties. Figure 27 shows the core structural model for a conventional structure.

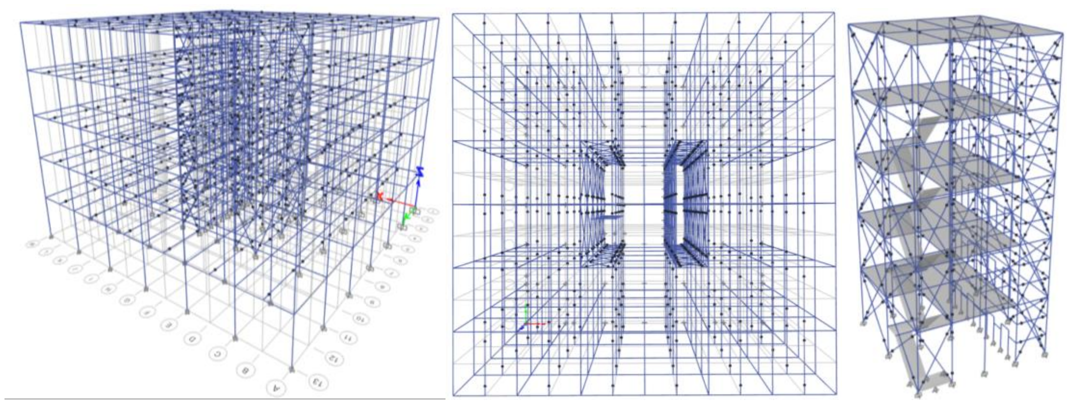

Figure 27: Core Design for 5 m spacing Conventional Design

3.8 Stability of the Frames

Frame assessment is carried out to see if the members sway hence if the second order analysis is needed. The frame structure used for this calculation is 5-meter regular frame structure. Selection of this structure are explained in Section 4.1.

To decide if a first order, sway or non-way approach is used, calculation of α_{cr} is done using equation 3.14:

$$\alpha_{cr} = \left(\frac{H_{Ed}}{V_{Ed}}\right)\left(\frac{h}{\delta_{H,Ed}}\right) \tag{3.14}$$

Where H_{Ed} is the design value of the horizontal reaction at the bottom of the storey to the horizontal loads and fictitious horizontal loads, $V_{Ed}$is the total design vertical load on the structure on the bottom of the storey, h is storey height and $\delta_{H,Ed}$ is horizontal displacement at the top of the storey, compared to the bottom of the storey. Figure 28 outlines the methodology for determining whether first-order, non-sway, or sway analysis should be applied:

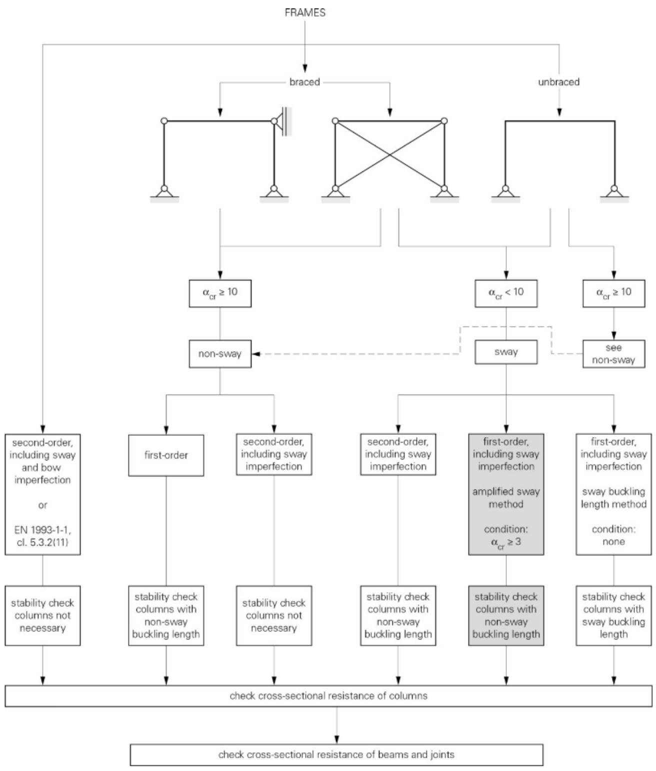

Figure 28: Methodology for stability checks of frames

Displacements in x and y direction, horizontal and vertical design forces of frames are obtained using ETABS software in order to calculated the α_{cr}. This calculation is done for each storey of the structure. Results of these analysis are shown in Table 5. Effects of displacement on the structure is found to be minimal since the lowest value of $\alpha_{cr} = 11$ which is greater than the limit of 10. This shows that a first order non-sway approach can be used for the structure. It is also observed that all of the design loads for the structural members are calculated from the software using the combination $1.35G_k + 1.5Q_k$. This means that the lateral loads are not critical for this given structure to have an affect on the design. However, if a taller, or an earthquake resistant structure is designed, second order effects will be critical and strcuture cannot be designed by the first order approach. That is the distinction between tall and short structures in the structural design framework. If the structure is susceptible to the second order effects, the structure is classified as a ‘tall structure’.

Table 5: Calculation of stability of frames of the structure for sway analysis and second order effects

Frame Stability Check								
Stories	Height (m	δx (mm)	δy (mm)	Ved (kN)	Hed (kN)	α_{cr} (x)	α_{cr} (y)	
Story5	4.50E+03	5.31E+00	4.81E+00	5.90E+03	-8.88E+01	1.28E+01	1.41E+01	αcr>10, Not required
Story4	4.50E+03	7.39E+00	8.70E+00	1.16E+04	-2.54E+02	1.33E+01	1.13E+01	αcr>10, Not required
Story3	4.50E+03	7.86E+00	7.91E+00	1.75E+04	-3.99E+02	1.31E+01	1.30E+01	αcr>10, Not required
Story2	4.50E+03	9.03E+00	9.05E+00	2.33E+04	-5.32E+02	1.14E+01	1.14E+01	αcr>10, Not required
Story1	4.50E+03	8.23E+00	7.81E+00	2.90E+04	-6.32E+02	1.19E+01	1.25E+01	αcr>10, Not required

3.9 Design and Verification Methodology

Resulting models and cross-sections are verified by using methodology and formulas following NEN-EN1993: Eurocode 3. Following methodology is not done by hand calculations, verifications are done using ETABS software and cross-sections are selected accordingly.

Verification of the elements are done using axial compression, shear, lateral torsional buckling, and combinations given in Eurocode 3 guidelines. All critical cases are checked and verified to select the most proper cross-section by ensuring that the Unity Checks (U.C.) are kept between 0.8 and 0.99999. However, these checks are done just like in the industry, designing for the most critical cross-section for each type of member. This is done to ensure the structure can be built with ease and without confusion for those constructing.

When there is lateral torsional buckling present on the structure, combination including lateral torsional buckling will be the most critical. First, axial compression and shear resistance are checked, and later flexural buckling and lateral torsional buckling combinations are checked to ensure safety of a member.

First, the cross-section is classified to start the calculations. The yield strength (f_y) EN 10219-1 S355 is selected by using Table 3.1: Nominal values of yield strength and ultimate strength for cross-sections (NEN-EN 1993-1-1).

Following calculations are an iterative process when done by hand. For the calculations, it is crucial to first start with a first cross-section, software calculations also work the same. Resulting calculations are the final iteration stage and cross-sections are withing the range for the Unity Checks. This is why the calculations start with a cross-section. The selected cross-sections are classified using the $\frac{c}{t}$ and $\frac{c_f}{t_f}$ ratios in Table 5.2: Largest width-to-thickness ratios for compression parts. Wherever the ratio falls, the cross-sections are classified appropriately.

For the flexural buckling verification, the design normal force N_{Ed} needs to be checked with the design resistance of normal force, $N_{b,Rd}$ using equations 3.14 and 3.15.

$$\frac{N_{Ed}}{N_{b,Rd}} \leq 1.0 \quad (U.C.) \tag{3.15}$$

$$N_{b,Rd} = \frac{\chi\, A\, f_y}{\Upsilon_{M1}} \tag{3.16}$$

$N_{Pl,Rd}$ is the design plastic resistance to normal forces of the gross cross-section, A is the cross-sectional area of the section; $\gamma_{M,1}$ is partial factor for resistance of members to instability assessed by member checks. Since for the flexural buckling calculations, a reduction factor is added to the compression resistance of the cross-section, no other compression checks are required.

In order to obtain the flexural buckling reduction factor, χ, Using Table 6.2: Selection of buckling curve for a cross-section (NEN-EN 1993-1-1), first the right buckling curve for the cross-section is selected from Figure 6.4: Buckling Curves (NEN-EN 1993-1-1). Following the buckling curve an imperfection factor, α, from the selected cross-section is obtained, and used to calculate the buckling factor Buckling length. Following sets of equations (3.17 to 3.22) from NEN-EN 1993-1-1 are used to obtain the reduction factor for buckling of the cross-section, none of the cross-sections are of the classified as Class 4:

$$\chi = \frac{1}{\phi + \sqrt{\phi^2 - \bar{\lambda}^2}} \quad but \quad \chi \leq 1.0 \tag{3.17}$$

Where:

$$\chi = \frac{1}{\phi + \sqrt{\phi^2 - \bar{\lambda}^2}} \quad but \quad \chi \leq 1.0 \tag{3.18}$$

$$\phi = 0.5\left[1 + \alpha\left(\bar{\lambda} - 0.2\right) + \bar{\lambda}^2\right] \tag{3.19}$$

$$\bar{\lambda} = \sqrt{\frac{A\, f_y}{N_{cr}}} \quad for\ Class\ 1, 2\ and\ 3\ cross\ sections \tag{3.20}$$

$$\bar{\lambda} = \sqrt{\frac{A\, f_y}{N_{cr}}} = \frac{N_{cr}}{i}\frac{1}{\lambda_1} \quad for\ Class\ 1, 2\ and\ 3\ cross\ sections \tag{3.21}$$

$$\lambda_1 = \pi\sqrt{\frac{E}{f_y}} = 93.9\varepsilon \tag{3.22}$$

$$\varepsilon = \sqrt{\frac{235}{f_y}} \quad (fy\ in\ N/mm^2) \tag{3.23}$$

Where $\bar{\lambda}$ is the non-dimensional slenderness, λ_1 is the slenderness value to figure out the relative slenderness be, E is the Elastic Modulus, N_{Cr} is the elastic critical force for the relevant buckling mode based on the gross cross-sectional properties, L_{Cr} is buckling length, i is the radius of gyration about the relevant axis and ϕ is the global initial sway imperfection.

Using the equations above the reduction factor χ is calculate. Which is then applied to the resistance of the cross-section, to then calculate the Unity check for flexural buckling. Design shear resistance $V_{c,Rd}$ is be taken as design plastic or elastic shear resistance depending on the cross-section, $V_{Pl(El),Rd}$ where A_v is shear area. Using equations 3.24 and 3.25 from NEN-EN 1993-1-1, shear is verified. If the equation $0.5 * V_{b,Rd} < V_{Ed}$ is satisfied, no shear check is needed. This is the case for most of the cross-sections of the structure since shear is usually not the critical design load.

$$\frac{V_{Ed}}{V_{c,Rd}} \leq 1.0\ (U.C.) \tag{3.24}$$

$$V_{c,Rd} = V_{Pl,Rd} = \frac{A_v\ (f_y/\sqrt{3})}{\Upsilon_{M0}} \tag{3.25}$$

There are several design combinations such as bending and shear, bending and axial force etc. However, it is obtained from the software (ETABS) lateral torsional buckling combination is always the most critical, which makes sense in theory as well. Shear is usually not the critical design force and combination with reduction coefficients and interaction factors usually give the highest unity check. For the lateral torsional buckling verification following equations 3.26 and 3.27 from NEN-EN 1993-1-1 needs to be used:

$$\frac{N_{Ed}}{\frac{\chi_y\ N_{Rk}}{\Upsilon_{M1}}} + \mathrm{k}_{yy}\frac{M_{y,Ed} + \Delta M_{y,Ed}}{\chi_{LT}\ \frac{M_{y,Rk}}{\Upsilon_{M1}}} + \mathrm{k}_{yz}\frac{M_{z,Ed} + \Delta M_{z,Ed}}{\frac{M_{z,Rk}}{\Upsilon_{M1}}} \leq 1 \tag{3.26}$$

$$\frac{N_{Ed}}{\frac{\chi_z\ N_{Rk}}{\Upsilon_{M1}}} + \mathrm{k}_{zy}\frac{M_{y,Ed} + \Delta M_{y,Ed}}{\chi_{LT}\ \frac{M_{y,Rk}}{\Upsilon_{M1}}} + \mathrm{k}_{zz}\frac{M_{z,Ed} + \Delta M_{z,Ed}}{\frac{M_{z,Rk}}{\Upsilon_{M1}}} \leq 1 \tag{3.27}$$

Where:

N_{Ed}, $M_{y,Ed}$ and $M_{z,Ed}$ are the design values of compression force and the maximum moments about the y-y and z-z axis along the member, respectively

$\Delta M_{y,Ed}$, $\Delta M_{z,Ed}$ are the moments due to shift of the centroidal axis

χ_y and χ_z are the reduction factors due to flexural buckling, explained previously

χ_{LT} is the reduction factor due to lateral torsional buckling

k_{yy}, k_{yz}, k_{zy}, k_{zz} are the interaction factors

Following methodology explains how to obtain the lateral torsional buckling reduction factors, and more importantly, the interaction factors. Formulas are in order.

Firstly, buckling curve is selected for y-y and z-z axis of the cross-sections to obtain α_{LT}. Where the appropriate section modulus, $W_y = W_{Pl(El),y}$ depending on the cross-section classification. For lateral torsional buckling resistance, a new design resisting moment is introduced, $M_{b,Rd} = \chi_{LT} M_{Pl(El),Rd}$ where χ_{LT} is reduction factor for lateral-torsional buckling.

Similar to flexural buckling calculations, buckling curves are selected for the cross-section using Table 6.4: Recommended values for lateral torsional buckling curves for cross-sections (NEN-EN 1993-1-1), and imperfection factor, α_{LT}, is later gathered using Table 6.3: Recommended values for imperfection factors for lateral torsional buckling curves (NEN-EN 1993-1-1).

$$\chi_{LT} = \frac{1}{\phi_{LT} + \sqrt{\phi_{LT}^2 - \beta\overline{\lambda_{LT}}^2}} \quad but \quad \begin{cases} \chi \leq 1.0 \\ \chi \leq \frac{1}{\overline{\lambda_{LT}}^2} \end{cases} \tag{3.28}$$

Where:

$$\phi_{LT} = 0.5\left[1 + \alpha_{LT}\left(\overline{\lambda_{LT}} - \overline{\lambda_{LT,0}}\right) + \beta\overline{\lambda_{LT}}^2\right] \tag{3.29}$$

$$\overline{\lambda_{LT}} = \sqrt{\frac{W_y\, f_y}{M_{cr}}} \tag{3.30}$$

Where factors $\overline{\lambda}_{LT,0} = 0.4\ (maximum\ value)\ and\ \beta = 0.75\ (minimum\ value)$ for rolled I and H Sections. Depending on the cross-section class and selected section W_y can be obtained from Eurocode as $W_{pl,y}$ or $W_{el,y}$. To calculate non-dimensional slenderness for LTB, $\overline{\lambda}_{LT}$, critical elastic moment, M_{cr} is calculated.

$$M_{cr} = k_{red} \cdot \frac{C}{L_g} \cdot \sqrt{E\ .\ I_z\ .\ G\ .\ I_t} \tag{3.31}$$

$$C = \frac{\pi\ .\ C_1\ .\ L_g}{L_{kip}} \cdot \left(\sqrt{1 + \left(\frac{\pi^2\ .\ S^2}{L_{kip}^2}\ .\ (C_2^2 + 1)\right)} + \frac{\pi\ .\ C_2\ .\ S}{L_{kip}}\right) \tag{3.32}$$

$$S = \sqrt{\frac{E\ .\ I_w}{G\ .\ I_t}} \tag{3.33}$$

Where k_{red} is the coefficient taking into account deformability of the cross-section, C is the coefficient taking into account lateral restraints, support and boundary conditions, and type of loading, C_1 is the coefficient taking into account the loading and boundary conditions, C_2 is the coefficient taking into account position of the load with respect to the shear centr, L_g is the length of the beam between the points with torsional restraints, L_{kip} s the length of an equivalent laterally unrestrained beam, S is the first moment of area, I_t is the torsion constant, I_w is the warping constant and G is the shear modulus.

C_1 and C_2 values are determined determined from the internal loads present on the structure. L_g and L_{kip} are calculated using the buckling shape of the cross-section. Using these coefficients, C is calculated, k_{red} is obtained for the selected cross-section and later, M_{cr} is calculated. χ_{LT} is then calculated following the equations. For the interaction factors there are 2 methods presented in Eurocode 3-1-1. Following Methodologies can be used to obtain the interaction factors. Annex A: Method 1: Interaction factors kij for interaction formula (NEN-EN 1993-1-1) and Annex B: Method 2: Interaction factors kij for interaction (NEN-EN 1993-1-1). These Section in Eurocode have step by step guide to calculate the interaction factors with Tables. Calculation also requires knowledge of the moment graph on the member, which are all obtained from the software. The highest values of interaction factors are combined and used in the verification to ensure sections fit the criteria.

Following combination of both methods, factors k_{yy}, k_{yz}, k_{zy} and k_{zz} are calculated. Using both interaction formulas Unity Check (U.C.) is done by the most critical method and cross-section is verified. These verifications are time consuming to be done by hand, especially for each member and for every design. ETABS software uses this methodology to verify the members and all the verifications are checked by the writer. Shown in Appendix C are the design specifications and Appendix D are the verification done for critical sections for each type of member. It can be seen from the ETABS report that same methodology is used to verify the cross-sections. These reports show that the software calculations and verifications follow Eurocode standards.

4 Structural Design and Analysis

The aim of this thesis is to minimize steel usage in structures through structural engineering, thereby achieving the lowest possible Environmental Cost Indicator (ECI) cost. The key strategies include:

- Identifying the most efficient structural system: Diagrid, X-braced, V-braced, and conservative systems.
- Determining the optimal column and beam spacing.
- Selecting the best cross-sections for beams (including composite beams), columns, and braces.
- Designing connections (bolted, welded, or demountable).

Previous research on tall buildings indicates that the best diagrid system is 33% more efficient than an outrigger system. Bracing systems significantly reduce horizontal displacement and second-order effects, resulting in material savings. For tall structures, Cho et al. (2012) reported a 24% material reduction for X-braced systems and 28% for V-braced systems. These percentages vary with the number of stories and floor area.

For this study, a 5-storey, 22.5-meter-tall office building was chosen, reflecting the average building height in the Netherlands (12-20 meters) and Rotterdam (25-30 meters) (Webmapper, Hoogste Gebouwen van Nederland). The focus on shorter structures addresses the fact that dynamic and lateral loads are less impactful, making some systems less effective than conventional designs. The selected structural systems were examined for their material efficiency in this context.

4.1 Optimal Column Spacing

Column spacing is a critical factor in structural design. For this 30x30 meter structure, symmetrical load cases allow for consistent column spacing. The studied spacings are 3, 5, 6, and 10 meters. Figure 33 illustrates these variations. Column spacings were examined in the regular structure, as diagrid systems are mainly influenced by angles, and braces, as well as the interior systems of diagrids, depend on the regular system. Figure 29-Figure 32 detail the tested systems. Floor systems for conventional, braced, and diagrid structures are detailed in Section 3.6. Specific floor systems for Diagrid Designs are elaborated in Section 4.3.2. Cross-sections (HEA for columns and IPE for beams) were kept constant to isolate the variable of column spacing. The loading cases and combinations were also consistent, as the loading area remains unchanged.

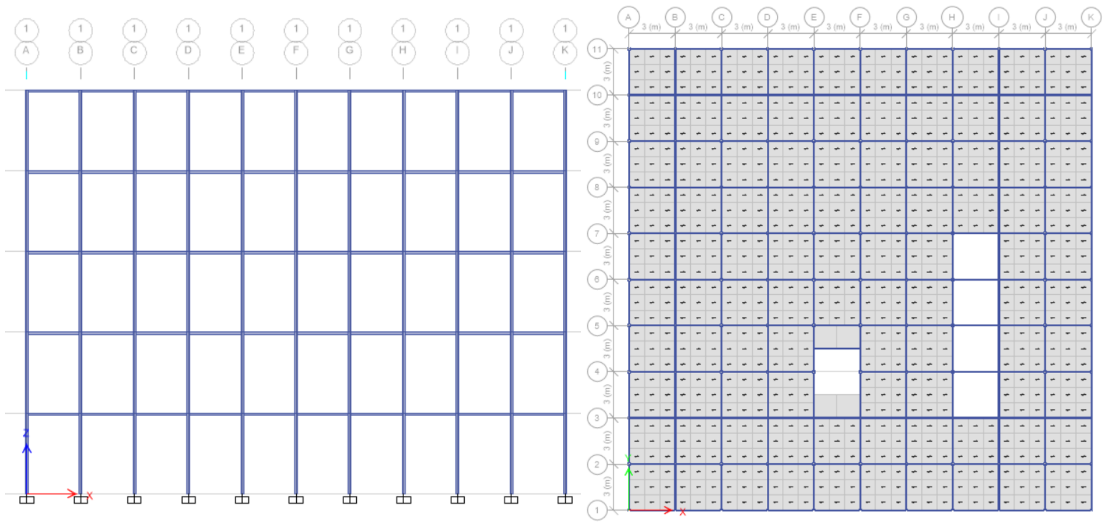

Figure 29: Floor plan and elevation of 3m column conservative design

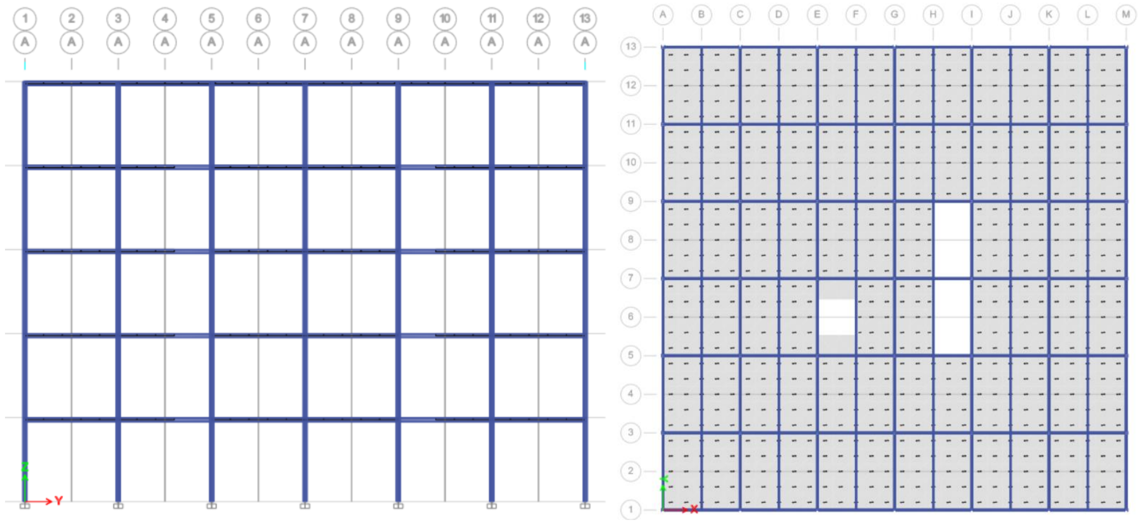

Figure 30: Floor plan and elevation of 5m column conservative design

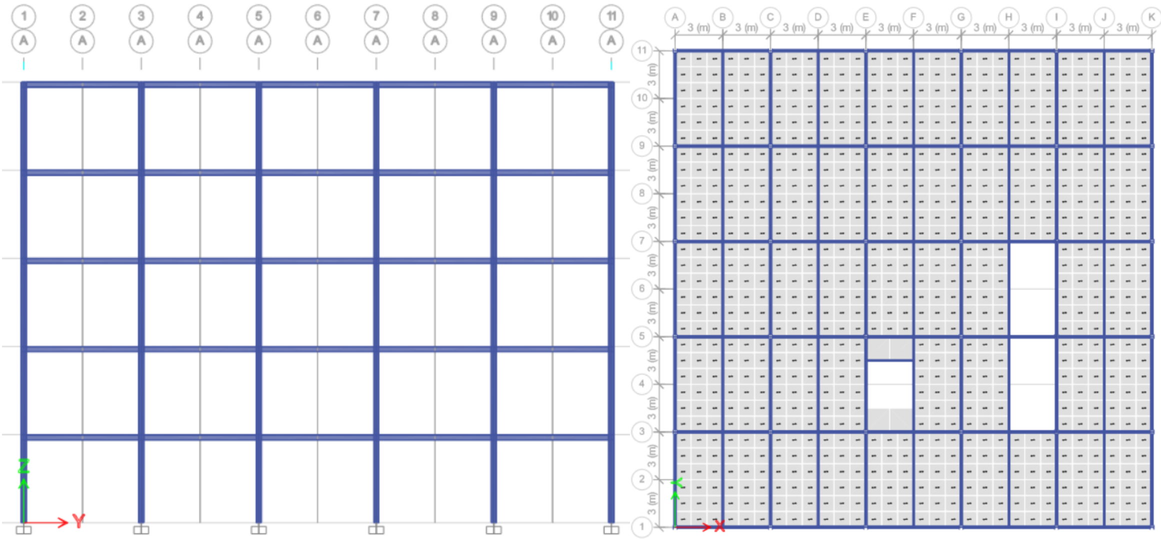

Figure 31: Floor plan and elevation of 6m column conservative design

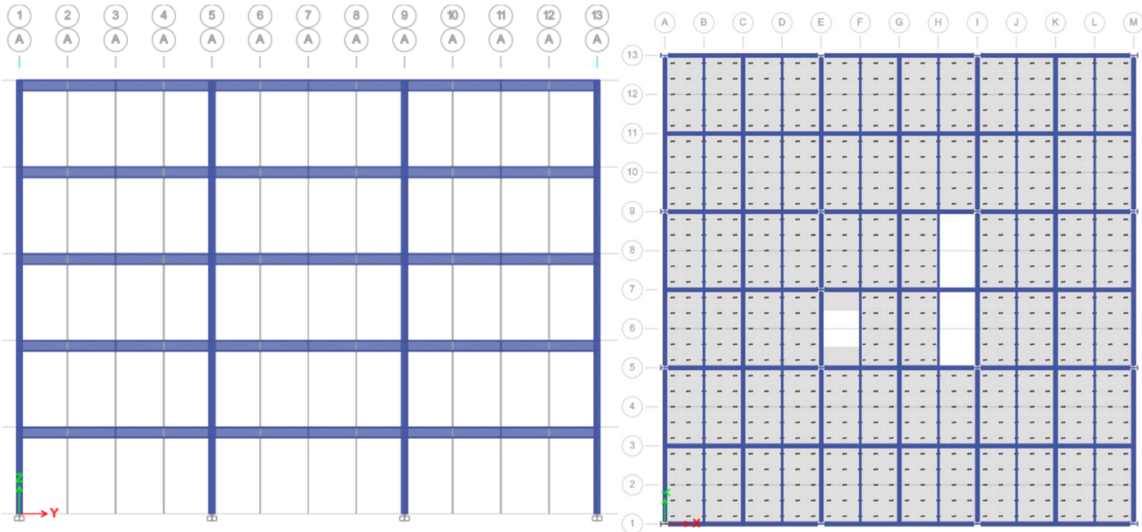

Figure 32: Floor plan and elevation of 10m column conservative design

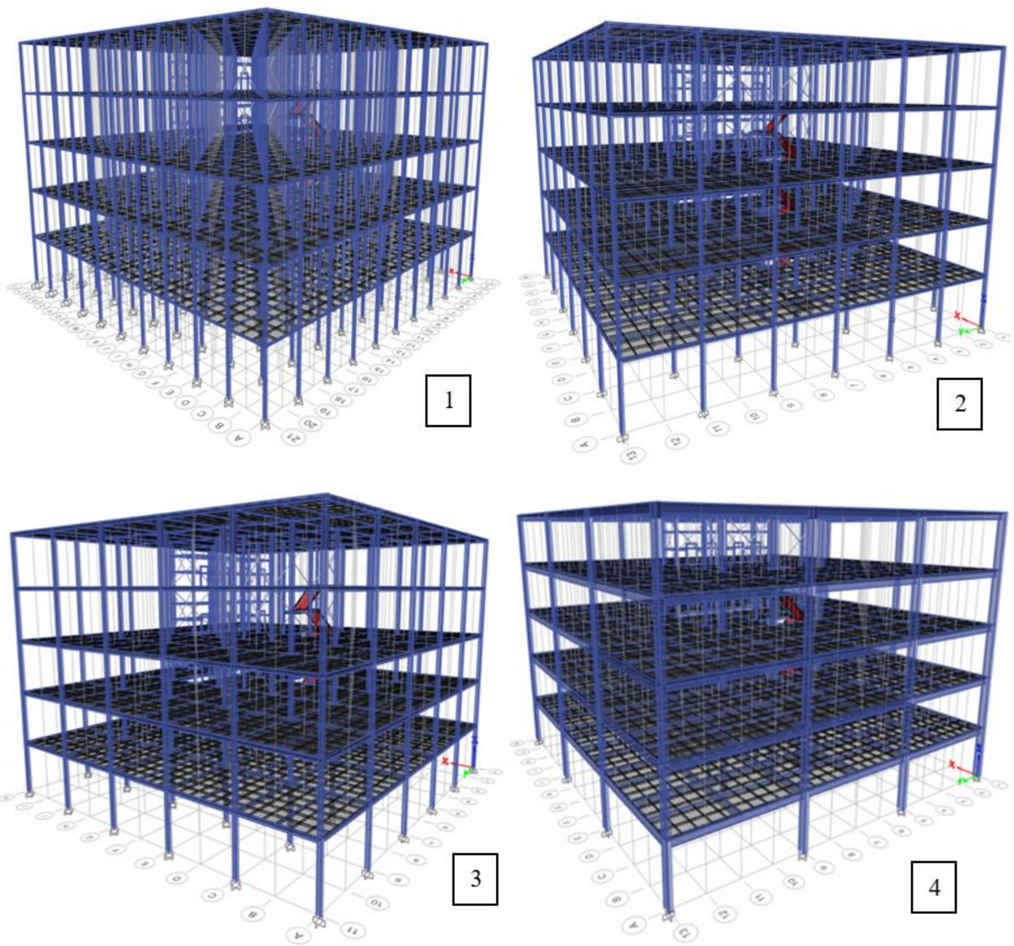

Figure 33: Modelled 3D and examined column spacings for regular system: 1) 3m column spacing 2) 5m column spacing 3) 6m column spacing 4) 10m column spacing

The analysis results, shown in Table 6, indicate that a 6-meter column spacing performs best for column performance but not for beam performance. The 3-meter spacing system, despite being the least efficient for columns, performed best overall due to beam optimization. However, practical design considerations make a 3-meter spacing impractical for most structures.

Table 6: Resulting weight of steel for different column spacings

	Model	Column (kN)	Beam (kN)	Braces (kN)	Total Steel (kN)
Column Spacing 3m	Regular System	8.32E+02	3.50E+02	3.92E+00	1.19E+03
Column Spacing 5m	Regular System (2.5m)	5.81E+02	6.69E+02	2.87E+00	1.25E+03
Column Spacing 6m	Regular System (2m)	5.79E+02	8.11E+02	2.41E+00	1.39E+03
	Regular System (3m)	5.84E+02	7.79E+02	4.49E+00	1.37E+03
Column Spacing 10m	Regular System (2.5m)	6.86E+02	2.29E+03	2.87E+00	2.98E+03

In this section, the column weight is analysed. Models show that a 6-meter column spacing performs best for column efficiency but not for beam performance. The 3-meter spacing system, although least efficient for columns, performs best overall due to beam optimization. However, a 3-meter spacing is impractical for most structures due to design requirements for room layouts and open spaces.

A 40% increase in column spacing results in a 5.66% material loss, while a 16.67% decrease yields an 9.2% material gain when switching from 6 to 5 meters. Therefore, a minimum column spacing of 5 meters is recommended. With composite slabs, beam length significantly influences material use, making lower column spacing more effective for reducing material consumption. Considering all findings and requirements, a 5-meter column spacing is identified as the most optimal for the designs. However, due to the critical influence of geometry in some systems, a 6-meter column spacing is also tested for stability systems.

4.2 Design of Beam and Composite Beam Spacings

As discussed in Section 4.1, beams contribute the most steel weight in structures. Ideally, the length of a regular beam should not exceed 6 meters. Beam spacing corresponds to column spacing, making a 5-meter column spacing also a 5-meter beam spacing.

For all floor systems, except for the conventional structure with 3-meter column spacing, intermediate beams are used. This approach keeps concrete as a near-constant variable. Steel-concrete composite floor systems offer several advantages over conventional concrete slabs, including a higher strength-to-weight ratio, flexibility, reduced labour and time due to prefabrication, and better performance under dynamic or cyclic loads. However, composite slabs are more complex and costly to construct and maintain, requiring skilled labour.

The optimal composite beam spacing maximizes spacing while minimizing steel use. Structural models indicate that reducing composite beam spacing does not significantly decrease cross-section sizes. Thus, higher spacings improve steel efficiency. Composite beam spacings typically range from 1.5 to 3.5 meters. The column spacing influences composite beam spacing, as a 5x5 meter slab cannot be divided into 3-meter segments. In all systems, maintaining the highest possible spacing within the range (e.g., 2.5 meters for a 5x5 slab) results in the lowest steel use. The 3-meter design lacks intermediate beams but is included for functional requirements and material use comparisons due to column spacing.

4.3 Stability Systems

Given that a 3-meter column spacing is impractical and a 10-meter spacing is not environmentally beneficial, the selected designs were applied to 5- and 6-meter column spacings to evaluate the total steel weight used for each design. Preliminary designs from Section 3.1 were used. The following sections outline the design of each structure type and present the resulting steel weights. These options are then compared to determine the optimal scenario for the parametric study.

The goal of this study is to understand the impact of each system and decision on the structure and steel use, rather than to design the perfect structure for the selected parameters. Therefore, all results are thoroughly examined, and their effects are investigated.

Comparisons are made using conventional structural systems with the most similar cases, as shown in Table 6 in Section 4.1. The 5-meter column spacing system was found to be the most effective, so most structural designs were tested against this baseline. Successful designs were then applied to a 6-meter spaced structure to evaluate potential improvements in material usage. Figure 34 illustrates the load-bearing systems examined, while Figure 18 in Section 3.2 provides 2D versions of the designs.

For consistency, cross-section types for each member and column spacings for stability system comparisons were kept similar. It should be noted that over 20 models were tested, varying in locations, angles (for diagrids), and spacings. The main types of load-bearing systems used are shown below.

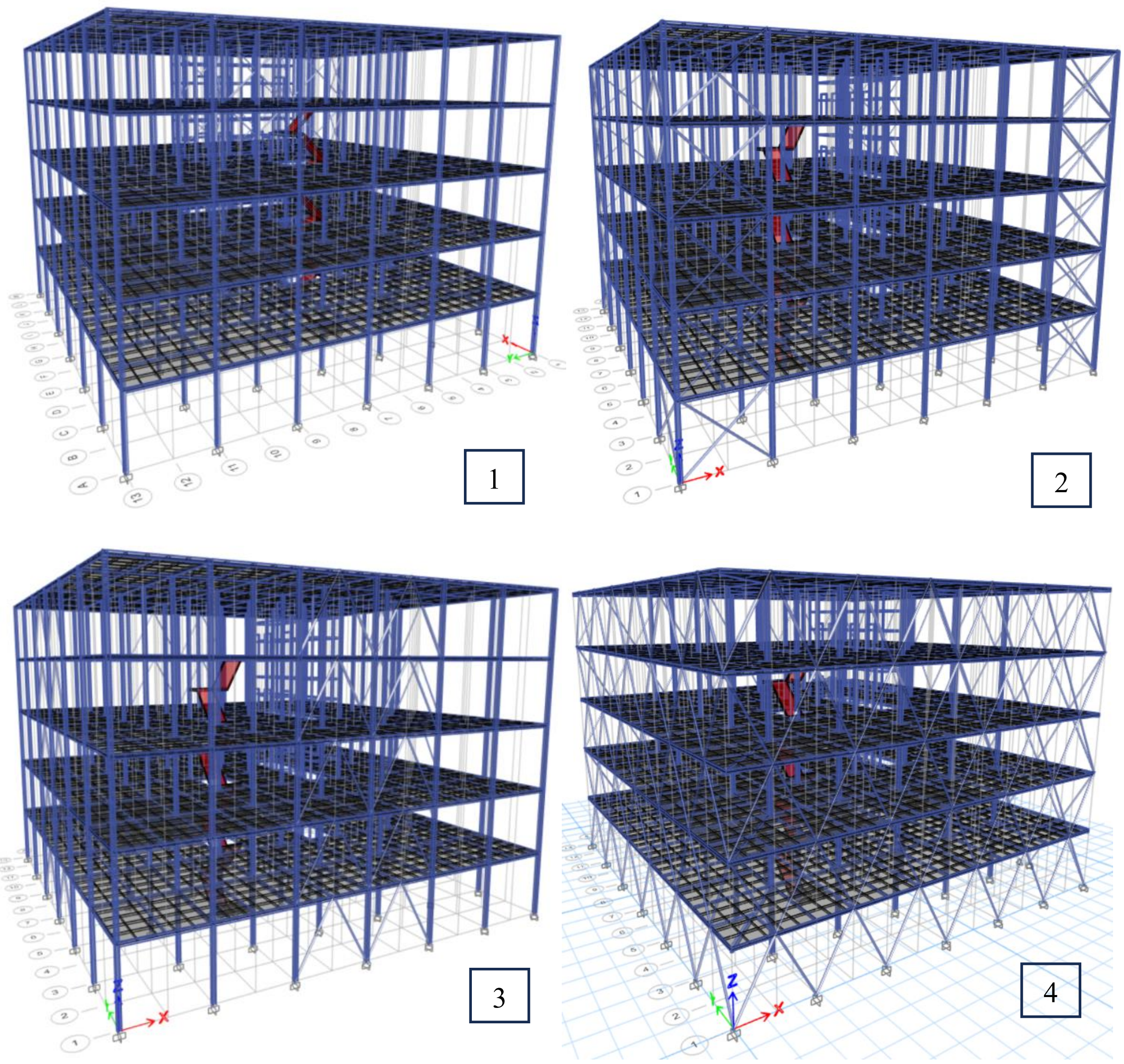

Figure 34: Types of load bearing systems used to obtain the optimal design 1) Conventional (Conservative) Design 2) X Braced Design 3) V (Chevron) Braced Design 4) Diagrid Design

4.3.1 X- and V- Braced Structure

This section outlines the tests and analysis results for both X and Chevron braced structural designs. Bracings mitigate lateral loads and second-order effects, as discussed in the literature review. Their effectiveness in structures primarily loaded with occupational loads is tested to determine whether bracing improves the design.

4.3.1.1 X-Braced Structure Tests

X-Bracing was applied using the '1 on 2 off' rule, but the structures with 5-meter column spacing are unsuitable for this configuration. This structure required testing both locations of this method (Figure 35). Analysis results are shown in Figure 36.

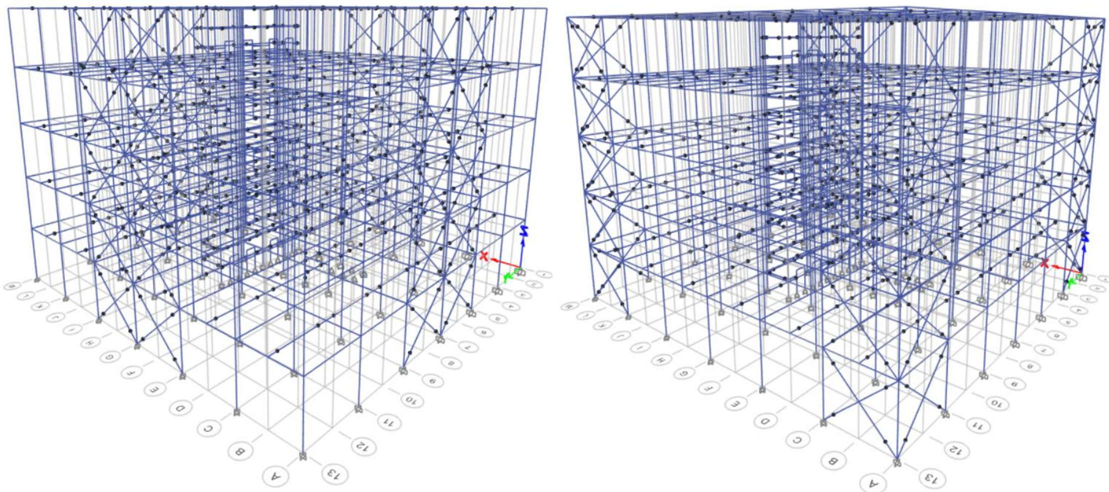

Figure 35: X braced systems with different exterior locations

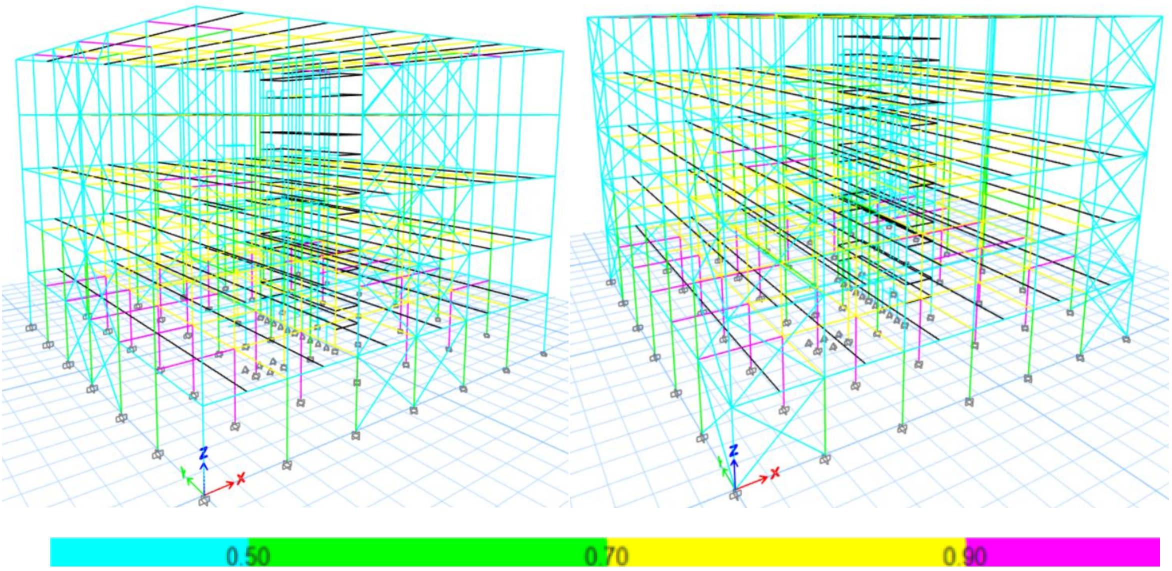

Figure 36: ETABS analysis results for exterior X-braced design

The results indicate no significant difference when using exterior braces, as lateral displacements are minimal for occupational and dead loads. The interior columns, loaded by half the area of four slabs, are the critical sections (Figure 36). This suggests that interior braces, similar to 4 steel cores on sides, connecting interior and exterior columns could reduce column loads.

Middle columns are uniformly loaded, so altering the critical cross-section does not change the overall column cross-section due to potential failure of another column. Figure 37 shows the model and analysis results of the proposed system.

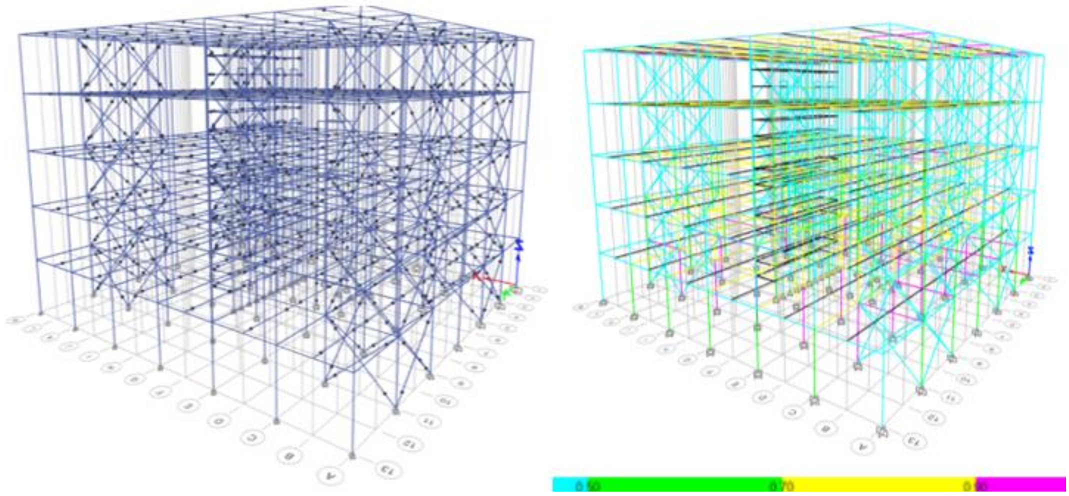

Figure 37: X-braced design connecting interior and exterior columns and ETABS analysis results

As expected, cross-section selection was unaffected by the new system. However, adding braces between loaded and half-loaded exterior columns reduced the unity check (U.C.) from 0.98 to 0.93, a significant improvement. Connecting the entire structure with braces is impractical due to spatial requirements. The weight of steel used for these designs is shown in Table 7.

Table 7: Resulting steel weight in X braced designs (for 5-meter column spacing)

Model	Column (kN)	Beam (kN)	Braces (kN)	Total Steel (kN)
Regular System 2.5 m	5.81E+02	6.69E+02	2.87E+00	1.25E+03
X Bracing Sides	5.72E+02	6.69E+02	3.25E+00	1.24E+03
X Bracing Sides Middle	5.72E+02	6.69E+02	3.25E+00	1.24E+03
X Braced to Exterior	5.72E+02	6.69E+02	6.51E+00	1.25E+03

4.3.1.2 V-Braced Structure Tests

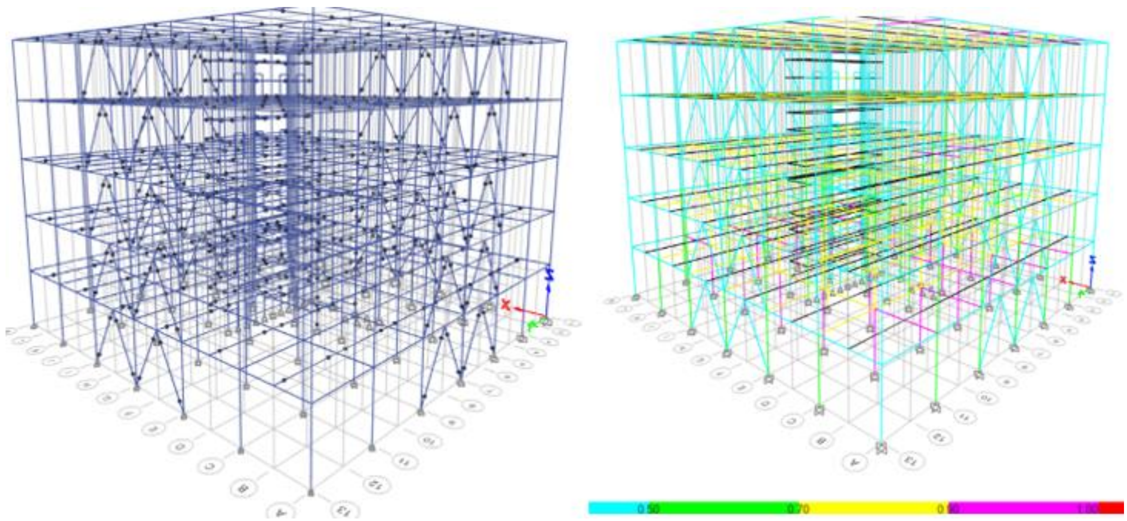

Figure 38: V (Chevron) braced design and analysis results

Figure 38 shows an exterior design and analysis results for the V-braced system. Both X- and V-Braced tests indicate that while bracings slightly improve load distribution, they do not significantly impact short structures as they do tall structures. Therefore, no additional V-brace models are presented, as the results are nearly identical to X-brace designs regardless of location.

4.3.2 Design of Diagrids

Diagrid design is complex due to the need to connect diagrids to interior column systems, which alters beam types and orientations compared to conventional systems. The stability system resists both lateral and vertical loads, allowing the design of internal columns to focus solely on vertical load-bearing criteria (Jani & Patel, 2013). Figure 11 in the literature review illustrates diagrid floorplans.

The changing position of diagrid nodes on each floor influences the orientation and spacing of secondary beams. These adapted beams ensure full connectivity between interior and exterior structures, preventing member overload. Although this alters beam orientation compared to conventional designs, consistent interior column spacings optimize structural integrity. Diagonal beams connect interior columns to diagrid sides on each floor, as structures are connected solely by composite beams.

Both the angle and size of diagrids are crucial. For a short structure like the parametric study office, small modules (2-4 storeys) are used. Small modules facilitate unusual shapes and eccentric loads (Boake, 2014). Figure 39 shows the analysis results for the optimal diagrid model: Diagrid 60.

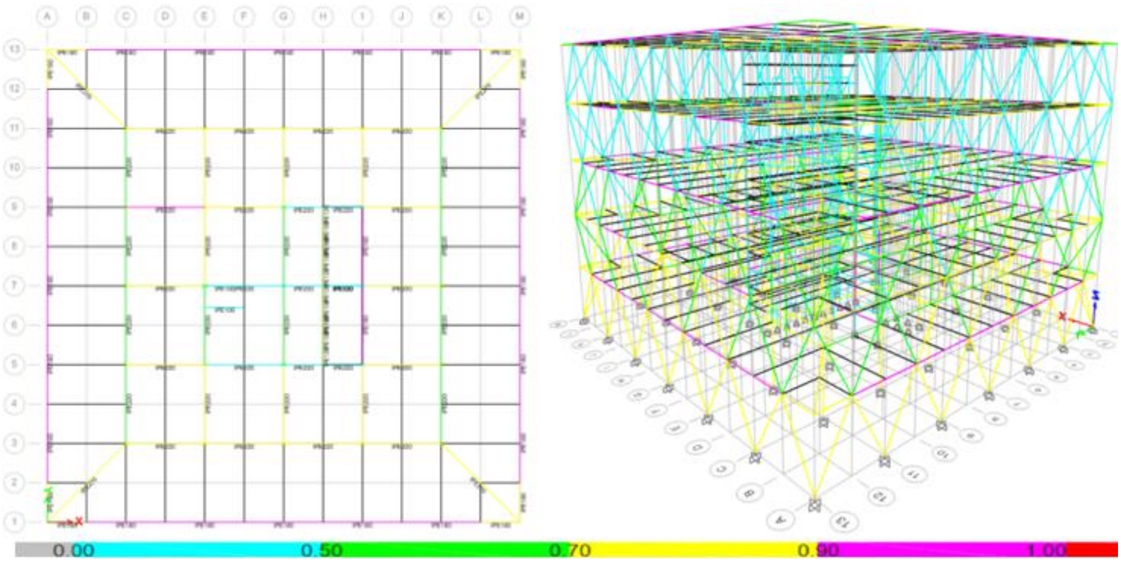

Figure 39: Analysis results of Diagrid 60 on ETABS a) floor plans and beams analysis b) 3D analysis for all structure

Loading patterns and stability systems are analysed using software results. Floor plans illustrate the connection between the interior and exterior systems through composite beams. The software's composite output verifies the beams, but the figures are more relevant for understanding load patterns. Floor plans in Figure 39 show load distribution to cross-sections. Compared to conventional designs, edge beams are better optimized due to the separation of inner and outer systems. In Figure 39, the exterior structure's optimization ranges from 0.7 to 0.99, whereas conventional designs optimize exterior members within 0.0 to 0.5 (blue range) as shown in Figure 36. Conventional designs would use IPE220 beams for exterior beams instead of IPE180, resulting in overdesigned cross-sections and increased steel weight. This explains why diagrid designs perform better, even for shorter structures.

The load distribution on inner beams is also examined. Horizontal beams bear more load, shown by the colour difference in the figures (in 2D, yellow or pink for horizontal, green for vertical). This variation is due to the composite beams; shorter spans for vertical beams reduce loads. This principle applies across all composite slab structures. Additionally, IPE270 diagonal beams are crucial for moment distribution and connecting inner and outer systems. Four diagonal beams on each floor transfer moments to or from the edges, integrating the interior and exterior systems. These longer, thicker cross-sections facilitate moment transfer to the diagrids and then to the ground.

Secondly, the right side of Figure 39 shows the beam loading. All columns and diagrid bracings experience maximum loads at the bottom cross-sections. This is primarily because diagrids do not resist moments, transferring them to the ground, resulting in higher stress in these sections. Additionally, the bottom member bears the cumulative load from all above members. Columns, while resisting moments at each floor, transfer the cumulative weight to the ground, making the bottom column the most critical section. This compression principle also applies to diagrids, with added torsion and moments causing greater differences between upper and lower sections.

The floor plan of Storey 1 shows edge beams are not optimized due to the lack of diagrid connections at the edges, resulting in a cantilever supported only by beams. This part does not contribute to load carrying or system connectivity. Some designers exclude these sections to optimize the structure and reduce material use. However, this approach was not adopted in the thesis due to minimal material savings for the 5-storey structure. For taller structures, the benefit could be more significant. Small diagrid modules do not create large cantilever spans, but medium and large modules do, increasing beam loads and moments. In such cases, edges must be cut off. For shorter buildings, the advantage is minimal, and the loss of space is not justified.

Diagrid effects were examined for 5 and 6 meters spacing, with 10 meters resulting in excessive material use and thus avoided. Previous research identifies the optimal diagrid angles as ranging between 55° and 75°. Diagrid structures with brace angles between 60° and 70° are found to be the most efficient in resisting both lateral and gravity loads (Kim & Lee, 2010). For this structure, 60-75-degree designs were explored. In diagrid design, angles are dictated by column spacing. The results for 5- and 6-meter spacings are shown in Table 8 to avoid excessive graphical content. Optimal designs for material use are selected and depicted as figures based on the results in Table 8 and Table 9.

Table 8: Steel weight for final designs for column spacing of 5 meters

Column Spacing 5 m				
Model	Column (kN)	Beam (kN)	Braces (kN)	Total Steel (kN)
Regular System 2.5 m	5.81E+02	6.69E+02	2.87E+00	1.25E+03
X Bracing Sides	5.72E+02	6.69E+02	3.25E+00	1.24E+03
X Bracing Sides Middle	5.72E+02	6.69E+02	3.25E+00	1.24E+03
V Bracing Middle	5.72E+02	6.69E+02	2.49E+00	1.24E+03
Diagrid 60	3.55E+02	6.06E+02	1.85E+02	1.15E+03
Diagrid 65	3.55E+02	6.37E+02	1.94E+02	1.19E+03
Diagrid 70	3.55E+02	5.75E+02	3.91E+02	1.32E+03
Diagrid 75	3.55E+02	7.78E+02	2.51E+02	1.38E+03
G+D60	4.18E+02	6.05E+02	1.42E+02	1.17E+03

Table 9: Steel weight for final designs for column spacing of 6 meters

Column Spacing 6 m				
Model	Column (kN)	Beam (kN)	Braces (kN)	Total Steel (kN)
Regular System 2 m	5.79E+02	8.11E+02	2.41E+00	1.39E+03
Regular System 3 m	5.84E+02	7.79E+02	4.49E+00	1.37E+03
Diagrid 60	3.73E+02	7.65E+02	1.85E+02	1.32E+03
Diagrid 65	3.04E+02	7.13E+02	2.12E+02	1.23E+03
Diagrid 70	3.08E+02	7.03E+02	2.26E+02	1.24E+03
Diagrid 75	3.10E+02	6.94E+02	2.67E+02	1.27E+03

Diagrids are compared with similar or identical composite spacings for regular systems. For a 5-meter column spacing, only a 2.5-meter composite spacing is feasible due to equal area considerations. Therefore, diagrids are only compared to the 2.5-meter alternative. Figures below show the top-performing diagrids, labelled in green in Table 8 and Table 9.

The optimal performance of these diagrids is not coincidental. As noted by Boake in "Diagrid Structures," small modules are essential for efficiency, thus all tested modules are small. A large module model was tested but found to use excessive material. The selected models include two for the 5-meter column spacing and two for the 6-meter spacing. Beyond the angles, geometric differences play a role. The structural efficiency of diagrids can be maximized by optimizing their grid geometries (Moon, 2009). Diagrid 60 for 5-meter spacing and Diagrid 70 for 6-meter spacing are geometrically symmetric in this structure, though this may vary in other structures. Both meet interior columns on the grid, preventing beam overload due to eccentricity.

This highlights the importance of diagrid design. The angle should not be fixed but within a recommended range, as it is case-specific. Designers must optimize the angle for their specific design and grid. The results indicate that Diagrid 60 with 5-meter spacing is the best for this structure, consistent with the lowest feasible column spacing determined in Section 4.1. Interior columns affect steel usage in diagrid structures. Optimal angles are discussed after presenting the designs. Figure 40 and Figure 41 show the designs and floor plans of the top four diagrids.

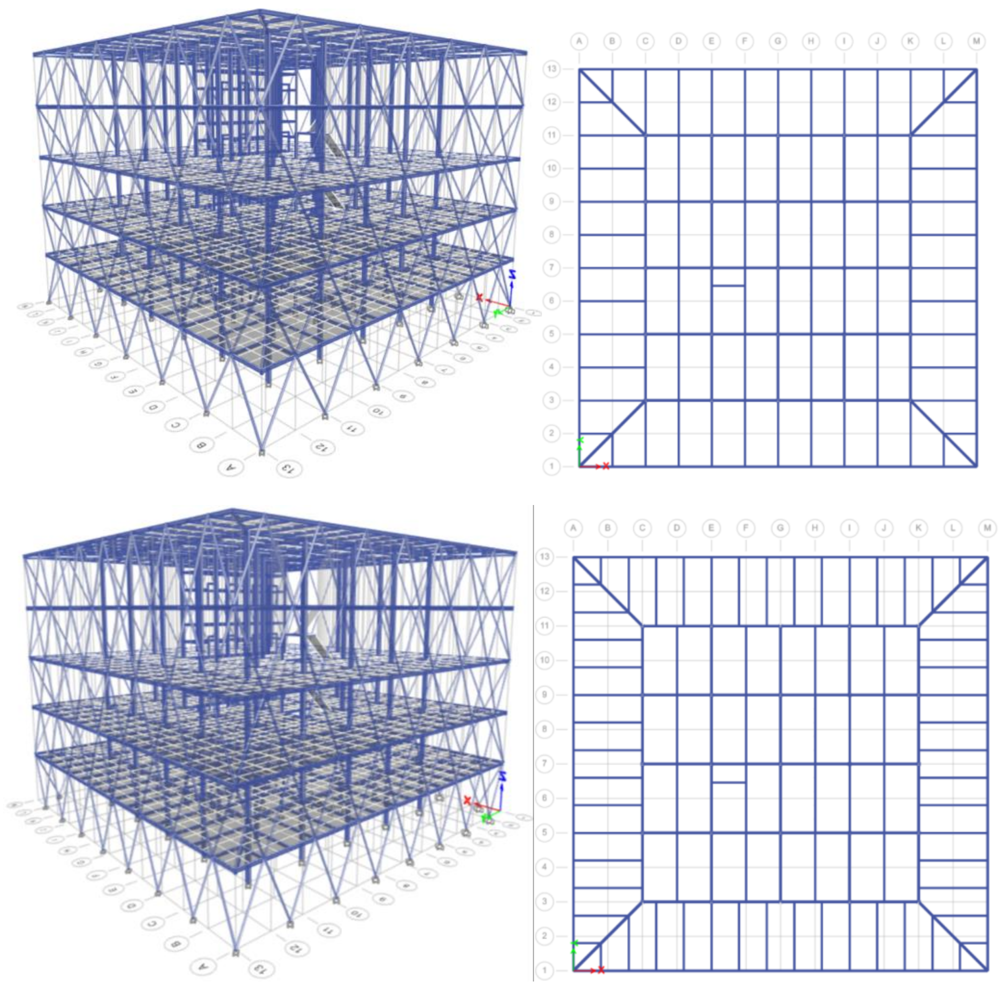

Figure 40: Best performing diagrid structures for 5-meter interior column spacing 1) 60-degree diagrid angle design (above) 2) 65-degree diagrid angle design (below)

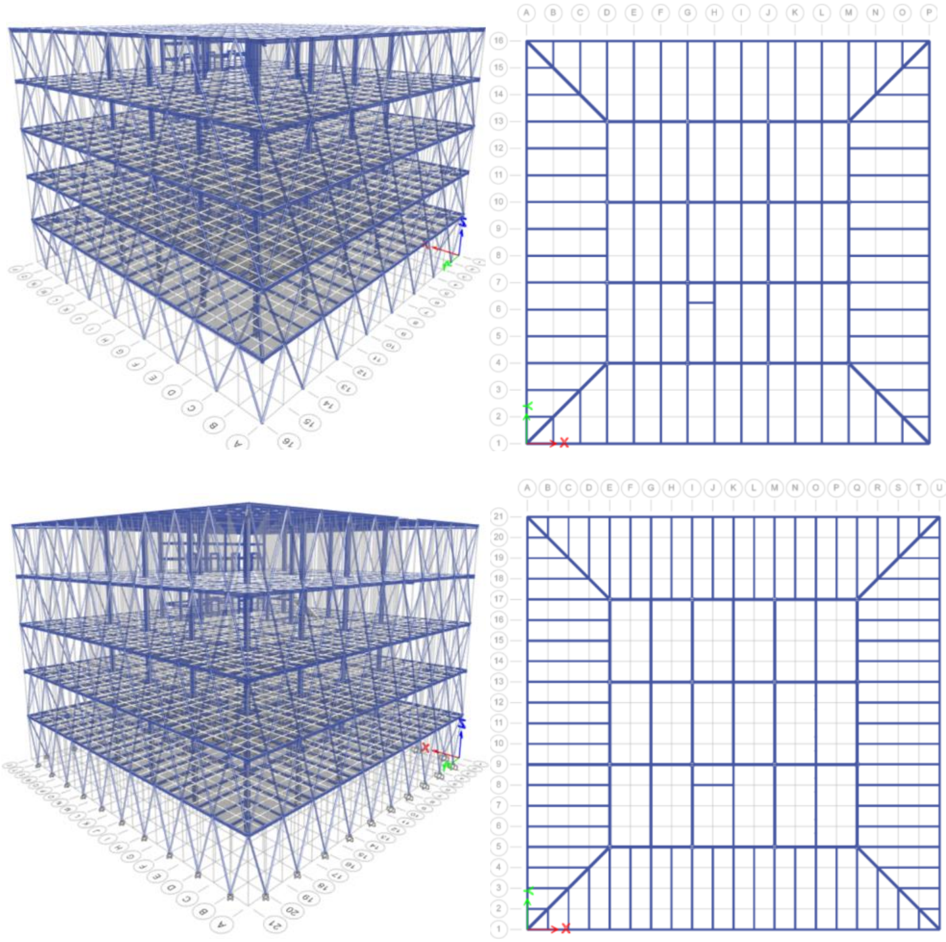

Figure 41: Best performing diagrid structures for 6-meter interior column spacing 1) 65-degree diagrid angle design (above) 2) 70-degree diagrid angle design (below)

The parametric study identified the optimal angles for diagrids: 60 degrees for 5-meter spacing and 70 degrees for 6-meter spacing, as shown in Table 8 and Table 9. Accurate floor system selection is crucial. Diagrids intersect with different parts of the exterior beams, necessitating secondary beam spacing at half the diagrid width. This alignment is discussed in the literature review.

Compared systems are highlighted in light brown in Table 8 and Table 9. The best-performing diagrid design features a 5-meter interior column spacing with a 60-degree angle. This configuration maintains a maximum 3-meter composite spacing, with 2.5-meter secondary beams providing optimal support. This system achieves an 8.5% steel saving compared to a conservative structure with the same column and beam spacings. However, the highest material saving percentage is observed with a 65-degree diagrid for 6-meter column spacing comparing with 6 and 3 m column and composite spacing respectively. The material saving of 11.7% compared to the conservative structure is substantial but not the highest performing design. This discrepancy arises because non-optimal column spacings increase steel weight, providing more opportunity for material savings with diagrids.

From the results in Table 8 and Table 9 the optimal diagrid design includes symmetrical alignment of secondary beams with inner columns. Two critical steps for optimal diagrid design are: selecting the best column spacing and ensuring the diagrid angle facilitates non-eccentric geometrical connections between interior and exterior load-bearing systems. Symmetrical systems offer superior performance due to even force distribution, while eccentric connections create stress concentrations and additional moments where primary and secondary beams meet.

4.4 Selection of Cross-sections

Selecting appropriate cross-sections for beams and columns is a critical decision in the design process. Optimized cross-section design enhances material efficiency and reduces construction material demand (Nijgh & Veljkovic, 2020). An integrated approach is essential for accurately defining, representing, and analysing cross-sections, ensuring that theoretical advancements are effectively applied to practical design (Anwar & Najam, 2017). Through trial and error, it has been found that thinner cross-sections provide the best material efficiency. Consequently, IPE sections are exclusively used for beams, HEA sections for columns, symmetrical and circular hollow sections for diagrids, and steel rods for braces. Table 10 presents the selected cross-sections for the best-performing system, Diagrid 60, and the conservative system (5m column spacing, 2.5m secondary beam spacing).

Table 10: Resulting cross-sections for the compared designs

Column Spacing = 5 meters				
System	Columns	Beams	Secondary Beams	Braces (Diagrids)
Diagrid 60	HEA240	IPE220 - IPE180	IPE140	TUBOD159x4
Conservative	HEA220	IPE220	IPE140	-

The material usage calculations are based on these optimized cross-sections, selected to be the thinnest possible for the given load case. Columns were switched to HEB sections, beams to HEA sections, and Rectangular Hollow Sections (RHS) were chosen for diagrids. Secondary beams were not changed to H sections due to insufficient depth, which would lead to a significant material increase without enhancing moment resistance. The new cross-sections are shown in Table 11, with unchanged sections labelled as '-' for clarity. All cross-sections were selected based on the member with a Unity Check value closest to 1.

Table 11: Resulting different cross-sections when different types of sections are selected for the compared designs

Column Spacing = 5 meters				
System	Columns	Beams	Secondary Beams	Braces (Diagrids)
Trial Diagrid 60	HEB220	HEA180 - HEA160 -HEA140	-	TUBO140x98x7.1
Trial Conservative	HEB200	HEA160	-	-

Switching columns from HEA to HEB results in a 21% increase in steel use for columns and a 9.7% increase for the entire structure, significantly impacting the material usage as columns constitute 46% of the material in the conservative structure. Changing primary beams from IPE220 to HEA160 results in a 13% increase in material usage for beams and a 6.7% increase for the structure. Combining these changes leads to a 16.2% increase in total steel usage, the most significant impact observed, even without altering composite beams.

For diagrids, switching from Circular Hollow Sections (CHS) to TUBO140x98x7.2 (RHS) increases steel use by 63% for braces and 10% for the total steel usage. Symmetrical cross-sections, such as CHS, perform better and are more efficient. If using RHS diagrids, the orientation angle is crucial, ideally closer to 45 degrees, although this is not the best alternative as not all variables were tested. This results in a more complex design and makes cross-sections more susceptible to construction orientation errors.

Table 12, Table 13, Figure 42 and Figure 43 illustrate the Diagrid 60 and Conservative models with different cross-sections. The differences are visualized for each cross-section selection and the total resulting steel weight. Secondary beams were not adjusted due to their smaller sizes and the difficulty of finding HEA alternatives. Regardless, if HEA or HEB cross-sections were used, the results would be similar to those for beams. Separate models were created for each scenario to ensure accuracy, as changes in one type of cross-section can impact the structural integrity and cross-section requirements of other members

Table 12: Resulting increase in material weight for each cross-section type for conservative (conventional) design

System	Column (kN)	Beam (kN)	Brace (kN)	Total Steel (kN)
Regular System 2.5 m	5.81E+02	6.69E+02	2.87E+00	1.25E+03
Regular HEA to HEB	7.00E+02	6.70E+02	2.87E+00	1.37E+03
Regular IPE to HEA	5.81E+02	7.55E+02	2.87E+00	1.34E+03
Regular All Different Cross Sections	7.00E+02	7.55E+02	2.87E+00	1.46E+03

Table 13: Resulting increase in material weight for each cross-section type for the diagrid (60) design

System	Column (kN)	Beam (kN)	Brace (kN)	Total Steel (kN)
Diagrid 60	3.55E+02	6.06E+02	1.85E+02	1.15E+03
Diagrid HEA to HEB	4.16E+02	6.06E+02	1.85E+02	1.21E+03
Diagrid IPE to HEA	3.55E+02	6.79E+02	1.85E+02	1.22E+03
Diagrid to RHS	3.55E+02	6.06E+02	3.02E+02	1.26E+03
Diagrid All Different Cross Sections	4.16E+02	6.79E+02	3.02E+02	1.40E+03

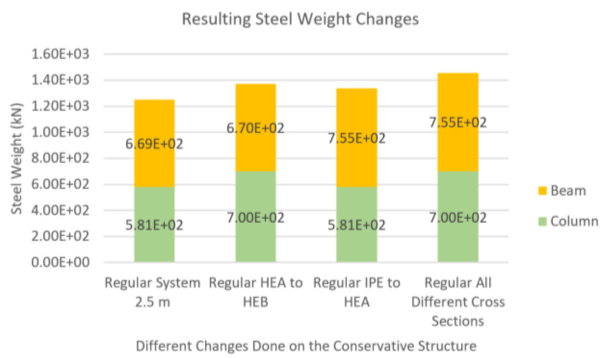

Figure 42: Representation of resulting changes in weight of steel due to change of cross-section in conservative (conventional) design

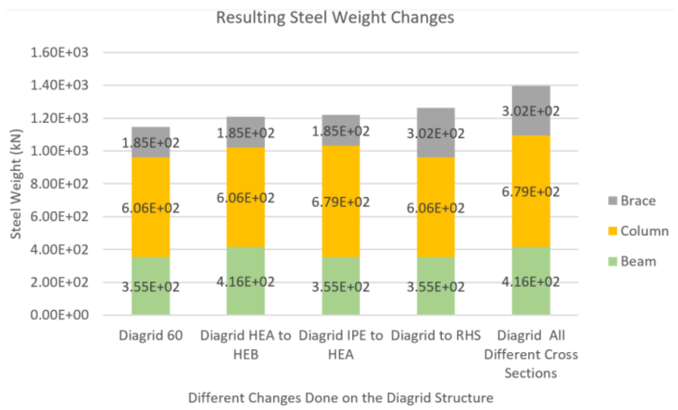

Figure 43: Representation of resulting changes in weight of steel due to change of cross-section in the diagrid (60) design

4.5 Design of Composite Slab

Structural design for buildings and bridges primarily focuses on supporting load-bearing horizontal surfaces, such as slabs in buildings (Johnson & Wong, 2019). In a 30x30 meter office building, columns can be spaced at 3, 5, 6, and 10 meters. According to Hauke et al. (2016), optimal material use is achieved when columns and beams intersect at every location with equal spacing. High spans necessitate thicker concrete slabs, which are undesirable. Thus, a 3x3 meter frame system without a composite slab was tested for feasibility and functional requirements. However, offices require open spaces, and a 3x3 meter frame complicates this requirement. The focus of this thesis is on steel use, thus all systems, including slab types, are designed to be steel based. To maintain concrete as a constant variable and assess the steel usage and system synergy, composite beam spacings are kept consistent to ensure a similar concrete deck depth.

The shear connection in a composite beam is vital for structural performance and integrity, ensuring a bond between components that prevents independent movement and enhances load-carrying capacity and stiffness (Kyvelou et al., 2017). The demountability of steel-concrete composite slab connections is also extensively studied in the literature. This thesis incorporates previous research to develop a demountable composite slab guide. The number of shear studs is calculated using ETABS and detailed in Appendix D: 8.4.4 Composite Beams.

The primary consideration is the design of the composite members, which is case-specific, but the critical aspect is ensuring demountability. Understanding the physics of composite action is essential. Composite slabs can be constructed either on-site with steel sheeting or with prefabricated concrete slabs. Prefabricated slabs offer the advantage of eliminating construction loading on steel beams. During the 20-30 days of concrete hardening, concrete has no load-bearing capacity, so all dead load is carried by steel beams, requiring temporary span supports. The primary disadvantage of prefabrication is transportation, but the benefits outweigh this drawback. Therefore, prefabricated designs are used in all models in this thesis.

Concrete slabs are connected to steel beams via shear studs (bolts) embedded in the concrete and through the steel beam flanges. Figure 44 illustrates a potential design for demountable composite connections. Compared to welded headed stud connectors, bolted connectors require fewer bolts and are thus selected (Nijgh & Veljkovic, 2020)

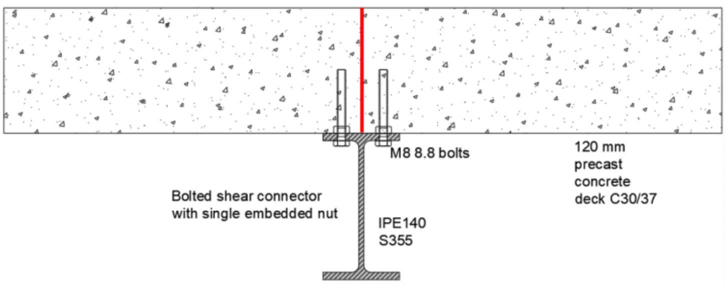

Figure 44: Composite Slab Design Representation

Slip occurs when self-weight is imposed into the design equations, hence oversized bolt holes cannot be 2 mm bigger than the bolt holes, but 22 mm oversize of the holes is required to keep the composite beam as a composite unit after loading of self-weight (Nijgh & Veljkovic, 2020). 22 mm oversize is required to achieve 95% demountability (Nijgh & Veljkovic, 2020) which is critical for the structure and full demountability. This oversizing, however, increases slab deflections. To mitigate this, bolt holes can be injected with resin post-construction.

4.6 Design of Connections

This section presents the three most complex connection locations within the selected designs. The primary goals for these connections are demountability and optimization. Multiple iterations were conducted to maximize the performance of members and connections. Welds were minimized, particularly between connected members, to enhance demountability. Minimizing drilling into members is crucial, leading to the selection of plated connections.

When using bolted connections, drilling into columns is unavoidable. Cleat connections, which require drilling through both members, were not selected. Although clamp-based and plug-in connections are innovative, they are not commonly used and could be topics for future research. Conventional connections, like end-plates and fin plates, offer simplicity and standardization, facilitating reuse (Dai et al., 2022). Therefore, end-plate connections were primarily employed due to their widespread use and ease of reuse. End plate connections involve welding the connecting member to a plate without bolting. Additionally, wideners and stiffeners were welded to members at various locations. These welds do not compromise demountability, as plates can be disassembled and reused with the members after bolts are removed.

To ensure demountability, several criteria were addressed after selecting the connection types. Elastic design was implemented for all structural designs and stability systems. Rotation capacity and failure mode for ductility were verified using IdeaStatica, ensuring all connections have a ductile failure mode, avoiding brittle failure (Veljkovic et al., 2020). Bolt holes on connecting members were oversized by 2 mm to prevent cross-section damage during disassembly.

The designs are detailed in Sections 4.6.1, 4.6.2, and 4.6.3. These sections model and present three critical connections for the Diagrid 60 design. Since Diagrid 60 is the final design, connections were specifically designed for it. However, the diagrid design also includes significant connections from conservative and braced structures with the inner columns and diagrids.

Figure 45: Grid System for Diagrid 60 Design

4.6.1 4 Beams – 2 Columns Connection

Figure 46 illustrates the four beam and two column connections located in Grid 3I, labelled as (1) in the Diagrid 60 Design (Figure 45). These connections are developed for the Diagrid 60 Design, identified as the optimal solution. Despite potential load variations across different structures and designs, these connections are crucial and widely applicable. Minor adjustments may be needed, but the same connection type can be used for most, if not all, structures.

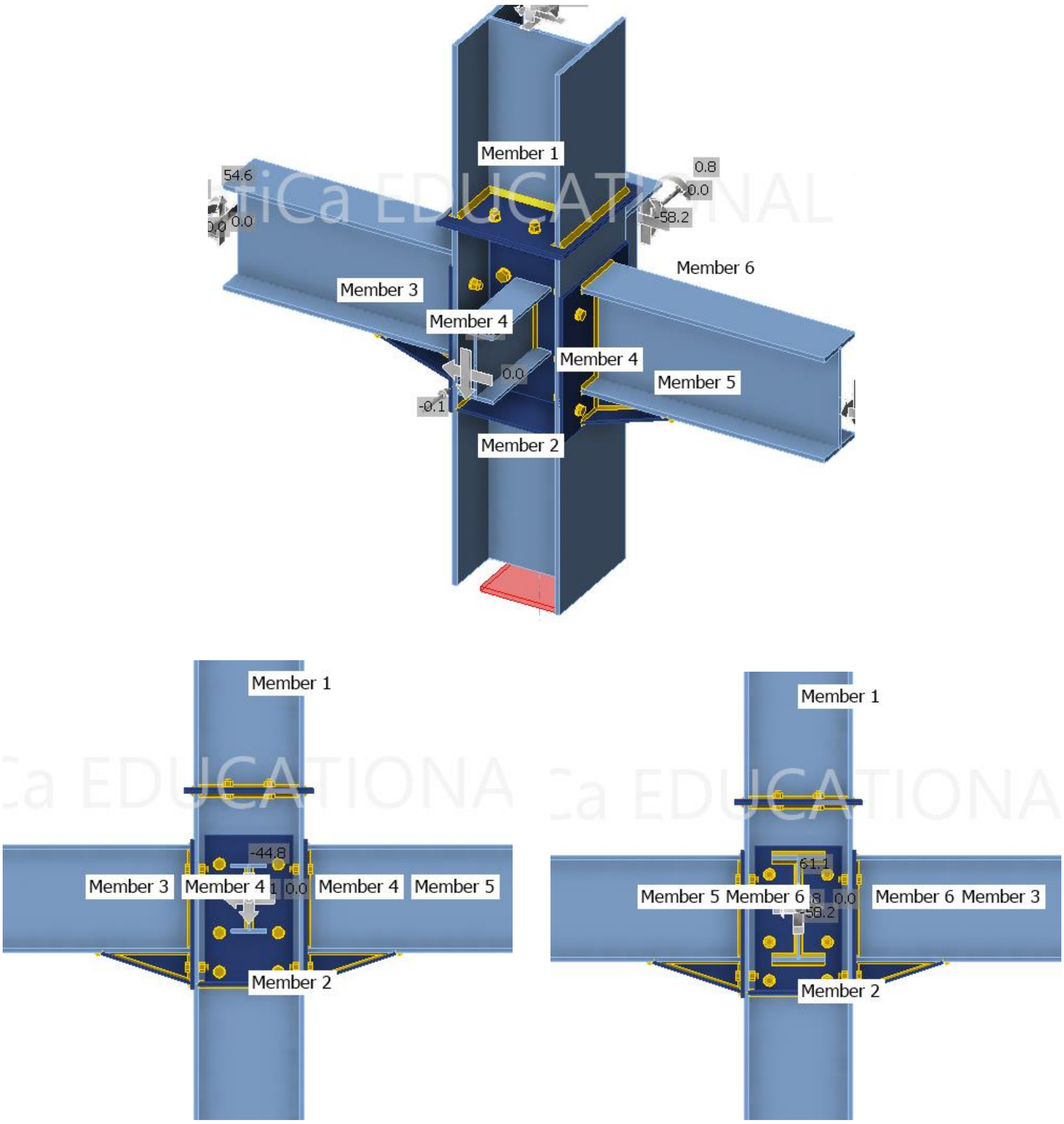

Figure 46: Connection Design for 4 beam 2 column connection using IdeaStatica

Connection is designed to be optimal, lower material use is the aim when connections are designed, hence several different iterations are done to finalize the connections. Shown below in Table 14 are the components used to each connection. Detailing of each connection can be found in Appendix F.

Table 14: Connection Detailing for 4 beams 2 columns connection

Connection	Number and Type of Bolts (c x r)	Plate (mm) (h x w x t)	Widener thickness (mm)	Widener location (mm) (d x l)	Weld Throat Thickness (Always both sides if possible)
Column Web to Beams IPE220 and IPE140	2 x 3 M14 10.9 Bolts	S355 300x180x18 On **each** side (x2)	-	-	Web: 4 mm Flange: 6.5 mm
Column (HEA240) Flange to Beam IPE220 (1)	2 x 2 M12 8.8 Bolts	S235 305x240x7	S355 $w_f = 110\ mm$ $t_f = 5\ mm$ $t_w = 5\ mm$	60x180 mm	Web: 4 mm Flange: 4 mm Widener: 4 mm
Column (HEA240) Flange to Beam IPE220 (2)	2 x 2 M12 8.8 Bolts	S235 305x240x7	S355 $w_f = 110\ mm$ $t_f = 5\ mm$ $t_w = 5\ mm$	60x180 mm	Web: 4 mm Flange: 4 mm Widener: 4 mm
Column (HEA240) to Column (HEA240)	2 x 2 M12 8.8 Bolts	S235 265x290x5 On **each** side (x2)	-	-	Web: 6 mm Flange: 6 mm

Cost of the connection is estimated to be 142 €. This estimate is done by IdeaStatica Software using following four basic entities:

- Steel parts (plates and added steel members, grade dependent)
- Welds (single and double fillet welds, ½ V and K butt welds, weld size dependent)
- Bolt assemblies (grade and diameter dependent)
- Hole drilling (as a percentage of bolt assembly cost)

All in detailed verifications including calculations for total cost and more specifically the material use for each connection design can be found in Appendix F.

4.6.2 5 Beams + 2 Columns

The second connection design involves five beams and two columns intersecting at Grid 3K, labelled as (2) in the Diagrid 60 Design (Figure 45). This design is specific to diagrids but can be adapted for use without them. The fifth beam, angled at 45 degrees, connects to the column flange at the same location as another beam. This angled beam integrates the exterior diagrids with the interior system. When used in non-diagrid designs, these angled beams are typically the same size or smaller than the beams oriented at 0 or 90 degrees, creating complexity in connection design. To avoid additional loading due to eccentricity, beams are connected at the midpoint where the web meets the flange. Given the angled beam's higher load resistance, this configuration optimizes load distribution. Figure 47 illustrates the connections for this scenario.

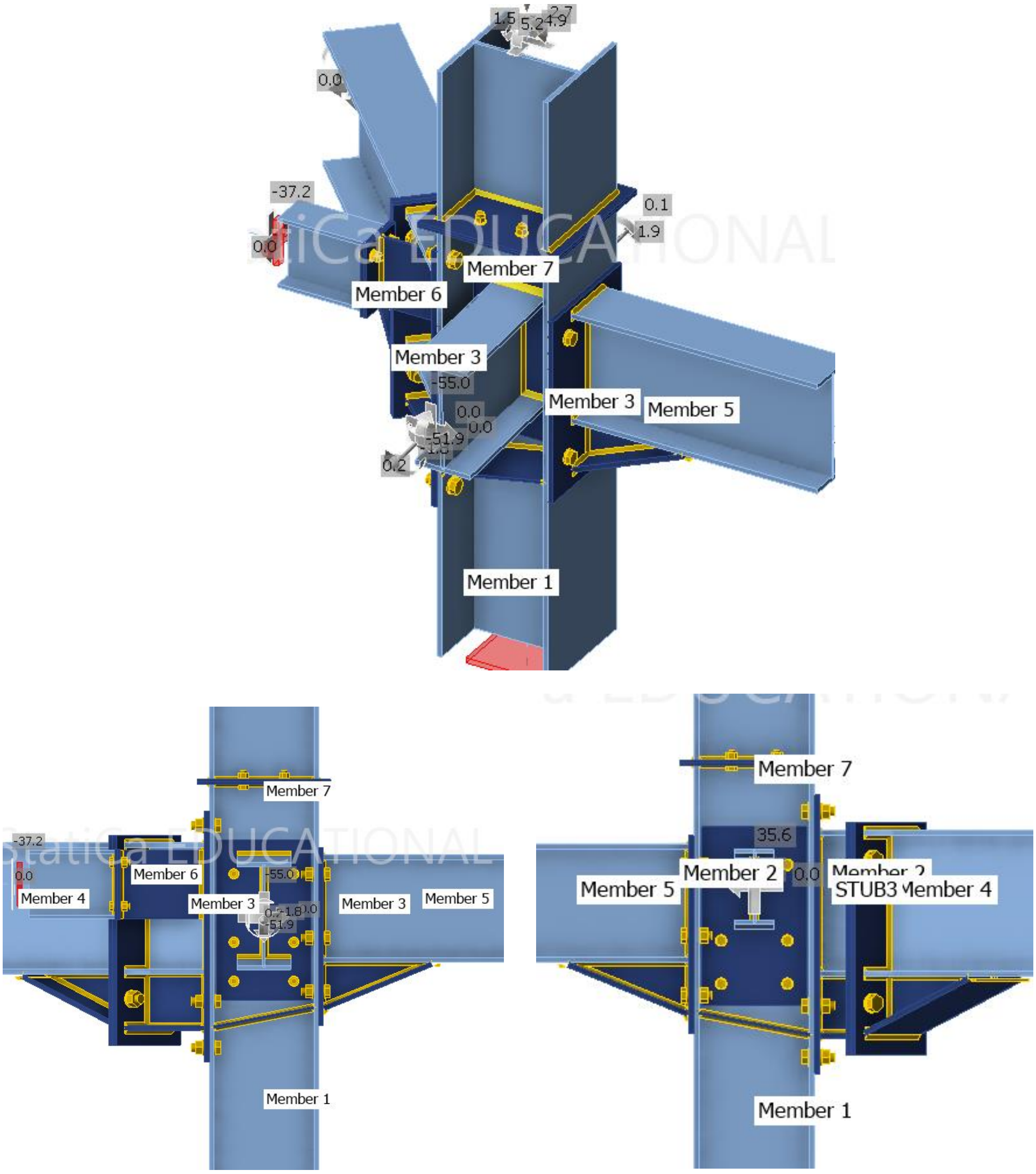

Figure 47: Connection Design for 5 beam 2 column connection using IdeaStatica

To connect two beams at the same point, a stub and end plate connection is used to avoid cutting, welding, or drilling of the cross-sections. The stub of the angled beam is connected to an angled member, which then connects to the column via an end plate. The stub of the smaller beam is welded to a stiffening plate and an end plate, which attaches to the column flange. This configuration avoids welding directly to the column flange and the need for flange stiffening. Figure 48 illustrates this connection of two beams to a column.

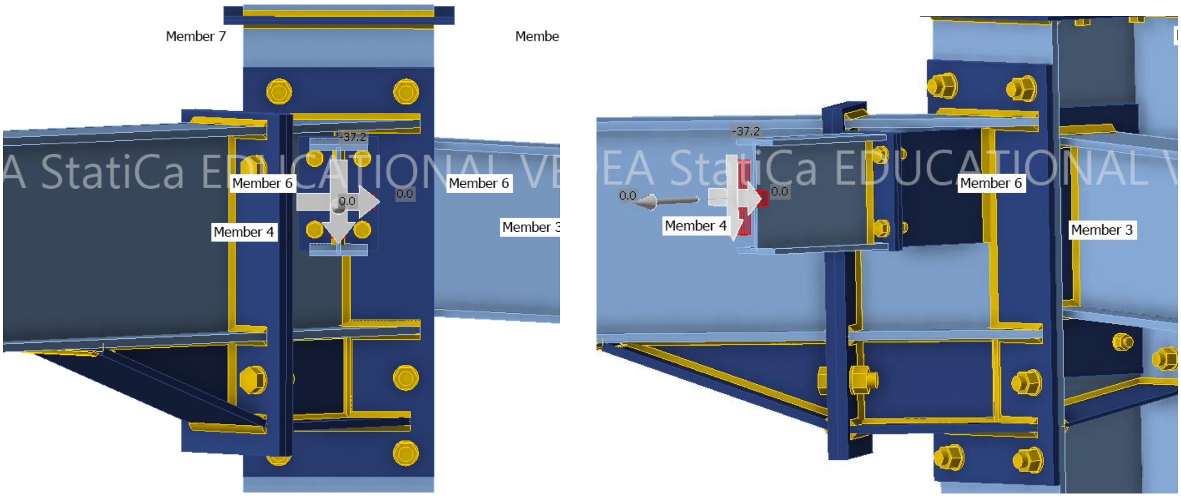

Figure 48: Closer look to the coinciding beam connections

The stiffener extends to the stub in the angled beam, and plates are placed at the stiffener location to connect the stub to the column, ensuring load transfer. Due to the angled connection of the biggest member, the stiffening plates are also angled for better load support. While this connection required welding, it was limited to the plates, maintaining the demountability standard.

Table 15 lists the components used for each connection. The estimated cost of the connection is 266 €, as calculated by IdeaStatica. Detailed verifications, including total cost and material use calculations for each connection design, can be found in Appendix F.

Table 15: Connection Detailing for 5 beams 2 columns connection

Connection	Number and Type of Bolts	Plate (mm) (h x w x t)	Widener thickness (mm)	Widener location (mm) (d x l)	Weld Throat Thickness
Column (HEA240) Web to Beam IPE220 and IPE140	2 x 3 M12 10.9 Bolts	S355 330x195x15 On **each** side (x2)	-	-	Web: 4 mm Flange: 6 mm
Column (HEA240) Flange to Beam IPE220	2 x 3 M16 10.9 Bolts	S355 365x240x10	S355 $w_f = 110\ mm$ $t_f = 9.2\ mm$ $t_w = 5.9\ mm$	90x220 mm	Web: 4 mm Flange: 4 mm Widener: 4 mm
Beam IPE140 (2) to Stub 1	2 x 2 M12 8.8 Bolts	S355 145x100x6 On **each** side (x2)	-	-	Web: 4 mm
Stub 1 to Plate (weld) to Column End Plate (Weld) (IPE140)	-	S355 140x165x5	-	-	All: 4 mm
Beam IPE270 (angle 45) to Stub 2 (IPE270)	2 x 2 M20 10.9 Bolts	S355 430x180x12 On **each** side (x2)	S355 $w_f = 135\ mm$ $t_f = 10.2\ mm$ $t_w = 6.6\ mm$	100x180 mm	Web: 4 mm Flange: 5 mm Widener: 5 mm
Stub 2 (IPE270) to End Plate	-	Connecting member: IPE270 cut	S355 $w_f = 135\ mm$ $t_f = 10.2\ mm$ $t_w = 6.6\ mm$	120x185 mm Constant plate	Widener: 5 mm Web: 4 mm Flange: 5 mm
End Plate to Column	2 x 3 M18 10.9	S355 515x240x10	-	-	-
Stiffener x2 (with angle) to Column	-	S355 (x2) Plate: 210x115x5 mm	-	-	Plate: 4 mm

4.6.3 Diagrid Connection

Diagrid connections are among the most complex in structural design due to the multiple member angles and beam considerations. The node connecting the diagrid members is designed to be stiff for constructability, facilitating erection but not intended as a moment-resisting element. The force transfer is similar to that in truss-type designs (Boake, 2014). Figure 49 illustrates the Diagrid connection in Grid 1J, labelled as (3) in the Diagrid 60 design shown in Figure 45. This connection involves four CHS columns (braces) at 60-degree angles, two side beams, and one smaller beam behind the plate. To ensure demountability, all members are connected to a stiffening plate with cap and end plate connections. The critical aspect is that a stiffening member must support all these elements in various directions. Unlike conventional structures, where a column typically serves as the supporting member, this design requires a solid plate and several angled stiffening plates for adequate support.

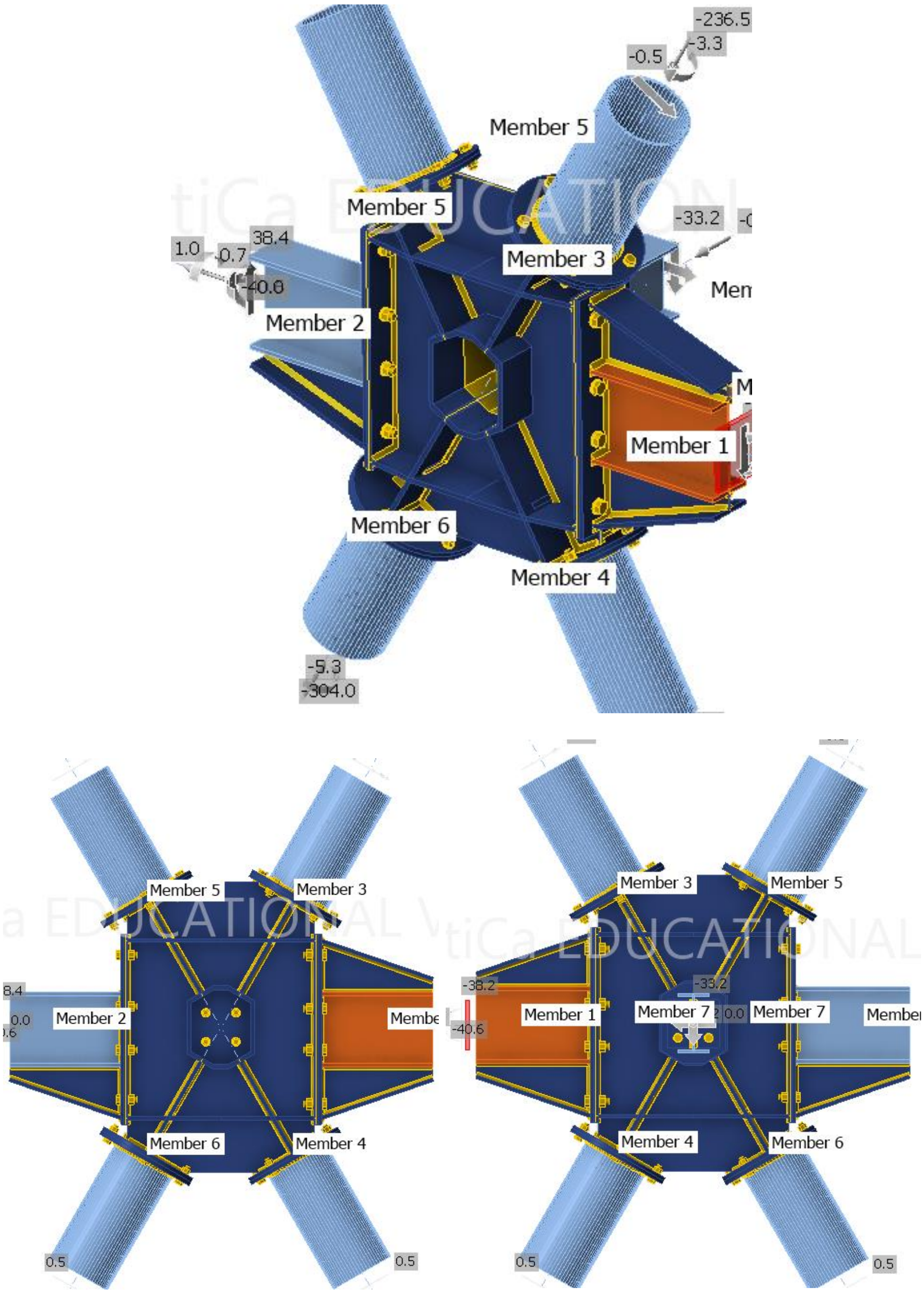

Figure 49: Connection design for diagrid connection with 7 members using IdeaStatica

Stiffening plates (t = 8 mm) are welded at 60-degree angles to the diameter of CHS beams, with two plates per beam. IPE beams on both sides are similarly supported by 8 mm thick stiffening plates on both flanges, ensuring stresses do not exceed the yield stress of the structural members. Without proper stiffening, connection stresses can surpass the yield stress due to insufficient support in load transfer directions. The plates distribute excessive loads across multiple locations. All stiffening plates are welded to a major plate (t = 10 mm) and a hexagonal prism, which provides support. The entire system is prefabricated as a single unit, minimizing on-site welding and ensuring structural integrity.

Subsequently, plate-to-plate connections are designed to join the end plates to the structure. Each connection uses two plates: a cap plate and an end plate. The cap plate is welded to the stiffening plates, while the end plates are bolted to the cap plates, facilitating disassembly. For the IPE beams, additional stiffening is required under load, necessitating wideners on flanges to meet space requirements. The smaller IPE beam, connected perpendicularly to the major plate, uses a similar configuration with two plates and bolts. The cap plate is welded to the hexagonal prism, and the end plate is bolted to the cap plate. Detailed dimensions and connections are provided in Table 16, with comprehensive reports available in Appendix F. The estimated cost of the connection is 692 € via IdeaStatica.

Table 16: Connection Detailing for 7-member diagrid connection

Connection	Number and Type of Bolts (c x r)	Plate (mm) (h x w x t)	Widener thickness (mm)	Widener location (mm) (d x l)	Weld Throat Thickness (Always both sides if possible)
Beam (1) (IPE180) End plate to Cap Plate (1)	2 x 4 M16 8.8 Bolts	S355 460x142x8 **Both** cap and end plate (x2)	x2 S355 $w_f = 90\ mm$ $t_f = 8\ mm$ $t_w = 5.3\ mm$	±120x350 mm	Web: 4 mm Flange: 6 mm Widener: 5.5 mm
Major Connecting Plate for Connection	-	S355 700x450x8 (Edges are cut off at locations of cap plates)	-	-	-
Cap Plate Cross Stiffening Plates (CHS) (x4) tapered plates (x2) and Stiffening Plate (prefabricated)	-	Cap plate: S355 255x175x8 2 Stiffening plates at stiffener level: (tapered from 140 to 175 until 100 mm) 175x225x8 (x2)	-	-	To stiffening plates: 6 mm To main (major) plate: 5 mm
Beam (2) (IPE180) End plate to Cap Plate (2)	2 x 4 M14 8.8 Bolts	S355 460x142x8 **Both** cap and end plate (x2)	x2 S355 $w_f = 90\ mm$ $t_f = 8\ mm$ $t_w = 5.3\ mm$	120x350 mm	Web: 4 mm Flange: 6 mm Widener: 5 mm
Cap Plate (2) to Major and Stiffening Plate (prefabricated)	-	Cap plate: S355 470x142x26 2 Stiffening plates at flange level: (tapered from 140 to 175 until 100 mm) 175x225x8 x2	-	-	To stiffening plates: 6 mm To main (major) plate: 4 mm
All CHS (159,4) End Plate to Cap Plate	5 M12 8.8 Bolts	S355 250x10 (d x t) **Both** cap and end plate (x2)	-	-	4 mm

5 Discussions and Framework

5.1 ECI Cost

Impact assessment is a procedure that evaluates the environmental effects of a product or system using both qualitative and quantitative methods. This analysis examines the impact of raw material usage, energy consumption, water production, effluent discharge, air emissions, and solid waste generation on the environment (Asif et al., 2007). The specific impact categories, outlined in Section 2.7, are essential for accurately calculating the Environmental Cost Indicator (ECI) value.

To calculate the ECI cost associated with the designs, using generic 'steel' material values is insufficient, as the production of cross-sections also contributes to the ECI cost. Therefore, for each design and cross-section, producers within Europe were identified. Relevant values were obtained from producer declarations on the EPD International website (EPD library). This thesis considers only the production (A1-A3) and end-of-life (C1-C4) stages, as construction optimization is excluded. Table 17 presents the ECI cost calculation coefficients for each cross-section, sourced from the producers' manuals. The producers and their manuals are listed below:

Circular Hollow Section: Seamless Hot Rolled Steel Tubes 2022

I and H Sections: Environmental Product Declaration: Steel Beams 2021

Rod (for Bracing): Dufuerco Danish Steel: Rolled Steel Products 2022

Table 17: Declared ECI Coefficients for the Cross-sections

			Steel Beam/ Column (I- H Sections)					Steel Pipe (CHS)					Steel Rod (Bracing)				
			Production Stage	End of life stage				Production Stage	End of life stage				Production Stage	End of life stage			
Impact Category	Unit	Cost (€)	A1-A3	C1	C2	C3	C4	A1-A3	C1	C2	C3	C4	A1-A3	C1	C2	C3	C4
GWP total	kg CO2e	1.33E-01	7.19E-01	3.30E-03	8.27E-03	2.21E-02	2.64E-04	5.61E-01	3.30E-03	8.34E-03	2.21E-02	2.64E-04	1.10E+00	2.06E-02	6.84E-03	1.13E-02	2.50E-04
GWP fossil	kg CO2e	1.33E-01	7.12E-01	3.30E-03	8.26E-03	2.34E-02	2.63E-04	5.38E-01	3.30E-03	8.33E-03	2.34E-02	2.63E-04	1.10E+00	2.06E-02	6.84E-03	1.11E-02	2.50E-04
GWP Biogenic	kg CO2e	1.33E-01	6.01E-03	9.17E-07	4.44E-06	-1.34E-03	5.22E-07	1.87E-02	9.17E-07	4.45E-06	-1.34E-03	5.22E-07	3.83E-03	1.00E-05	0.00E+00	1.20E-04	0.00E+00
GWP LULUC	kg CO2e	1.33E-01	8.09E-04	2.79E-07	2.96E-06	2.66E-05	7.82E-08	4.17E-03	2.79E-07	2.96E-06	2.66E-05	7.82E-08	3.70E-04	0.00E+00	0.00E+00	1.00E-05	0.00E+00
Ozone depletion pot	kg CFC11e	3.00E+01	8.68E-08	7.12E-10	1.89E-09	3.37E-09	1.08E-10	7.79E-08	7.12E-10	1.89E-09	3.37E-09	1.08E-10	6.28E-08	4.60E-09	1.64E-09	1.90E-09	5.24E-11
Acidification pot	mol H+e	7.65E+00	3.81E-03	3.45E-05	4.20E-05	2.84E-04	2.50E-06	1.33E-03	3.45E-05	3.40E-05	2.84E-04	2.50E-06	4.79E-03	2.20E-04	3.00E-05	1.00E-05	0.00E+00
EP-freshwater	kg Pe	1.65E+01	4.08E-05	1.33E-08	6.97E-08	1.62E-06	3.18E-09	9.89E-06	1.33E-08	6.97E-08	1.62E-06	3.18E-09	8.13E-08	1.45E-08	3.53E-09	3.73E-07	8.96E-10
EP-marine	kg Ne	2.00E+01	8.16E-04	1.52E-05	1.43E-05	6.27E-05	8.61E-07	2.85E-04	1.52E-05	1.01E-05	6.27E-05	8.61E-07	1.10E-03	1.00E-04	1.00E-05	4.00E-05	0.00E+00
EP-terrestrial	mol Ne	3.11E+01	9.38E-03	1.67E-04	1.58E-04	7.28E-04	9.48E-06	3.17E-03	1.67E-04	1.12E-04	7.28E-04	9.48E-06	1.23E-02	1.09E-03	1.30E-04	4.40E-04	1.00E-05
POCP ("smog")	kg NMVOCe	1.55E+00	3.26E-03	4.59E-05	4.50E-05	1.99E-04	2.75E-06	1.24E-03	4.59E-05	3.42E-05	1.99E-04	2.75E-06	3.94E-03	3.00E-04	3.00E-05	1.20E-04	0.00E+00
ADP-minerals & metals	kg Sbe	0.00E+00	1.33E-06	5.03E-09	2.25E-07	1.30E-06	2.41E-09	9.84E-07	5.03E-09	2.25E-07	1.30E-06	2.41E-09	4.57E-06	1.06E-09	3.00E-10	5.86E-10	1.22E-11
ADP- fossil resources	MJ	0.00E+00	1.16E+01	4.54E-02	1.26E-01	3.25E-01	7.36E-03	1.12E+01	4.54E-02	1.26E-01	3.25E-01	7.36E-03	1.42E+01	2.84E-01	9.78E-02	1.80E-01	3.36E-03
Water use	m3e depr.	0.00E+00	1.29E+00	8.46E-05	4.05E-04	4.61E-03	3.40E-04	1.69E-01	8.46E-05	4.05E-04	4.61E-03	3.40E-04	1.22E-01	7.00E-05	-2.00E-05	8.20E-04	0.00E+00

All three producer documents declare the end of life similarly: demolition using machinery, 95% recycling of steel, and 5% disposal as landfill. The resulting ECI costs for all designs are shown in Figure 50 and Figure 51. To maintain conciseness, detailed calculations are included in Appendix G. This section presents a summary of the ECI costs for the designs and column spacings, with calculations and graphs provided. Discussions and analysis are in Section 5.5.1.5.

The calculation methodology is as follows:

- Calculate ECI coefficients for each cross-section type using the EPD International software.
- Obtain the weight of steel for the entire structure and each specific type of steel from ETABS for every design.
- Multiply the kilograms of material used by the coefficients for each stage and category, then by the monetary cost to determine the total ECI cost in Euros.

5.1.1 Column Spacing 5 meters:

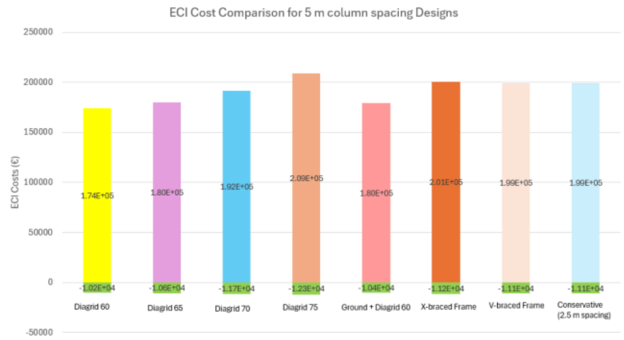

Figure 50: Resulting ECI Cost Calculations for 5 m Desings

5.1.2 Column Spacing 6 meters

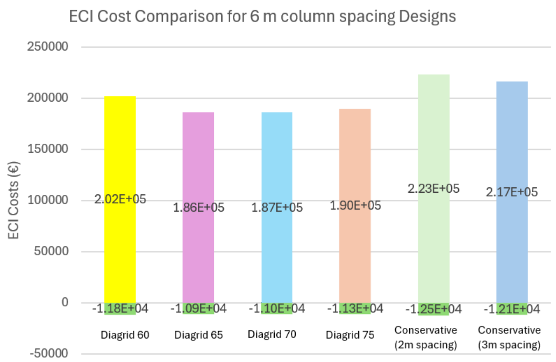

Figure 51: Resulting ECI Cost Calculations for 6 m Desings

All calculated ECI Costs are shown in Figure 52. 5- and 6-meter designs are all compared on the same graph. ECI values for every used design can be compared using results in Figure 52.

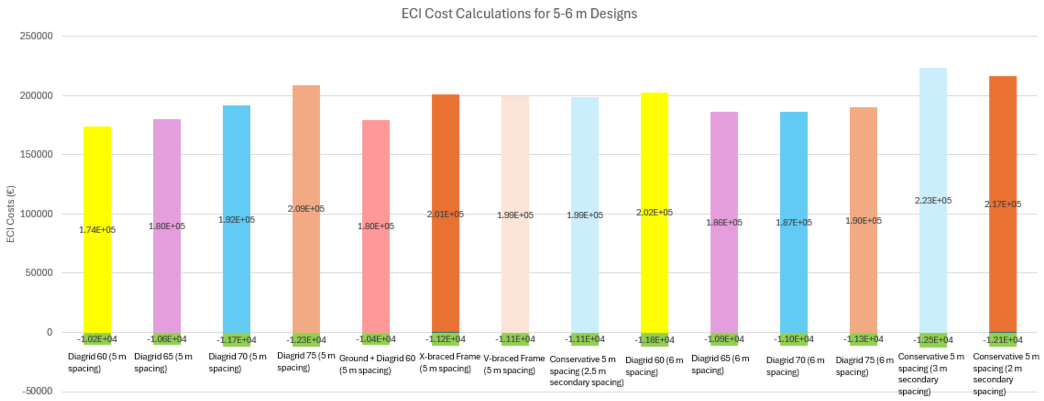

Figure 52: Resulting ECI Cost Calculations for all Accounted Designs

5.2 Demountability and Reuse Between Designs

The final resulting designs and their ECI costs are analysed in Section 5.1. The analysis highlights that demountability is the most critical factor influencing ECI costs for both initial and subsequent designs. This is primarily because reused materials in later designs incur no production ECI costs. This section examines the reusability of various designs, quantifying the percentage of material reuse to evaluate their sustainability.

To investigate, 4 main design types are investigated within each other: Design 1: Conservative Design, Design 2: Braced Design, Design 3: Ground+Diagrid Design and Design 4: Diagrid Design. Shown below in Figure 53, Figure 54, Figure 55 and Figure 56 are the selected designs, the optimal for each design is selected.

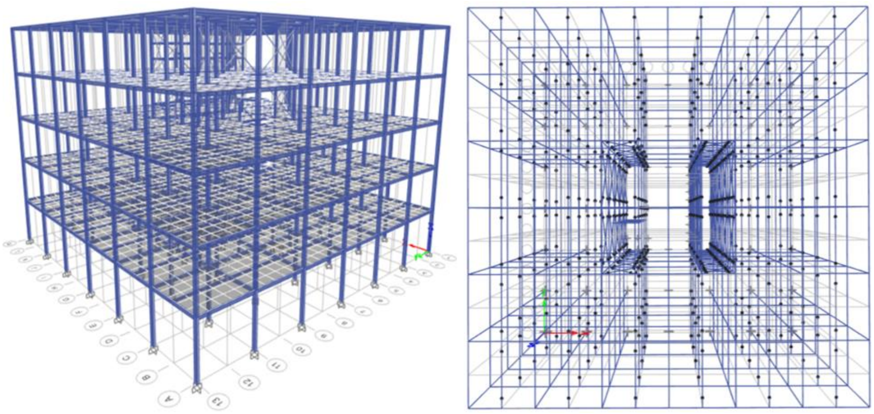

Figure 53: Design 1: Conservative (5m spacing) Design with Core

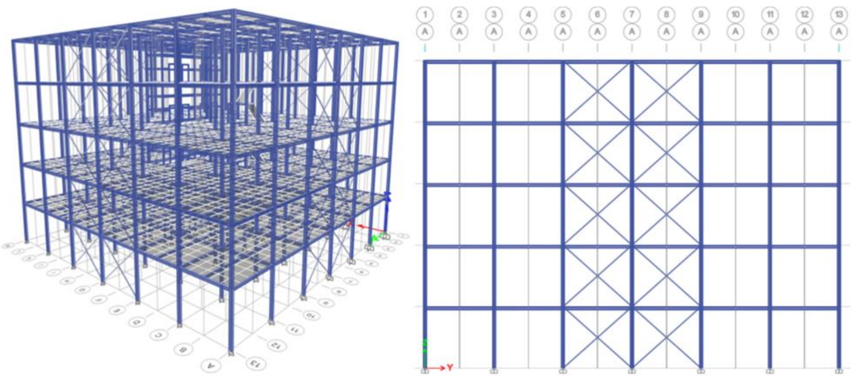

Figure 54: Design 2: X-Braced Design (5 m spacing: Middle Columns)

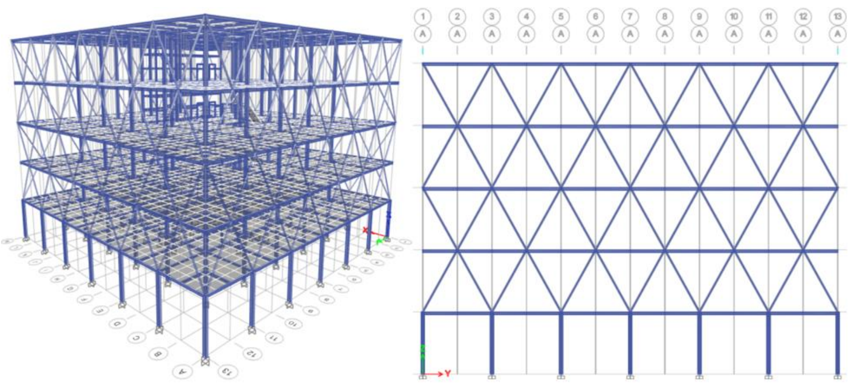

Figure 55: Design 3: Ground + Diagrid Design (5 m spacing: 60 Degrees)

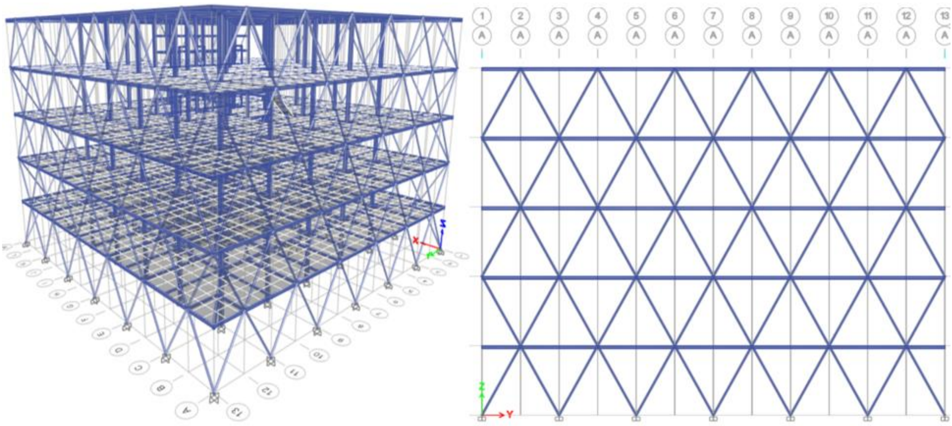

Figure 56: Design 4: Diagrid Design (5 m spacing: 60 Degrees)

Shown below in Table 18 are the steel uses of members for the given designs.

Table 18: ECI Cost for the Selected Designs

	ECI Cost (€)			
	Column	Beam	Braces (CHS)	Braces (Rod)
Conservative Design (5 m Spacing)	8.79E+04	1.01E+05	-	5.89E+02
X Braced Design (5 m Spacing: Middle)	8.65E+04	1.01E+05	-	6.67E+02
Diagrid Design (5 m spacing: 60 degrees)	5.36E+04	9.16E+04	1.87E+04	-
Ground +Diagrid Design (5 m spacing: 60 degrees)	6.33E+04	9.15E+04	1.43E+04	-

The models indicate varying levels of reuse potential among different designs. The bracing and column systems in Design 1 (Conservative Design) and Design 2 (X-Braced Design) show high reusability. Both designs use the same beam and column members (HEA220 and IPE220) and rod bracing with a diameter of 10 mm. The X-Braced Design uses slightly more rods and fewer columns, resulting in additional material when reused.

Similarly, the Diagrid Design and Ground+Diagrid Design feature similar diagrid angles and members. The Diagrid Design employs CHS diagrid braces of TUBOD159x4 mm, while the Ground+Diagrid Design uses TUBOD152.4x4 mm. Although the CHS members are slightly larger in the Diagrid Design, they are 100% reusable in the Ground+Diagrid Design. However, additional columns are needed to provide exterior support, increasing the ECI cost for columns.

Due to member similarities, demountability between design types is investigated starting from Design 1. The percentage of reuse and additional material costs are assessed for each subsequent design (2, 3, and 4) to evaluate demountability. This analysis assumes that similar members (e.g., HEA220 and HEA240, IPE220 and IPE240) are equivalent for both designs. This assumption maximizes demountability and reuse potential across different stability systems. In practice, engineers may reinforce existing members (e.g., HEA220) to meet new requirements (e.g., HEA240) rather than discarding them. Additionally, members are designed elastically, ensuring safety even if the lower member operates in the plastic range.

Demountability assessment for the various designs are explained more in detail in page 77, highlighting the reuse potential and additional material costs. Additionally, page 76 presents a graphical explanation of the reuse potential between stability systems.

Shown in red boxes are reused members and black boxes, non-reused members. Not all can be shown in the representation. Please also read descriptions. Explanations show what members are reused in between stability systems.

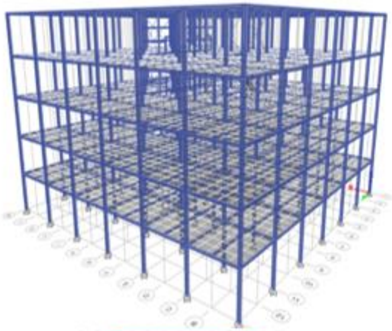

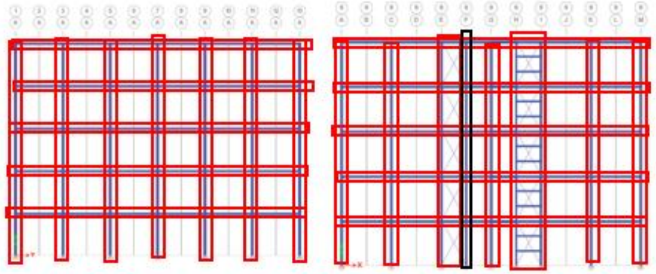

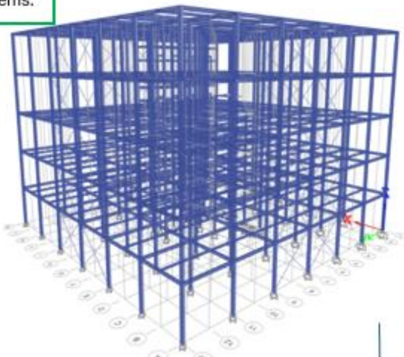

100% beam, 100% brace and 97.5% column reuse. Non-reused column is placed in the conventional system for core, no core hence no need. Braces for the core are reused on the exterior sections as X braced design with similar rod bracings. Additional Bracing is required.

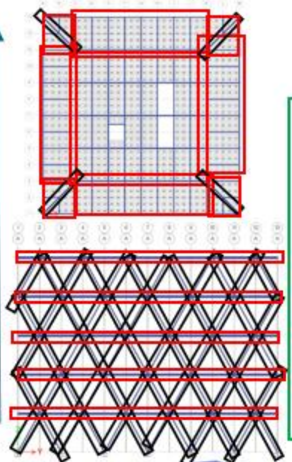

100% of columns, 95% of beams and 0% of diagrid members are reused. All interior columns are reused. Interior system is preserved to ensure optimal reuse between stability systems. All exterior diagrid CHS members are removed, and additional columns are placed instead. Additionally, braces and an additional column is required to design the core.

To ensure maximum reusability, same column spacing designs are selected.

Elevator shaft and stairs are always constant in the designs and reused for all.

Interior system is kept as similar as possible

All are done to see what the maximum reuse possibility between stability systems are.

It is assumed that similar members can be reused, 100% demountability is achieved and all demounted members are used for same secondary structure, no division.

67% of columns, 95% of beams and 0% of braces are reused. All interior columns are reused. Interior system is preserved to ensure optimal reuse. Starting from first storey, all exterior columns are not reused. There is no need for braces in Ground+Diagrid System. Additional beams (20xIPE270) and Diagrid Members are required.

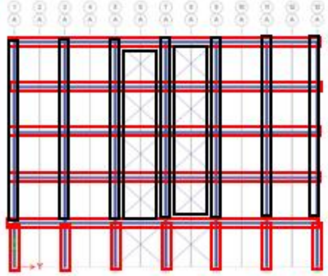

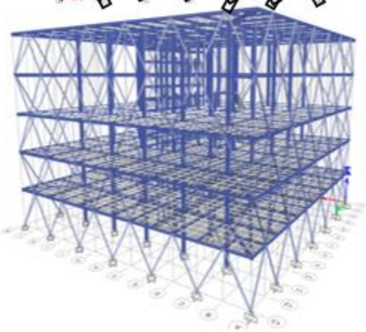

100% beam, and 100% diagrid members are reused. Interior system is kept consistent hence no changes. Bottom exterior columns are replaced with additional diagrid members.

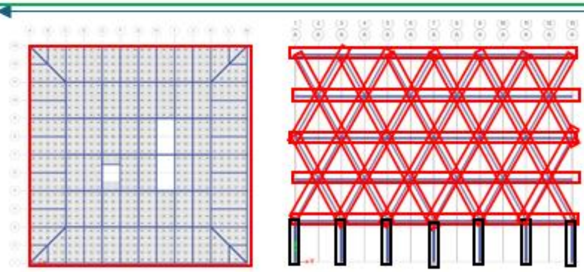

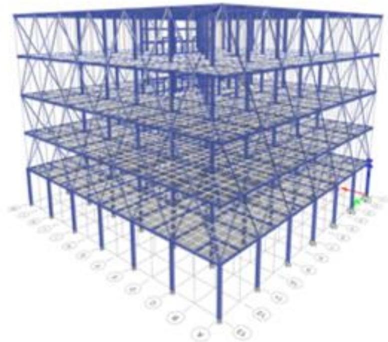

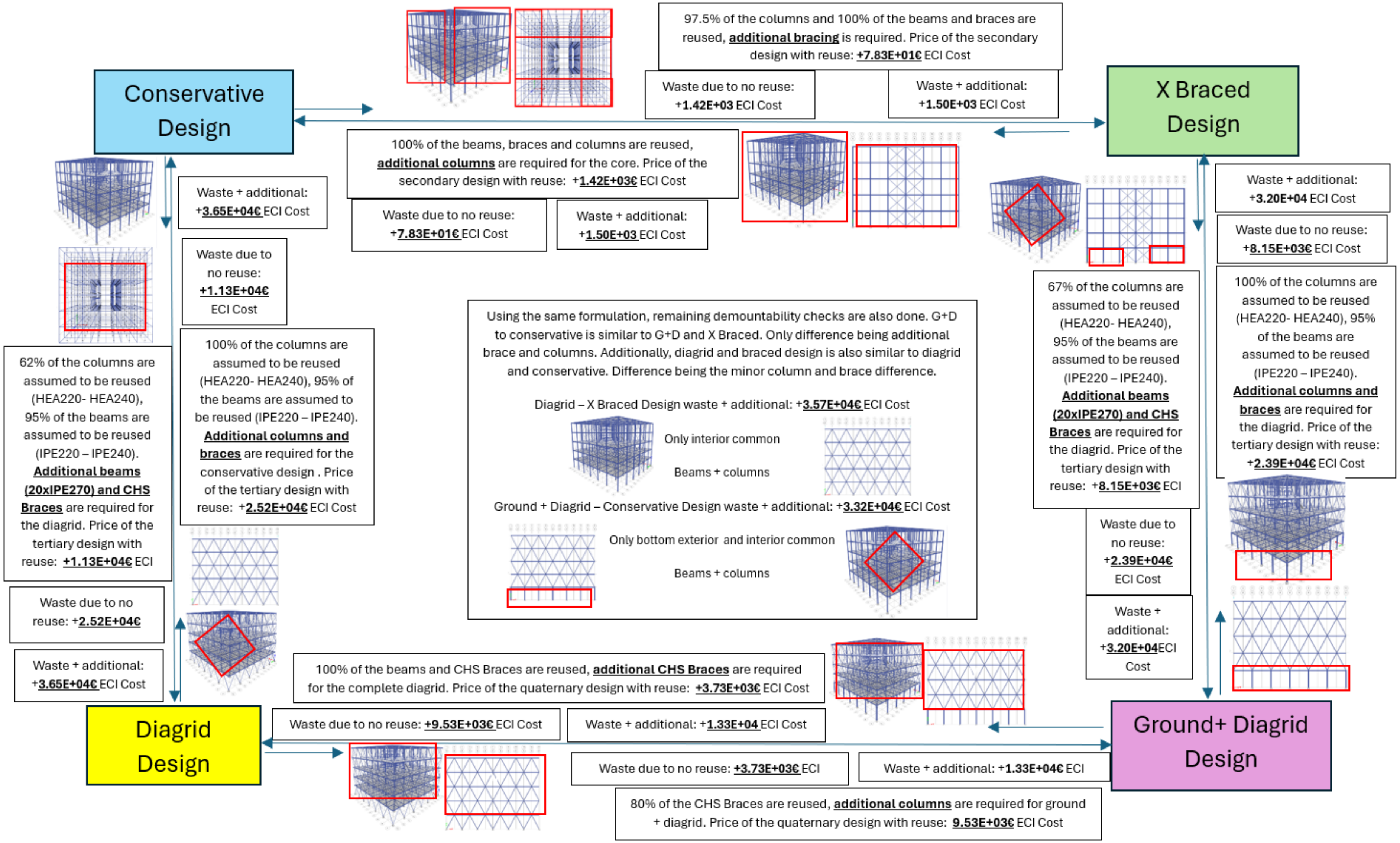

Conservative Design
X Braced Design
Diagrid Design
Ground+ Diagrid Design
97.5% of the columns and 100% of the beams and braces are reused, additional bracing is required. Price of the secondary design with reuse: +7.83E+01€ ECI Cost
Waste due to no reuse: +1.42E+03 ECI Cost
Waste + additional: +1.50E+03 ECI Cost
100% of the beams, braces and columns are reused, additional columns are required for the core. Price of the secondary design with reuse: +1.42E+03€ ECI Cost
Waste due to no reuse: +7.83E+01€ ECI Cost
Waste + additional: +1.50E+03 ECI Cost
Waste + additional: +3.65E+04€ ECI Cost
Waste due to no reuse: +1.13E+04€ ECI Cost
62% of the columns are assumed to be reused (HEA220- HEA240), 95% of the beams are assumed to be reused (IPE220 – IPE240). Additional beams (20xIPE270) and CHS Braces are required for the diagrid. Price of the tertiary design with reuse: +1.13E+04€ ECI
100% of the columns are assumed to be reused (HEA220- HEA240), 95% of the beams are assumed to be reused (IPE220 – IPE240). Additional columns and braces are required for the conservative design . Price of the tertiary design with reuse: +2.52E+04€ ECI Cost
Waste due to no reuse: +2.52E+04€
Waste + additional: +3.65E+04€ ECI Cost
Using the same formulation, remaining demountability checks are also done. G+D to conservative is similar to G+D and X Braced. Only difference being additional brace and columns. Additionally, diagrid and braced design is also similar to diagrid and conservative. Difference being the minor column and brace difference.
Diagrid – X Braced Design waste + additional: +3.57E+04€ ECI Cost
Only interior common
Beams + columns
Ground + Diagrid – Conservative Design waste + additional: +3.32E+04€ ECI Cost
Only bottom exterior and interior common
Beams + columns
Waste + additional: +3.20E+04 ECI Cost
Waste due to no reuse: +8.15E+03€ ECI Cost
67% of the columns are assumed to be reused (HEA220- HEA240), 95% of the beams are assumed to be reused (IPE220 – IPE240). Additional beams (20xIPE270) and CHS Braces are required for the diagrid. Price of the tertiary design with reuse: +8.15E+03€ ECI
100% of the columns are assumed to be reused (HEA220- HEA240), 95% of the beams are assumed to be reused (IPE220 – IPE240). Additional columns and braces are required for the diagrid. Price of the tertiary design with reuse: +2.39E+04€ ECI Cost
Waste due to no reuse: +2.39E+04€ ECI Cost
Waste + additional: +3.20E+04ECI Cost
100% of the beams and CHS Braces are reused, additional CHS Braces are required for the complete diagrid. Price of the quaternary design with reuse: +3.73E+03€ ECI Cost
Waste due to no reuse: +9.53E+03€ ECI Cost
Waste + additional: +1.33E+04 ECI Cost
Waste due to no reuse: +3.73E+03€ ECI
Waste + additional: +1.33E+04€ ECI
80% of the CHS Braces are reused, additional columns are required for ground + diagrid. Price of the quaternary design with reuse: 9.53E+03€ ECI Cost

5.3 Final Optimal Design

5.3.1 Resulting Design and Floor Plans

Figure 57 and Figure 58 illustrate the floor plan designs for the final structure. The elevator and stairs are centrally located to ensure accessibility. The office layout features open work areas, combining different workspaces without partitions. Toilets are included in the floor plans to accommodate the large number of occupants, addressing a critical functional requirement for offices.

These floor plans pertain to the current design iteration and are flexible since no structural members, except for the elevators and stairs, are fixed. The presented floor plans represent one of many potential interior design configurations, but the inclusion of elevator and stair designs is essential.

5.3.1.1 Floor Plans for Final Design

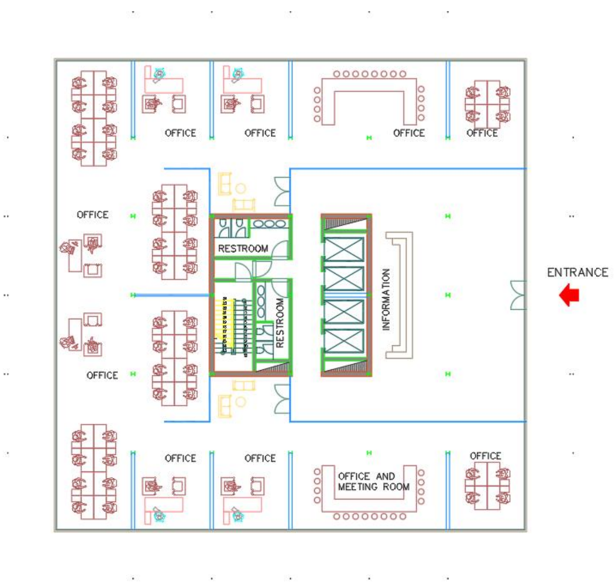

Figure 57: Floor Plan of ground floor

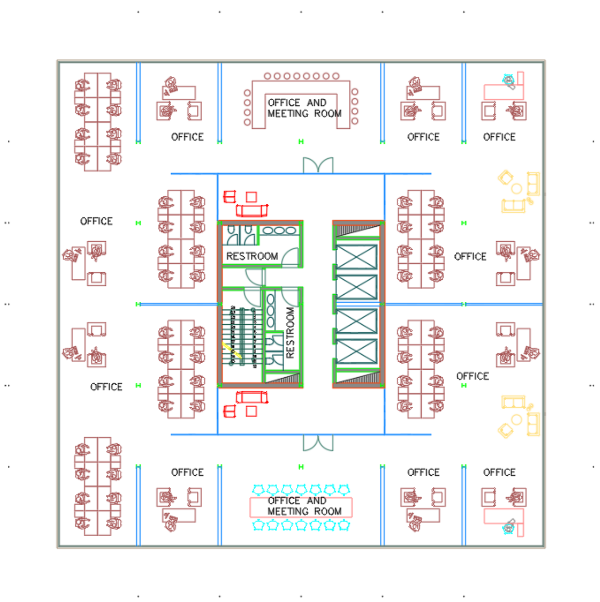

Figure 58: Floor plan of stories 2-4

5.3.1.2 Structural Design of the Final Design

Section 5.3.1.2 details the final structural design of the structure based on the floor plans in Figure 57 and Figure 58.

Figure 59 shows verification of the final Diagrid 60 design model, including the elevator shaft and stairs. All structural members have been validated. The stairs are modelled with a slab depth of 150 mm using C30/37 concrete. The stair shaft features IPE100 for door support, IPE120 for secondary beams, and IPE160 for the additional beam between the HEA100 columns supporting the elevators.

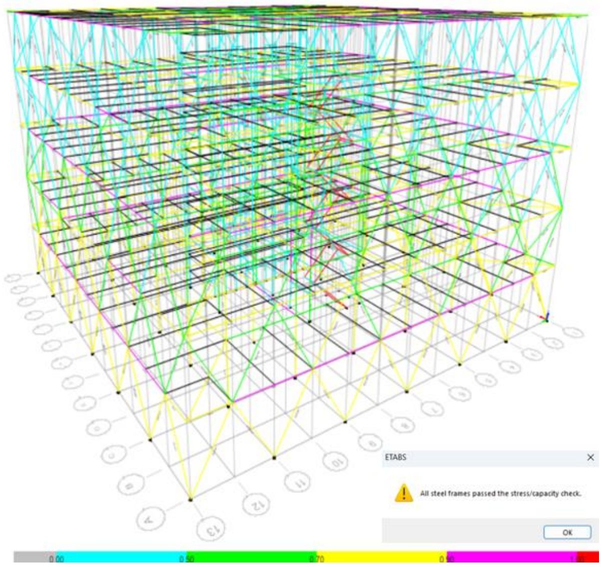

Figure 59: Verification of Final Version of Diagrid 60 with elevators and stairs

Figure 60 and Figure 59 present the final Diagrid 60 design model with extruded frames, providing a realistic depiction of the structural system's dimensions. Figure 61 illustrates the final floor plan for the Diagrid 60 model, noting that all floors are identical except for the base and roof. Roof access is not included in the design as it is an office building, hence the roof plan is consistent with Figure 40. The final ECI costs and steel weight for the optimal design are summarized in Table 19 and Table 20.

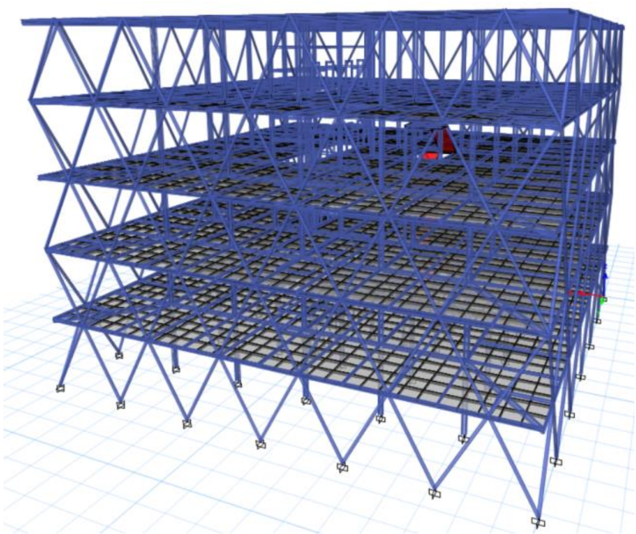

Figure 60: Final Structural Design with Stairs and Elevator Shaft and Extruded Frames in ETABS

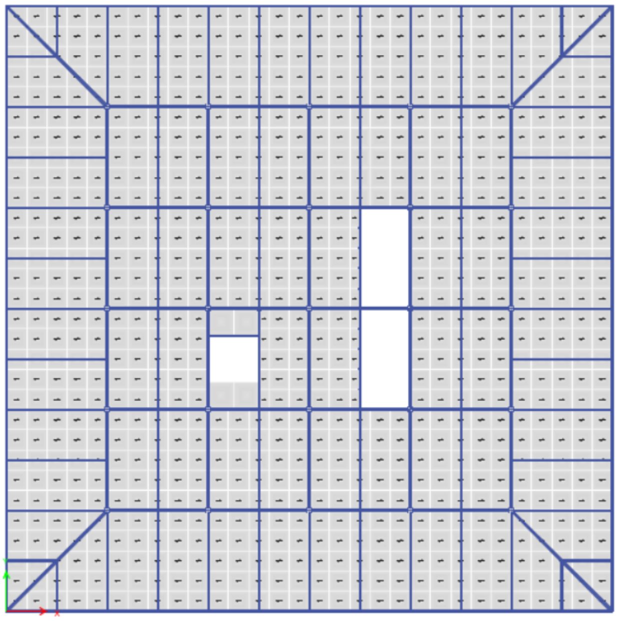

Figure 61: Final Resulting Floor Plans due to the addition of stairs and elevator shaft

Table 19: Diagrid 60 Final Design Resulting Steel Weight

Final Design	
Diagrid 60 (5 m) Final Design	
Beams (kN)	6.06E+02
Columns (kN)	3.55E+02
Braces (kN)	1.85E+02
Total Steel (kN)	1.15E+03

Table 20: Diagrid 60 Final Design Resulting ECI Cost and Calculations

Diagrid 60 Final Design					
Production Stage			End of Life Stage		
Beam	Braces (Diagrid)	Column	Beam	Braces (Diagrid)	Column
A1-A3	A1-A3	A1-A3	C1-C4	C1-C4	C1-C4
5.91E+03	1.41E+03	3.46E+03	2.79E+02	8.54E+01	1.63E+02
5.85E+03	1.35E+03	3.42E+03	2.89E+02	8.87E+01	1.69E+02
4.94E+01	4.70E+01	2.89E+01	-1.10E+01	-3.35E+00	-6.42E+00
6.65E+00	1.05E+01	3.89E+00	2.46E-01	7.52E-02	1.44E-01
1.61E-01	4.41E-02	9.42E-02	1.13E-02	3.45E-03	6.60E-03
1.80E+03	1.92E+02	1.05E+03	1.72E+02	5.13E+01	1.00E+02
4.15E+01	3.08E+00	2.43E+01	1.74E+00	5.31E-01	1.02E+00
1.01E+03	1.08E+02	5.90E+02	1.15E+02	3.36E+01	6.73E+01
1.80E+04	1.86E+03	1.05E+04	2.04E+03	5.96E+02	1.19E+03
3.12E+02	3.62E+01	1.82E+02	2.80E+01	8.24E+00	1.64E+01
1.75E-01	3.96E-02	1.03E-01	2.02E-01	6.17E-02	1.18E-01
1.21E+04	3.58E+03	7.09E+03	5.26E+02	1.61E+02	3.08E+02
5.18E+03	2.08E+02	3.03E+03	2.18E+01	6.68E+00	1.28E+01
9.16E+04	1.87E+04	5.36E+04	5.41E+03	1.63E+03	3.17E+03
	1.64E+05		Tot eol	1.02E+04	
Total ECI	1.74E+05	Demountable cost	1.64E+05	-1.02E+04	

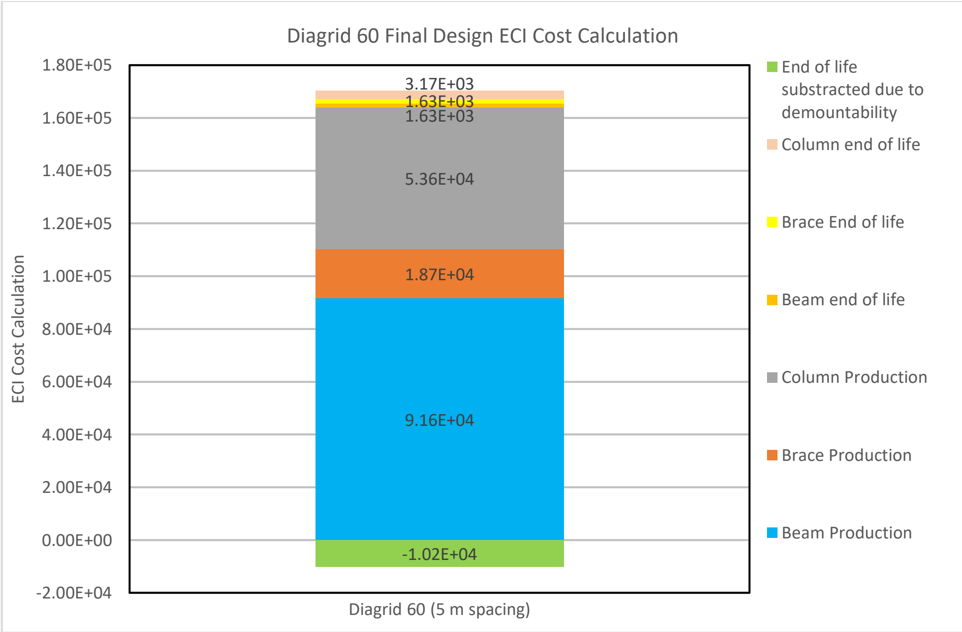

Figure 62: Resulting ECI Cost for Final Diagrid 60 Design

5.4 Tall Structures

The evolution of structural systems for tall buildings has prioritized efficiency and economy (Moon, 2008). As materials science advances, producing higher-strength materials, structural design is increasingly governed by stiffness requirements due to the imbalance between material stiffness and strength (Connor, 2003). To refine the framework, stability systems for tall structures have been rigorously tested to evaluate their performance under lateral loading and second-order effects. Achieving optimal deformation modes enables structural design to meet stiffness criteria with maximum efficiency, improving performance under second-order effects (Connor, 2003). This optimal deformation mode is achieved through the implementation of stability systems.

5.4.1 Stability Systems for Tall Structures

This section evaluates stability systems for tall structures, extending the analysis beyond the 5-storey, 22.5-meter-tall structures previously examined. While the optimal spacings, cross-sections, and diagrid angles identified for shorter structures remain applicable due to their height-independent principles, the geometric considerations for diagrid angles depend on width rather than height. Both literature and parametric studies consistently indicate that the optimal diagrid angle lies between 60 and 70 degrees, consistent with findings for shorter structures.

To assess the stability systems for tall structures, a 15-storey, 67.5-meter-tall steel multistorey office was designed. The optimal 5-meter beam and column spacing and 2.5-meter composite beam spacing from the conservative and diagrid structures were preserved. However, second-order effects required re-evaluation for this new structure. Table 21 illustrates the second-order calculations for the 67.5-meter structure.

Table 21: Second Order Checks for 15-Storey Steel Multistorey Office Structure

Frame Stability Check									
Stories	Height (mm)	δx (mm)	δy (mm)	Ved (kN)	Hedx (kN)	Hedy (kN)	α_{cr} (x)	α_{cr} (y)	
Story15	4.50E+03	1.64E+01	2.10E+01	2.85E+03	-1.86E+02	-1.83E+02	1.79E+01	1.37E+01	αcr<10 Second Order
Story14	4.50E+03	2.95E+01	3.91E+01	8.38E+03	-5.51E+02	-5.44E+02	1.00E+01	7.47E+00	αcr<10 Second Order
Story13	4.50E+03	4.20E+01	5.06E+01	1.39E+04	-9.08E+02	-9.02E+02	7.00E+00	5.78E+00	αcr<10 Second Order
Story12	4.50E+03	5.45E+01	6.16E+01	1.94E+04	-1.26E+03	-1.25E+03	5.35E+00	4.71E+00	αcr<10 Second Order
Story11	4.50E+03	6.68E+01	7.24E+01	2.50E+04	-1.60E+03	-1.59E+03	4.32E+00	3.97E+00	αcr<10 Second Order
Story10	4.50E+03	7.88E+01	8.28E+01	3.05E+04	-1.93E+03	-1.93E+03	3.62E+00	3.44E+00	αcr<10 Second Order
Story9	4.50E+03	9.02E+01	9.25E+01	3.60E+04	-2.26E+03	-2.25E+03	3.13E+00	3.04E+00	αcr<10 Second Order
Story8	4.50E+03	1.00E+02	1.01E+02	4.15E+04	-2.54E+03	-2.54E+03	2.75E+00	2.72E+00	αcr<10 Second Order
Story7	4.50E+03	1.09E+02	1.08E+02	4.71E+04	-2.79E+03	-2.79E+03	2.45E+00	2.47E+00	αcr<10 Second Order
Story6	4.50E+03	1.16E+02	1.13E+02	5.26E+04	-3.03E+03	-3.02E+03	2.22E+00	2.28E+00	αcr<10 Second Order
Story5	4.50E+03	1.22E+02	1.18E+02	5.81E+04	-3.24E+03	-3.23E+03	2.05E+00	2.13E+00	αcr<10 Second Order
Story4	4.50E+03	1.24E+02	1.18E+02	6.32E+04	-3.40E+03	-3.43E+03	1.95E+00	2.07E+00	αcr<10 Second Order
Story3	4.50E+03	1.26E+02	1.20E+02	6.91E+04	-3.62E+03	-3.61E+03	1.87E+00	1.96E+00	αcr<10 Second Order
Story2	4.50E+03	1.24E+02	1.20E+02	7.47E+04	-3.78E+03	-3.77E+03	1.84E+00	1.90E+00	αcr<10 Second Order
Story1	4.50E+03	7.80E+01	9.91E+01	8.02E+04	-3.90E+03	-3.89E+03	2.80E+00	2.20E+00	αcr<10 Second Order

The lowest value of α_{cr} is significantly less than 10, indicating that second-order effects must be incorporated into the design loads for the members. Significant deflections generate additional moments due to the eccentricity of axial load application points. The axial loads on columns are already substantial; hence, the deflection-induced moments at the member's base become significant.

Figure 63 - Figure 67 present the selected tested stability systems and verified design models for the tall structure. To streamline the presentation, only the best-performing model of each stability system is shown.

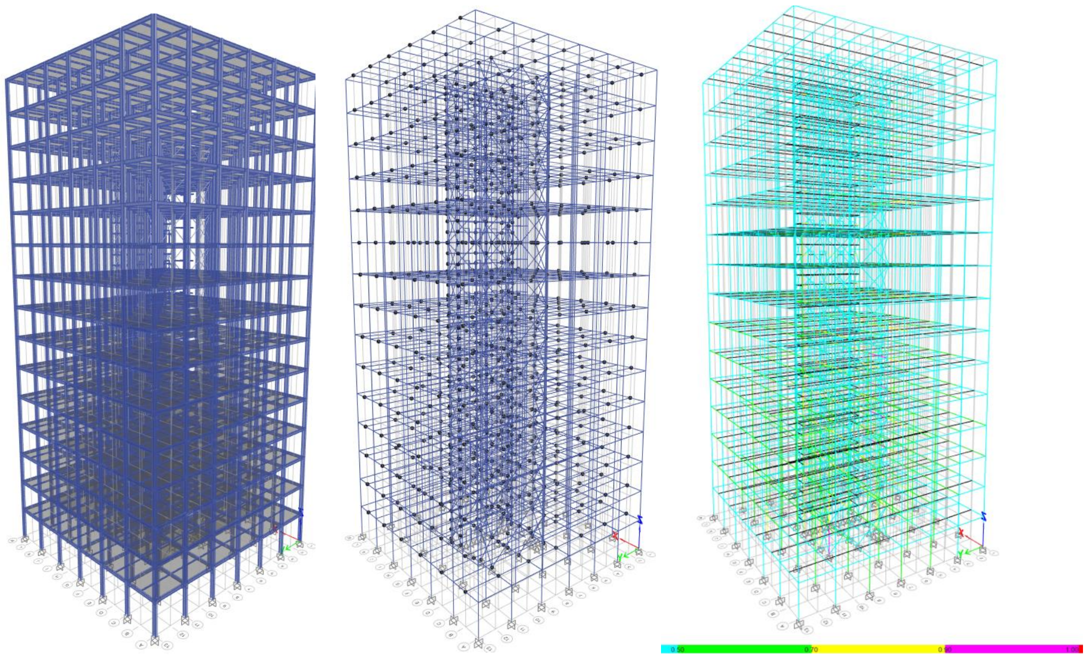

Figure 63: 15-Storey Steel Office Building Conservative Design with Core

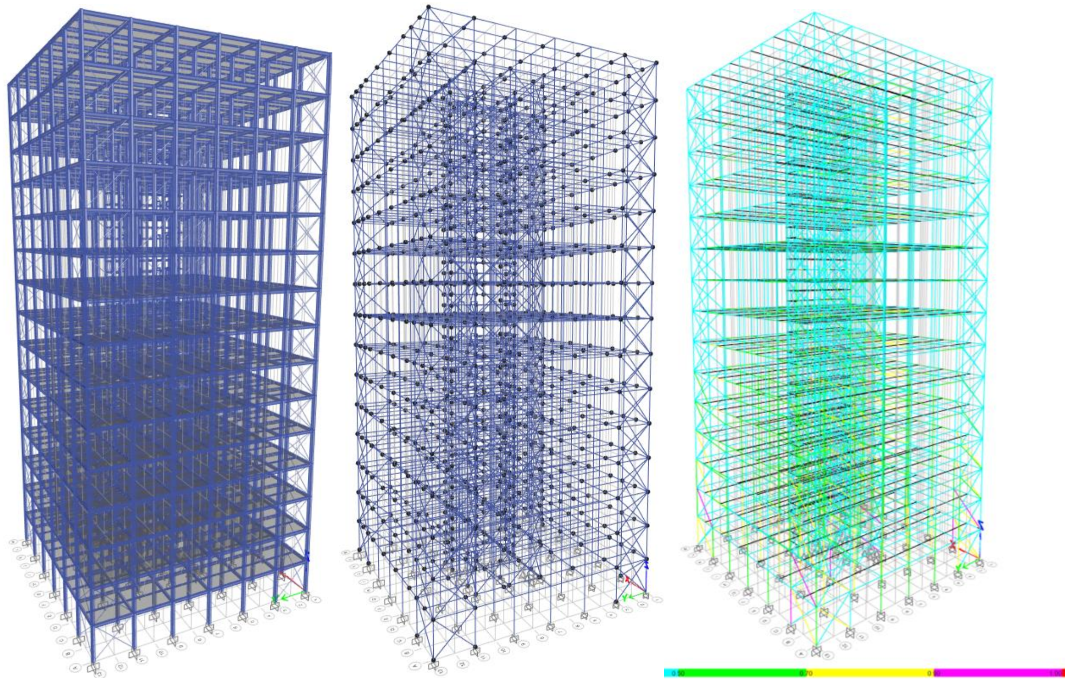

Figure 64: 15-Storey Steel Office Building X-Braced Frame with Core

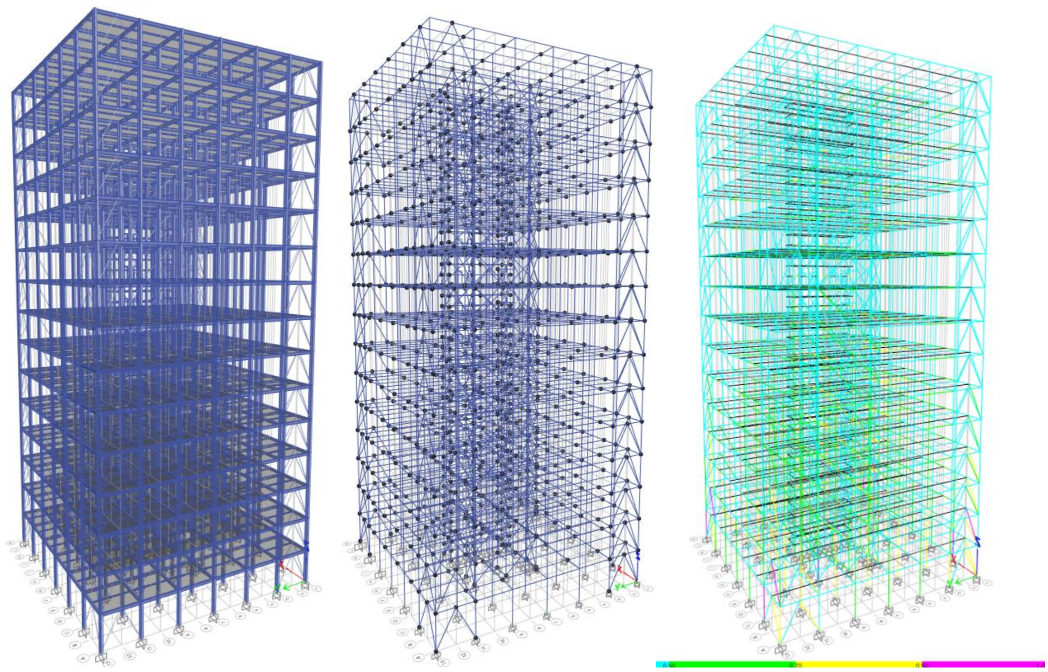

Figure 65: 15-Storey Steel Office Building V-Braced Frame with Core

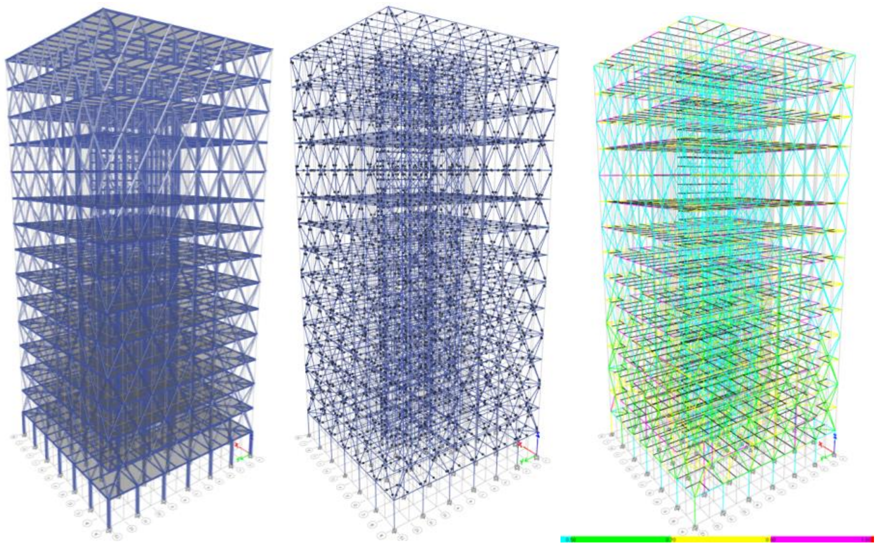

Figure 66: 15-Storey Steel Office Building Ground + Diagrid with Core

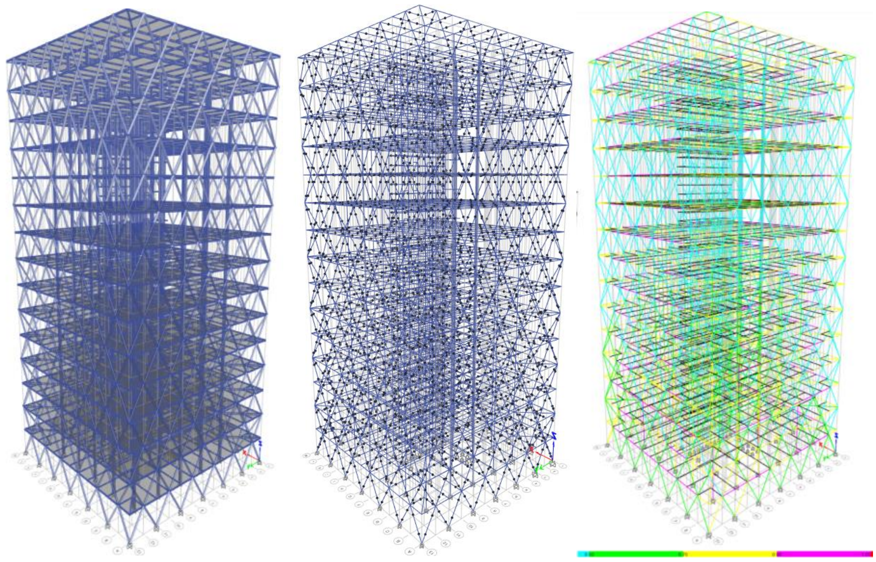

Figure 67: 15-Storey Steel Office Building Diagrid

Table 22 and Figure 68 present the resulting steel weight and ECI costs for the tested stability systems. Table 22 and Figure 68 summarizes all tested alternatives, including variations in location and the presence or absence of a braced core. The inclusion of second-order calculations underscores the enhanced performance of lateral stability systems.

Table 22: Resulting Steel Weight for Stability Systems 15-Storey Steel Multistorey Tall Structure

Column Spacing 5 m				
Model	Column (kN)	Beam (kN)	Braces (kN)	Total Steel (kN)
Conservative with Core	4.90E+03	3.75E+03	4.85E+02	9.14E+03
X Bracing and middle	4.90E+03	3.75E+03	4.88E+02	9.14E+03
X Bracing Sides + Core	4.39E+03	3.30E+03	4.13E+02	8.11E+03
V Bracing and middle	4.39E+03	3.77E+03	5.38E+02	8.70E+03
V Bracing Sides + Core	4.39E+03	3.30E+03	4.84E+02	8.18E+03
Diagrid 60	2.19E+03	1.80E+03	1.55E+03	5.54E+03
Diagrid 60 + core	2.37E+03	1.80E+03	1.60E+03	5.77E+03
Ground +Diagrid 60	2.60E+03	2.69E+03	1.25E+03	6.54E+03
Ground +Diagrid 60 + cor	2.50E+03	1.79E+03	1.67E+03	5.97E+03

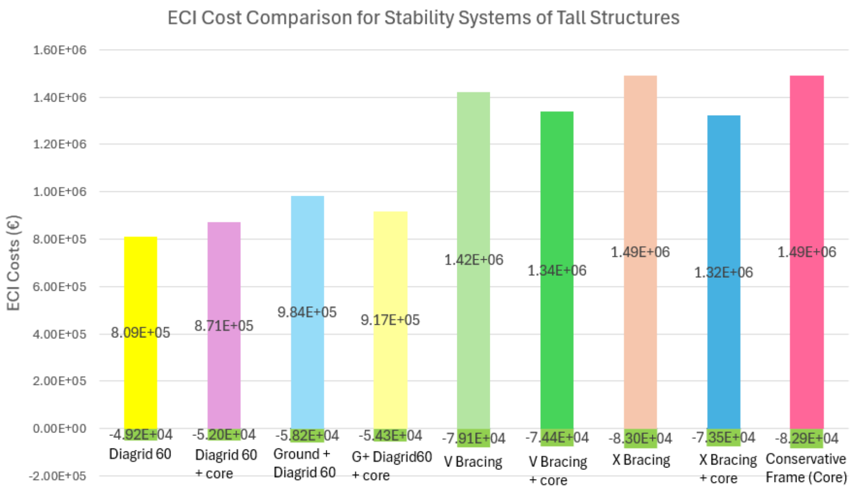

Figure 68: ECI Costs for Stability Systems for Tall Structures

The optimal stability systems were identified as Diagrid, Ground + Diagrid, V-Braced, X-Braced, and Conservative, respectively. Most optimal models, except for the Diagrid, included a core addition, which enhanced lateral stability and supported all exterior vertical columns. Braced structures without a core required substantial external bracing, optimally bracing 4 out of 6 column-beam frames. Testing different bracing locations and varying the number of braced frames showed that fewer braced locations led to critical columns and stress concentrations, necessitating thicker cross-sections. The inclusion of a braced core effectively shifted the structure's centre of mass, provided additional lateral bracing, and reduced lateral displacement and second-order effects, resulting in smaller cross-sections.

Beam cross-sections also influenced storey displacement. Optimized smaller beams resulted in larger column sections due to decreased self-weight, which increased storey displacement and second-order effects. Therefore, stronger beams performed better in the optimized structures, optimizing the steel weight.

The X-Braced Frame, V-Braced Frame, Ground + Diagrid Design, and Diagrid Design resulted in steel weight changes of +0.04%, -4.83%, -28.41%, and -39.39%, respectively, compared to the Conservative Frame with a braced core. However, adding a braced core improved the performance of the braced frames, reducing the steel weight by -11.26%, -10.48%, and -34.66% for the X-Braced, V-Braced, and Ground + Diagrid designs, respectively.

A similar pattern was observed in ECI costs, which were significantly influenced by cross-section choices and did not always align with steel usage. The ECI cost differences were +0.05%, -4.53%, -33.97%, and -45.75% for the X-Braced, V-Braced, Ground + Diagrid, and Diagrid Designs, respectively, compared to the Conservative Frame with a braced core. Implementing the braced core reduced ECI cost differences to -11.32%, -10.29%, and -38.51% for the X-Braced, V-Braced, and Ground + Diagrid designs, respectively, compared to the conservative design.

5.5 Discussions

5.5.1 Research and Results

This thesis examines the impact of various design choices on the Environmental Cost Indicator (ECI) and steel usage in steel structures. A parametric study was conducted to evaluate different design options, offering a comprehensive analysis of potential real-life scenarios. This approach enhances the understanding of design changes and enables the exploration of innovative design strategies.

The findings from this thesis are applicable to all the included types of structures, although the specific numbers and percentages for steel use and ECI cost will vary for each structure. Despite these variations, the principles identified in the analysis can be universally applied to any design within the scope of the studied structures, offering a general framework for optimization.

5.5.1.1 Design Choices and Optimization

Key design choices impacting material use and ECI cost include:

- Column and Beam Spacing
- Secondary (Composite) Beam Spacing
- Cross-section Selection
- Selection of Stability (Load Bearing) Systems
- Connections and End-of-life and Reuse of a structure

To optimize these design selections, various models were developed and tested. These design choices are interdependent; for instance, column spacing, beam spacing, and span directly influence each other. Composite beam spacing depends on the primary beam and column spacing. While several composite beam spacings can be tested within the primary beam spacings, certain spans (e.g., 6 m) preclude testing of intervals like 4 m or 2.5 m.

To capture all relevant details, distinctive designs were developed by combining different spacings. Stability systems significantly affect design selections, especially with diagrids, where load-carrying members change due to the elimination of exterior columns. This results in two different load-carrying systems: interior columns and exterior bracings. The location where diagrid nodes meet the beams changes on each floor within a given interval, aligning with composite spacings.

Over 50 different models were tested to examine the effects of diagrids with varying angles and composite spacings. Varying diagrid angles were tested and found less effective. Models with 10 m column spacing used significantly more steel compared to more optimal models. All braced models, irrespective of location, showed consistent material use due to the tested structure being 'short'.

Optimization involved testing all models and combining the most effective design choices to achieve optimal designs. The effects of each choice on steel use and ECI cost were evaluated, with increasingly optimal models tested to identify the best design for the current study. Although the final design changes across different scenarios, the underlying principles remain consistent. Each tested section thus presents generalized results applicable to all types of accounted structures.

5.5.1.2 Optimal Spacings and Cross-sections

Optimal spacings were derived from five primary models based on a 30x30 m floor plan, resulting in column spacings of 3, 4, 5, 6, and 10 meters. Each spacing was designed under consistent load conditions, selecting the most critical cross-sections within $0.8 < U.C. < 1.0$. The tested models revealed that increasing column spacing and beam span results in:

- Fewer columns, but thicker cross-sections
- Increased span for beams, and thicker beam sections

This trend is intuitive, but determining the optimal spacing is more complex. Tests showed that for designs with primary and secondary beams, minimizing beam steel weight is crucial, as both span and spacing lead to thicker beam sections. The number of beam sections is significantly higher than columns, indicating that the lowest possible column spacing minimizes material use. However, the framework is developed for office needs, requiring open spacings for functional requirements. Consequently, 3-meter column spacing was eliminated due to minimal open space and slight steel weight savings. The 10-meter spacing significantly increased material usage, making it less optimal. The 5-meter spacing was identified as the most optimal, with 6-meter spacing also performing adequately, warranting further testing with stability systems and design variations.

For composite beams, the optimal scenario reverses. Within the recommended maximum of 3.5-meter spacings, the highest spacings performed best. The cross-sections did not change significantly across different spacings, with most composite beams being IPE140 or IPE160. Minimizing cross-sections within 1-2 meters resulted in adding another cross-section rather than using smaller beams. Future studies could explore changes in concrete use.

Cross-section types significantly impact steel weight if not selected correctly. Recommended cross-sections are IPE for beams, HE and IPE for columns, and circular hollow sections for diagrid braces. The most optimal cross-sections, tested close to 1.0 U.C., revealed the following:

- IPE sections performed best for beams due to depth being more critical than thickness.
- HE sections had excessive thickness for the required depths for beams.
- For columns, thickness was more critical, and IPE sections had excessive depths, resulting in more steel use. HEA sections were found to be the most optimal.
- Hollow Sections (CHS) were optimal for diagrid braces due to member orientation and torsion. RHS and SHS performed less effectively due to symmetry and edge inefficiencies. The orientation angle of SHS and RHS also affects optimization, making CHS sections the best choice.

These principles apply universally to similar scenarios, ensuring consistent optimal cross-sections for all steel structures, excluding special beams for cases like movable cranes.

5.5.1.3 Stability Systems

Stability systems are classified into two categories: short structures and tall structures. This classification is based not on height or width but on the presence of second-order effects on the structural loading. The initial step in evaluating each stability system involves checking the frame stability to assess frame movement and the impact of load eccentricity on cross-sections.

Short structures and tall structures have different critical loading points. Short structures are primarily loaded in the interior columns due to occupancy loads, while tall structures are loaded in the exterior columns due to lateral loads and second-order effects. This distinction leads to different design approaches for each type.

Short structures were the focus of the parametric study, where frame displacement was not critical enough to warrant the inclusion of second-order effects. Despite the critical loading on middle columns, stability systems were tested for optimal designs, including diagrid with various angles, ground plus diagrid, X and V-braced frames, and conventional frames.

- **Diagrid Systems:** Perform best within the 55–75-degree range, with 60 degrees being optimal for the final model. Diagrids excel due to their ability to separate inner and outer designs, optimizing exterior members.
- **Conservative Design:** Sufficient for short structures as long as the exterior system is not overloaded. This design is efficient since the interior system remains consistent across different structures.

- **Braced Frames:** Commonly used in areas prone to earthquakes and high winds. Braced frames are less efficient for short structures where lateral loads are non-critical. The additional bracing material adds unnecessary weight, which can be avoided.

An inclusive parametric study requires testing tall structures where frame displacement necessitates incorporating second-order effects. In this context, frame stiffness becomes as critical as, if not more critical than, strength. Effective resistance to lateral loads and displacement is essential, with self-weight and core stability significantly impacting overall design stability. Beams become critical members, enhancing self-weight and improving the lateral resistance of columns. Exterior columns are increasingly critical due to higher wind loads, while braces and diagrids show greater effectiveness in load resistance. Various stability systems, including the optimal diagrid, ground plus diagrid, X and V-braced frames, conventional frames, and designs with additional braced cores, were evaluated for optimal performance.

- **Diagrid Systems:** Perform optimally within the 55–75-degree range, with 60 degrees being ideal for the final model. Diagrids are highly effective in resisting both lateral and vertical loads, and the angled beams connecting the exterior frame to inner columns reduce overall storey displacement and second-order effects.
- **Conservative Design:** Becomes less effective for tall structures as cross-sections thicken, reducing efficiency. Even with a braced core, significant thickening of frame members indicates the need for an exterior load-resisting stability system at greater heights.
- **Braced Frames:** While effective for tall structures, braces alone are insufficient. Without a stable (braced) core, lateral displacement increases significantly, requiring thicker frame members. Although braces alone offer limited improvement over conservative designs, the performance of V- and X-braced frames improves considerably with a braced core.

In summary, diagrids offer benefits for both short and tall structures due to their system separation and second-order load handling. Braces are essential for tall structures but less effective for short ones. Conservative designs work until second-order effects and lateral loads become significant.

Additionally, the reuse potential and ECI costs for subsequent designs were analysed. This analysis revealed that conservative and braced structures are more easily reusable, resulting in lower subsequent ECI costs due to their highly reusable sections and conventional designs. Ground Diagrid and Diagrid designs show lower reuse potential with each other, and the cost is closer to that of an actual building when compared to conventional and braced designs. Although reuse can eventually occur due to demountable members, it requires a longer time span. Consequently, braced and conservative designs are labelled as yellow, rather than orange or red, in the framework.

5.5.1.4 Demountability

Demountability is crucial for two types of connections: composite slab connections and steel-to-steel connections. This thesis does not delve into composite research as it is already a well-explored topic. Correct orientation of composite beams and slabs, combined with 22 mm oversized holes filled with resin, achieves 95% demountability.

Steel-to-steel connections, particularly in complex designs like diagrids, require more intricate solutions. Three different connection types are designed to address key factors. For beam-to-column connections, three main considerations are:

1. **Avoiding Welds**: Welding between members creates undesirable stress concentrations and is not demountable. High heat from welding also disturbs the cross-section at weld locations.
2. **Minimizing Drilling:** Drilling cross-sections should be minimized. Bolted connections are preferred for ease of calculation, well-known codes, and production practicality. While columns may need to be drilled for bolted connections, beam-to-beam and column-to-column connections can be achieved without drilling the cross-section.
3. **Connection Types:** Cleat connections are avoided to prevent drilling both members. End plates are used where possible, connecting plates are used when end plates are not feasible. Plates welded to plates do not affect demountability since they can be disassembled and reused. Fin plates for the connection designs are not found feasible due to drilling of beams.

For demountability, designs must also be elastic to facilitate reuse. These principles ensure the structure and connections are demountable. Demountability increases material use due to the need for elastic design. However, the Environmental Cost Indicator (ECI) calculations reveal both short- and long-term benefits. This thesis considers ECI for production (A) and end-of-life (C) stages. Demountability reduces end-of-life costs, effectively making the ECI cost the production cost of the cross-sections, excluding construction and occupation. For subsequent structures, reused sections incur minimal production costs, bringing ECI at the production stage close to zero. If cross-sections are reused after the second structure, the ECI cost will mainly consist of construction and occupation, significantly improving overall sustainability.

5.5.1.5 ECI Cost

To discuss the results, ECI Cost calculations must be conducted for all cross-sections being compared. This is necessary because ECI cost does not always correlate with material weight, occasionally altering the ranking of results. While these differences do not significantly impact the optimal design, it is essential to investigate which stability systems are more ECI cost-efficient. Table 23 presents the ECI costs for each cross-section type used in the designs.

Table 23: ECI Cost Calculations for 1 kg of all cross-section types

IPE/HE/UPE			CHS tube			Steel Rod Bracing		
Production	EOL	Demountable	Production	EOL	Demountable	Production	EOL	Demountable
9.56E-02	4.51E-03	9.56E-02	7.46E-02	4.52E-03	7.46E-02	1.46E-01	5.17E-03	1.46E-01
9.47E-02	4.68E-03	9.47E-02	7.16E-02	4.69E-03	7.16E-02	1.46E-01	5.16E-03	1.46E-01
7.99E-04	-1.77E-04	7.99E-04	2.49E-03	-1.77E-04	2.49E-03	5.09E-04	1.73E-05	5.09E-04
1.08E-04	3.98E-06	1.08E-04	5.55E-04	3.98E-06	5.55E-04	4.92E-05	1.33E-06	4.92E-05
2.60E-06	1.82E-07	2.60E-06	2.34E-06	1.82E-07	2.34E-06	1.88E-06	2.46E-07	1.88E-06
2.91E-02	2.78E-03	2.91E-02	1.02E-02	2.72E-03	1.02E-02	3.66E-02	1.99E-03	3.66E-02
6.72E-04	2.81E-05	6.72E-04	1.63E-04	2.81E-05	1.63E-04	1.34E-06	6.45E-06	1.34E-06
1.63E-02	1.86E-03	1.63E-02	5.70E-03	1.78E-03	5.70E-03	2.20E-02	3.00E-03	2.20E-02
2.91E-01	3.30E-02	2.91E-01	9.84E-02	3.16E-02	9.84E-02	3.82E-01	5.19E-02	3.82E-01
5.04E-03	4.53E-04	5.04E-03	1.92E-03	4.36E-04	1.92E-03	6.10E-03	6.96E-04	6.10E-03
2.84E-06	3.27E-06	2.84E-06	2.10E-06	3.27E-06	2.10E-06	9.74E-06	4.17E-09	9.74E-06
1.96E-01	8.51E-03	1.96E-01	1.89E-01	8.51E-03	1.89E-01	2.39E-01	9.56E-03	2.39E-01
8.39E-02	3.54E-04	8.39E-02	1.10E-02	3.54E-04	1.10E-02	7.90E-03	5.66E-05	7.90E-03
Total ECI	1.57E+00	1.48E+00	Total ECI	1.07E+00	9.88E-01	Total ECI	2.12E+00	2.01E+00

Based on the calculations, CHS tube sections have a slightly lower ECI cost in Euros compared to IPE, HE, or UPE sections, while steel rods have a slightly higher ECI cost. Rods, used only as bracings for frames, are not substitutes for IPE or CHS sections and are not used excessively in designs. Despite their higher ECI cost, rods remain advantageous in braced designs where significant lateral displacement occurs.

CHS sections replace exterior HE columns in diagrid designs, and the difference in ECI cost between cross-sections can be attributed to production methods. I/H beams in cold-rolled production require fixing and welding at two connected locations, whereas CHS sections only have one connection. Although hot rolling uses significant energy, it is preferred due to fewer defects and the absence of welding. I and H sections are initially produced as filled rectangular sections and then trimmed with high heat. In contrast, CHS sections are rolled around a tube and fabricated in a single heating process, resulting in a lower ECI cost.

This difference in ECI cost explains why several diagrid designs outperformed conservative designs in terms of ECI Costs. Material use alone does not always correlate with the environmental impact of a design, highlighting the importance of accounting for ECI costs.

5.5.1.6 Framework

The framework integrates all previously discussed sections, providing a comprehensive guide for designing the most optimal multistorey steel office structure. This framework serves as both a representation of the results and a practical tool for engineers. By generalizing the findings without specific numerical values, it enables engineers to design more efficiently, optimizing material use and minimizing ECI cost.

5.6 Framework

Two distinct frameworks have been developed from the thesis analysis. The first framework leverages all previously discussed tests, examining column spacing, beam and composite beam spacings, cross-section selection, diagrid angle, and choice of stability system for both steel use and ECI Cost. This case-specific framework includes percentages indicating ECI Costs added or subtracted based on design choices. Comparisons are made with conventional or optimal designs, as detailed in Sections 4 and 5. For tall structures, design choices are presented using tall structural models and relevant sources from the literature review. In this framework, a negative %ECI indicates a beneficial design choice, while a positive %ECI is disadvantageous.

The numbers in the case-specific framework are unique to each design, but the underlying principles universally aim to reduce ECI Costs. The second framework, without numerical values, uses a colour scheme to convey design recommendations: red for designs to avoid, orange for caution, yellow for acceptable designs, light green for good designs, and green for optimal choices.

This second framework serves as a general tool for engineers, guiding them in selecting optimal design choices for material use and ECI Costs across various steel structures. While software analysis is still necessary for refining cross-sections and finalizing the structure, this tool aims to reduce the number of models required, streamlining the design process.

5.6.1 Case Specific Numbers

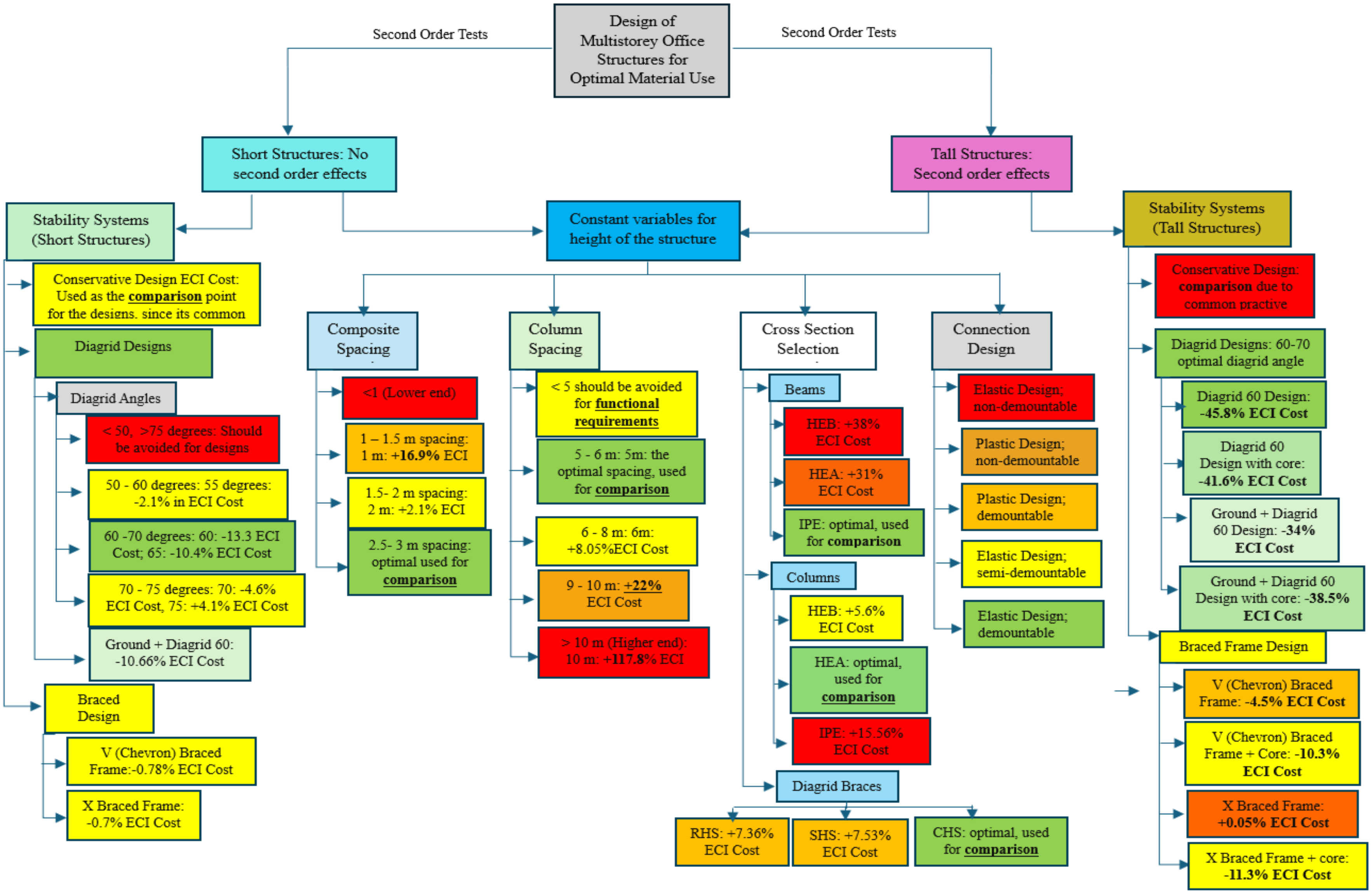

5.6.2 General Framework (Tool)

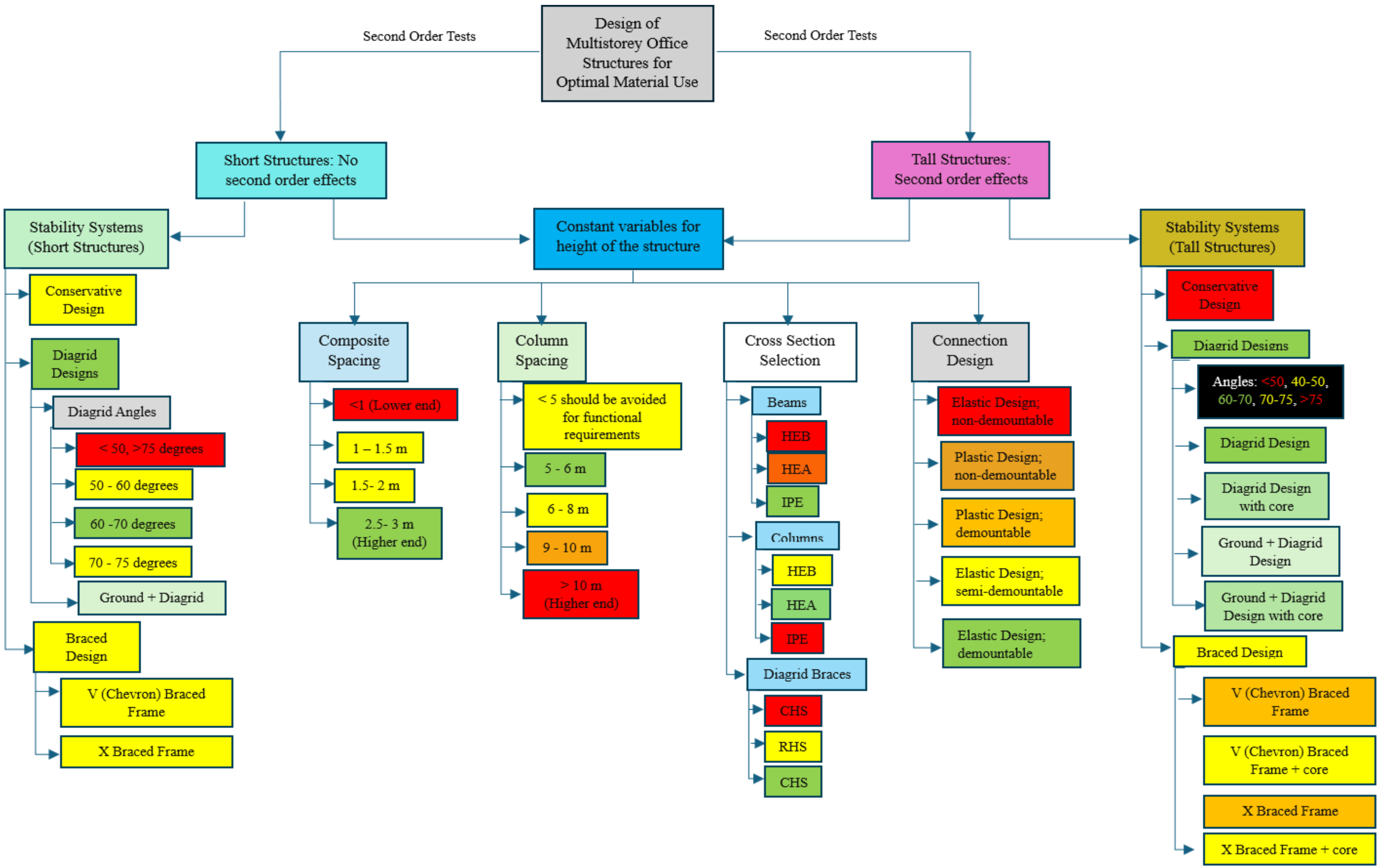

6 Conclusions and Recommendations

The thesis aimed to develop a framework to optimize the steel use and ECI Cost of multistorey steel office structures, focusing solely on steel stability systems. The central research question was:

- How can a step-by-step structural design framework for multistorey steel offices be developed to optimize structural steel use, reuse potential, and resulting ECI costs in comparison to conventional steel structures, by conducting a parametric study on a 5-storey 30x30m office building?

To address this, a parametric study was conducted on a 5-storey, 30x30m office structure designed for snow loads, wind loads, and live loads. Several design choices were identified and tested to reduce material use and ECI Cost:

- Stability Systems and their Reuse Potential
- Column Spacing
- Beam Spacing and Composite Beams
- Cross-Section Types
- Slab Type
- Connection Design

Over 50 models were developed to evaluate each alternative and combination. Key findings from the parametric study are summarized as follows:

Column Spacings:

- Column spacings of 3, 5, 6, and 10 meters were tested in the parametric study. The optimal spacings, ranked by performance, are 3, 5, 6, and 10 meters. The primary reason for this ranking is that increasing beam and composite beam spans require larger cross-sections, leading to greater steel use. While a 3-meter spacing reduces steel use by 5.7% compared to a 5-meter spacing, this reduction is not practical due to functional requirements. Generally, beams contribute more to steel weight than columns. Increasing column spacing increases beam spans, necessitating thicker sections. Compared to a 5-meter column spacing, 6-meter and 10-meter spacings increase ECI Costs by 8.05% and 117.8%, respectively.

Beam and Composite Spacings

- Beam and column spacings are interdependent variables. Composite beam spacings are determined by beam spacings, which are influenced by column spacings. For optimal steel weight, the highest feasible composite beam spacings should be used, typically 2-3 meters for 5 and 6-meter beam spacings. Composite spacings below 1 meter and above 3.5 meters should be avoided. Spacings of 1 meter and 2 meters result in additional ECI Costs of 16.9% and 2.1%, respectively, compared to 2.5-3-meter spacings.

Cross Sections:

- **Recommended Cross Sections**: Optimal cross sections for columns and beams are IPE, HEB, and HEA. For diagrid braces, RHS, SHS, and CHS are recommended due to their superior torsional resistance. Each member type was tested for optimal performance with cross sections selected based on proximity to a 1.0 Unity Check. The most optimal cross sections identified are IPE for beams, HEA for columns, and CHS for diagrid braces.

- **ECI Cost Comparisons:**
  - Using HEB and HEA sections for beams increases ECI Costs by 38% and 31% respectively, compared to IPE sections.
  - Using HEB and IPE sections for columns increases ECI Costs by 5.6% and 15.6% respectively, compared to HEA sections.
  - Using RHS and SHS sections for diagrid braces increases ECI Costs by 7.36% and 7.53% respectively, compared to CHS sections. The orientation of RHS and SHS sections is also critical for diagrid design verification.
- **Performance Analysis:** Larger but thinner cross sections generally performed better than smaller but thicker sections. However, IPE sections are less effective for columns, indicating that thinner sections are not always preferable.
- **ECI Cost Calculation:** Different cross sections have specific coefficients provided by manufacturers for ECI Cost calculations. The ECI Cost per kg of steel is 1.57€ for I/H sections, 1.07€ for CHS sections, and 2.12€ for steel rods.
- **Manufacturing Procedures:** The ECI cost differences are due to manufacturing processes. IPE/HE sections are produced by heating steel twice: first to shape the steel into a rectangular form, and second to cut the I/H shape. In contrast, CHS sections are produced by heating and rolling the steel around a cylinder, requiring only one heating process.

<u>**Stability Systems:**</u>

- **Focus and Selection**: This thesis investigates stability systems using solely steel. The selected systems include braced frames, conservative frames, and diagrid designs. Various configurations for X- and V-braced designs and different angles for diagrid designs were tested.
- **Optimal Spacings and Angles**: The optimal configuration for a conventional structure was found to be a 5 m column-beam spacing with a 2.5 m composite beam spacing. For diagrids, a 60-degree angle was optimal for the current design. However, the geometry of a structure significantly affects diagrid performance, with optimal angles generally falling between 60-70 degrees for different designs.
- **Comparison and Loading Conditions**: Stability systems were compared under identical loading conditions. Performance varies significantly with the height of the structure due to second-order effects. Tall structures are critically loaded by lateral forces and second-order effects, while short structures are more affected by occupational loads, making middle columns the most loaded.

  <u>**Short Structures**</u>:
- **Performance Analysis**: For short structures, conventional systems perform adequately, but diagrid designs show superior performance. The 60-degree diagrid design resulted in a 13.3% reduction in ECI Cost compared to the optimal conservative design. Diagrid designs excel due to their ability to separate the loading of exterior and interior sections, allowing for more precise optimization of cross-sections, thereby reducing steel use and ECI Costs. Braced systems are less effective for short structures as they primarily add braces to exterior columns without optimizing cross-sections.
- **Ranking and ECI Costs**: For short structures, the best-performing stability systems were Diagrid 60 and Diagrid 65, with ECI Cost reductions of 13.3% and 10.4%, respectively. Conservative designs outperformed several diagrids and similar to all braced systems in terms of steel use. The ECI Cost does not directly correlate with steel use due to varying ECI coefficients for different cross-sections. This discrepancy makes diagrid designs more favourable compared to conservative designs. For instance, Diagrid 70 had 5.37% and 4.67% more steel weight than the best conservative

and Diagrid 75 designs, respectively. However, ECI Cost calculations showed Diagrid 70 with 4.6% and 9.1% lower costs compared to conventional (2.5 m; 5 m) and Diagrid 75 designs, respectively.

Tall Structures:

- **Performance Analysis**: Diagrid designs and their variations demonstrate superior performance for tall structures compared to braced and conservative designs. The 60-degree diagrid design achieved a 45.75% reduction in ECI Cost compared to the optimal conservative design. Diagrids are highly effective in resisting both lateral and gravity loads, significantly contributing to structural stiffness, reducing steel use, and lowering ECI Costs. While braced systems are effective for tall structures, their performance improves with the addition of a core, which enhances lateral stability, reduces lateral displacement, and distributes loads more evenly between inner and outer columns.
- **Ranking and ECI Costs**: Among stability systems for tall structures, Diagrid 60 is the top performer, with a 45.75% reduction in ECI Cost compared to the conservative design. The Ground + Diagrid design also outperforms conservative and braced systems, achieving ECI Cost reductions of 33.97% without a core and 38.51% with a core. X- and V-braced frames show similar performance, but V-bracing is more favourable without a core. ECI Cost changes for X- and V-braced frames are +0.05% and -4.53% without a core, and -11.32% and -10.29% with a core, respectively, compared to the conservative design.

Demountability

- **Elastic Design and Feasibility**: Demountability initially increases steel use due to the requirements of elastic design. However, the end-of-life ECI cost is subtracted from the total ECI cost. For secondary structures reusing these disassembled members, the production ECI cost can be assumed zero, significantly reducing the overall ECI Cost. If members are designed to be demountable again after the second structure, the production ECI cost remains zero. Hence, demountability is critical for ECI Cost efficiency.
- **Composite Slabs**: Demountability begins with composite slabs. For the composite connection to be demountable, 22 mm oversized bolt holes filled with resin are necessary for initial settlement and safe demountability. These oversized holes ensure 95% demountability in composite slabs. Bolted connectors are preferred over welded headed stud connectors as they require fewer bolts, resulting in fewer critical locations for demountability. Construction loading on the beams should be avoided, either by supporting the slabs during the concrete hardening phase or, preferably, by using prefabricated slabs.
- **Steel Member Connections**: Demountable connections between steel members should also be achieved. Welding between members must be avoided, and the use of welds should be minimized. Three different connection possibilities have been selected from the diagrid design, given their unique and complex connections. Three demountable connection designs are provided to guide the principles and requirements of steel-to-steel demountable connections.
- **Impact on ECI Cost**: Only about 6% of the total ECI cost is subtracted due to demountability. While 6% might seem insignificant, the second design benefits from the remaining 94% becoming zero, highlighting the long-term benefits of demountability.

<u>Reuse between Stability Systems</u>:

- Conventional and braced designs, as well as diagrid and ground plus diagrid designs, exhibit high demountability and reuse potential within their respective categories.
- The highest reuse potential is observed between braced and conservative designs, achieving the lowest ECI Cost of 1.5E+03€.
- Diagrid designs have significantly lower reuse potential compared to conventional designs due to the specialized nature of diagrid members.
- The reuse potential from Ground+Diagrid to diagrid designs is higher than between braced or conventional designs, despite the additional columns, resulting in an ECI Cost of 1.33E+04€.
- Interchanging the main load-carrying systems significantly reduces reuse potential. The worst scenario is the transition from diagrid to conservative design, with an ECI Cost of 3.65E+05€.
- Reuse of diagrid designs is more challenging due to the use of uncommon sections. While they remain demountable, the time required for reuse will increase. However, they will ultimately be reused.

Contribution to Literature

This thesis aimed to address four significant gaps in the literature:

1. **Stability Systems for Short Structures**: There is a lack of significant analysis of stability systems for short structures in current research. This thesis addresses this by conducting a parametric study on short structural designs, testing braced frames, conservative frame designs, and diagrids. The findings reveal that diagrids, typically designed for tall structures, remain the most optimal for short structures as well.
2. **Optimal Member Spacing**: Existing literature and practice recommend intervals for member spacings, but there is no detailed analysis on the efficiency of different spacings within these intervals. This thesis contributes to the literature by testing various spacings (maximum, minimum, and intermediate values) and identifying the most efficient spacings for steel use. The study concludes that minimum column and beam spacing, along with maximum composite beam spacing, are the best for reducing steel weight and ECI Cost, within functional requirements.
3. **Cross-Section Selection**: While IPE, HEA, and HEB sections are commonly recommended for beams and columns, and SHS, RHS, and CHS sections for diagrid braces or angled columns, there is no consensus on the optimal cross-sections for steel use. This thesis fills this gap by testing all recommended cross-sections under identical conditions for different structural members. The results indicate that IPE sections are optimal for beams, HEA sections for columns, and CHS sections for diagrid braces and angled columns in terms of steel weight efficiency under the same loading conditions.
4. **Design Tool for ECI Costs and Material Use**: There is no existing design tool to help engineers optimize ECI Costs and material use during the design phase. This thesis develops a practical tool that can significantly reduce the time required for design by eliminating suboptimal designs before the modelling process. This tool also has the potential to improve or contribute to innovative design ideas.

Recommendations

This thesis can be enhanced in the future by incorporating several new elements:

- **Concrete in Slabs and Stability Systems**: While this thesis focuses on steel frameworks, future work could integrate concrete considerations, especially in composite structures and slabs, accounting for concrete thickness more comprehensively.
- **Occupation, Construction, and Transportation**: These are critical contributors to ECI Costs in the construction industry. Future research could develop frameworks that address the occupation phase, potentially lowering ECI Costs significantly. Buildings contribute 39% of global carbon emissions, with 28% from operational emissions. Addressing this could yield substantial improvements in ECI Costs.
- **Project Management**: Transportation and construction processes could be optimized in a future project management thesis. Effective route planning and supplier selection could reduce ECI Costs by minimizing fuel consumption.
- **Site Management**: Proper project planning and site management can reduce the need for construction machinery, further lowering fuel usage. This area could benefit from a guiding tool or framework similar to the one developed in this thesis.
- **Advanced Connection Methods**: Future analyses could include clamped and plug-in connections, exploring their potential for enhancing demountability and further optimizing construction practices.
- **Reuse potential of Stability Systems:** The thesis topic and research can be enhanced by incorporating reusability considerations. While reusability does not directly correlate with the ECI calculations made for stability systems, future research could potentially develop a method to integrate reusability into these calculations.

7 References

(No date) GPT-4 - OpenAI. Available at: https://openai.com/index/gpt-4/ (Accessed: 19 June 2024).

'Dufuerco Danish Steel: Rolled Steel Products' (2022) *EPD International* [Preprint]. Available at: https://environdec.com/library/epd5669 (Accessed: 16 April 2024).

'Environmental Product Declaration: Steel Beams' (2021) *EPD International* [Preprint]. Available at: https://environdec.com/library/epd2936 (Accessed: 18 April 2024).

'Seamless Hot Rolled Steel Tubes' (2022) *EPD International* [Preprint]. Available at: https://environdec.com/library/epd5359 (Accessed: 15 April 2024).

12 office design considerations that will increase your productivity at work (2023) *Bowens Interiors*. Available at: https://boweninteriors.com.au/office-design-considerations/ (Accessed: 17 April 2024).

Ali, M. M. and Moon, K. S. (2007) "Structural Developments in Tall Buildings: Current Trends and Future Prospects." Architectural Science Review, 50 (3): pp. 205–223.

Amato, A. and Eaton, K. (1998) "A comparative Life Cycle Assessment of Modern Office Buildings." The Steel Construction Institute, Berkshire.

Anwar, N. and Najam, F.A. (2017) *Structural cross-sections: Analysis and design*. Kidlington, Oxford: Butterworth-Heinemann.

Asadi, E., Li, Y. and Heo, Y. (2018) 'Seismic Performance Assessment and loss estimation of steel diagrid structures', *Journal of Structural Engineering*, 144(10). doi:10.1061/(asce)st.1943-541x.0002164.

Asif, M., Muneer, T. and Kelley, R. (2007) 'Life cycle assessment: A case study of a dwelling home in Scotland', *Building and Environment*, 42(3), pp. 1391–1394. doi:10.1016/j.buildenv.2005.11.023.

Blengini, G.A. and Di Carlo, T. (2010) 'The changing role of life cycle phases, subsystems and materials in the LCA of low energy buildings', *Energy and Buildings*, 42(6), pp. 869–880. doi:10.1016/j.enbuild.2009.12.009.

Boake, T.M. (2014) *Diagrid structures: Systems, connections, details*. Basel: Birkhäuser.

Brambilla, G. *et al.* (2019) 'Environmental benefits arising from demountable steel-concrete composite floor systems in buildings', *Resources, Conservation and Recycling*, 141, pp. 133–142. doi:10.1016/j.resconrec.2018.10.014.

Bruyn, S.M. de (2018a) *Environmental prices handbook 2017: Methods and numbers for valuation of environmental impacts*. Delft: CE Delft.

Cabaleiro, M. *et al.* (2023) 'Removable, reconfigurable, and sustainable steel structures: A state-of-the-art review of Clamp-based steel connections', *Sustainability*, 15(10), p. 7808. doi:10.3390/su15107808.

Catherine De Wolf. Material quantities in building structures and their environmental impact. PhD thesis, Massachusetts Institute of Technology, 2014.

Ceiling Height Office Specifications (no date) *Ceiling Height Office Specifications: Office Leasing in Japan*. Mori Building Co., Ltd.

Cho, Y.S. *et al.* (2012) 'LCA application in the optimum design of high rise steel structures', *Renewable and Sustainable Energy Reviews*, 16(5), pp. 3146–3153. doi:10.1016/j.rser.2012.01.076.

Cole, R.J., (1999) *'Building environmental assessment methods: clarifying intentions.'* Building Research and Information 27 (4/5), 230–246.

Connor, J.J. (2003). 'Introduction to Structural Motion Control', New York: Prentice Hall

Crawley, D., Aho, I., (1999) *'Building environmental assessment methods: application and development trends.'* Building Research and Information 27 (4/5), 300–308.

D'Amico, B. and Pomponi, F. (2018) 'Sustainability Tool to optimise material quantities of steel in the construction industry', Procedia CIRP, 69, pp. 184–188. doi:10.1016/j.procir.2017.10.006.

Dai, X. et al. (2022) '*Experiment and numerical modelling of a demountable Steel Connection System for Reuse', Journal of Constructional Steel Research*, 198, p. 107534. doi:10.1016/j.jcsr.2022.107534.

de Klijn-Chevalerias, M. and Javed, S. (2017). The Dutch approach for assessing and reducing environmental impacts of building materials. *Building and Environment*, 111, pp.147–159. doi:https://doi.org/10.1016/j.buildenv.2016.11.003.

Dimopoulos, C.A. and Gantes, C.J. (2008) 'Design of circular steel arches with hollow circular cross-sections according to EC3', *Journal of Constructional Steel Research*, 64(10), pp. 1077–1085. doi:10.1016/j.jcsr.2007.09.009.

Ding, G.K.C. (2008) 'Sustainable construction—the role of Environmental Assessment Tools', *Journal of Environmental Management*, 86(3), pp. 451–464. doi:10.1016/j.jenvman.2006.12.025.

Dixit M.K., Fernández-Solís J.L., Lavy S. and Culp C.H. (2012). *Need for an embodied energy measurement protocol for buildings: A review paper.* Renewable and Sustainable Energy Reviews, 16 (6), pp. 3730-3743.

Eco-costs emissions (2023) *Sustainability Impact Metrics*. Available at: https://www.ecocostsvalue.com/ecocosts/eco-costs-emissions/ (Accessed: 08 January 2024).

Embodied carbon (2022) *World Green Building Council*. Available at: https://worldgbc.org/advancing-net-zero/embodied-carbon/#:~:text=Buildings%20are%20currently%20responsible%20for,11%25%20from%20materials%20and%20construction (Accessed: 11 June 2023).

Faggiano, B. et. al. (2016). 'Appraisal of seismic design criteria for concentric bracing steel structures according to Italian and European codes.' *Ing. Sismica*, *33*, 42-50.

Fazlur R. Khan and Walter P. Moore. Tall Building Systems and Concepts. American Society of Civil Engineers, 1980.

Gan, V.J.L. *et al.* (2017) 'Developing a CO2-e accounting method for quantification and analysis of embodied carbon in high-rise buildings', *Journal of Cleaner Production*, 141, pp. 825–836. doi:10.1016/j.jclepro.2016.09.126.

Hauke, B. *et al.* (2016) *Sustainable steel buildings: A practical guide for structures and Envelopes*. Chichester, West Sussex: John Wiley & Sons, Ltd.

Holmes, J., Hudson, G., (2000) '*An evaluation of the objectives of the BREEAM scheme for offices: a local case study'. In: Proceedings of Cutting Edge 2000, RICS Research Foundation*, RICS, London.

Huberman, N. and Pearlmutter, D. (2008). A life-cycle energy analysis of building materials in the Negev desert. *Energy and Buildings*, 40(5), pp.837–848. doi:https://doi.org/10.1016/j.enbuild.2007.06.002.

Jani, K. and Patel, P.V. (2013) 'Analysis and design of diagrid structural system for High Rise Steel Buildings', Procedia Engineering, 51, pp. 92–100. doi:10.1016/j.proeng.2013.01.015.

Johnson, R.P. and Wong, Y.C. (2019) *Composite structures of steel and concrete: Beams, slabs, columns and frames for buildings*. Hoboken, NJ, USA: Wiley.

Kaethner, S. and Burridge, J. (2012) "Embodied CO2 of structural frames." The Structural Engineer, May, pp. 33-40.

Kamath, K. and Rao, A. (2012) 'A study on static and dynamic behavior of outrigger structural system for Tall Buildings', *Bonfring International Journal of Industrial Engineering and Management Science*, 2(4), pp. 15–20. doi:10.9756/bijiems.1655.

Kim, J. and Lee, Y. (2010) 'Seismic Performance Evaluation of Diagrid System Buildings', *The Structural Design of Tall and Special Buildings*, 21(10), pp. 736–749. doi:10.1002/tal.643.

Kim, S. and Kim, S.-A. (2020) 'Framework for designing sustainable structures through steel beam reuse', *Sustainability*, 12(22), p. 9494. doi:10.3390/su12229494.

Kyvelou, P., Gardner, L. and Nethercot, D.A. (2017) 'Design of composite cold-formed steel flooring systems', *Structures*, 12, pp. 242–252. doi:10.1016/j.istruc.2017.09.006.

Lempriere, M. (2023) *Steel industry makes 'pivotal' shift towards lower-carbon production*, *Carbon Brief*. Available at: https://www.carbonbrief.org/steel-industry-makes-pivotal-shift-towards-lower-carbon-production/ (Accessed: 11 January 2024).

Marique, A.-F. and Rossi, B. (2018). Cradle-to-grave life-cycle assessment within the built environment: Comparison between the refurbishment and the complete reconstruction of an office building in Belgium. *Journal of Environmental Management*, 224, pp.396–405. doi:https://doi.org/10.1016/j.jenvman.2018.02.055.

Milana, G., Gkoumas, K. and Bontempi, F. (2014) 'Sustainability Concepts in the Design of High-Rise Buildings: The Case of Diagrid Systems', in *Proceedings of the 3rd International Workshop on Design in Civil and Environmental Engineering*, pp. 170–179.

Moon, K. (2009). 'Design and construction of steel diagrid structures', *School of Architecture. Yale University. New Haven. USA*, 398-405.

Moon, K.S. (2008) 'Sustainable Structural Engineering Strategies for Tall Buildings', *The Structural Design of Tall and Special Buildings*, 17(5), pp. 895–914. doi:10.1002/tal.475.

N.d. *Sustainable steelmaking*. Available at: https://www.steel.org/wp-content/uploads/2021/11/AISI_FactSheet_SteelSustainability-11-3-21.pdf (Accessed: 03 January 2024).

Nidheesh, P.V. and Kumar, M.S. (2019) 'An overview of environmental sustainability in cement and steel production', *Journal of Cleaner Production*, 231, pp. 856–871. doi:10.1016/j.jclepro.2019.05.251.

Nijgh, M.P. (Martin) and Veljkovic, M. (Milan) (2020) 'Requirements for oversized holes for reusable steel-concrete composite floor systems', *Structures*, 24, pp. 489–498. doi:10.1016/j.istruc.2020.01.021.

Nijgh, M.P. and Veljkovic, M. (2020) '*An optimisation strategy for the (in- and out-of-plane) resistance of steel beams in demountable Composite Floor Systems', Structures*, 24, pp. 880–889. doi:10.1016/j.istruc.2020.01.049.

Nijgh, M.P., Gîrbacea, I.A. and Veljkovic, M. (2019) 'Elastic behaviour of a tapered steel-concrete composite beam optimized for reuse', *Engineering Structures*, 183, pp. 366–374. doi:10.1016/j.engstruct.2019.01.022.

Ottelé, M. and Jonkers, H.M. (2022) 'Lecture 3 Introduction to LCA', *CIE4100: Materials and Ecological Engineering Lecture 3*. *CIE4100: Materials and Ecological Engineering Lecture 3*, Delft: Netherlands, 17 January.

Paolo Foraboschi, Mattia Mercanzin, and Dario Trabucco. Sustainable structural design of tall buildings based on embodied energy. Energy and Buildings, 68:254–269, 2014. doi: 10.1016/j.enbuild.2013.09.003.

Payam Ashtari *et al.* (2021) *Optimum geometrical pattern and design of real-size diagrid structures using accelerated fuzzy-genetic algorithm with bilinear membership function*, *Applied Soft Computing*. Available at: https://www.sciencedirect.com/science/article/abs/pii/S1568494621005676 (Accessed: 11 January 2024).

Philip, R.B. et al. (2022) 'Comparative study of conventional slab with slab constructed using AAC block and Steel Grid', Materials Today: Proceedings, 65, pp. 448–454. doi:10.1016/j.matpr.2022.02.634.

Pomponi, F. and Moncaster, A. (2016). Embodied carbon mitigation and reduction in the built environment – What does the evidence say? Journal of Environmental Management, 181, pp.687–700. doi:https://doi.org/10.1016/j.jenvman.2016.08.036.

Sameer, M. and Dahake, H.B. (2017) 'Comparative Study of Conventional R.C.C & Composite Structure', International Journal of Innovative Science and Research Technology, 2(4). doi:10.38124/volume-2-2017_issue-4-april.

Search the EPD library (no date) EPD Library | EPD International. Available at: https://environdec.com/library (Accessed: 21 December 2023).

Subramanian, N. (2013) *Design of Reinforced Concrete Structures*. New Delhi: Oxford University.

Sun Moon, K. (2011) 'Diagrid structures for complex-shaped tall buildings', *Procedia Engineering*, 14, pp. 1343–1350. doi:10.1016/j.proeng.2011.07.169.

Taranath, B.S. (2016) *Structural analysis and design of Tall Buildings: Steel and Composite Construction*. CRC Press.

Team, G.S.W.E. (2022) *Steelmaking in EAFS produces 75% lower CO2 emissions, validates independent study*, *GreenSteelWorld.com*. Available at: https://greensteelworld.com/steelmaking-in-eafs-produces-75-lower-co2-emissions-validates-independent-study (Accessed: 03 January 2024).

Uy, B. et al. (2017) '*Behaviour and design of connections for Demountable Steel and composite structures', Structures,* 9, pp. 1–12. doi:10.1016/j.istruc.2016.06.005.

Veljkovic, M., Kavoura, F. and de Vries, P. (2020) 'Steel Structures 2 Lecture 12: Bolted Connections', *Steel Structures 2*. *Steel Structures 2*, Delft: Netherlands, 30 September.

Wagh, S.A. and Waghe, U.P. (2014) 'Comparative Study of R.C.C and Steel Concrete Composite Structures', International Journal of Engineering Research and Applications, 4(4). doi:10.9790/9622-44.

Webmapper (no date) *Hoogste Gebouwen van Nederland*, *Webmapper*. Available at: https://apps.webmapper.nl/bag_3D/#11.93/51.90462/4.50517/-58.4/6 (Accessed: 11 January 2024).

Webster M. D., Meryman H., Slivers A., Rodriguez-Nikl T., Lemay L. and Simonen K. (2012) "Strucutre and Carbon – How Materials Affect the Climate." SEI Sustainability Committee, Carbon Working Group, American Society of Civil Engineers or ASCE, Reston.

Zhang, Q., Li, Y., Xu, J., Jia, G., (2018). *Carbon element flow analysis and CO2emission reduction in iron and steel works*. J. Clean. Prod. 172, 709e723. https://doi.org/10.1016/j.jclepro.2017.10.211.

8 Appendices

8.1 Appendix A: Resulting Loads on Structural Model

8.1.1 Wind Load Cases

8.1.1.1 Case 1: 90 Degree Wind (1)

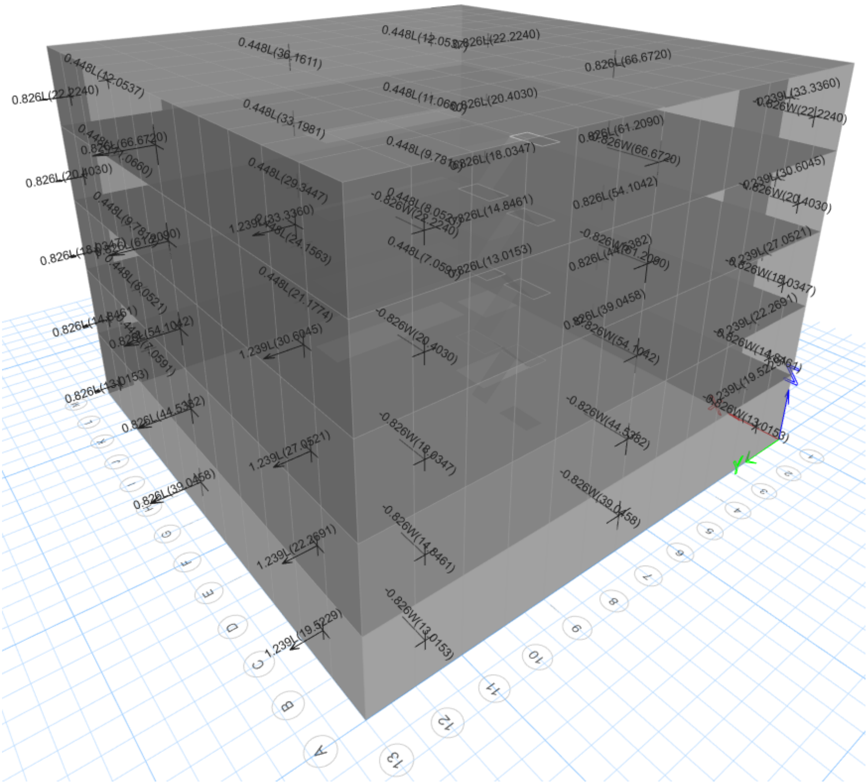

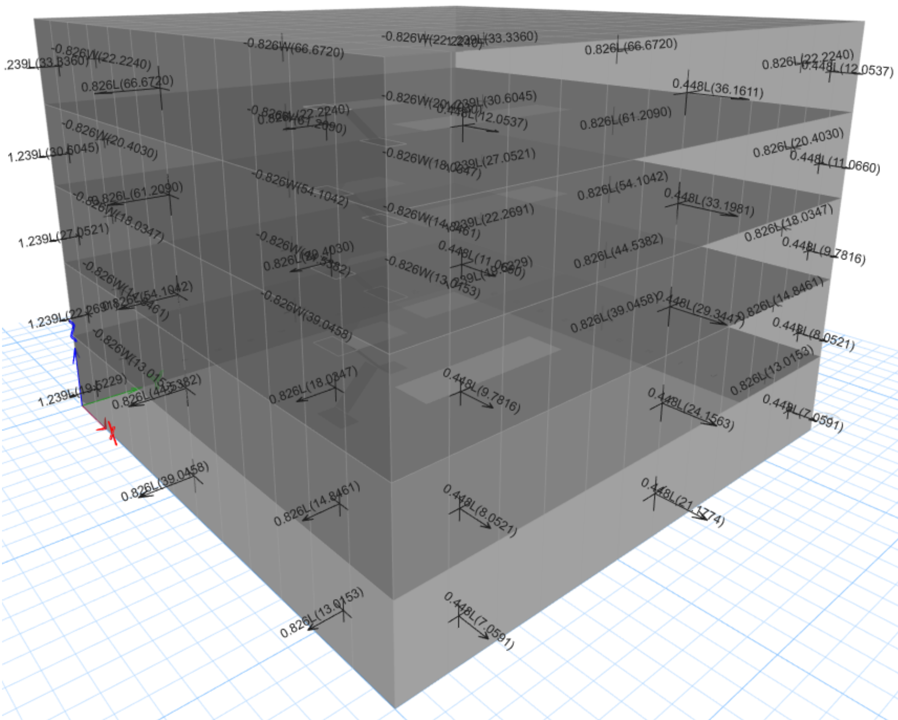

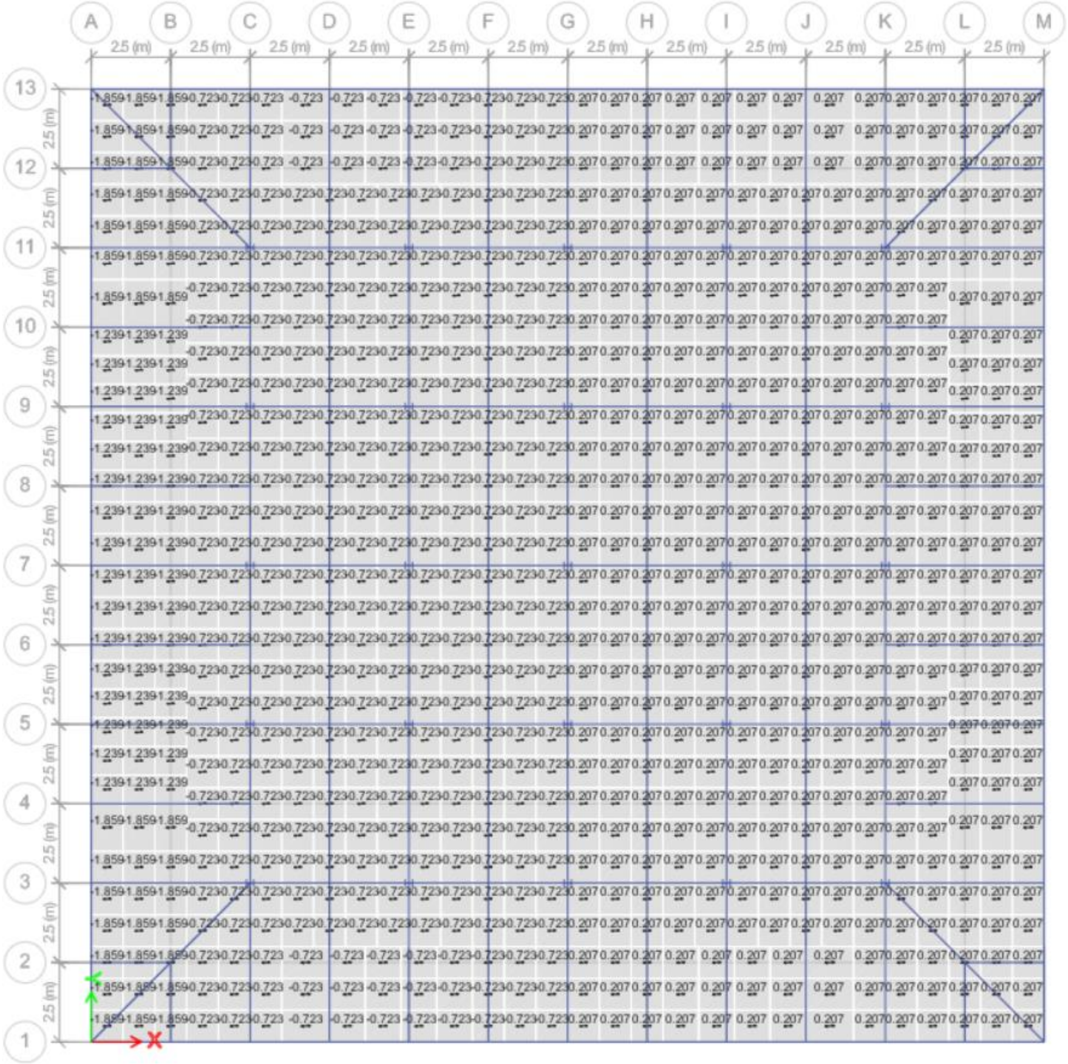
A
B
C
D
E
F
G
H
I
J
K
L
M
2.5 (m)
13
12
11
10
9
8
7
6
5
4
3
2
1

8.1.1.2 Case 2: 90 Degree Wind (2)

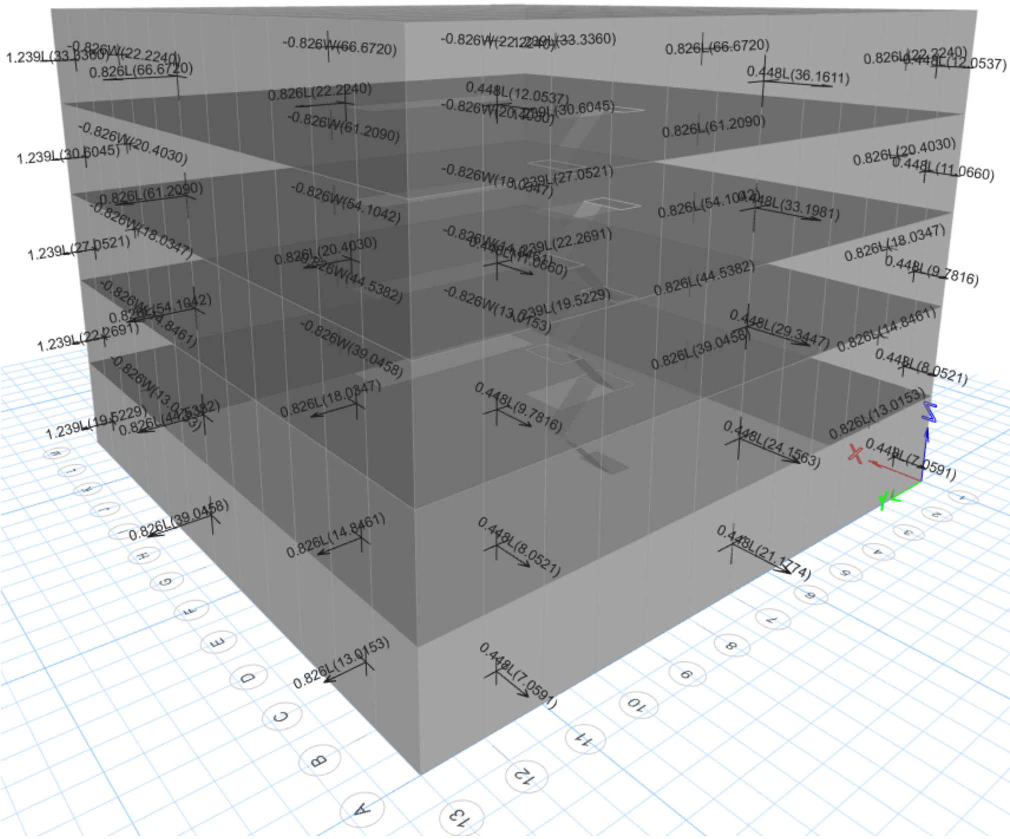

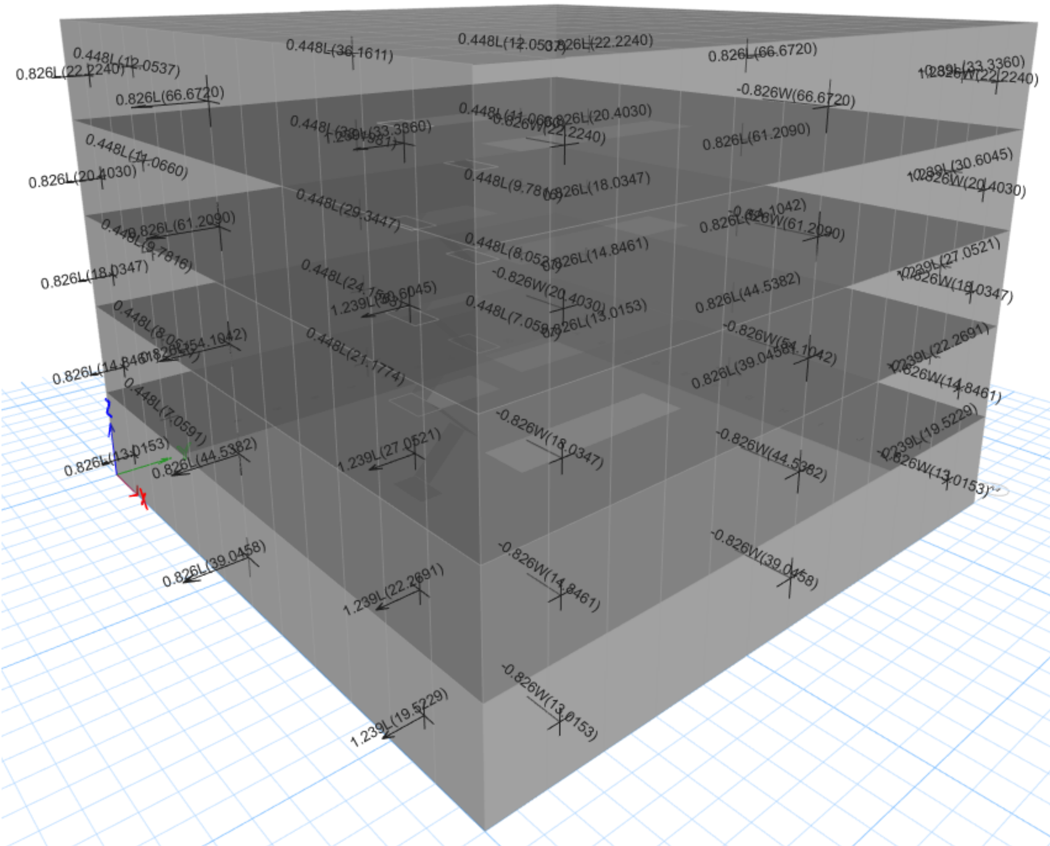

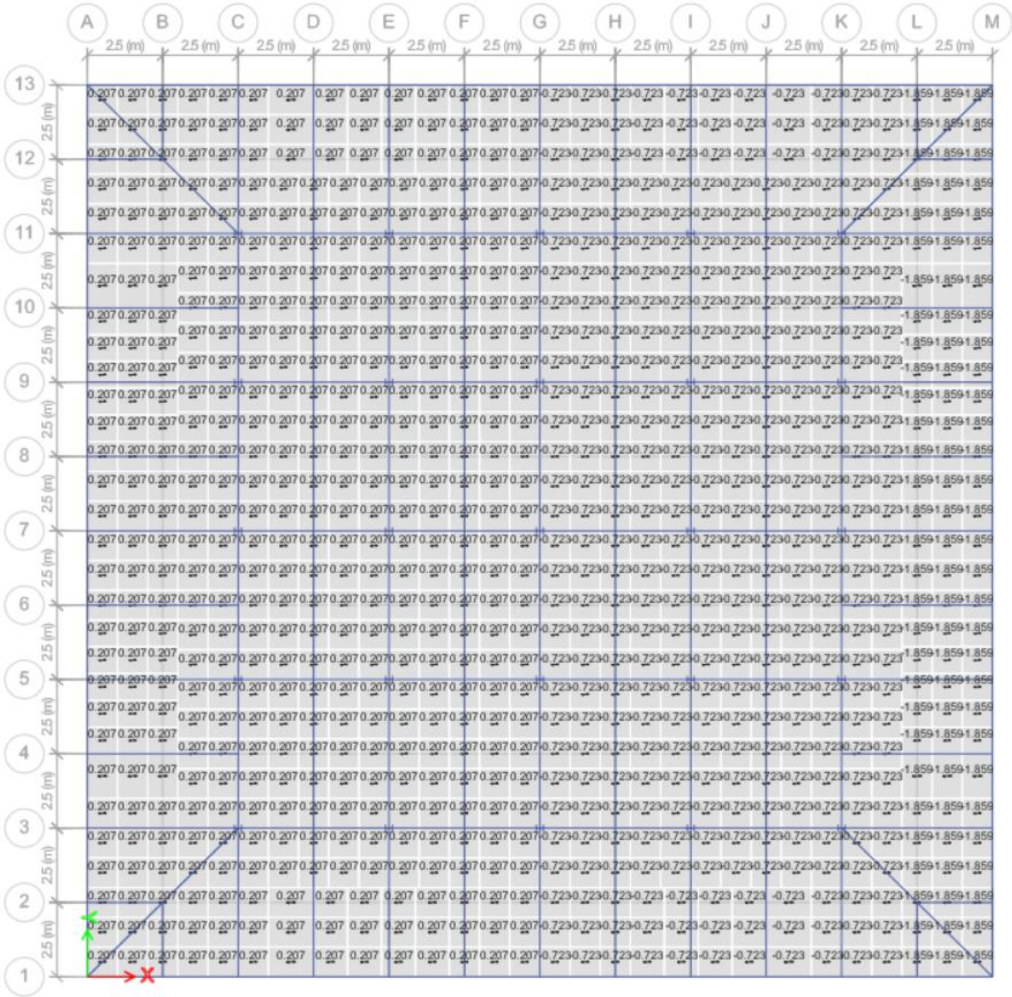
A B C D E F G H I J K L M
2.5 (m)
1 2 3 4 5 6 7 8 9 10 11 12 13
0.207
-0.723
-1.859
X
Y

8.1.1.3 Case 3: 0 Degree Wind (1)

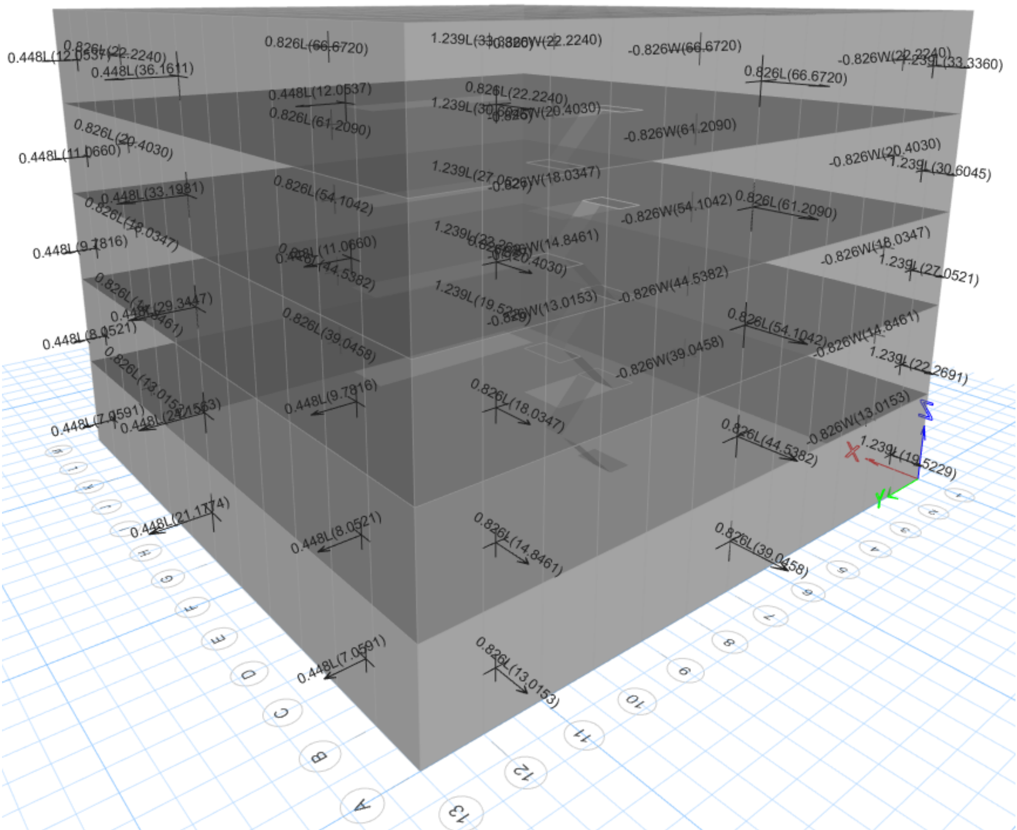

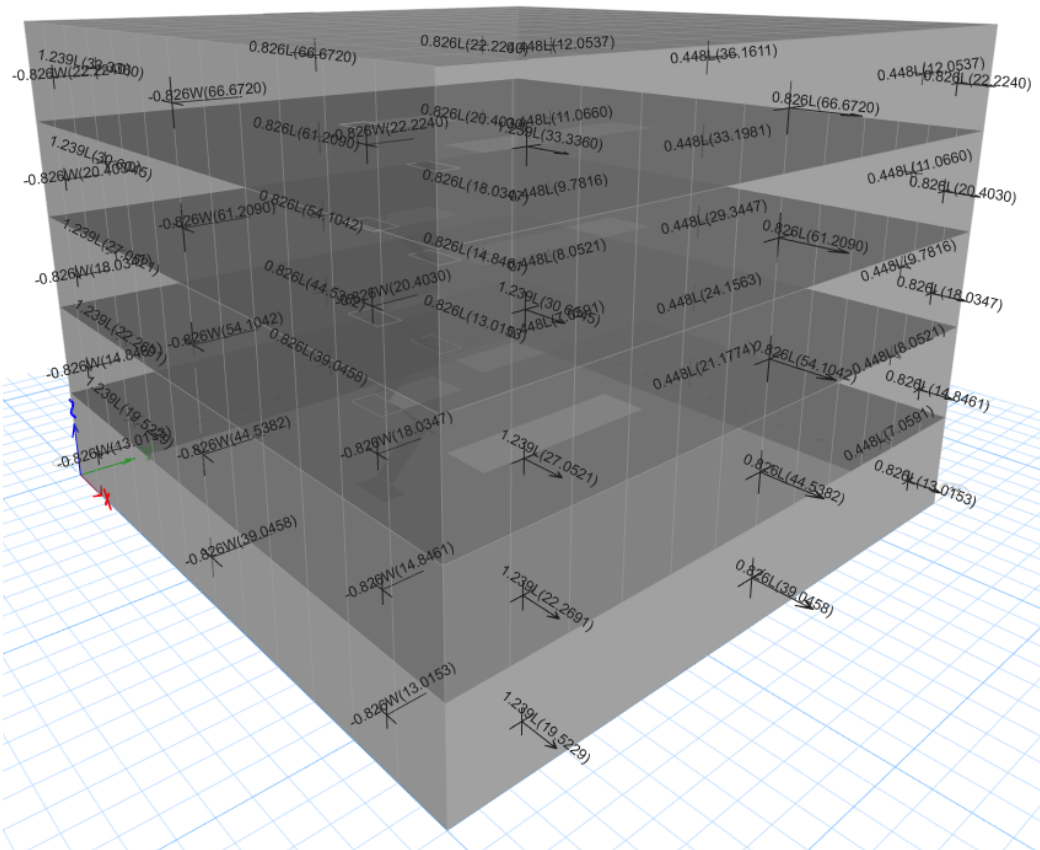

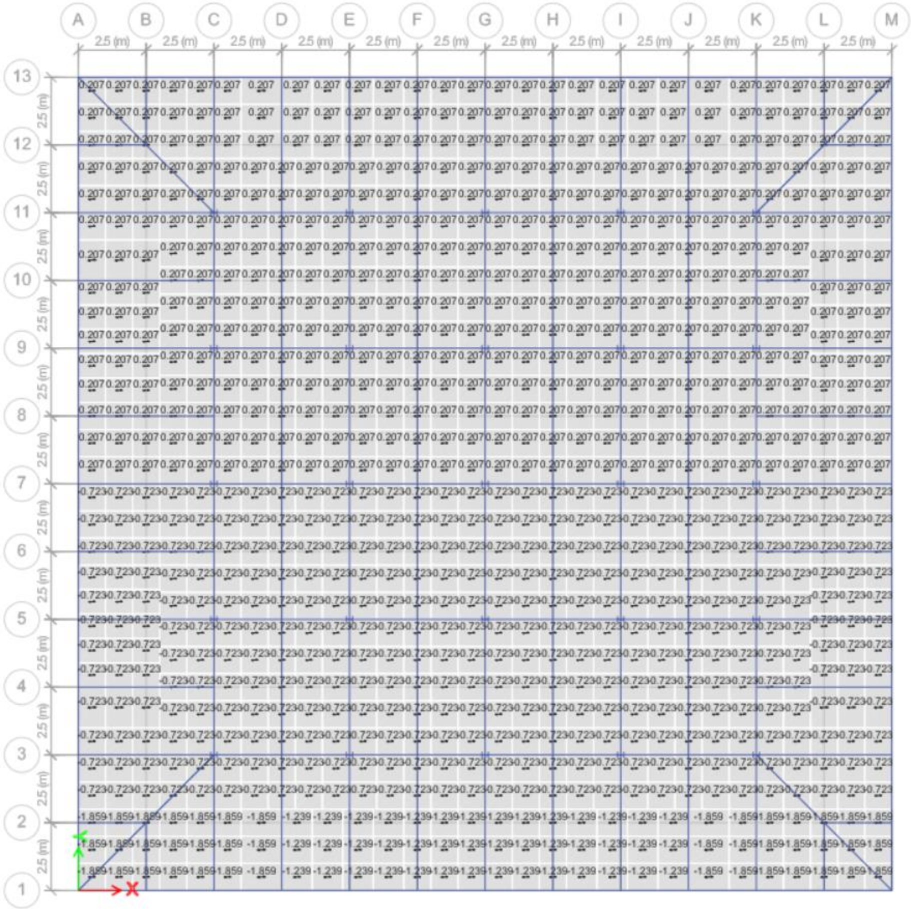
A B C D E F G H I J K L M
2.5 (m)
13 12 11 10 9 8 7 6 5 4 3 2 1
X
Y

8.1.1.4 Case 4: 0 Degree Wind (2)

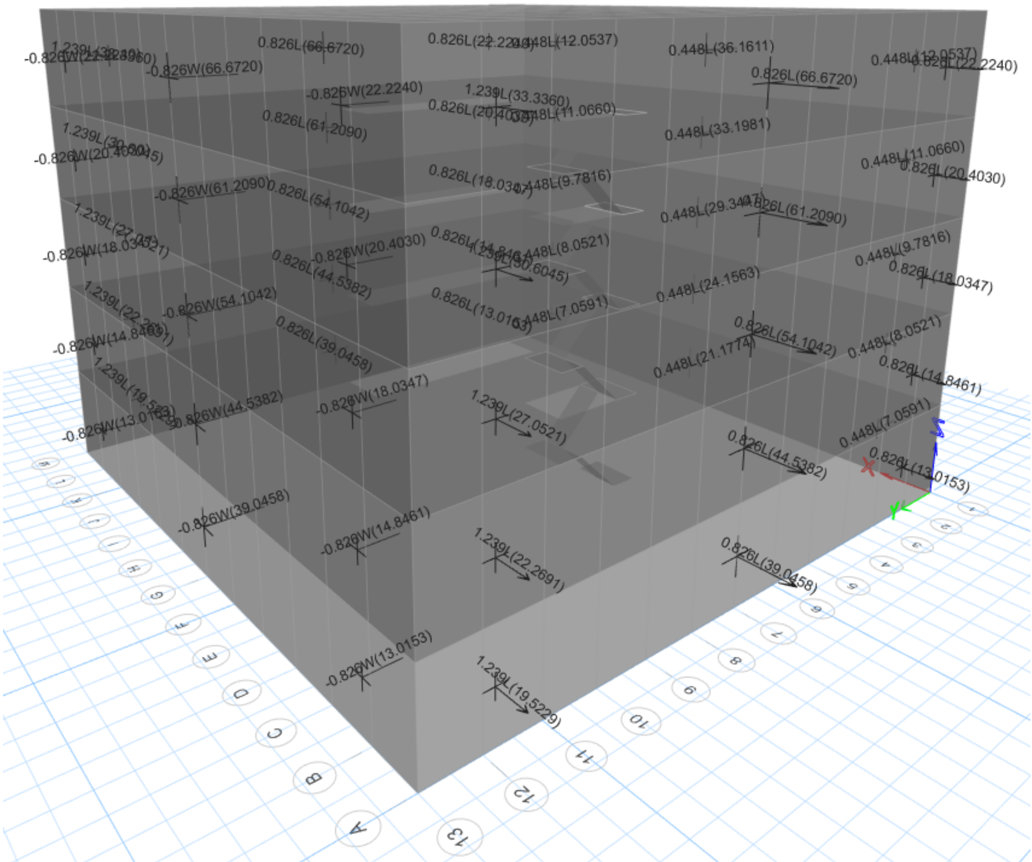

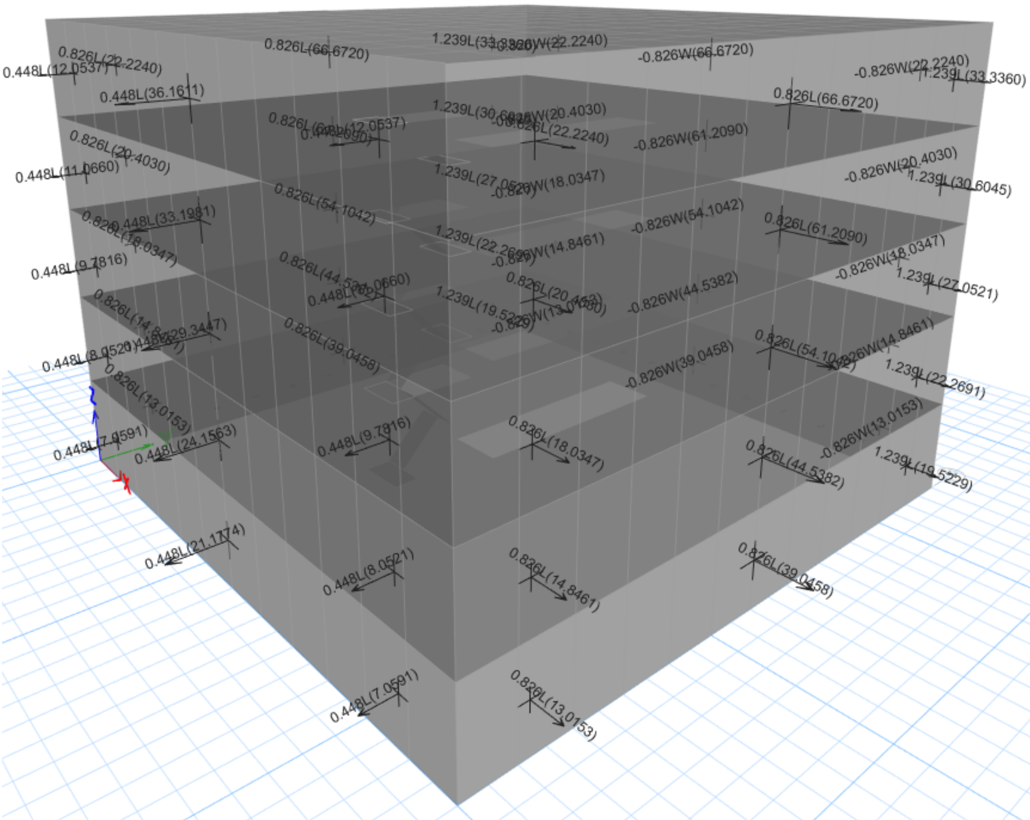

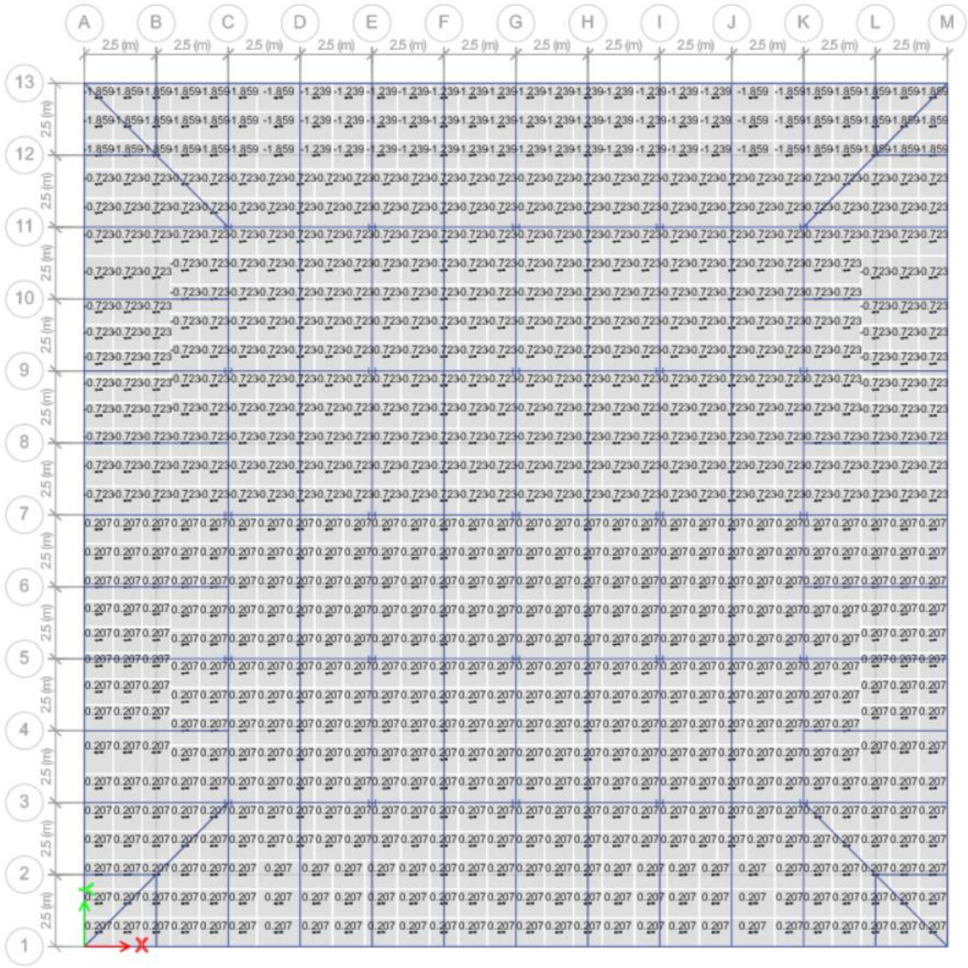
A B C D E F G H I J K L M
2.5 (m)
13 12 11 10 9 8 7 6 5 4 3 2 1
X

8.1.2 Live Load

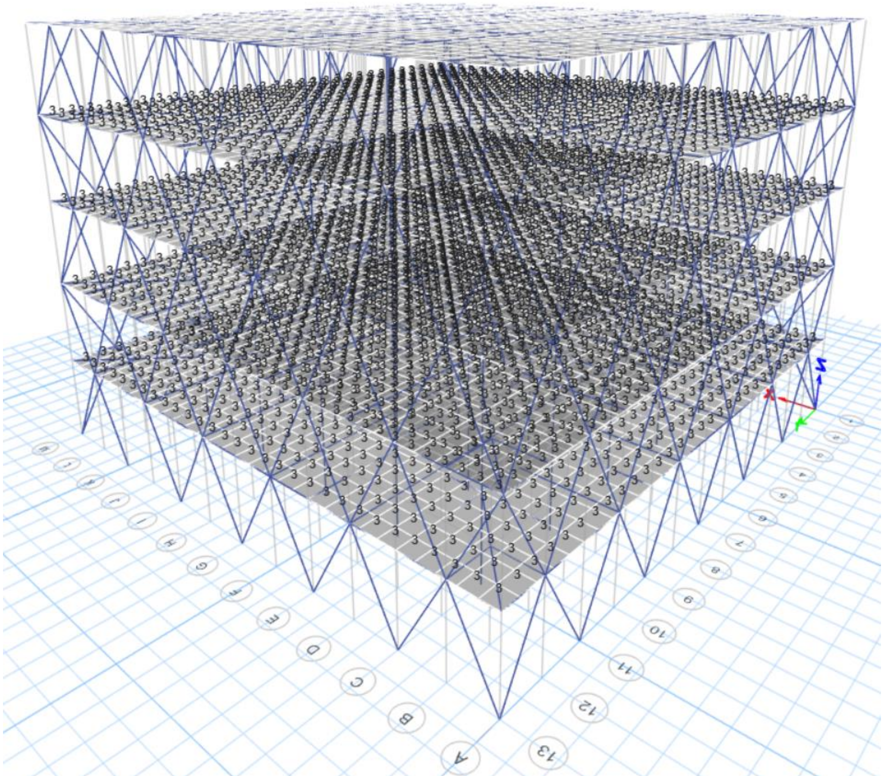

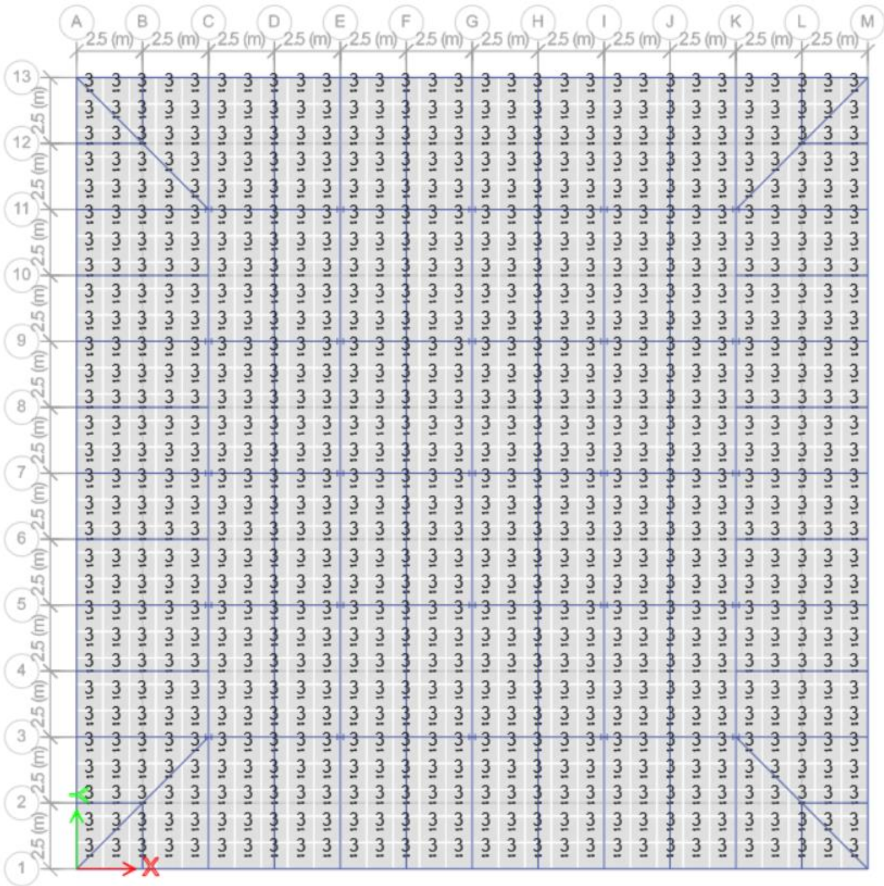

8.1.3 Snow Load

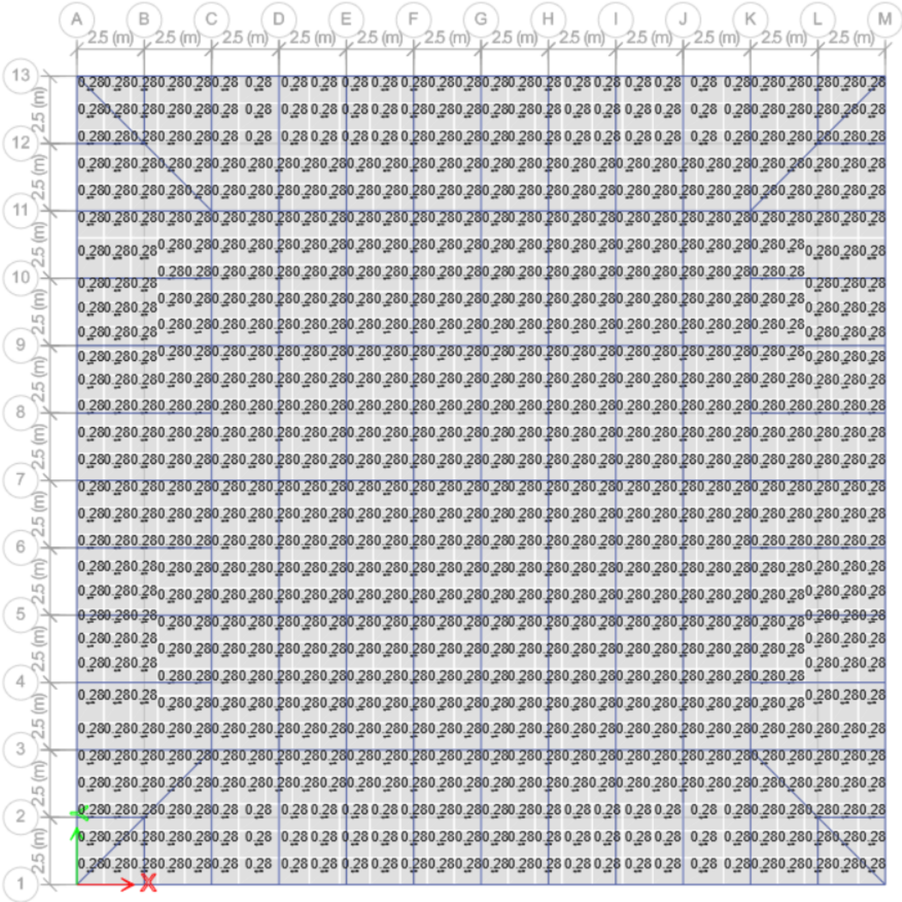

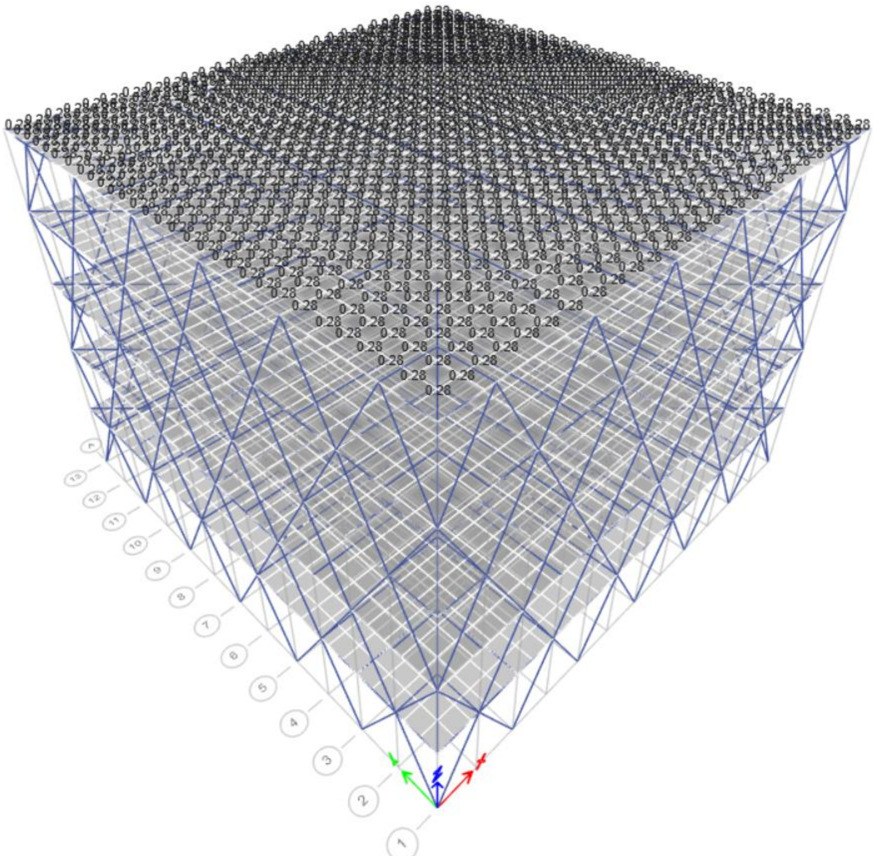

8.2 Appendix B: Load Combinations

W1 and W2 are labelled twice (for W01 W02 for W1 and W901 and W902 for W2)

ULS STR

L.C. 201: 1.35Gk+1.50Qi (Eq.6.10)
L.C. 202: 1.35Gk+1.50Qs1 (Eq.6.10)
L.C. 203: 1.35Gk+1.50Qs2 (Eq.6.10)
L.C. 204: 1.35Gk+1.50Qs3 (Eq.6.10)
L.C. 205: 1.35Gk+1.50Qw1 (Eq.6.10)
L.C. 206: 1.35Gk+1.50Qw2 (Eq.6.10)
L.C. 210: 1.00Gk+1.50Qw1 (Eq.6.10)
L.C. 211: 1.35xGk+1.50Qs1+0.90Qw1 (Eq.6.10)
L.C. 212: 1.35xGk+1.50Qs1+0.90Qw2 (Eq.6.10)
L.C. 213: 1.35xGk+1.50Qs2+0.90Qw1 (Eq.6.10)
L.C. 214: 1.35xGk+1.50Qs2+0.90Qw2 (Eq.6.10)
L.C. 215: 1.35xGk+1.50Qs3+0.90Qw1 (Eq.6.10)
L.C. 216: 1.35xGk+1.50Qs3+0.90Qw2 (Eq.6.10)
L.C. 217: 1.35xGk+1.50Qw1+0.75Qs1 (Eq.6.10)
L.C. 218: 1.35xGk+1.50Qw1+0.75Qs2 (Eq.6.10)
L.C. 219: 1.35xGk+1.50Qw1+0.75Qs3 (Eq.6.10)
L.C. 220: 1.35xGk+1.50Qw2+0.75Qs1 (Eq.6.10)
L.C. 221: 1.35xGk+1.50Qw2+0.75Qs2 (Eq.6.10)
L.C. 222: 1.35xGk+1.50Qw2+0.75Qs3 (Eq.6.10)
L.C. 231: 1.35xG+0.75Qs1+0.90Qw1 (Eq.6.10a)
L.C. 232: 1.35xG+0.75Qs1+0.90Qw2 (Eq.6.10a)
L.C. 233: 1.35xG+0.75Qs2+0.90Qw1 (Eq.6.10a)
L.C. 234: 1.35xG+0.75Qs2+0.90Qw2 (Eq.6.10a)
L.C. 235: 1.35xG+0.75Qs3+0.90Qw1 (Eq.6.10a)
L.C. 236: 1.35xG+0.75Qs3+0.90Qw2 (Eq.6.10a)
L.C. 251: 1.15xG+1.50Qs1+0.90Qw1 (Eq.6.10b)
L.C. 252: 1.15xG+1.50Qs1+0.90Qw2 (Eq.6.10b)
L.C. 253: 1.15xG+1.50Qs2+0.90Qw1 (Eq.6.10b)
L.C. 254: 1.15xG+1.50Qs2+0.90Qw2 (Eq.6.10b)
L.C. 255: 1.15xG+1.50Qs3+0.90Qw1 (Eq.6.10b)
L.C. 256: 1.15xG+1.50Qs3+0.90Qw2 (Eq.6.10b)
L.C. 257: 1.15xG+1.50Qw1+0.75Qs1 (Eq.6.10b)
L.C. 258: 1.15xG+1.50Qw1+0.75Qs2 (Eq.6.10b)
L.C. 259: 1.15xG+1.50Qw1+0.75Qs3 (Eq.6.10b)
L.C. 260: 1.15xG+1.50Qw2+0.75Qs1 (Eq.6.10b)
L.C. 261: 1.15xG+1.50Qw2+0.75Qs2 (Eq.6.10b)
L.C. 262: 1.15xG+1.50Qw2+0.75Qs3 (Eq.6.10b)

SLS

L.C. 301: Gk + Qi (Eq.6.14a)
L.C. 302: Gk + Qs1 (Eq.6.14a)
L.C. 303: Gk + Qs2 (Eq.6.14a)
L.C. 304: Gk + Qs3 (Eq.6.14a)
L.C. 305: Gk + Qw1 (Eq.6.14a)
L.C. 306: Gk + Qw2 (Eq.6.14a)
L.C. 311: Gk + Qs1 + 0.60Qw1 (Eq.6.14a)
L.C. 312: Gk + Qs1 + 0.60Qw2 (Eq.6.14a)
L.C. 313: Gk + Qs2 + 0.60Qw1 (Eq.6.14a)
L.C. 314: Gk + Qs2 + 0.60Qw2 (Eq.6.14a)
L.C. 315: Gk + Qs3 + 0.60Qw1 (Eq.6.14a)
L.C. 316: Gk + Qs3 + 0.60Qw2 (Eq.6.14a)
L.C. 317: Gk + Qw1 + 0.50Qs1 (Eq.6.14a)
L.C. 318: Gk + Qw1 + 0.50Qs2 (Eq.6.14a)
L.C. 319: Gk + Qw1 + 0.50Qs3 (Eq.6.14a)
L.C. 320: Gk + Qw2 + 0.50Qs1 (Eq.6.14a)

L.C. 321: Gk + Qw2 + 0.50Qs2 (Eq.6.14a)
L.C. 322: Gk + Qw2 + 0.50Qs3 (Eq.6.14a)
L.C. 331: Gk + 0.20Qs1 + 0.00Qw1 (Eq.6.15a)
L.C. 332: Gk + 0.20Qs1 + 0.00Qw2 (Eq.6.15a)
L.C. 333: Gk + 0.20Qs2 + 0.00Qw1 (Eq.6.15a)
L.C. 334: Gk + 0.20Qs2 + 0.00Qw2 (Eq.6.15a)
L.C. 335: Gk + 0.20Qs3 + 0.00Qw1 (Eq.6.15a)
L.C. 336: Gk + 0.20Qs3 + 0.00Qw2 (Eq.6.15a)
L.C. 337: Gk + 0.20Qw1 + 0.00Qs1 (Eq.6.15a)
L.C. 338: Gk + 0.20Qw1 + 0.00Qs2 (Eq.6.15a)
L.C. 339: Gk + 0.20Qw1 + 0.00Qs3 (Eq.6.15a)
L.C. 340: Gk + 0.20Qw2 + 0.00Qs1 (Eq.6.15a)
L.C. 341: Gk + 0.20Qw2 + 0.00Qs2 (Eq.6.15a)
L.C. 342: Gk + 0.20Qw2 + 0.00Qs3 (Eq.6.15a)
L.C. 351: Gk + 0.00Qs1 + 0.00Qw1 (Eq.6.16a)
L.C. 352: Gk + 0.00Qs1 + 0.00Qw2 (Eq.6.16a)
L.C. 353: Gk + 0.00Qs2 + 0.00Qw1 (Eq.6.16a)
L.C. 354: Gk + 0.00Qs2 + 0.00Qw2 (Eq.6.16a)
L.C. 355: Gk + 0.00Qs3 + 0.00Qw1 (Eq.6.16a)
L.C. 356: Gk + 0.00Qs3 + 0.00Qw2 (Eq.6.16a)

8.3 Appendix C: Design Specifications

8.3.1 For Steel Members

Steel Frame Design Preferences for Eurocode 3-2005

	Item	Value
01	Design Code	Eurocode 3-2005
02	Country	CEN Default
03	Combinations Equation	Eq. 6.10
04	Reliability Class	Class 2
05	Interaction Factors Method	Method 2 (Annex B)
06	Multi-Response Case Design	Step-by-Step - All
07	Framing Type	DCH-MRF
08	Behavior Factor, q	4
09	System Overstrength Factor, Omega	1
10	Consider P-Delta Done?	Yes
11	Consider Torsion?	No
12	GammaM0	1
13	GammaM1	1
14	GammaM2	1.25
15	Ignore Seismic Code?	No
16	Ignore Special Seismic Load?	No
17	Is Doubler Plate Plug-Welded?	Yes
18	Consider Deflection?	Yes
19	DL Limit, L /	120
20	Super DL+LL Limit, L /	120
21	Live Load Limit, L /	360
22	Total Limit, L/	240
23	Total-Camber Limit, L/	240
24	Pattern Live Load Factor	0.75
25	Demand/Capacity Ratio Limit	0.999
26	Max Number of Auto Iterations	1

Set To Default Values: All Items | Selected Items

Reset To Previous Values: All Items | Selected Items

OK | Cancel

8.3.2 For Composite Design

Beam | Shear Studs | Camber | Deflection | Vibration | Prices | Factors

	Item	Value
01	Country	CEN Default
02	Combinations Equation	Eq. 6.10
03	Reliability Class	Class 2
04	Interaction Factors Method	Method 2 (Annex B)
05	γM0 (Steel)	1
06	γM1 (Steel)	1
07	γM2 (Steel)	1.25
08	γV (Steel)	1.25
09	γC (Concrete)	1.5
10	Reaction Factor	1

Beam | Shear Studs | Camber | Deflection | Vibration | Prices | Factors

	Item	Value
1	Minimum PCC, %	40
2	Maximum PCC, %	100
3	Single Segment?	No
4	Min. Long. Spacing, mm	114
5	Max. Long. Spacing, mm	1000
6	Min. Trans. Spacing, mm	76
7	Max. Studs Per Row	3

Beam | Shear Studs | Camber | Deflection | Vibration | Prices | Factors

	Item	Value
1	PreComp DL Limit, L /	0
2	Super DL+LL Limit, L /	240
3	Live Load Limit, L /	360
4	Total-Camber Limit, L/	240
5	Free Shrinkage Strain	0.0008
6	Creep Factor	2

Beam | Shear Studs | Camber | Deflection | Vibration | Prices | Factors

	Item	Value
1	Shored Construction?	Yes
2	Middle Range, %	70
3	Pattern Live Load Factor	0.75
4	Stress Ratio Limit	1

8.4 Appendix D: Verifications of Diagrid 60 Members on ETABS

8.4.1 Verifications of Column

ETABS Steel Frame Design

Eurocode 3-2005 Steel Section Check (Strength Summary)

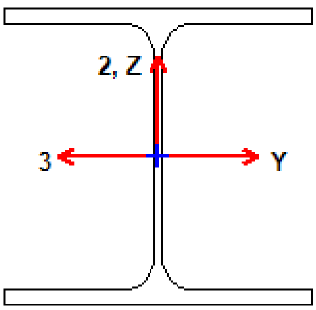

Element Details

Level	Element	Unique Name	Length (mm)	Location (mm)	Combo	Design Type	Element Type	Section
Storey1	C47	1481	4500	2140	1.35DL+1.5LL	Column	DCH MRF	HE240A

Classification	MultiResponse	P-Delta Done?	Rolled	Consider Torsion?
Class 2	Step-by-Step - All	Yes	Yes	No

Design Parameters

National Annex	Combination Equation	Analysis Type	Reliability
CEN Default	Eq. 6.10	Method 2 (Annex B)	Class 2

Design Code Parameters

γ_{M0}	γ_{M1}	γ_{M2}	A_n / A_g	LLRF	PLLF	D/C Limit
1	1	1.25	1	0.441	0.75	1

Section Properties

A (cm^2)	I_y (cm^4)	i_y (mm)	$W_{el,y}$ (cm^3)	$A_{v,2}$ (cm^2)	$W_{pl,y}$ (cm^3)	I_t (cm^4)	I_w (cm^6)	I_{yz} (cm^4)
76.8	7763	100.5	675	25.1	745	42.1	328485.9	0

I_z (cm^4)	i_z (mm)	$W_{el,z}$ (cm^3)	$A_{v,3}$ (cm^2)	$W_{pl,z}$ (cm^3)	h (mm)
2769	60	230.8	61.4	352	230

A_{eff} (cm^2)	e_{Ny} (mm)	e_{Nz} (mm)	$W_{ef,y}$ (cm^3)	$W_{ef,z}$ (cm^3)	Angle of principal axes (deg)
76.8	0	0	675	230.8	0

Material Properties

E (MPa)	f_y (MPa)	f_u (MPa)
210000	355	355

Stress Check Forces and Moments

Location (mm)	N_{Ed} (kN)	$M_{y,Ed}$ (kN-m)	$M_{z,Ed}$ (kN-m)	$V_{2,Ed}$ (kN)	$V_{3,Ed}$ (kN)	T_{Ed} (kN-m)
2140	-1310.7759	-3.2987	-3.4994	1.2217	1.2565	4.234E-06

Demand/Capacity (D/C) Ratio EC3 6.3.3(4)-6.62

D/C Ratio =	$N_{Ed} /(\chi_z N_{Rk} /\gamma_{M1}) + k_{zy} [M_{y,span,Ed} /(\chi_{LT} M_{y,Rk} /\gamma_{M1})] + k_{zz} [M_{z,span,Ed} /(M_{z,Rk} /\gamma_{M1})]$
0.855 =	0.829 + 0.01 + 0.016

Basic Factors

Buckling Mode	K Factor	L Factor	L Length (mm)	L_{cr} /i
Y-Y	1	0.951	4280	42.571
Y-Y Braced	0.683	0.951	4280	29.092
Z-Z	1	0.951	4280	71.279
Z-Z Braced	0.659	0.951	4280	47
LTB	1	0.951	4280	71.279

Axial Force Design

	N_{Ed} (kN)	$N_{c,Rd}$ (kN)	$N_{t,Rd}$ (kN)
Axial	-1310.7759	2726.4	1963.008

$N_{pl,Rd}$ (kN)	$N_{u,Rd}$ (kN)	$N_{cr,T}$ (kN)	$N_{cr,TF}$ (kN)	A_n /A_g (Unitless)
2726.4	1963.008	5189.7652	5189.7645	1

Design Parameters for Axial Design

	Curve	α	N_{cr} (kN)	λ	φ	χ	$N_{b,Rd}$ (kN)
Y-Y	b	0.34	8783.3682	0.557	0.716	0.858	2339.2411

	Curve	α	N_{cr} (kN)	λ	ϕ	χ	$N_{b,Rd}$ (kN)
Y-Y Braced	b	0.34	18807.4995	0.381	0.603	0.934	2545.4898
Z-Z	c	0.49	3132.9572	0.933	1.115	0.58	1580.7131
Z-Z Braced	c	0.49	7205.7017	0.615	0.791	0.776	2116.7481
Torsional TF	c	0.49	5189.7645	0.725	0.891	0.709	1933.7788

Moment Design

	M_{Ed} (kN-m)	$M_{Ed,span}$ (kN-m)	$M_{c,Rd}$ (kN-m)	$M_{v,Rd}$ (kN-m)	$M_{n,Rd}$ (kN-m)	$M_{b,Rd}$ (kN-m)
Y-Y	-0.6843	-3.2987	264.475	264.475	156.9405	248.0344
Z-Z	-0.8105	-3.4994	124.96	124.96	113.1292	

Compactness

Section	Flange	Web	ε	α	ψ
Class 2	Class 2	Class 1	0.814	1	-0.038

LTB Factors

Curve	α_{LT}	λ_{LT}	ϕ_{LT}	χ_{LT}	I_w (cm⁶)	M_{cr} (kN-m)
a	0.21	0.454	0.63	0.938	328485.9	1280.3655

k_w	C_1	C_2	C_3	z_a (mm)	z_s (mm)	z_g (mm)	z_z (mm)	z_j (mm)
1	2.711	0	0.586	115	0	115	0	0

C_{my}	C_{mz}	C_{mLT}	k_{yy}	k_{yz}	k_{zy}	k_{zz}
0.4	0.4	0.4	0.437	0.334	0.746	0.556

	V_{Ed} (kN)	$V_{pl,Rd}$ (kN)	V_{Ed} /$V_{pl,Rd}$	ρ
2-Axis	1.2217	515.2676	0.002	1
3-Axis	1.2565	1257.425	0.001	1

Shear Design

	V_{Ed} (kN)	T_{Ed} (kN-m)	$V_{c,Rd}$ (kN)	Stress Ratio	Status Check
2-Axis	1.2217	4.234E-06	515.2676	0.002	OK
3-Axis	1.2565	4.234E-06	1257.425	0.001	OK

	$V_{pl,Rd}$ (kN)	η	λ_{bar}	X
2-Axis	515.2676	1.2	0.391	1.2
3-Axis	1257.425	1.2	0	1

8.4.2 Verifications of Beam

ETABS Steel Frame Design

Eurocode 3-2005 Steel Section Check (Strength Summary)

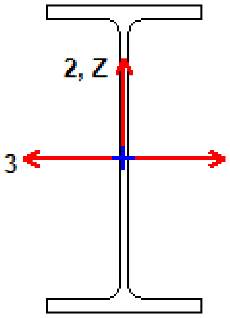

Element Details

Level	Element	Unique Name	Length (mm)	Location (mm)	Combo	Design Type	Element Type	Section
Storey1	B13	97	5000	0	1.35DL+1.5LL	Beam	DCH MRF	IPE180

Classification	MultiResponse	P-Delta Done?	Rolled	Consider Torsion?
Class 1	Step-by-Step - All	Yes	Yes	No

Design Parameters

National Annex	Combination Equation	Analysis Type	Reliability
CEN Default	Eq. 6.10	Method 2 (Annex B)	Class 2

Design Code Parameters

γ_{M0}	γ_{M1}	γ_{M2}	A_n / A_g	LLRF	PLLF	D/C Limit
1	1	1.25	1	1	0.75	1

Section Properties

A (cm^2)	I_y (cm^4)	i_y (mm)	$W_{el,y}$ (cm^3)	$A_{v,2}$ (cm^2)	$W_{pl,y}$ (cm^3)	I_t (cm^4)	I_w (cm^6)	I_{yz} (cm^4)
23.9	1317	74.2	146.3	11.2	166	4.7	7431.2	0

I_z (cm^4)	i_z (mm)	$W_{el,z}$ (cm^3)	$A_{v,3}$ (cm^2)	$W_{pl,z}$ (cm^3)	h (mm)
101	20.6	22.2	15.2	34.6	180

A_{eff} (cm^2)	e_{Ny} (mm)	e_{Nz} (mm)	$W_{ef,y}$ (cm^3)	$W_{ef,z}$ (cm^3)	Angle of principal axes (deg)
23.9	0	0	146.3	22.2	0

Material Properties

E (MPa)	f_y (MPa)	f_u (MPa)
210000	355	355

Stress Check Forces and Moments

Location (mm)	N_{Ed} (kN)	$M_{y,Ed}$ (kN-m)	$M_{z,Ed}$ (kN-m)	$V_{2,Ed}$ (kN)	$V_{3,Ed}$ (kN)	T_{Ed} (kN-m)
0	1.7757	-41.0986	0.0525	33.9429	0.1093	0.7561

Demand/Capacity (D/C) Ratio EC3 6.3.3(4)-6.62

D/C Ratio =	$N_{Ed} /(\chi_z N_{Rk} /\gamma_{M1}) + k_{zy} [M_{y,span,Ed} /(\chi_{LT} M_{y,Rk} /\gamma_{M1})] + k_{zz} [M_{z,span,Ed} /(M_{z,Rk} /\gamma_{M1})]$
0.975 =	0 + 0.973 + 0.002

Basic Factors

Buckling Mode	K Factor	L Factor	L Length (mm)	L_{cr} /i
Y-Y	1	1	5000	67.356
Y-Y Braced	1	1	5000	67.356
Z-Z	1	0.5	2500	121.613
Z-Z Braced	1	0.5	2500	121.613
LTB	1	0.5	2500	121.613

Axial Force Design

	N_{Ed} (kN)	$N_{c,Rd}$ (kN)	$N_{t,Rd}$ (kN)
Axial	1.7757	848.45	610.884

$N_{pl,Rd}$ (kN)	$N_{u,Rd}$ (kN)	$N_{cr,T}$ (kN)	$N_{cr,TF}$ (kN)	A_n /A_g (Unitless)
848.45	610.884	1059.2713	1059.2714	1

Design Parameters for Axial Design

	Curve	α	N_{cr} (kN)	λ	ϕ	χ	$N_{b,Rd}$ (kN)
Y-Y	a	0.21	1091.8546	0.882	0.96	0.746	632.9334
Y-Y Braced	a	0.21	1091.8546	0.882	0.96	0.746	632.9334
Z-Z	b	0.34	334.9349	1.592	2.003	0.311	263.535
Z-Z Braced	b	0.34	334.9349	1.592	2.003	0.311	263.535
Torsional TF	b	0.34	1059.2713	0.895	1.019	0.664	563.7215

Moment Design

	M_{Ed} (kN-m)	$M_{Ed,span}$ (kN-m)	$M_{c,Rd}$ (kN-m)	$M_{v,Rd}$ (kN-m)	$M_{n,Rd}$ (kN-m)	$M_{b,Rd}$ (kN-m)
Y-Y	-31.2674	-41.0986	58.93	58.93	58.93	42.24
Z-Z	0.0525	0.0525	12.283	12.283	12.283	

Compactness

Section	Flange	Web	ε	α	ψ
Class 1	Class 1	Class 1	0.814	0.497	-1.004

LTB Factors

Curve	α_{LT}	λ_{LT}	ϕ_{LT}	χ_{LT}	I_w (cm^6)	M_{cr} (kN-m)
a	0.21	0.926	1.005	0.717	7431.2	68.7633

k_w	C_1	C_2	C_3	z_a (mm)	z_s (mm)	z_g (mm)	z_z (mm)	z_j (mm)
1	2.017	0.459	0.525	90	0	90	0	0

C_{my}	C_{mz}	C_{mLT}	k_{yy}	k_{yz}	k_{zy}	k_{zz}
0.65	0.4	0.4	0.65	0.24	1	0.4

	V_{Ed} (kN)	$V_{pl,Rd}$ (kN)	V_{Ed} /$V_{pl,Rd}$	ρ
2-Axis	33.9429	229.6363	0.148	1
3-Axis	0.1093	311.702	3.506E-04	1

Shear Design

	V_{Ed} (kN)	T_{Ed} (kN-m)	$V_{c,Rd}$ (kN)	Stress Ratio	Status Check
2-Axis	33.9429	0.7561	229.6363	0.148	OK
3-Axis	0.1093	0.7561	311.702	3.506E-04	OK

	$V_{pl,Rd}$ (kN)	η	λ_{bar}	X
2-Axis	229.6363	1.2	0.44	1.2
3-Axis	311.702	1.2	0	1

8.4.3 Verifications of the Diagrid

ETABS Steel Frame Design

Eurocode 3-2005 Steel Section Check (Strength Summary)

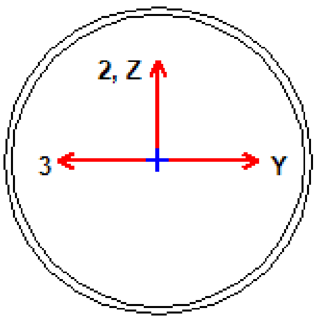

Element Details (Part 1 of 2)

Level	Element	Unique Name	Length (mm)	Location (mm)	Combo	Design Type	Element Type
Storey1	D77	40	5147.8	0	1.35DL+1.5LL	Brace	DCH MRF

Element Details (Part 2 of 2)

Section
TUBO-D159X4

Classification	MultiResponse	P-Delta Done?	Rolled	Consider Torsion?
Class 2	Step-by-Step - All	Yes	Yes	No

Design Parameters

National Annex	Combination Equation	Analysis Type	Reliability
CEN Default	Eq. 6.10	Method 2 (Annex B)	Class 2

Design Code Parameters

γ_{M0}	γ_{M1}	γ_{M2}	A_n / A_g	LLRF	PLLF	D/C Limit
1	1	1.25	1	1	0.75	1

Section Properties

A (cm^2)	I_y (cm^4)	i_y (mm)	$W_{el,y}$ (cm^3)	$A_{v,2}$ (cm^2)	$W_{pl,y}$ (cm^3)	I_t (cm^4)	I_w (cm^6)	I_{yz} (cm^4)
19.5	585.3	54.8	73.6	12.4	96.1	1170	0	0

I_z (cm^4)	i_z (mm)	$W_{el,z}$ (cm^3)	$A_{v,3}$ (cm^2)	$W_{pl,z}$ (cm^3)	h (mm)
585.3	54.8	73.6	12.4	96.1	159

A_{eff} (cm^2)	e_{Ny} (mm)	e_{Nz} (mm)	$W_{ef,y}$ (cm^3)	$W_{ef,z}$ (cm^3)	Angle of principal axes (deg)
19.5	0	0	73.6	73.6	0

Material Properties

E (MPa)	f_y (MPa)	f_u (MPa)
210000	355	355

Stress Check Forces and Moments

Location (mm)	N_{Ed} (kN)	$M_{y,Ed}$ (kN-m)	$M_{z,Ed}$ (kN-m)	$V_{2,Ed}$ (kN)	$V_{3,Ed}$ (kN)	T_{Ed} (kN-m)
0	-306.4024	0.6875	0	0.5342	0	5.3509

Demand/Capacity (D/C) Ratio EC3 6.3.3(4)-6.61

D/C Ratio =	$N_{Ed} /(\chi_y N_{Rk} /\gamma_{M1}) + Sqrt[(k_{yy} [M_{y,span,Ed} /(\chi_{LT} M_{y,Rk} /\gamma_{M1})])^2 + (k_{yz} [M_{z,span,Ed} /(M_{z,Rk} /\gamma_{M1})])^2]$
0.898 =	0.866 + Sqrt[$(0.033)^2$ + $(0)^2$]

Basic Factors

Buckling Mode	K Factor	L Factor	L Length (mm)	L_{cr} /i
Y-Y	1	1	5147.8	93.914
Y-Y Braced	1	1	5147.8	93.914
Z-Z	1	1	5147.8	93.914
Z-Z Braced	1	1	5147.8	93.914
LTB	1	1	5147.8	93.914

Axial Force Design

	N_{Ed} (kN)	$N_{c,Rd}$ (kN)	$N_{t,Rd}$ (kN)
Axial	-306.4024	691.54	497.9088

$N_{pl,Rd}$ (kN)	$N_{u,Rd}$ (kN)	$N_{cr,T}$ (kN)	$N_{cr,TF}$ (kN)	A_n /A_g (Unitless)
691.54	497.9088	157257.8468	457.7745	1

Design Parameters for Axial Design

	Curve	α	N_{cr} (kN)	λ	ϕ	χ	$N_{b,Rd}$ (kN)
Y-Y	a	0.21	457.7746	1.229	1.363	0.512	354.0134
Y-Y Braced	a	0.21	457.7746	1.229	1.363	0.512	354.0134
Z-Z	a	0.21	457.7746	1.229	1.363	0.512	354.0134
Z-Z Braced	a	0.21	457.7746	1.229	1.363	0.512	354.0134
Torsional TF	a	0.21	457.7745	1.229	1.363	0.512	354.0133

Moment Design

	M_{Ed} (kN-m)	$M_{Ed,span}$ (kN-m)	$M_{c,Rd}$ (kN-m)	$M_{v,Rd}$ (kN-m)	$M_{n,Rd}$ (kN-m)	$M_{b,Rd}$ (kN-m)
Y-Y	0	0.6875	34.1226	34.1226	34.1226	34.1226
Z-Z	0	0	34.1226	34.1226	34.1226	

Compactness

Section	Flange	Web	ε	α	ψ
Class 2	Class 2	Class 2	0.814	1	-0.114

LTB Factors

Curve	α_{LT}	λ_{LT}	ϕ_{LT}	χ_{LT}	I_w (cm^6)	M_{cr} (kN-m)
d	0.76	0.217	0.53	0.987	0	725.8709

k_w	C_1	C_2	C_3	z_a (mm)	z_s (mm)	z_g (mm)	z_z (mm)	z_j (mm)
1	1.132	0.459	0.525	79.5	0	79.5	0	0

C_{my}	C_{mz}	C_{mLT}	k_{yy}	k_{yz}	k_{zy}	k_{zz}
0.95	1	0.95	1.608	1.015	0.965	1.692

	V_{Ed} (kN)	$V_{pl,Rd}$ (kN)	V_{Ed} /$V_{pl,Rd}$	ρ
2-Axis	0.5342	254.1772	0.002	1
3-Axis	0	254.1772	0	1

Shear Design

	V_{Ed} (kN)	T_{Ed} (kN-m)	$V_{c,Rd}$ (kN)	Stress Ratio	Status Check
2-Axis	0.5342	5.3509	254.1772	0.002	OK
3-Axis	0	5.3509	254.1772	0	OK

	$V_{pl,Rd}$ (kN)	η	λ_{bar}	X
2-Axis	254.1772	1.2	0	1
3-Axis	254.1772	1.2	0	1

End Reaction Axial Forces

Left End Reaction (kN)	Load Combo	Right End Reaction (kN)	Load Combo
-306.4024	1.35DL+1.5LL	-304.4794	1.35DL+1.5LL

8.4.4 Verifications of Composite Beam

Storey Storey1	**Beam B92**	Length: 5 m Trib. Area: 10.05 m²
Location: X= 27.5 m Y= 20 m		8 19 mm Ø studs
S355	**IPE140**	Shored

Composite Deck Properties

	Slab	Depth (mm)	w_c (kN/m³)	f_{ck} (MPa)	b_{eff} (mm)	E_{cm} (S) (MPa)	E_{cm} (D) (MPa)	E_{cm} (V) (MPa)	P_R (kN)
At Left, at Right	D120	120	24.9926	30	625	16500	16500	22275	72.6

Loading (1.35DL+1.5LL combo)

	Constr.	Dead	SDL	Live NR	Factored
Line Load (kN/m) 0 m→1 m	0.000	0.126→0.000	0.000	0.000	0.360→0.000
Line Load (kN/m) 1 m→4 m	0.000	6.124→0.000	0.000	0.000	17.455→0.000
Line Load (kN/m) 4 m→5 m	0.000	0.126	0.000	0.000	0.360
Point Load (kN) @ 1 m	0.0000	3.9188	0.0000	0.0000	11.1685
Point Load (kN) @ 2 m	0.0000	2.1534	0.0000	0.0000	6.1373
Point Load (kN) @ 3 m	0.0000	2.1534	0.0000	0.0000	6.1373
Point Load (kN) @ 4 m	0.0000	3.9188	0.0000	0.0000	11.1685

End Reactions

	Top Cope	Bot. Cope	Constr.	Dead	SDL	Live NR	Combo	Factored
I end (kN)	0 mm	0 mm	0.0000	15.7326	0.0000	0.0000	1.35DL+1.5LL	44.8380
J end (kN)	13 mm	0 mm	0.0000	15.0231	0.0000	0.0000	1.35DL+1.5LL	42.8159

Strength Checks

	Combo	Loc.	E_d	R_d	Ratio	Pass
Shear at Ends (kN)	1.35DL+1.5LL	5 m	42.8159	122.3402	0.350	✓
Partial Comp. Bending (kN-m)	1.35DL+1.5LL	2.5591 m	66.9363	72.7889	0.920	✓

Constructability and Serviceability Checks

	Combo	I (cm⁴)	Actual	Allowable	Ratio	Pass
Shear Studs Distribution	N/A	N/A	8	1 * [4819/114] = 42	0.19	✓
Dead Load Defl. (mm)	DL+LL	4002.5	13.7	No Limit	N/A	N/A
SDL + LL Defl. (mm)	DL+LL	4002.5	0	20.8	0.000	✓
Live Load Defl. (mm)	DL+LL	4002.5	0	13.9	0.000	✓
Total Defl. (mm)	DL+LL	4002.5	13.7	20.8	0.658	✓

Section Properties

	Y1 (mm)	Y2 (mm)	Area (cm²)	S_{bot} (cm³)	I (cm⁴)	M_{Rd} (kN-m)	$N_{pl,a}$ $N_{c,f}$ or N_c (kN)
Steel fully braced	70	N/A	16.4	77.3	541	N/A	582.2
Full composite (plastic)	0	106.3	N/A	N/A	N/A	102.6425	582.2
Full composite (elastic)	N/A	55.3	79.9	204.9	4002.5	N/A	N/A
Partial composite (50%)	5.6	113.2	N/A	204.9	4002.5	72.7889	4 * 72.6 = 290.3
Vibrations Check (E_c = 22275)	52.1	N/A	271	N/A	6199.7	N/A	N/A

8.5 Appendix E: ETABS Modelling Results

8.5.1 Diagrid 60 5m Column Spacing

Axial Force:

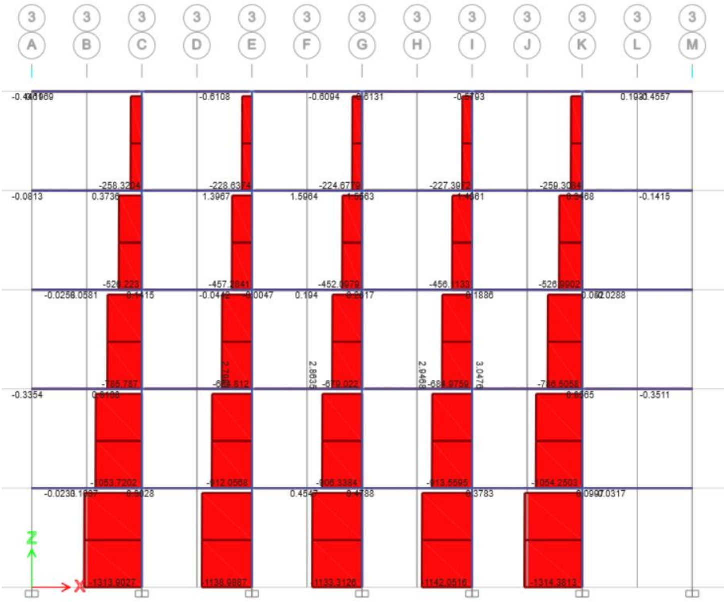

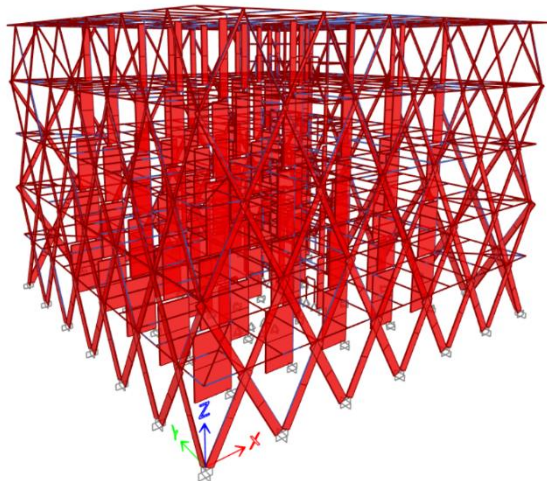

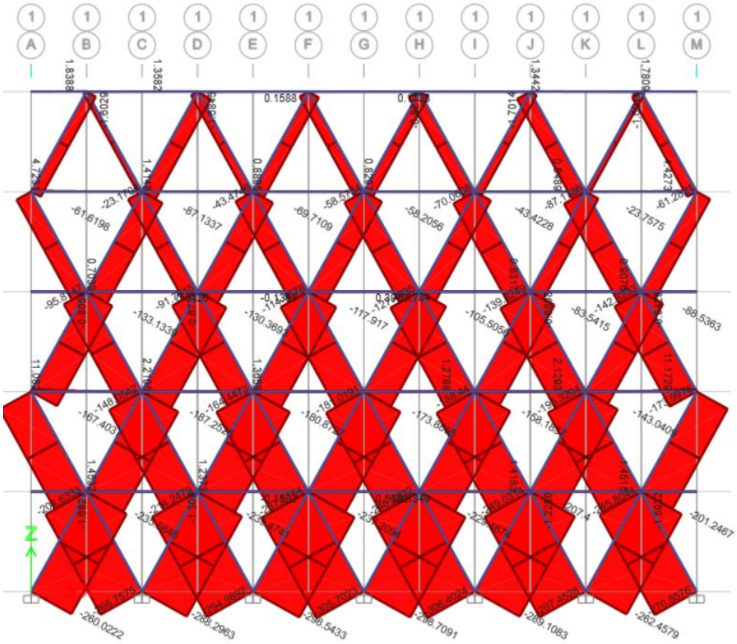

Shear z-z:

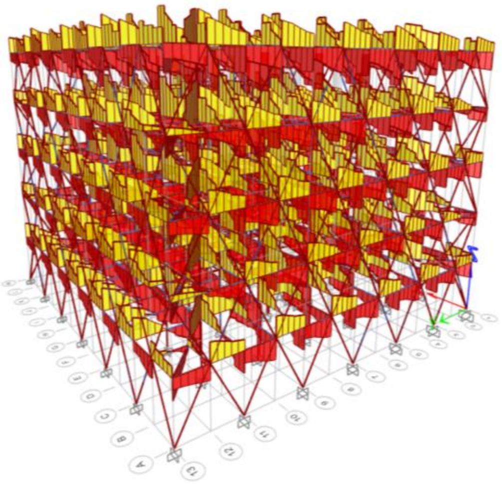

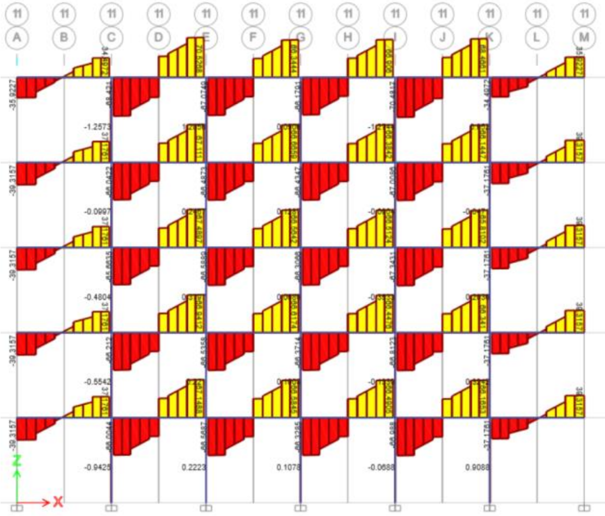

Shear y-y:

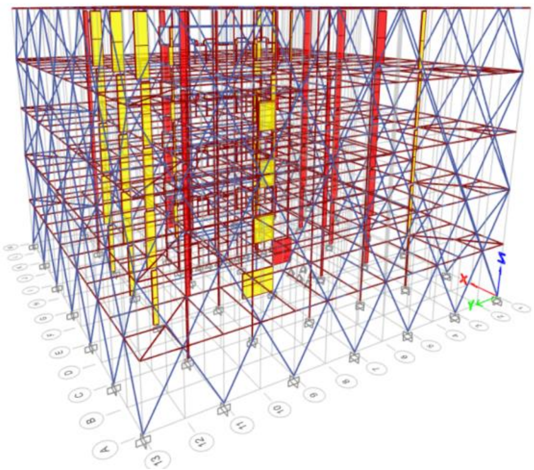

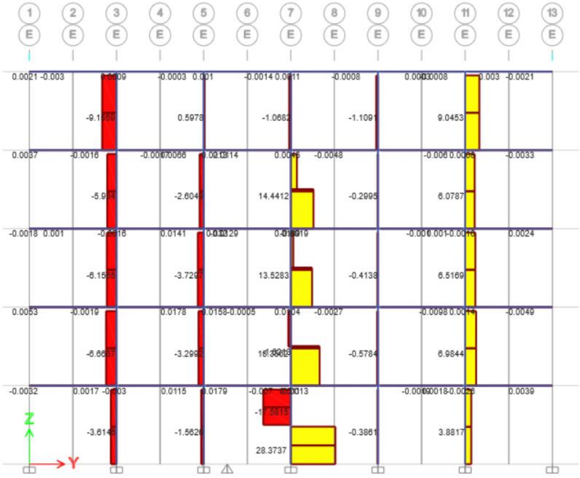

Moment z-z:

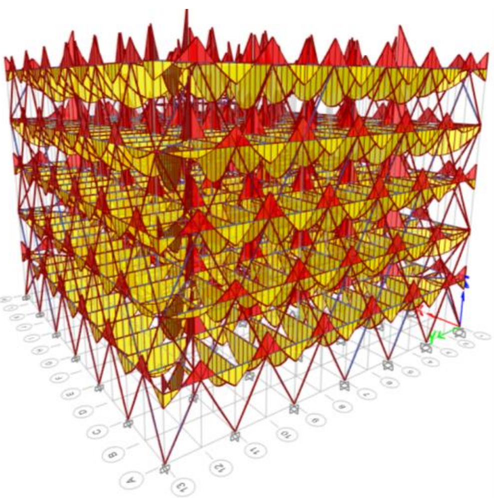

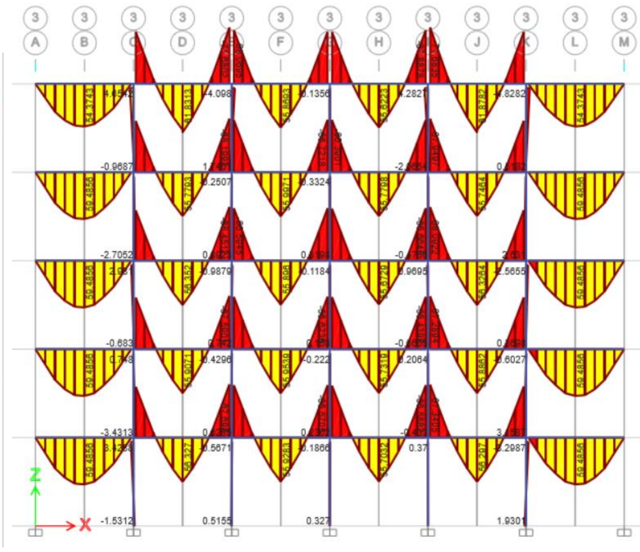

Moment y-y:

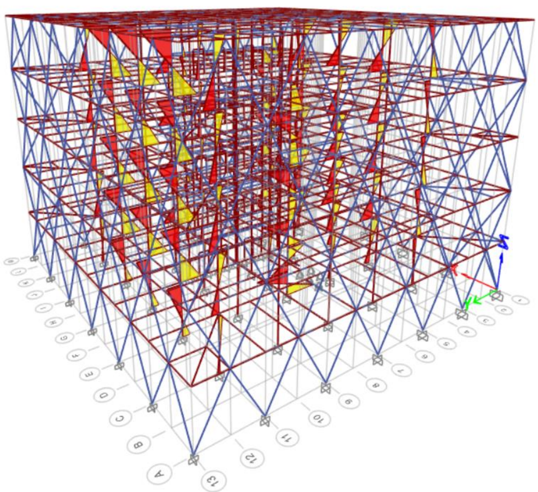

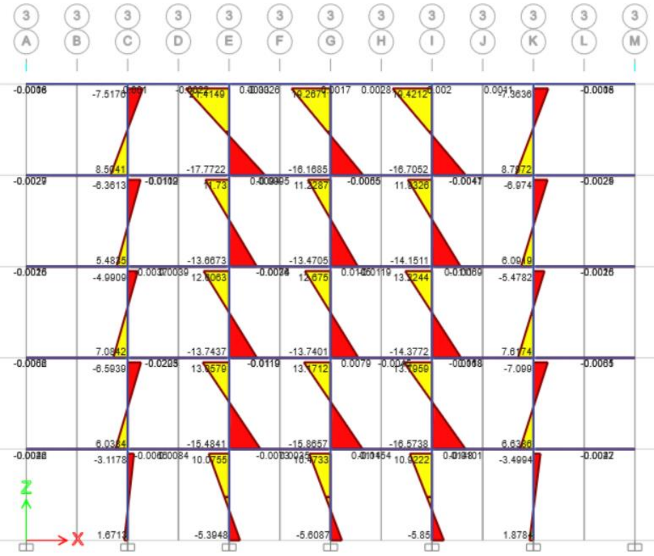

Torsion:

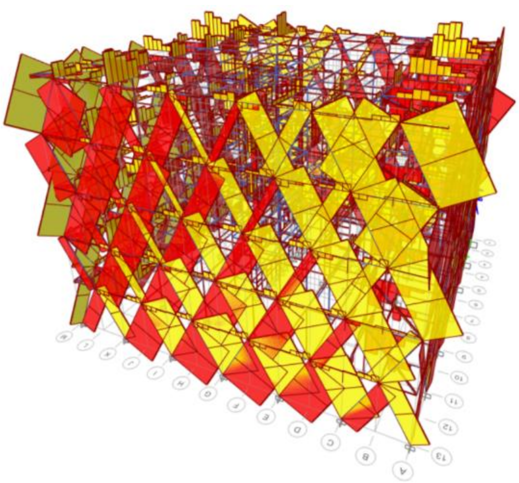

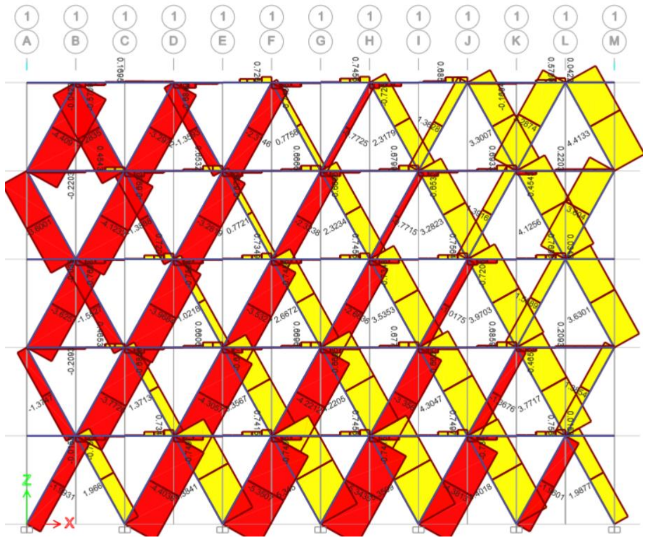

8.5.2 Conservative Design 5 m ; 2.5 m Composite Spacing

Axial Force:

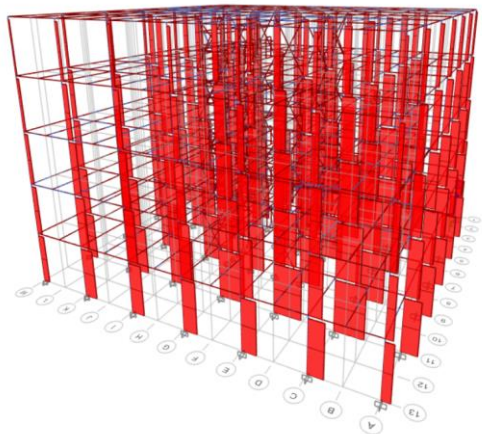

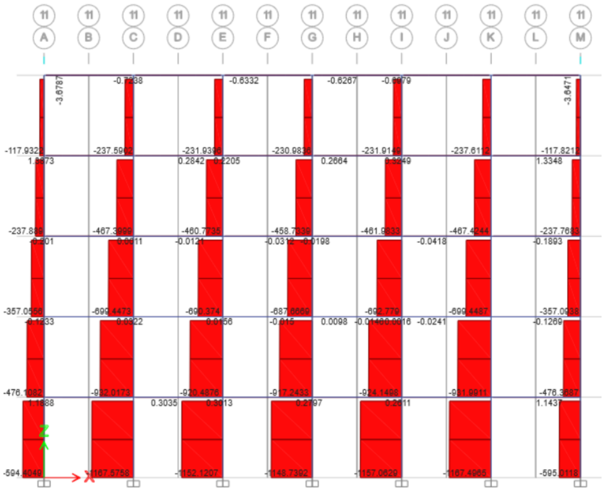

Shear z-z:

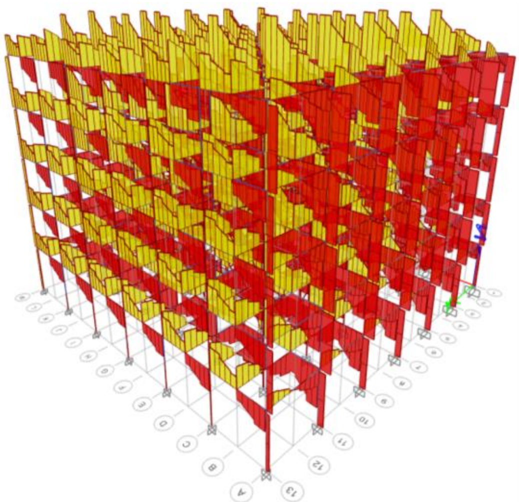

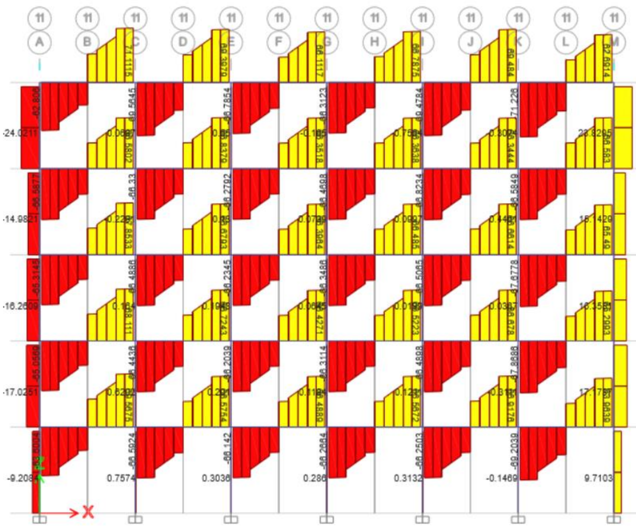

Shear y-y:

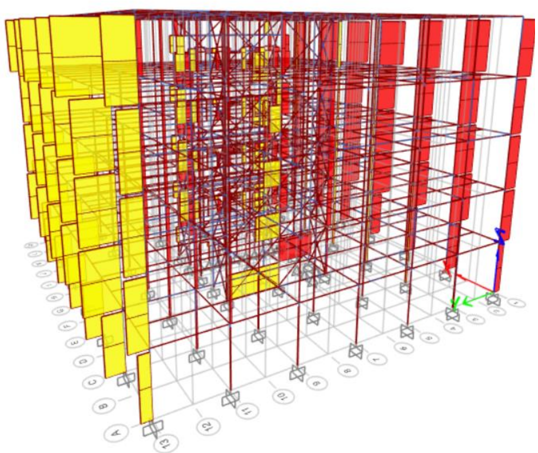

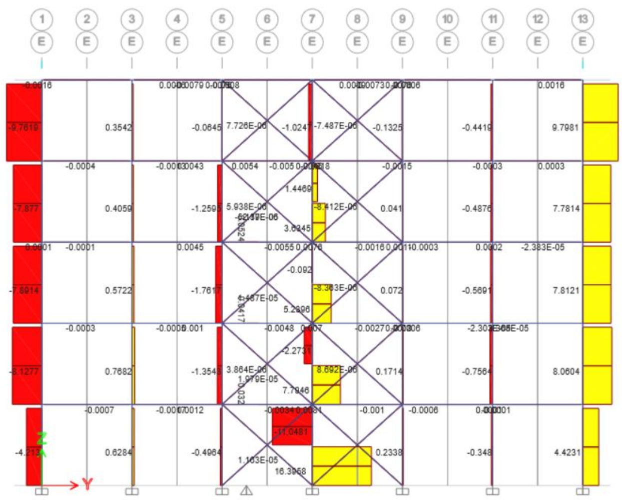

Moment z-z:

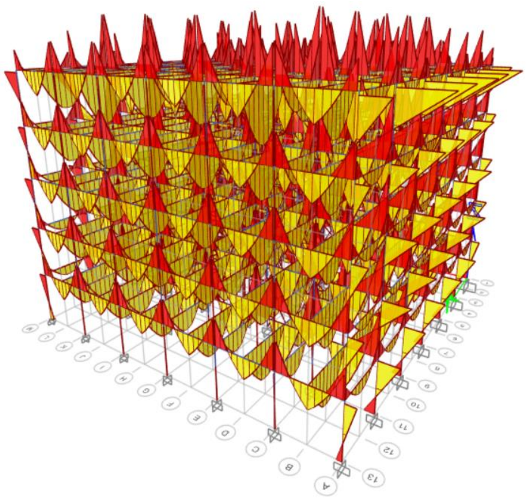

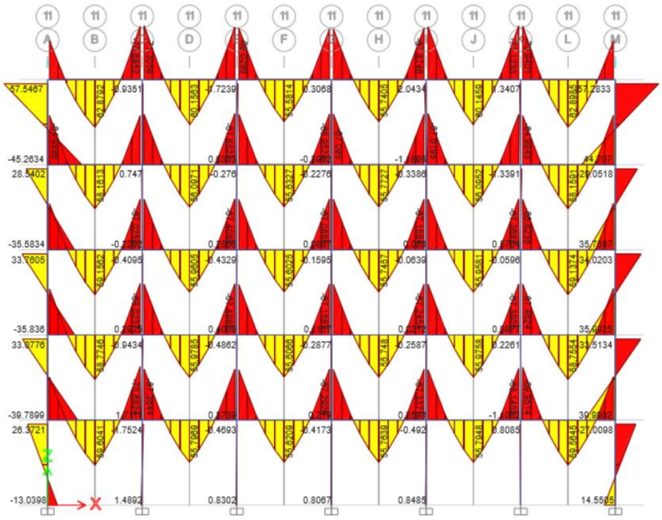

Moment y-y:

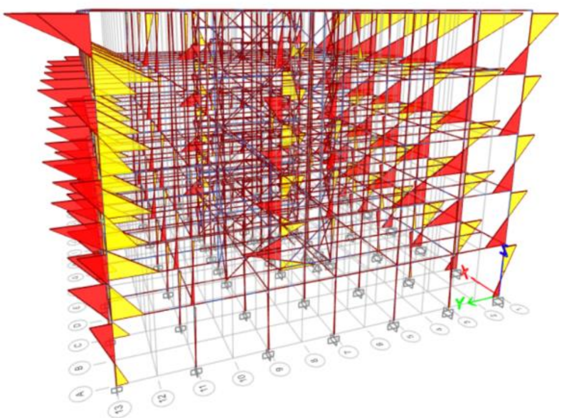

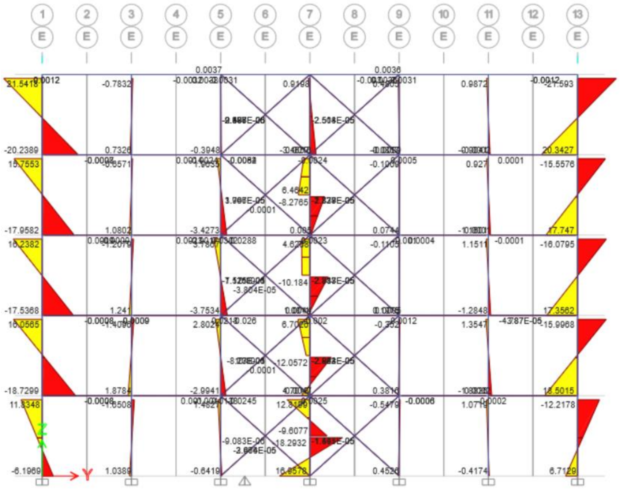

Torsion:

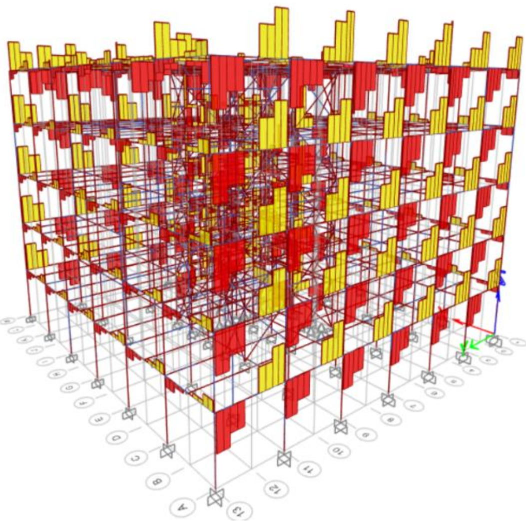

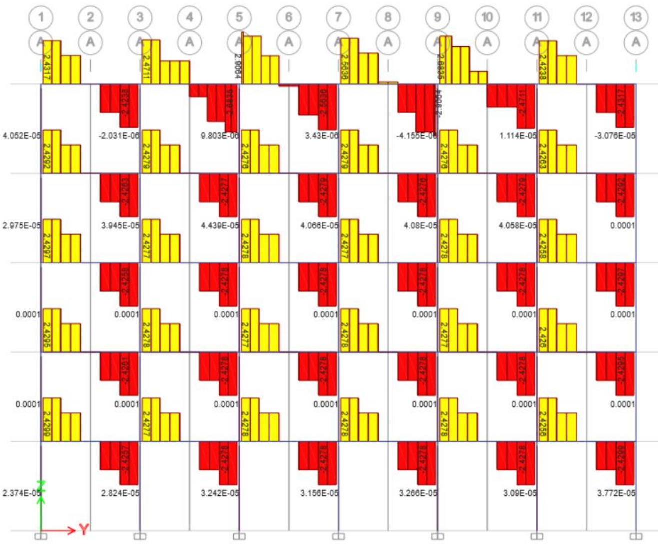

8.5.3 Ground+Diagrid 60: 5m Column Spacing

Axial Force:

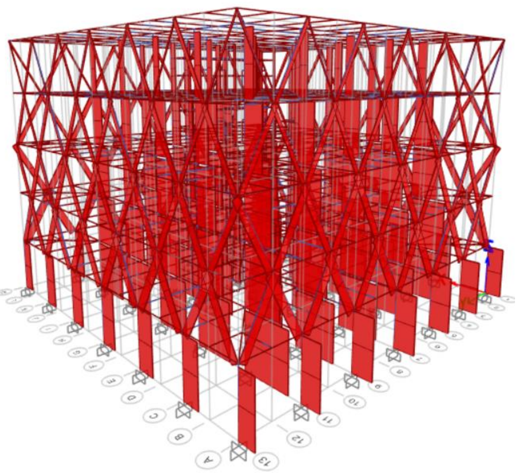

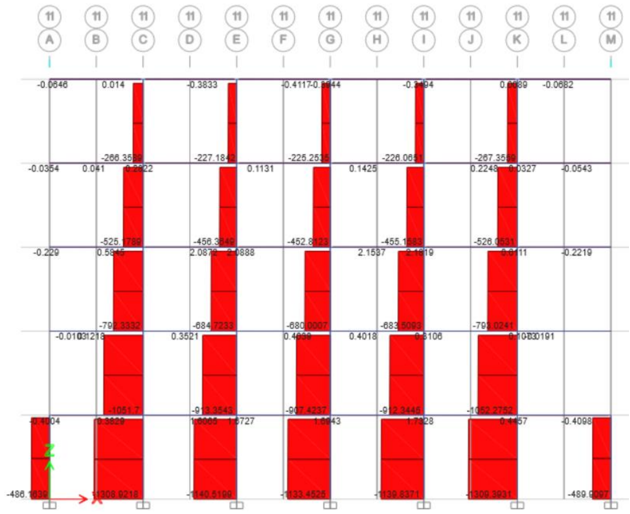

Shear z-z:

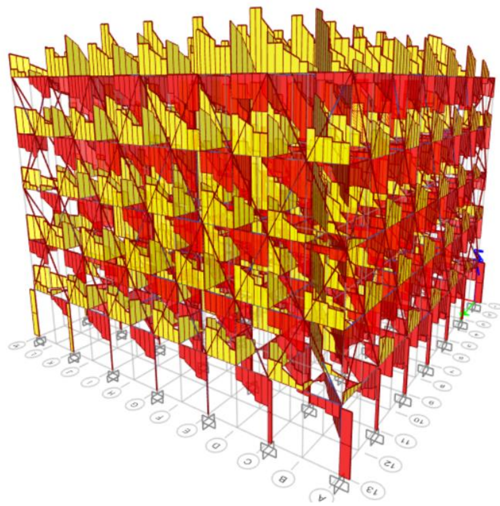

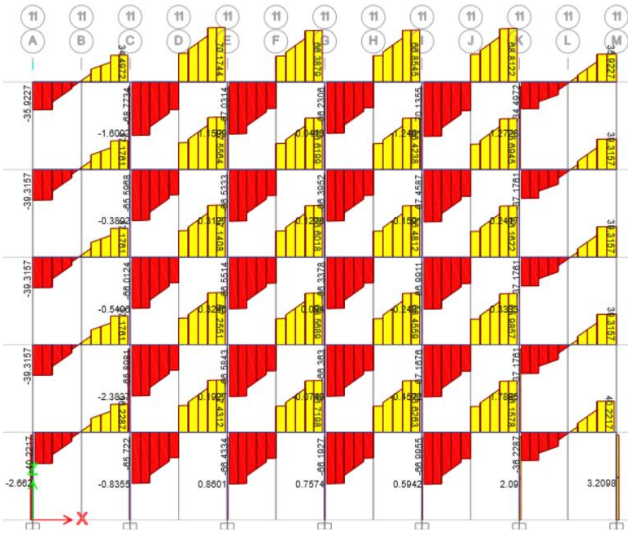

Shear y-y:

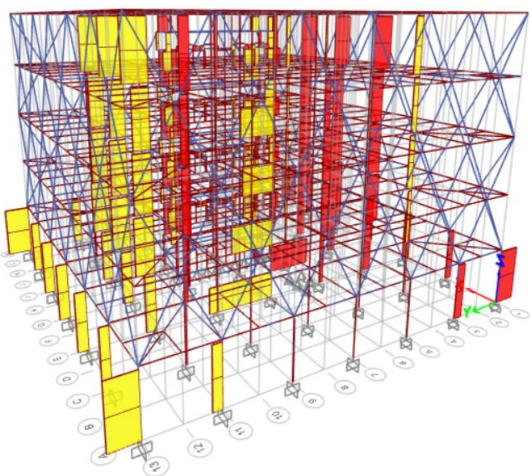

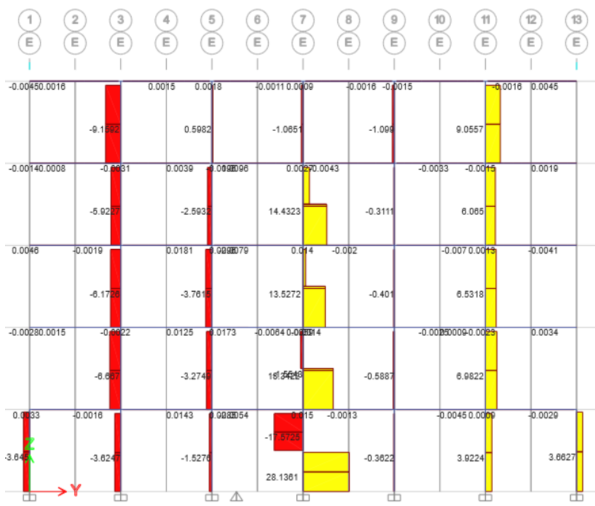

Moment z-z:

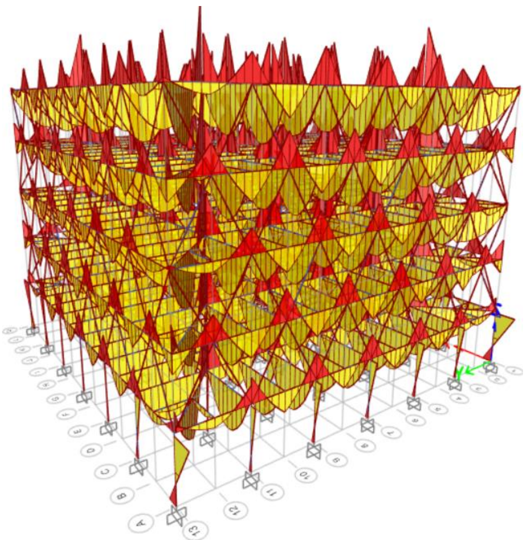

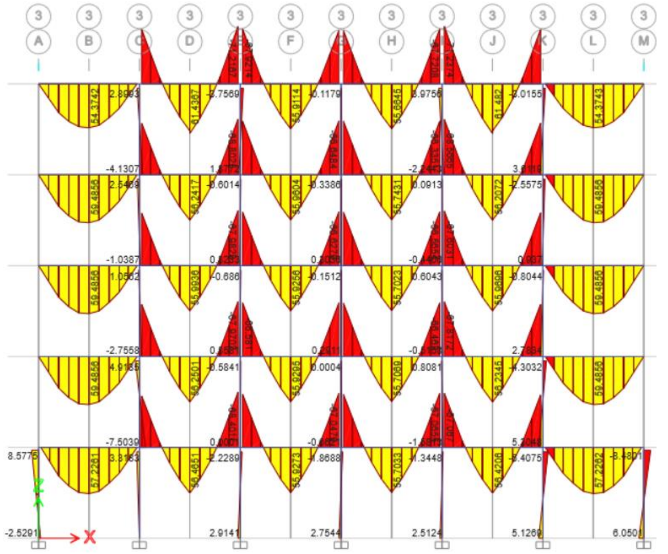

Moment y-y:

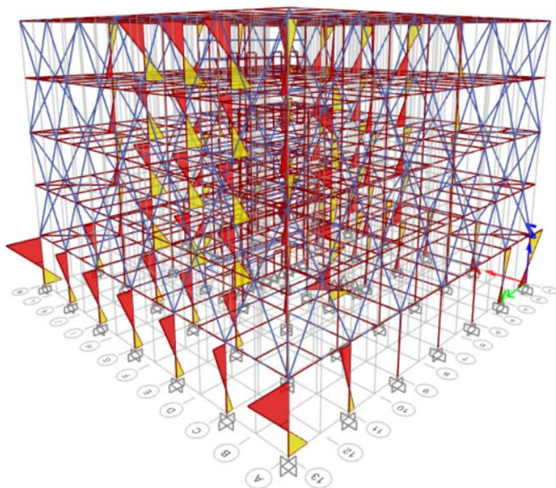

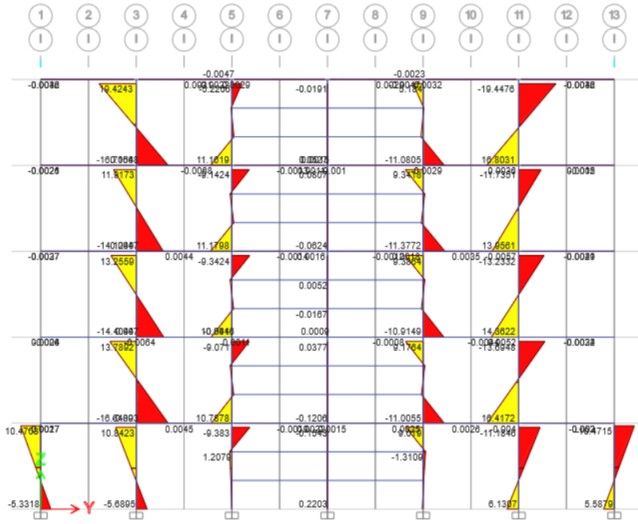

Torsion:

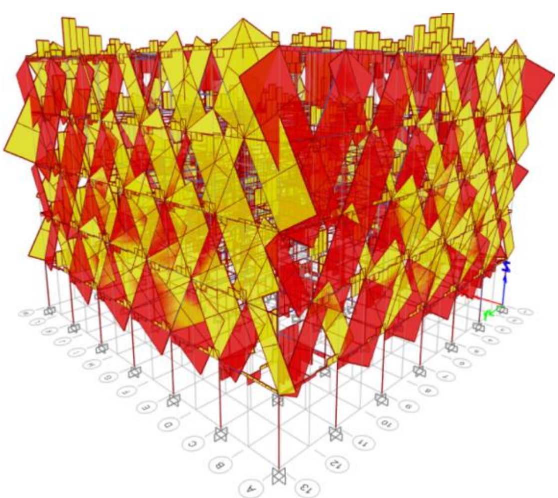

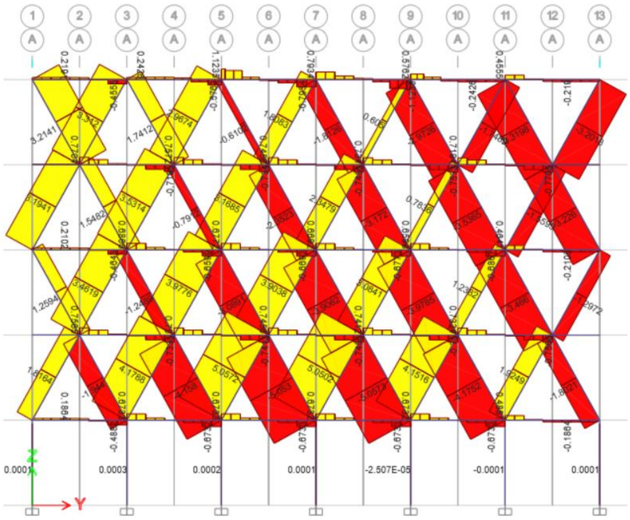

8.5.4 X- Braced Frame (Sides) 5 m Column Spacing

Axial Force:

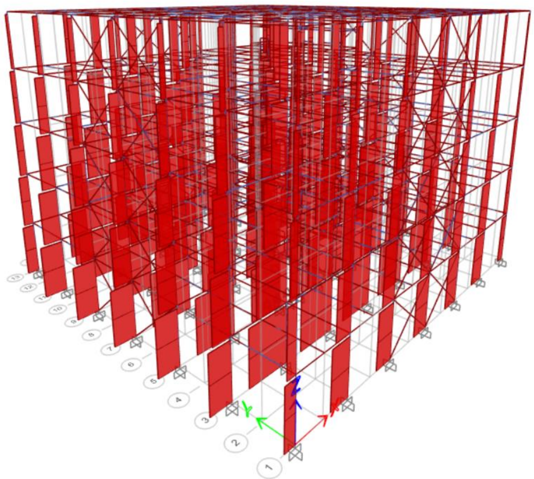

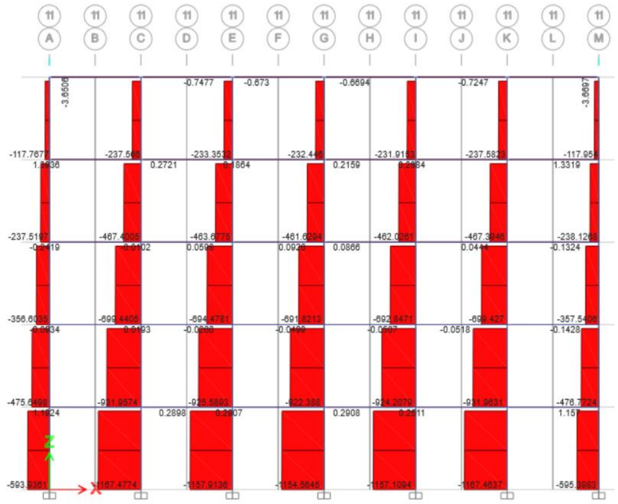

Shear z-z:

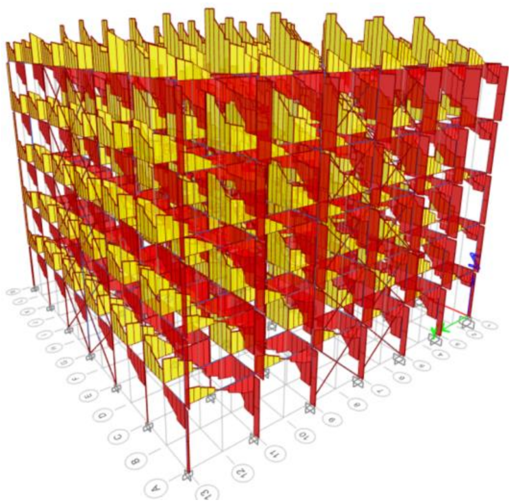

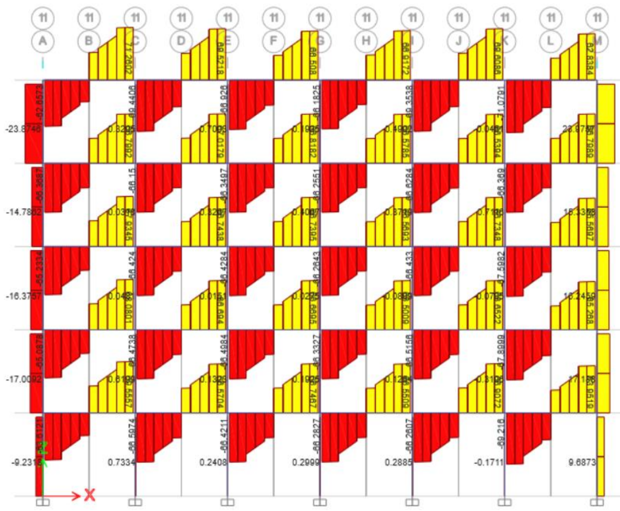

Shear y-y:

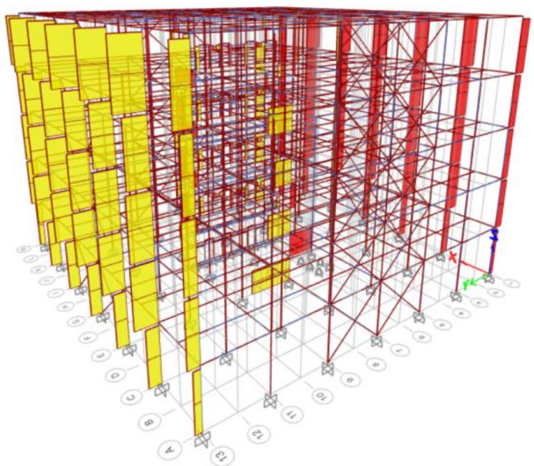

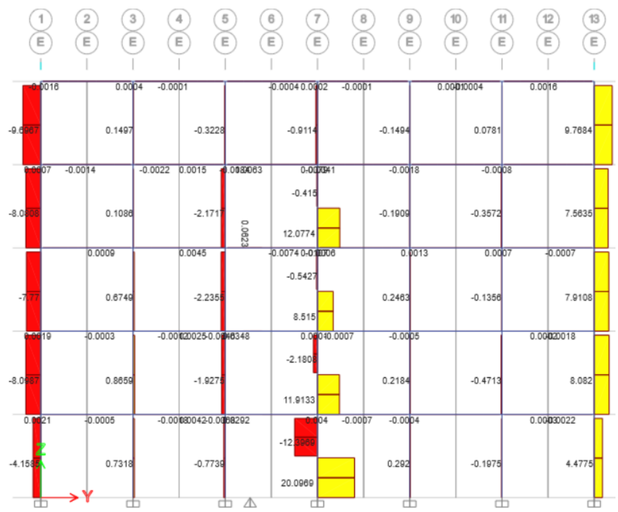

Moment z-z:

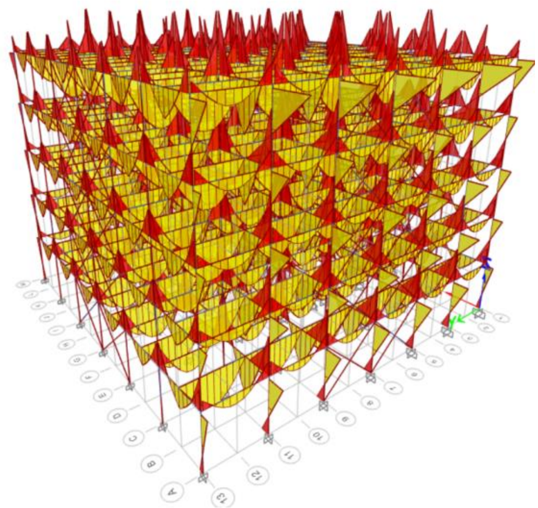

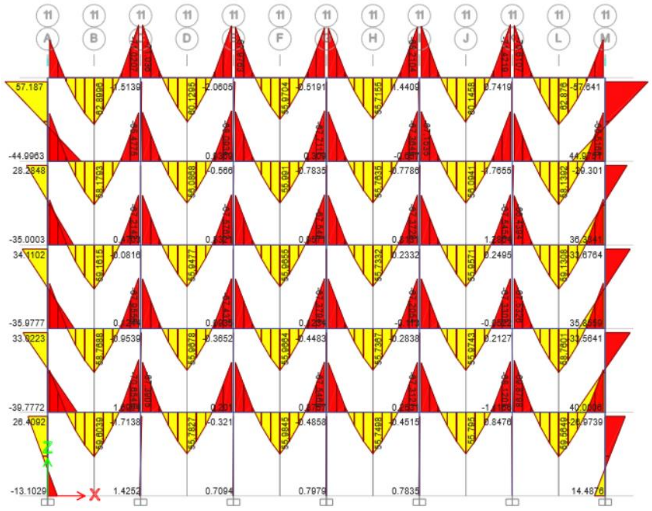

Moment y-y:

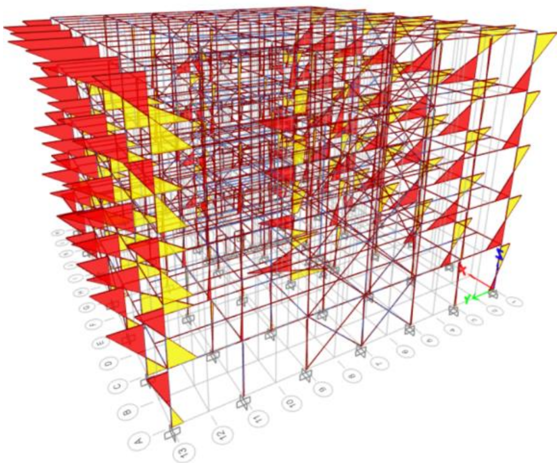

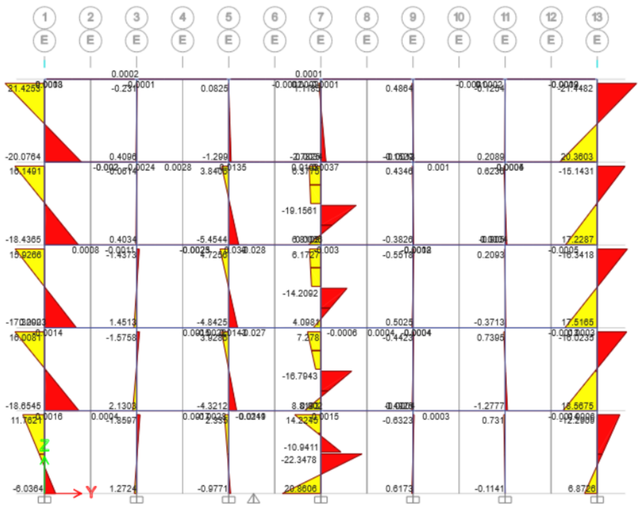

Torsion:

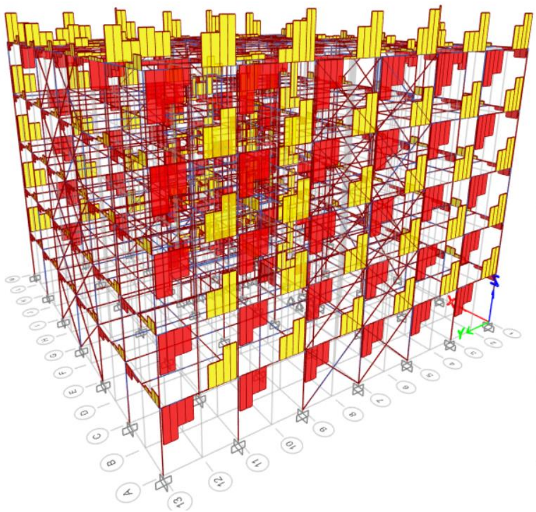

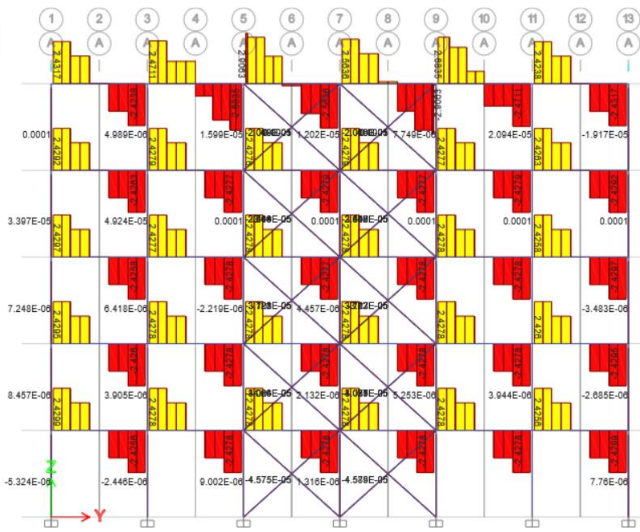

8.5.5 V- Braced Frame (Sides) 5 m Column Spacing

Axial Force:

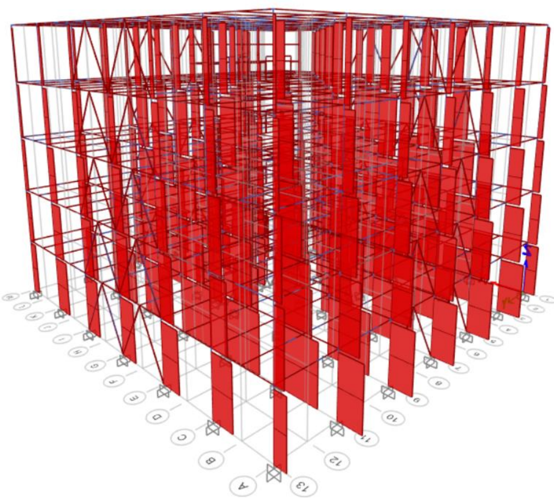

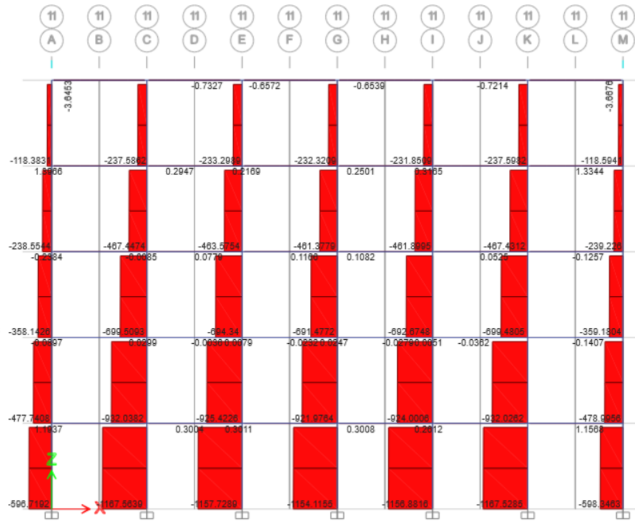

Shear z-z:

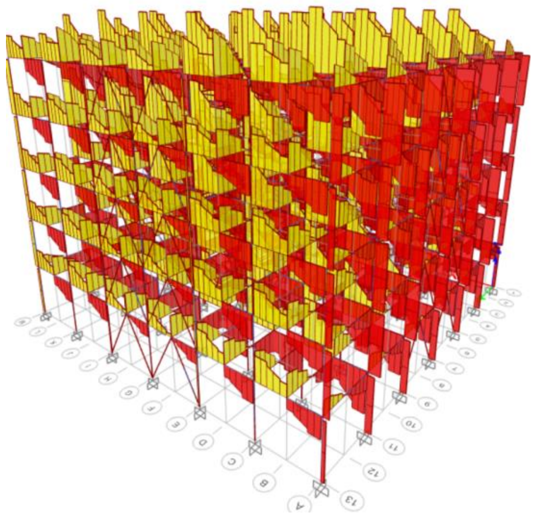

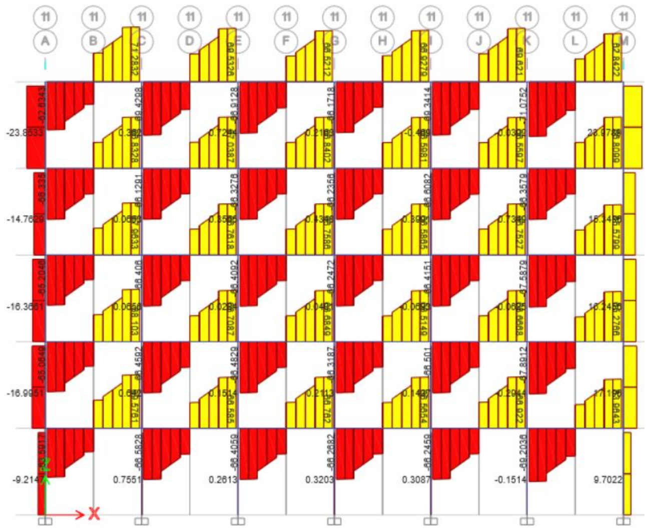

Shear y-y:

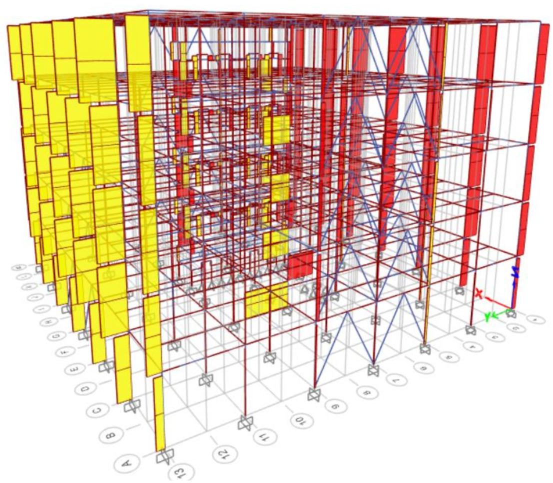

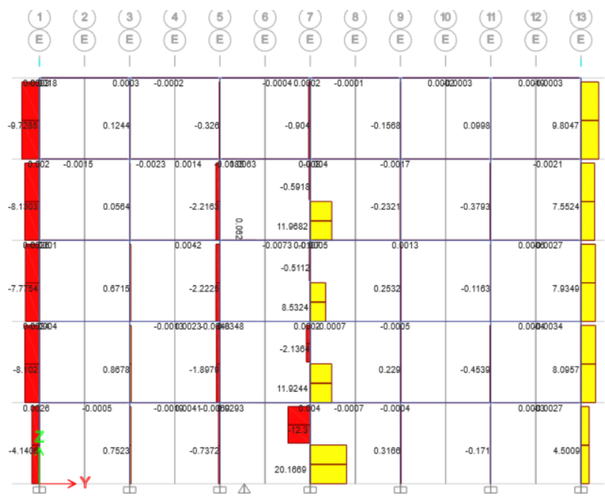

Moment z-z:

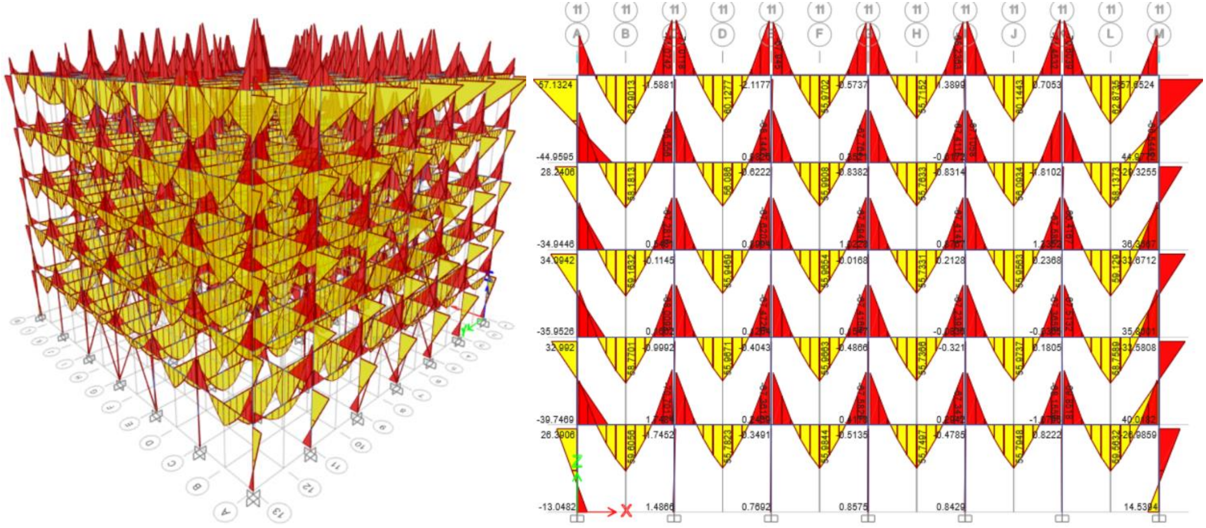

Moment y-y:

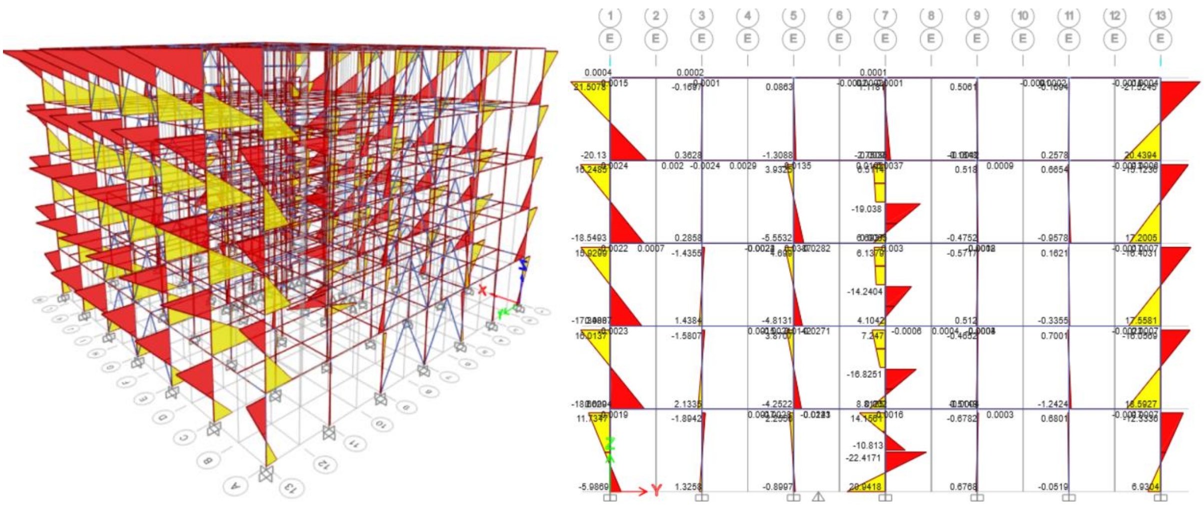

Torsion:

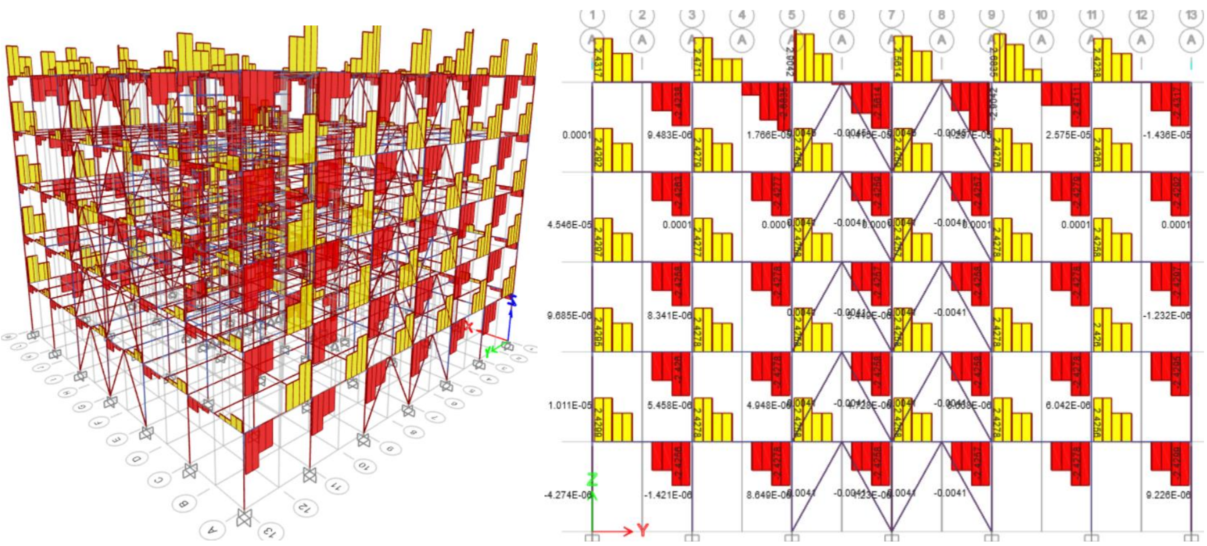

8.5.6 Diagrid 70 6 m Column Spacing

Axial Force:

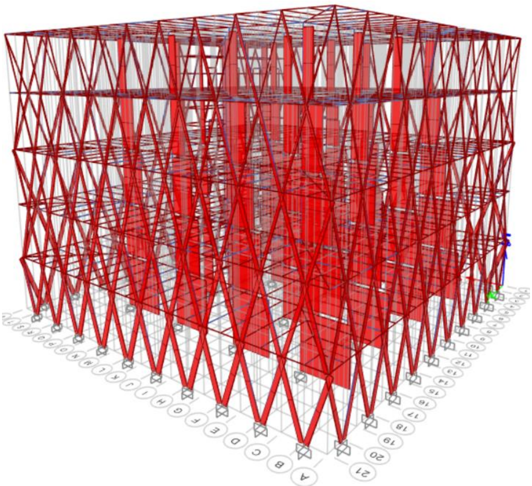

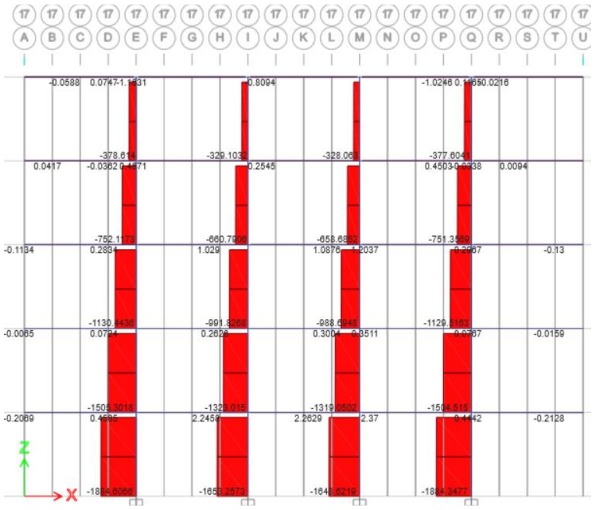

Shear z-z:

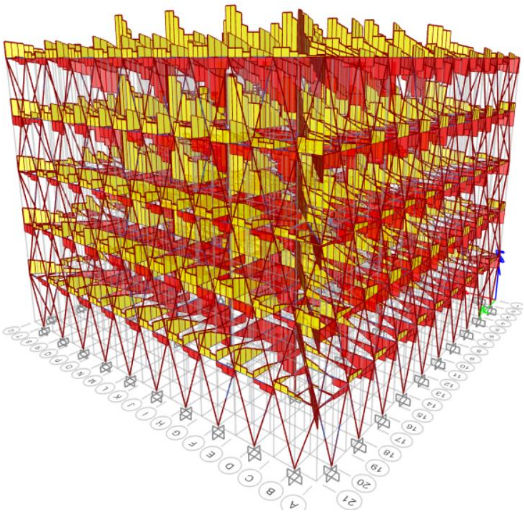

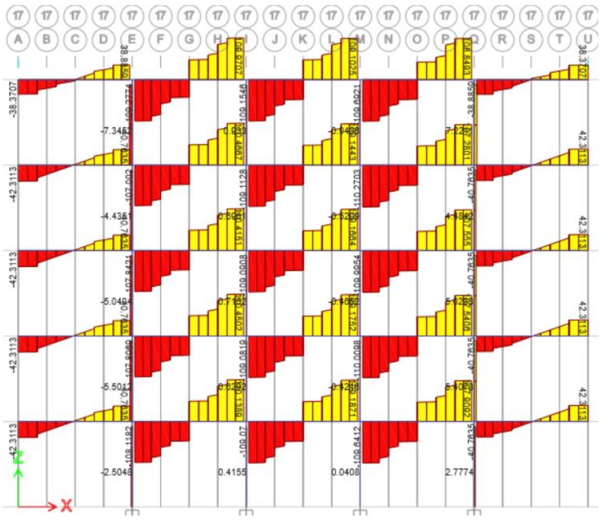

Shear y-y:

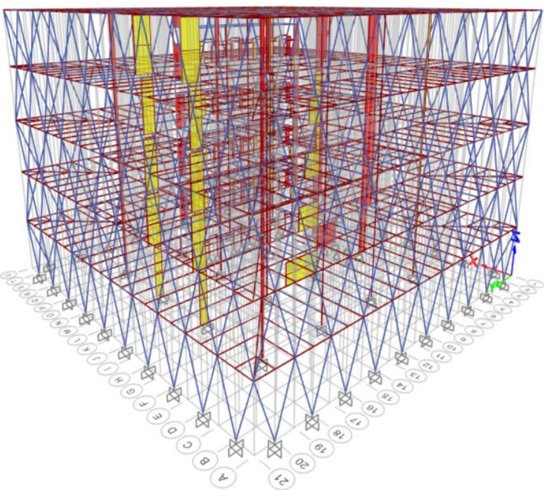

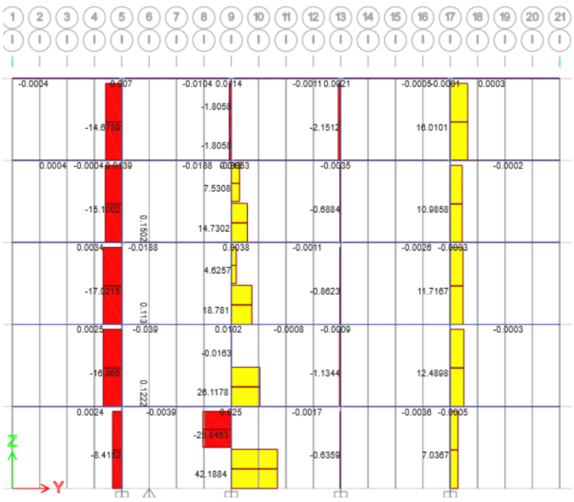

Moment z-z:

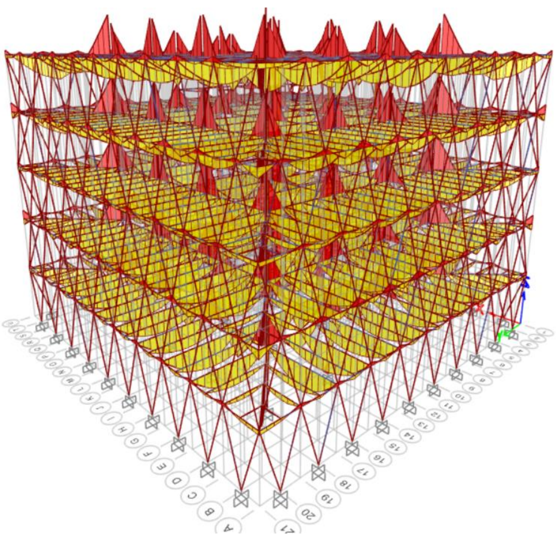

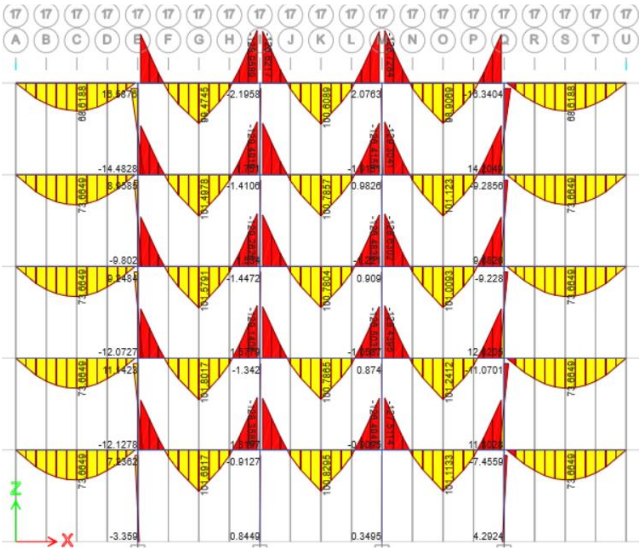

Moment y-y:

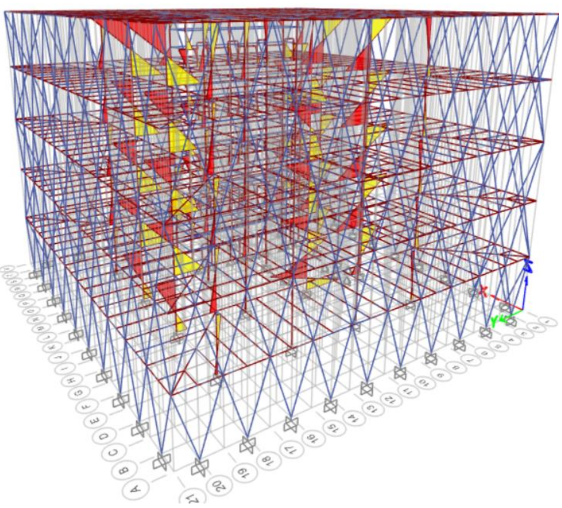

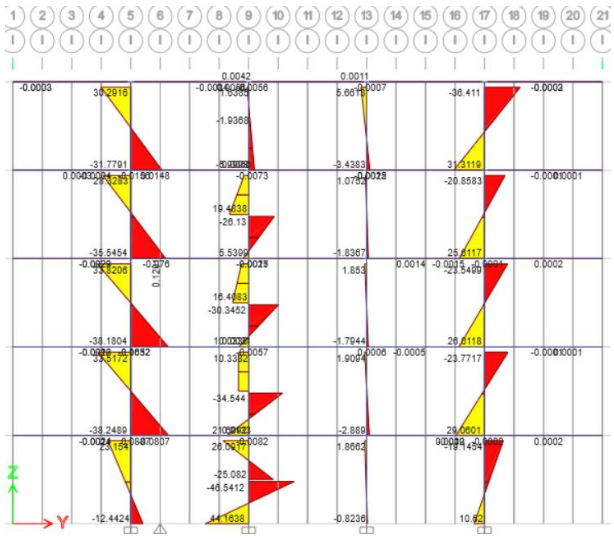

Torsion:

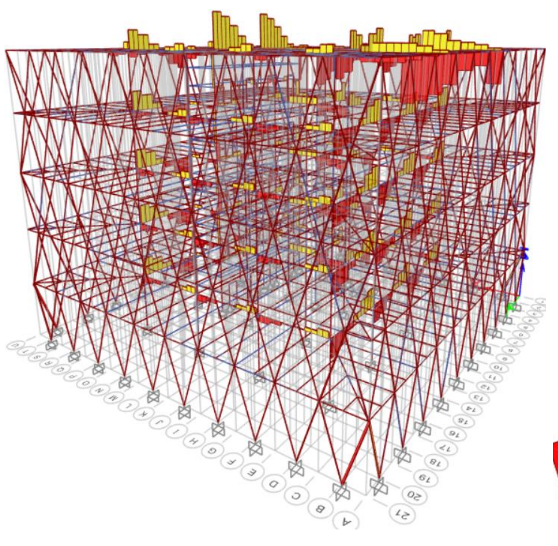

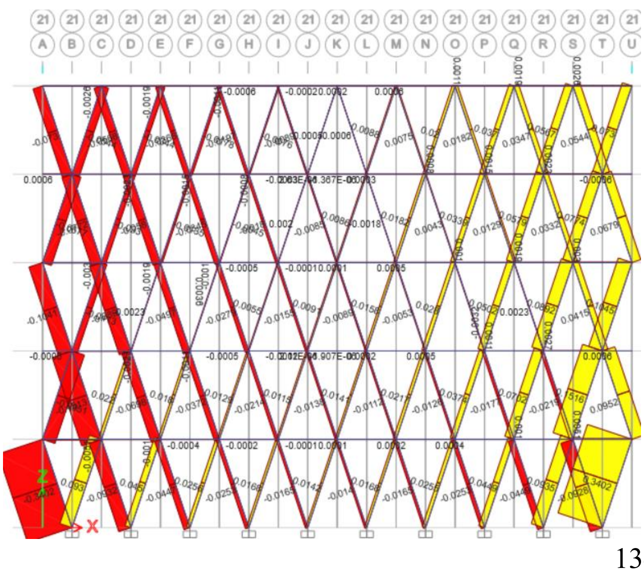

8.5.7 Conservative Design 6 m ; 3 m Composite Spacing

Axial Force:

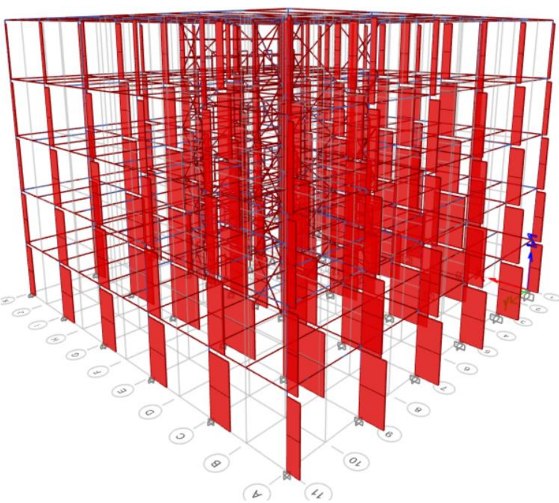

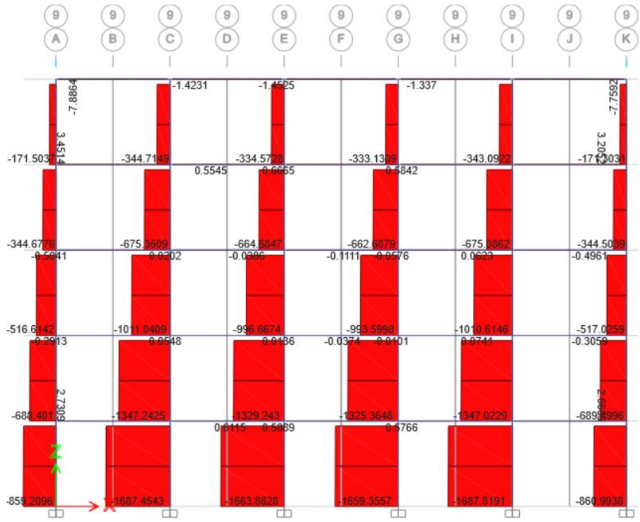

Shear z-z:

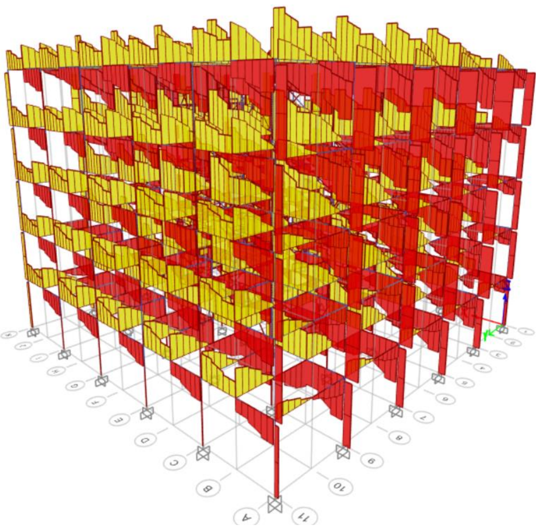

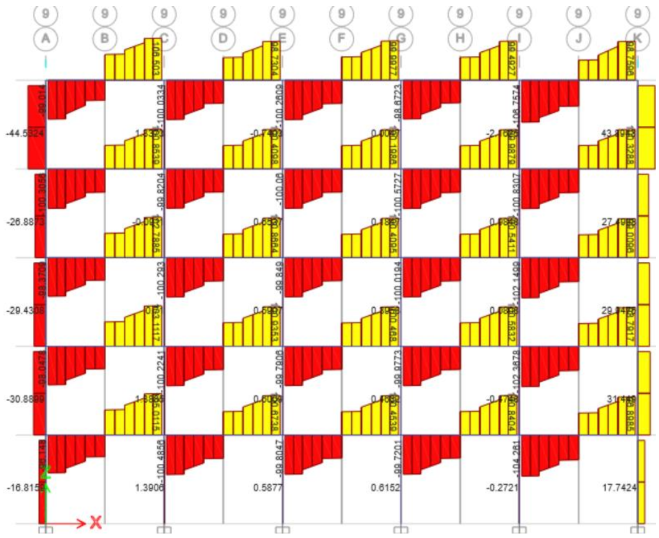

Shear y-y:

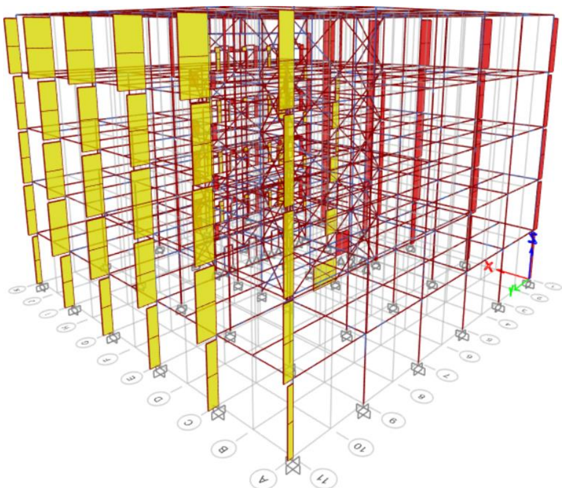

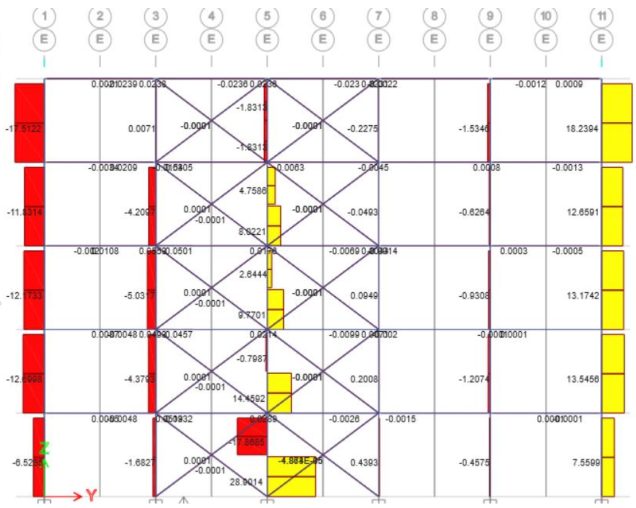

Moment z-z:

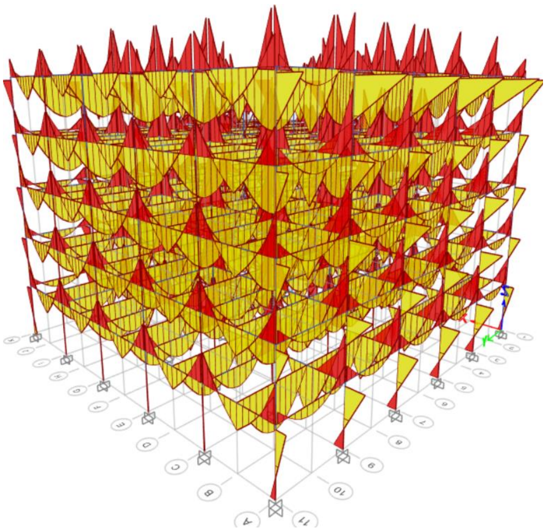

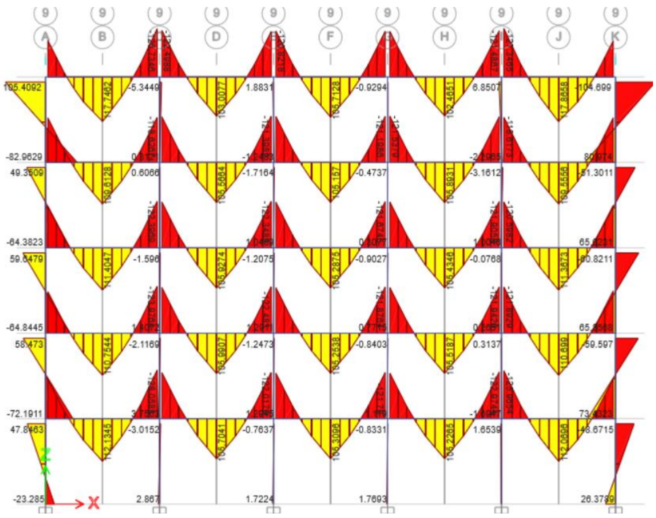

Moment y-y:

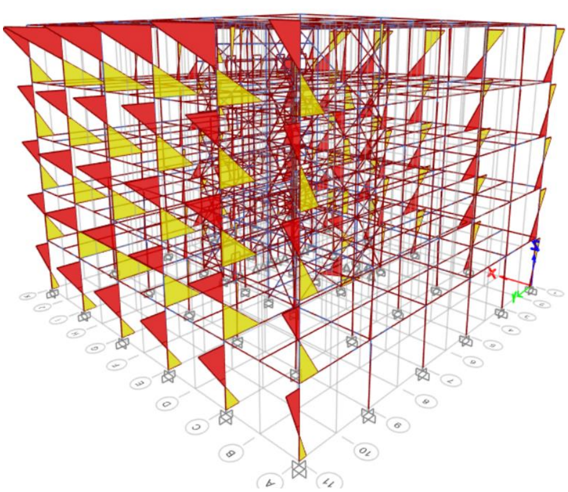

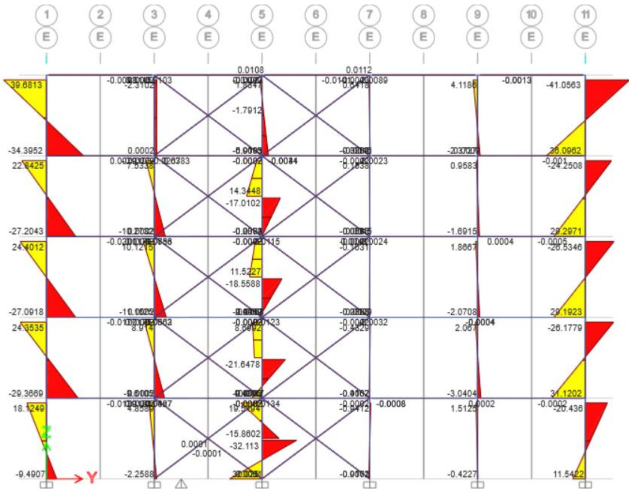

Torsion:

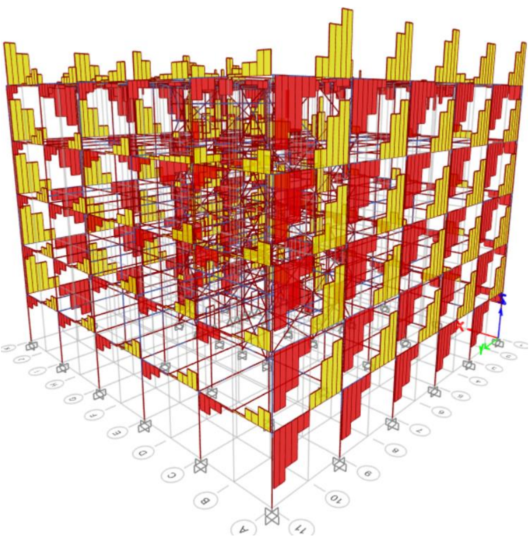

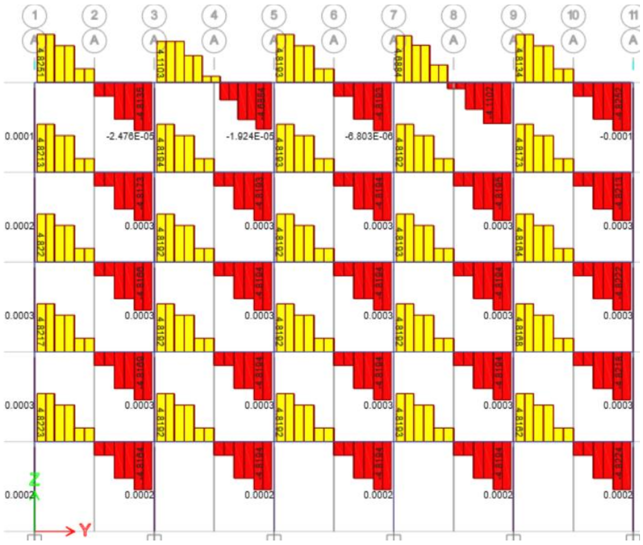

8.6 Appendix F: Connection Detailing

8.6.1 4 Beam 2 Column Connection

Members

Geometry

Name	Cross-section	β – Direction [°]	γ - Pitch [°]	α - Rotation [°]	Offset ex [mm]	Offset ey [mm]	Offset ez [mm]
Member 1	39 - HEA240A	0.0	90.0	0.0	0	0	0
Member 2	41 - HEA240A	0.0	-90.0	-180.0	0	0	0
Member 3	38 - IPE220	180.0	0.0	0.0	0	0	-170
Member 4	40 - IPE140	-90.0	0.0	0.0	0	0	-170
Member 5	38 - IPE220	0.0	0.0	0.0	0	0	-170
Member 6	38 - IPE220	90.0	0.0	0.0	0	0	-170

Supports and forces

Name	Support	Forces in	X [mm]
Member 1 / end		Node	0
Member 2 / end	N-Vy-Vz-Mx-My-Mz	Node	0
Member 3 / end		Node	0
Member 4 / end		Node	0
Member 5 / end		Node	0
Member 6 / end		Node	0

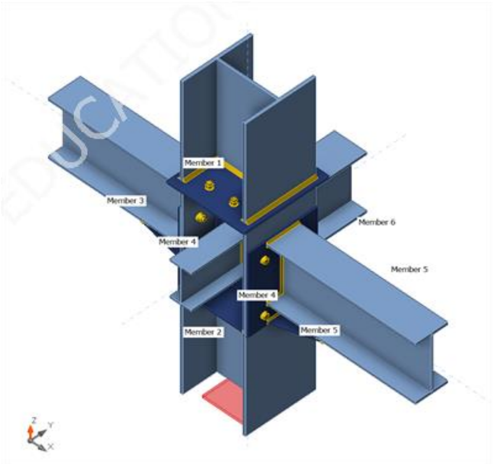

Cross-sections

Name	Material
39 - HEA240A	S 355
41 - HEA240A	S 355
38 - IPE220	S 355
40 - IPE140	S 355

Bolts

Name	Diameter [mm]	f_y [MPa]	f_u [MPa]	Gross area [mm^2]
M12 8.8	12	640.0	800.0	113
M14 10.9	14	900.0	1000.0	154

Load effects (Equilibrium not required)

Name	Member	N [kN]	Vy [kN]	Vz [kN]	Mx [kNm]	My [kNm]	Mz [kNm]
LE1	Member 1 / End	-909.5	0.1	15.7	0.0	37.0	0.2
	Member 3 / End	0.4	0.0	54.6	1.8	-50.5	0.0
	Member 4 / End	-0.1	0.0	-44.8	0.0	0.0	0.0
	Member 5 / End	0.2	0.0	-54.4	-1.8	-50.3	0.0
	Member 6 / End	0.8	0.0	61.1	0.0	-58.2	0.0

Check

Summary

Name	Value	Check status
Analysis	100.0%	OK
Plates	3.3 < 5.0%	OK
Bolts	95.2 < 100%	OK
Welds	99.7 < 100%	OK
Buckling	2.70	

Plates

Name	Material	t_p [mm]	Loads	σ_{Ed} [MPa]	ε_{Pl} [%]	$\sigma_{c,Ed}$ [MPa]	Status
Member 1-bfl 1	S 355	9.0	LE1	347.2	0.0	0.0	OK
Member 1-tfl 1	S 355	9.0	LE1	220.5	0.0	0.0	OK
Member 1-w 1	S 355	6.5	LE1	235.5	0.0	0.0	OK
Member 2-bfl 1	S 355	9.0	LE1	356.5	0.7	70.1	OK
Member 2-tfl 1	S 355	9.0	LE1	355.3	0.1	54.0	OK
Member 2-w 1	S 355	6.5	LE1	361.3	3.0	75.2	OK
Member 3-bfl 1	S 355	9.2	LE1	353.7	0.0	0.0	OK
Member 3-tfl 1	S 355	9.2	LE1	244.5	0.0	0.0	OK
Member 3-w 1	S 355	5.9	LE1	342.9	0.0	0.0	OK
Member 4-bfl 1	S 355	6.9	LE1	132.5	0.0	0.0	OK
Member 4-tfl 1	S 355	6.9	LE1	132.7	0.0	0.0	OK
Member 4-w 1	S 355	4.7	LE1	351.2	0.1	0.0	OK
Member 5-bfl 1	S 355	9.2	LE1	355.3	0.2	0.0	OK
Member 5-tfl 1	S 355	9.2	LE1	355.1	0.0	0.0	OK
Member 5-w 1	S 355	5.9	LE1	340.0	0.0	0.0	OK
Member 6-bfl 1	S 355	9.2	LE1	355.7	0.3	0.0	OK
Member 6-tfl 1	S 355	9.2	LE1	300.5	0.2	0.0	OK
Member 6-w 1	S 355	5.9	LE1	352.7	0.1	0.0	OK
Operation 1a	S 235	5.0	LE1	235.0	0.0	102.9	OK
Operation 1b	S 235	5.0	LE1	142.9	0.0	102.9	OK
Operation 2	S 235	7.0	LE1	235.1	0.0	84.3	OK
Operation 3a	S 355	18.0	LE1	356.1	0.5	149.6	OK
Operation 3b	S 355	18.0	LE1	361.9	3.3	391.4	OK
Operation 4	S 235	7.0	LE1	235.3	0.1	102.1	OK
WID1a	S 355	5.0	LE1	359.9	2.3	0.0	OK
WID1b	S 355	5.0	LE1	356.7	0.8	0.0	OK
WID2a	S 355	5.0	LE1	338.1	0.1	0.0	OK
WID2b	S 355	5.0	LE1	321.2	0.0	0.0	OK
STIFF2a	S 355	5.0	LE1	335.8	0.0	0.0	OK

STIFF2b	S 355	5.0	LE1	344.9	0.0	0.0	OK

Design data

Material	f_y [MPa]	ε_{lim} [%]
S 355	355.0	5.0
S 235	235.0	5.0

Detailed result for Operation 3b Design values used in the analysis

$$f_{yd} = \frac{f_{yk}}{\gamma_{M0}} = 355.0 \text{ MPa}$$

Where:

f_{yk} = 355.0 MPa – characteristic yield strength

γ_{M0} = 1.00 – partial safety factor for steel material EN 1993-1-1 – 6.1

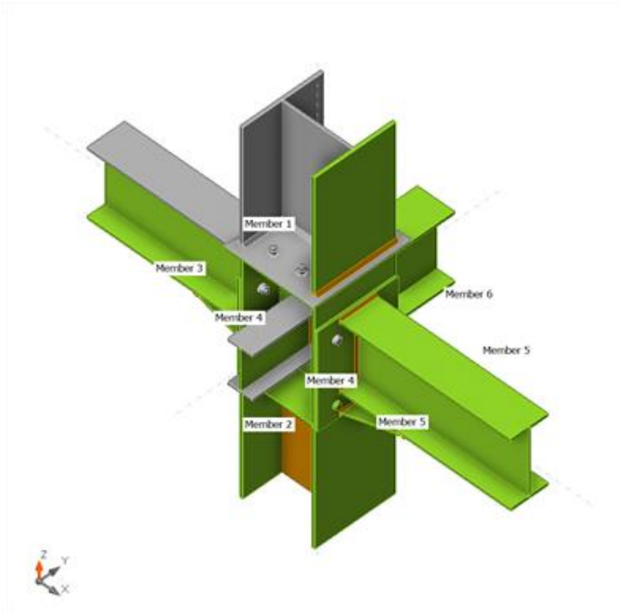

Overall check, LE1

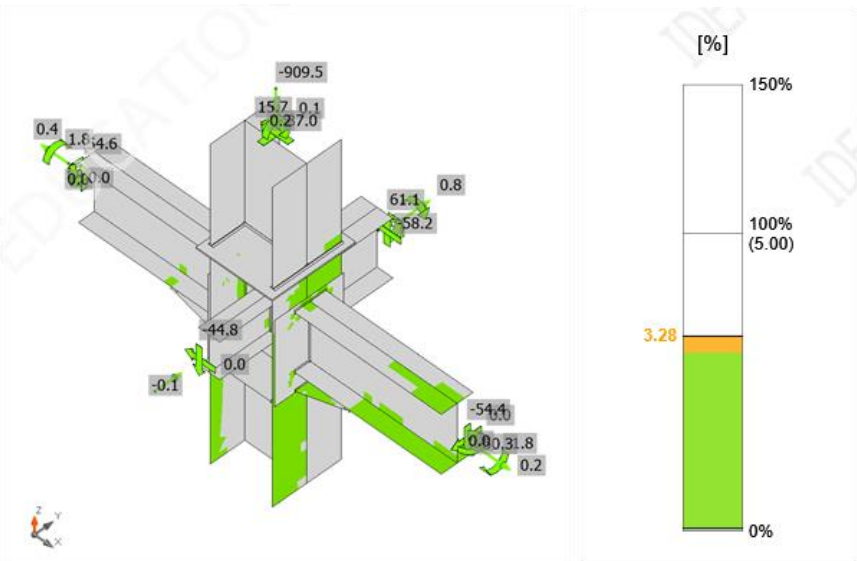

Strain check, LE1

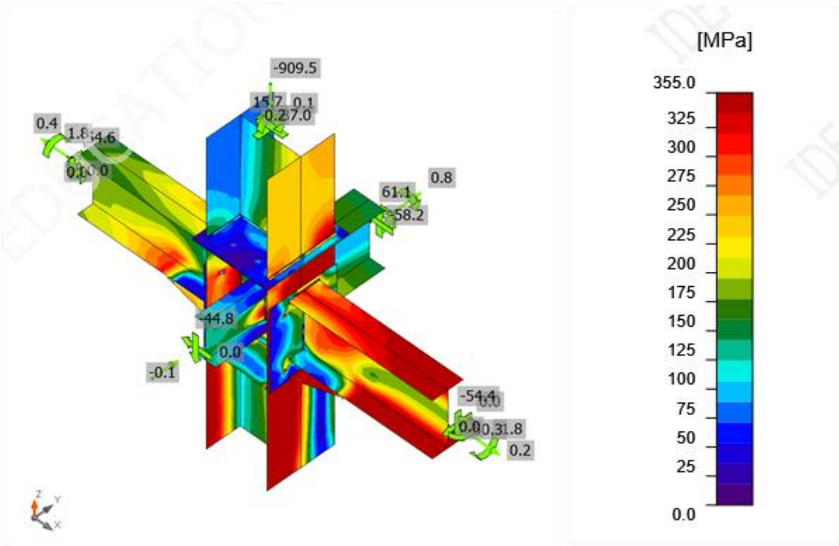

Equivalent stress, LE1

Bolts

Shape	Item	Grade	Loads	$F_{t,Ed}$ [kN]	$F_{v,Ed}$ [kN]	$F_{b,Rd}$ [kN]	Ut_t [%]	Ut_s [%]	Ut_{ts} [%]	Detailing	Status
	B1	M12 8.8 - 1	LE1	0.6	3.8	43.2	1.1	11.7	12.5	OK	OK
	B2	M12 8.8 - 1	LE1	0.3	4.0	43.2	0.5	12.4	12.8	OK	OK
	B3	M12 8.8 - 1	LE1	0.6	4.1	43.2	1.2	12.8	13.6	OK	OK
	B4	M12 8.8 - 1	LE1	0.3	3.8	43.2	0.7	11.8	12.3	OK	OK
	B5	M12 8.8 - 2	LE1	8.7	4.7	60.5	18.0	14.5	27.4	OK	OK
	B6	M12 8.8 - 2	LE1	3.0	2.9	60.5	6.1	8.8	13.2	OK	OK
	B7	M12 8.8 - 2	LE1	1.5	1.2	60.5	3.0	3.8	6.0	OK	OK
	B8	M12 8.8 - 2	LE1	5.7	0.8	60.5	11.7	2.5	10.8	OK	OK
	B9	M14 10.9 - 3	LE1	48.5	15.6	89.2	58.3	33.8	75.4	OK	OK
	B10	M14 10.9 - 3	LE1	48.1	14.8	89.2	57.9	32.1	73.5	OK	OK
	B11	M14 10.9 - 3	LE1	63.0	11.7	247.0	75.9	25.4	79.6	OK	OK
	B12	M14 10.9 - 3	LE1	65.0	11.8	244.2	78.2	25.5	81.4	OK	OK
	B13	M14 10.9 - 3	LE1	78.7	10.6	77.9	94.7	22.9	90.6	OK	OK
	B14	M14 10.9 - 3	LE1	79.1	10.4	102.9	95.2	22.6	90.6	OK	OK
	B15	M12 8.8 - 2	LE1	4.0	14.9	60.5	8.2	46.1	52.0	OK	OK
	B16	M12 8.8 - 2	LE1	10.7	11.2	60.5	22.1	34.5	50.3	OK	OK
	B17	M12 8.8 - 2	LE1	20.6	14.9	60.5	42.3	45.9	76.2	OK	OK
	B18	M12 8.8 - 2	LE1	10.6	16.1	60.5	21.8	49.8	65.4	OK	OK

Design data

Grade	$F_{t,Rd}$ [kN]	$B_{p,Rd}$ [kN]	$F_{v,Rd}$ [kN]
M12 8.8 - 1	48.6	51.6	32.4
M12 8.8 - 2	48.6	72.3	32.4
M14 10.9 - 3	83.1	295.0	46.2

Detailed result for B14

Tension resistance check (EN 1993-1-8 – Table 3.4)

$F_{t,Rd} = \frac{k_2 f_{ub} A_s}{\gamma_{M2}} =$ 83.1 kN ≥ $F_{t,Ed} =$ 79.1 kN

Where:

k_2 = 0.90 – Factor

f_{ub} = 1000.0 MPa – Ultimate tensile strength of the bolt

A_s = 115 mm^2 – Tensile stress area of the bolt

γ_{M2} = 1.25 – Safety factor

Punching resistance check (EN 1993-1-8 – Table 3.4)

$B_{p,Rd} = \frac{0.6\,\pi\, d_m\, t_p\, f_u}{\gamma_{M2}} =$ 295.0 kN ≥ $F_{t,Ed} =$ 79.1 kN

Where:

d_m = 22 mm – The mean of the across points and across flats dimensions of the bolt head or the nut, whichever is smaller

t_p = 18 mm – Plate thickness

f_u = 490.0 MPa – Ultimate strength

γ_{M2} = 1.25 – Safety factor

Shear resistance check (EN 1993-1-8 – Table 3.4)

$F_{v,Rd} = \frac{\beta_p\, \alpha_v f_{ub} A}{\gamma_{M2}} =$ 46.2 kN ≥ $F_{v,Ed} =$ 10.4 kN

Where:

β_p = 1.00 – Reduction factor for packing

α_v = 0.50 – Reduction factor for shear stress

f_{ub} = 1000.0 MPa – Ultimate tensile strength of the bolt

A = 115 mm^2 – Tensile stress area of the bolt

γ_{M2} = 1.25 – Safety factor

Bearing resistance check (EN 1993-1-8 – Table 3.4)

$F_{b,Rd} = \frac{k_1\, \alpha_b\, f_u\, d t}{\gamma_{M2}} =$ 102.9 kN ≥ $F_{b,Ed} =$ 8.2 kN

Where:

$k_1 = \min(2.8\frac{e_2}{d_0} - 1.7, 1.4\frac{p_2}{d_0} - 1.7, 2.5) =$ 2.50 – Factor for edge distance and bolt spacing perpendicular to the direction of load transfer

$\alpha_b = \min(\frac{e_1}{3d_0}, \frac{p_1}{3d_0} - \frac{1}{4}, \frac{f_{ub}}{f_u}, 1) =$ 0.42 – Factor for end distance and bolt spacing in direction of load transfer

e_2 = 30 mm – Distance to the plate edge perpendicular to the shear force

p_2 = ∞ mm – Distance between bolts perpendicular to the shear force

d_0 = 16 mm – Bolt hole diameter

e_1 = 20 mm – Distance to the plate edge in the direction of the shear force

p_1 = ∞ mm – Distance between bolts in the direction of the shear force

f_{ub} = 1000.0 MPa – Ultimate tensile strength of the bolt

f_u = 490.0 MPa – Ultimate strength of the plate

d = 14 mm – Nominal diameter of the fastener

t = 18 mm – Thickness of the plate

γ_{M2} = 1.25 – Safety factor

Utilization in tension

$\frac{F_{t,Ed}}{\min(F_{t,Rd}; B_{p,Rd})} =$ 0.95 ≤ 1.0

Where:

$F_{t,Ed}$ = 79.1 kN – Tensile force

$F_{t,Rd}$ = 83.1 kN – Tension resistance

$B_{p,Rd}$ = 295.0 kN – Punching resistance

Utilization in shear

$\max(\frac{F_{v,Ed}}{F_{v,Rd}}; \frac{F_{b,Ed}}{F_{b,Rd}}) =$ 0.23 ≤ 1.0

Where:

$F_{v,Ed}$ = 10.4 kN – Shear force (in decisive shear plane)

$F_{v,Rd}$ = 46.2 kN – Shear resistance

$F_{b,Ed}$ = 8.2 kN – Bearing force (for decisive plate)

$F_{b,Rd}$ = 102.9 kN – Bearing resistance

Interaction of tension and shear (EN 1993-1-8 – Table 3.4)

$$\frac{F_{v,Ed}}{F_{v,Rd}} + \frac{F_{t,Ed}}{1.4\,F_{t,Rd}} = \quad 0.91 \quad \leq \quad 1.0$$

Where:

$F_{v,Ed} = 10.4$ kN – Shear force (in decisive shear plane)

$F_{v,Rd} = 46.2$ kN – Shear resistance

$F_{t,Ed} = 79.1$ kN – Tensile force

$F_{t,Rd} = 83.1$ kN – Tension resistance

Welds

Item	Edge	Material	T_w [mm]	L [mm]	Loads	$\sigma_{w,Ed}$ [MPa]	ε_{Pl} [%]	$\sigma_{\perp}$ [MPa]	$\tau_{\perp}$ [MPa]	$\tau_{\parallel}$ [MPa]	Ut [%]	Ut_c [%]	Detailing	Status
Operation 1a	Member 2-bfl 1	S 235	6.0	239	LE1	353.1	0.2	-175.9	-173.1	36.1	98.1	78.2	OK	OK
		S 235	6.0	239	LE1	323.3	0.0	-165.6	159.5	-16.1	89.8	71.2	OK	OK
Operation 1a	Member 2-tfl 1	S 235	6.0	239	LE1	145.0	0.0	-76.3	-68.9	18.1	40.3	30.5	OK	OK
		S 235	6.0	239	LE1	193.4	0.0	-99.4	95.2	-11.2	53.7	40.8	OK	OK
Operation 1a	Member 2-w 1	S 235	6.0	214	LE1	250.8	0.0	-127.2	-121.7	-27.6	69.7	54.0	OK	OK
		S 235	6.0	214	LE1	139.4	0.0	-61.4	70.5	-15.7	38.7	27.6	OK	OK
Operation 1b	Member 1-bfl 1	S 235	6.0	239	LE1	345.3	0.0	-178.3	-170.5	-8.2	95.9	80.8	OK	OK
		S 235	6.0	239	LE1	295.5	0.0	-150.1	146.7	-8.9	82.1	68.1	OK	OK
Operation 1b	Member 1-tfl 1	S 235	6.0	239	LE1	128.8	0.0	-66.0	-63.2	9.1	35.8	25.5	OK	OK
		S 235	6.0	239	LE1	143.4	0.0	-68.9	53.4	49.2	39.8	33.0	OK	OK
Operation 1b	Member 1-w 1	S 235	6.0	214	LE1	170.3	0.0	-88.2	-83.4	-10.9	47.3	39.0	OK	OK
		S 235	6.0	214	LE1	171.9	0.0	-81.2	83.2	-27.1	47.8	36.0	OK	OK
Operation 2	Member 3-bfl 1	S 235	4.0	110	LE1	189.9	0.0	-102.0	-46.2	-80.1	52.8	48.1	OK	OK
		S 235	4.0	109	LE1	111.3	0.0	22.5	-15.5	-61.0	30.9	24.4	OK	OK
Operation 2	Member 3-tfl 1	S 235	4.0	109	LE1	353.3	0.4	-122.6	-129.8	140.5	98.1	75.2	OK	OK
		S 235	4.0	110	LE1	353.3	0.3	-154.5	146.8	-109.9	98.1	91.6	OK	OK
Operation 2	Member 3-w 1	S 235	4.0	210	LE1	239.0	0.0	-120.4	-119.1	-4.6	66.4	29.7	OK	OK

Item	Edge	Material	T_w [mm]	L [mm]	Loads	$\sigma_{w,Ed}$ [MPa]	ε_{Pl} [%]	$\sigma_{\perp}$ [MPa]	$\tau_{\perp}$ [MPa]	$\tau_{\parallel}$ [MPa]	Ut [%]	Ut_c [%]	Detailing	Status
		S 235	4.0	210	LE1	285.4	0.0	-75.0	103.0	121.2	79.3	34.5	OK	OK
Operation 3a	Member 4-w 1	S 355	4.0	133	LE1	429.0	1.2	-167.2	-167.7	-154.6	98.5	95.1	OK	OK
		S 355	4.0	133	LE1	429.1	1.3	-168.9	168.3	153.4	98.5	96.2	OK	OK
Operation 3b	Member 6-w 1	S 355	4.0	210	LE1	283.2	0.0	-144.0	-139.9	16.1	65.0	35.2	OK	OK
		S 355	4.0	210	LE1	280.7	0.0	-137.3	141.3	4.4	64.5	36.5	OK	OK
Operation 4	Member 5-bfl 1	S 235	4.0	110	LE1	297.8	0.0	81.9	123.2	110.1	82.7	64.1	OK	OK
		S 235	4.0	110	LE1	352.9	0.1	149.2	-122.4	-138.3	98.0	86.1	OK	OK
Operation 4	Member 5-tfl 1	S 235	4.0	109	LE1	354.4	1.1	-210.4	-164.7	-0.2	98.5	91.7	OK	OK
		S 235	4.0	110	LE1	354.1	0.9	-132.4	189.6	3.8	98.4	87.8	OK	OK
Operation 4	Member 5-w 1	S 235	4.0	210	LE1	352.8	0.0	-80.1	-97.2	-172.9	98.0	80.6	OK	OK
		S 235	4.0	210	LE1	352.8	0.0	-192.7	168.3	28.4	98.0	57.6	OK	OK
Member 2-bfl 1	WID1a	S 355	4.0	60	LE1	429.4	1.5	66.5	7.6	244.8	98.6	82.7	OK	OK
		S 355	4.0	60	LE1	430.3	2.0	19.9	-65.1	-239.5	98.8	85.5	OK	OK
Member 5-bfl 1	WID1a	S 355	4.0	179	LE1	429.3	1.4	-227.3	-208.8	24.7	98.6	78.1	OK	OK
		S 355	4.0	179	LE1	429.6	1.6	-200.9	217.2	-30.0	98.6	75.2	OK	OK
WID1b	WID1a	S 355	4.0	188	LE1	235.1	0.0	73.0	72.8	106.5	54.0	26.4	OK	OK
		S 355	4.0	188	LE1	279.8	0.0	-53.1	48.9	150.9	64.2	37.2	OK	OK
Member 2-bfl 1	WID1b	S 355	4.0	110	LE1	428.0	0.7	144.8	223.5	64.2	98.3	90.4	OK	OK

Item	Edge	Material	T_w [mm]	L [mm]	Loads	$\sigma_{w,Ed}$ [MPa]	ε_{Pl} [%]	$\sigma_{\perp}$ [MPa]	$\tau_{\perp}$ [MPa]	$\tau_{\parallel}$ [MPa]	Ut [%]	Ut_c [%]	Detailing	Status
		S 355	4.0	110	LE1	427.3	0.3	211.4	-108.7	-184.8	98.1	81.6	OK	OK
Member 5-bfl 1	WID1b	S 355	4.0	109	LE1	429.1	1.3	14.3	218.2	-117.0	98.5	87.5	OK	OK
		S 355	4.0	109	LE1	333.2	0.0	108.6	20.2	-180.8	76.5	42.4	OK	OK
Member 2-tfl 1	WID2a	S 355	4.0	60	LE1	382.1	0.0	132.9	194.6	70.1	87.7	67.6	OK	OK

		S 355	4.0	60	LE1	309.1	0.0	195.0	-133.1	38.1	71.0	55.0	OK	OK
Member 3-bfl 1	WID2a	S 355	4.0	179	LE1	424.1	0.0	-40.8	-134.1	203.5	97.4	62.3	OK	OK
		S 355	4.0	179	LE1	252.3	0.0	-62.3	-31.1	-137.7	57.9	37.7	OK	OK
WID2b	WID2a	S 355	4.0	188	LE1	86.7	0.0	23.4	21.2	43.3	19.9	15.4	OK	OK
		S 355	4.0	188	LE1	132.0	0.0	20.0	-22.2	-72.0	30.3	15.5	OK	OK
Member 2-tfl 1	WID2b	S 355	4.0	110	LE1	427.0	0.1	147.6	202.6	-111.8	98.0	74.7	OK	OK
		S 355	4.0	110	LE1	412.9	0.0	188.4	-133.4	164.9	94.8	68.7	OK	OK
Member 3-bfl 1	WID2b	S 355	4.0	109	LE1	428.2	0.8	12.0	232.0	85.2	98.3	93.2	OK	OK
		S 355	4.0	109	LE1	269.0	0.0	30.5	8.8	154.0	61.8	36.1	OK	OK
Operation 3b	Member 6-tfl 1	S 355	6.5	109	LE1	434.1	4.2	-162.9	-132.7	-190.7	99.7	99.7	OK	OK
		S 355	6.5	109	LE1	433.2	3.6	-113.2	147.7	190.9	99.4	99.4	OK	OK
Operation 3b	Member 6-bfl 1	S 355	6.0	109	LE1	428.7	1.0	144.3	139.9	186.4	98.4	97.2	OK	OK
		S 355	6.0	109	LE1	430.3	2.0	176.2	-178.6	-139.6	98.8	96.8	OK	OK
Member 2-bfl 1	STIFF2a	S 355	3.0	116	LE1	280.3	0.0	154.1	135.2	-0.5	64.4	46.4	OK	OK

Item	Edge	Material	T_w [mm]	L [mm]	Loads	$\sigma_{w,Ed}$ [MPa]	ε_{Pl} [%]	$\sigma_{\perp}$ [MPa]	$\tau_{\perp}$ [MPa]	$\tau_{\parallel}$ [MPa]	Ut [%]	Ut_c [%]	Detailing	Status
		S 355	3.0	116	LE1	321.3	0.0	85.2	-127.6	125.3	73.8	57.8	OK	OK
Member 2-w 1	STIFF2a	S 355	3.0	206	LE1	162.8	0.0	123.1	52.2	-32.6	37.4	30.0	OK	OK
		S 355	3.0	206	LE1	351.6	0.0	110.3	-181.1	-66.0	80.7	70.7	OK	OK
Member 2-tfl 1	STIFF2a	S 355	3.0	116	LE1	234.8	0.0	131.7	109.8	23.2	53.9	44.0	OK	OK
		S 355	3.0	116	LE1	275.1	0.0	84.1	-106.6	-107.2	63.2	40.2	OK	OK
Member 2-bfl 1	STIFF2b	S 355	3.0	116	LE1	426.9	0.0	198.4	214.7	38.7	98.0	41.1	OK	OK
		S 355	3.0	116	LE1	262.3	0.0	134.2	-116.4	-58.0	60.2	49.2	OK	OK
Member 2-w 1	STIFF2b	S 355	3.0	205	LE1	277.0	0.0	5.0	-53.6	150.7	63.6	56.4	OK	OK

		S 355	◢ 3.0 L	205	LE1	179.3	0.0	-66.3	94.8	-15.9	41.2	29.5	OK	OK
Member 2-tfl 1	STIFF2b	S 355	◢ 3.0 L	116	LE1	370.6	0.0	173.0	171.0	-81.0	85.1	43.8	OK	OK
		S 355	◢ 3.0 L	116	LE1	242.9	0.0	83.9	-100.4	85.1	55.8	43.0	OK	OK

Design data

Material	f_u [MPa]	β_w [-]	$\sigma_{w,Rd}$ [MPa]	0.9 σ [MPa]
S 235	360.0	0.80	360.0	259.2
S 355	490.0	0.90	435.6	352.8

Weld resistance check (EN 1993-1-8 – Cl. 4.5.3.2)

$\sigma_{w,Rd} = f_u/(\beta_w \gamma_{M2}) =$ 435.6 MPa $\geq$ $\sigma_{w,Ed} = [\sigma_\perp^2 + 3(\tau_\perp^2 + \tau_\parallel^2)]^{0.5} =$ 434.1 MPa

$\sigma_{\perp,Rd} = 0.9\, f_u \,/\, \gamma_{M2} =$ 352.8 MPa $\geq$ $|\sigma_\perp| =$ 192.0 MPa

where:

$f_u = 490.0$ MPa – Ultimate strength

$\beta_w = 0.90$ – Correlation factor EN 1993-1-8 – Tab. 4.1

$\gamma_{M2} = 1.25$ – Safety factor

Stress utilization

$U_t = \max\left(\frac{\sigma_{w,Ed}}{\sigma_{w,Rd}};\ \frac{|\sigma_\perp|}{\sigma_{\perp,Rd}}\right) =$ 1.00 $\leq$ 1.0

Where:

$\sigma_{w,Ed} = 434.1$ MPa – Maximum normal stress transverse to the axis of the weld

$\sigma_{w,Rd} = 435.6$ MPa – Equivalent stress resistance

$\sigma_\perp = -192.0$ MPa – Normal stress perpendicular to the throat

$\sigma_{\perp,Rd} = 352.8$ MPa – Perpendicular stress resistance

Buckling

Loads	Shape	Factor [-]
LE1	1	2.70
	2	3.03
	3	3.66
	4	3.90
	5	4.00
	6	4.62

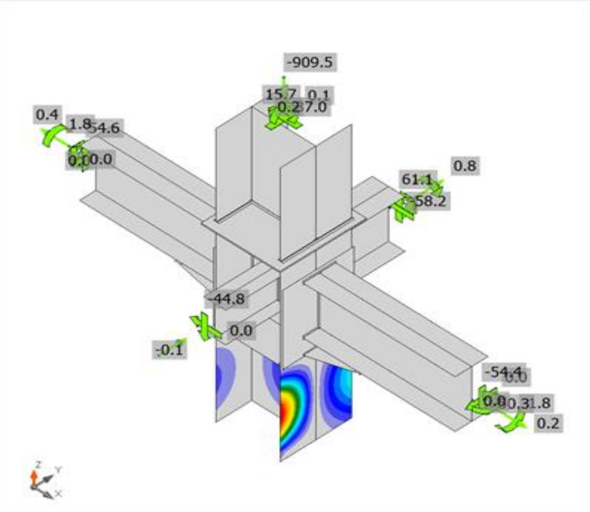

Cost estimation

Steel

Steel grade	Total weight [kg]	Unit cost [€/kg]	Cost [€]
S 235	14.05	2.00	28.11
S 355	17.57	2.00	35.14

Bolts

Bolt assembly	Total weight [kg]	Unit cost [€/kg]	Cost [€]
M12 8.8	0.90	5.00	4.49
M14 10.9	0.88	5.00	4.41

Welds

Weld type	Throat thickness [mm]	Leg size [mm]	Total weight [kg]	Unit cost [€/kg]	Cost [€]
Double fillet	6.0	8.5	0.60	40.00	24.19
Double fillet	6.0	8.5	0.24	40.00	9.72
Double fillet	4.0	5.7	0.63	40.00	25.17
Double fillet	6.5	9.2	0.07	40.00	2.92
Double fillet	3.0	4.2	0.12	40.00	4.97

Hole drilling

Bolt assembly cost [€]	Percentage of bolt assembly cost [%]	Cost [€]
8.90	30.0	2.67

Cost summary

Cost estimation summary	Cost [€]
Total estimated cost	141.79

Bill of Material

Manufacturing Operations

Name	Plates [mm]	Shape	Nr.	Welds Throat thickness [mm]	Length [mm]	Bolts	Nr.
Operation 1	P5.0x290.0-264.0 (S 235)	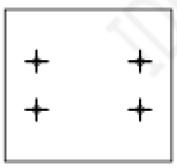	1	Double fillet: 6.0	1390.0	M12 8.8	4
	P5.0x290.0-264.0 (S 235)	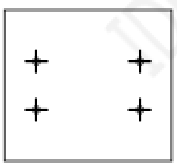	1				
Operation 2	P7.0x240.0-305.0 (S 235)		1	Double fillet: 4.0	430.8	M12 8.8	4

		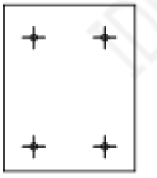					
Operation 3	P18.0x180.0-300.0 (S 355)	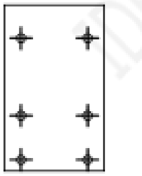	1	Double fillet: 4.0	343.9	M14 10.9	6
	P18.0x180.0-300.0 (S 355)	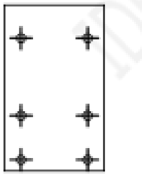	1				
Operation 4	P7.0x240.0-305.0 (S 235)	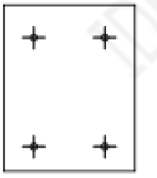	1	Double fillet: 4.0	430.8	M12 8.8	4
WID1	P5.0x60.0-180.0 (S 355)	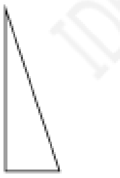	1	Double fillet: 4.0	649.7		
	P5.0x110.0-189.7 (S 355)	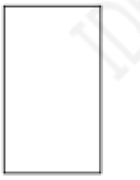	1				

Name	Plates [mm]	Shape	Nr.	Welds Throat thickness [mm]	Length [mm]	Bolts	Nr.
WID2	P5.0x60.0-180.0 (S 355)	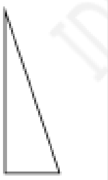	1	Double fillet: 4.0	649.7		

	P5.0x110.0-189.7 (S 355)	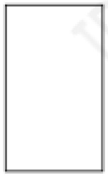	1				
STIFF2	P5.0x116.7-206.0 (S 355)	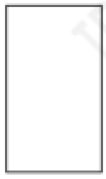	2	Double fillet: 3.0	879.0		

Welds

Type	Material	Throat thickness [mm]	Leg size [mm]	Length [mm]
Double fillet	S 235	6.0	8.5	1390.0
Double fillet	S 235	4.0	5.7	861.6
Double fillet	S 355	4.0	5.7	1643.4
Double fillet	S 355	6.5	9.2	110.0
Double fillet	S 355	6.0	8.5	110.0
Double fillet	S 355	3.0	4.2	879.0

Bolts

Name	Grip length [mm]	Count
M12 8.8	10	4
M12 8.8	16	8
M14 10.9	42	6

Symbol Explanation (only presented for this connection)

Symbol	Explanation
t_p	Plate thickness
σ_{Ed}	Equivalent stress
ε_{Pl}	Plastic strain
$\sigma_{c,Ed}$	Contact stress
f_y	Yield strength
ε_{lim}	Limit of plastic strain
$F_{t,Ed}$	Tension force
$F_{v,Ed}$	Resultant of bolt shear forces Vy and Vz in shear planes
$F_{b,Rd}$	Plate bearing resistance EN 1993-1-8 – Tab. 3.4
Ut_t	Utilization in tension
Ut_s	Utilization in shear
Ut_{ts}	Interaction of tension and shear EN 1993-1-8 – Tab. 3.4
$F_{t,Rd}$	Bolt tension resistance EN 1993-1-8 – Tab. 3.4
$B_{p,Rd}$	Punching shear resistance EN 1993-1-8 – Tab. 3.4
$F_{v,Rd}$	Bolt shear resistance EN 1993-1-8 – Tab. 3.4
T_w	Throat thickness a
L	Length
$\sigma_{w,Ed}$	Equivalent stress

$\sigma_{\perp}$	Perpendicular stress
$\tau_{\perp}$	Shear stress perpendicular to weld axis
$\tau_{\parallel}$	Shear stress parallel to weld axis
Ut	Utilization
Ut_c	Weld capacity estimation
◢	Fillet weld
f_u	Ultimate strength of weld
β_w	Correlation factor EN 1993-1-8 – Tab. 4.1
$\sigma_{w,Rd}$	Equivalent stress resistance
0.9 σ	Perpendicular stress resistance: 0.9*fu/γM2

Code settings (only presented for this connection)

Item	Value	Unit	Reference
Safety factor γ_{M0}	1.00	-	EN 1993-1-1: 6.1
Safety factor γ_{M1}	1.00	-	EN 1993-1-1: 6.1
Safety factor γ_{M2}	1.25	-	EN 1993-1-1: 6.1
Safety factor γ_{M3}	1.25	-	EN 1993-1-8: 2.2
Safety factor γ_{C}	1.50	-	EN 1992-1-1: 2.4.2.4
Safety factor γ_{Inst}	1.20	-	EN 1992-4: Table 4.1
Joint coefficient βj	0.67	-	EN 1993-1-8: 6.2.5
Effective area - influence of mesh size	0.10	-	
Friction coefficient - concrete	0.25	-	EN 1993-1-8
Friction coefficient in slip-resistance	0.30	-	EN 1993-1-8 tab 3.7
Limit plastic strain	0.05	-	EN 1993-1-5
Detailing	Yes		
Distance between bolts [d]	2.20	-	EN 1993-1-8: tab 3.3
Distance between bolts and edge [d]	1.20	-	EN 1993-1-8: tab 3.3
Concrete breakout resistance check	Both		EN 1992-4: 7.2.1.4 and 7.2.2.5
Use calculated αb in bearing check.	Yes		EN 1993-1-8: tab 3.4
Cracked concrete	Yes		EN 1992-4
Local deformation check	Yes		CIDECT DG 1, 3 - 1.1
Local deformation limit	0.03	-	CIDECT DG 1, 3 - 1.1
Geometrical nonlinearity (GMNA)	Yes		Analysis with large deformations for hollow section joints
Braced system	No		EN 1993-1-8: 5.2.2.5

8.6.2 5 Beam 2 Column Connection

Members

Geometry

Name	Cross-section	β – Direction [°]	γ - Pitch [°]	α - Rotation [°]	Offset ex [mm]	Offset ey [mm]	Offset ez [mm]
Member 1	84 - HEA240A	0.0	-90.0	0.0	0	0	0
Member 2	85 - IPE140	90.0	3.0	0.0	0	0	160
Member 3	86 - IPE220	-90.0	-3.0	0.0	0	0	140
Member 4	83 - IPE270	133.0	0.0	0.0	0	92	140
Member 5	86 - IPE220	0.0	0.0	0.0	0	0	140
Member 6	85 - IPE140	180.0	0.0	0.0	0	0	190
Member 7	84 - HEA240A	0.0	90.0	0.0	0	0	0

Supports and forces

Name	Support	Forces in	X [mm]
Member 1 / end	N-Vy-Vz-Mx-My-Mz	Node	0
Member 2 / end		Position	0
Member 3 / end		Position	200
Member 4 / end		Bolts	0
Member 5 / end		Bolts	0
Member 6 / end	Mx-My-Mz	Bolts	0
Member 7 / end		Bolts	0

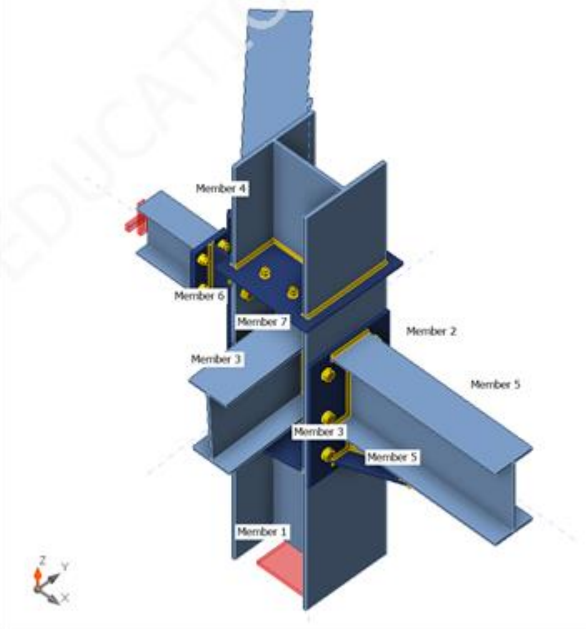

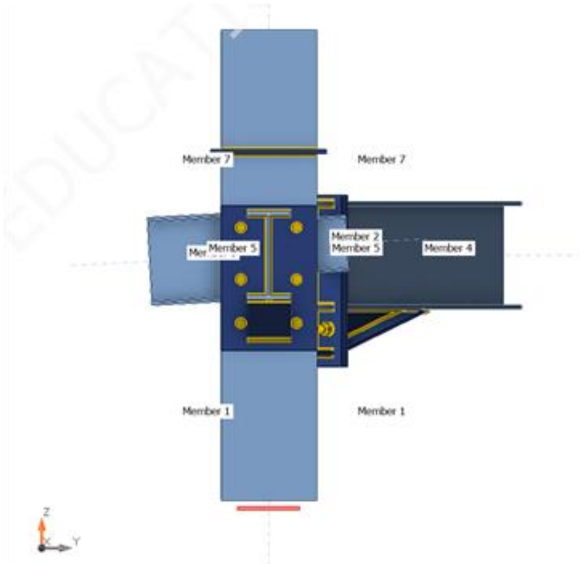

Cross-sections

Name	Material
84 - HEA240A	S 355
85 - IPE140	S 355
86 - IPE220	S 355
83 - IPE270	S 355

Bolts

Name	Diameter [mm]	f_y [MPa]	f_u [MPa]	Gross area [mm^2]
M12 8.8	12	640.0	800.0	113
M12 10.9	12	900.0	1000.0	113
M16 10.9	16	900.0	1000.0	201
M18 10.9	18	900.0	1000.0	254
M20 10.9	20	900.0	1000.0	314

Load effects (Equilibrium not required)

Name	Member	N [kN]	Vy [kN]	Vz [kN]	Mx [kNm]	My [kNm]	Mz [kNm]
LE1	Member 2 / End	0.1	0.0	35.6	1.9	0.0	0.0
	Member 3 / End	0.2	0.0	-55.0	-1.8	-51.9	0.0
	Member 4 / End	0.9	0.0	-55.2	0.3	-80.7	0.0
	Member 5 / End	0.3	0.0	65.9	0.0	-64.4	0.0
	Member 6 / End	0.0	0.0	-37.2	0.0	0.0	0.0
	Member 7 / End	-1047.2	2.7	1.5	0.0	4.9	5.2

Check

Summary

Name	Value	Check status
Analysis	100.0%	OK
Plates	3.1 < 5.0%	OK
Bolts	99.8 < 100%	OK
Welds	99.9 < 100%	OK
Buckling	3.07	

Plates

Name	t_p [mm]	Loads	σ_{Ed} [MPa]	ε_{Pl} [%]	$\sigma_{c,Ed}$ [MPa]	Status
Member 1-bfl 1	9.0	LE1	357.6	1.2	125.6	OK
Member 1-tfl 1	9.0	LE1	360.9	2.8	347.4	OK
Member 1-w 1	6.5	LE1	361.1	2.9	124.2	OK
Member 2-bfl 1	6.9	LE1	355.4	0.2	0.0	OK
Member 2-tfl 1	6.9	LE1	355.4	0.2	0.0	OK
Member 2-w 1	4.7	LE1	361.4	3.1	0.0	OK
Member 3-bfl 1	9.2	LE1	355.7	0.4	0.0	OK
Member 3-tfl 1	9.2	LE1	356.4	0.7	0.0	OK
Member 3-w 1	5.9	LE1	348.9	0.0	0.0	OK
Member 4-bfl 1	10.2	LE1	355.3	0.1	0.0	OK
Member 4-tfl 1	10.2	LE1	348.0	0.0	0.0	OK
Member 4-w 1	6.6	LE1	280.4	0.0	0.0	OK
Member 5-bfl 1	9.2	LE1	325.9	0.0	0.0	OK
Member 5-tfl 1	9.2	LE1	355.2	0.1	0.0	OK
Member 5-w 1	5.9	LE1	294.3	0.0	0.0	OK
Member 6-bfl 1	6.9	LE1	84.8	0.0	0.0	OK
Member 6-tfl 1	6.9	LE1	75.9	0.0	0.0	OK
Member 6-w 1	4.7	LE1	197.4	0.0	0.0	OK

Member 7-bfl 1	9.0	LE1	296.0	0.0	0.0	OK
Member 7-tfl 1	9.0	LE1	308.9	0.0	0.0	OK
Member 7-w 1	6.5	LE1	275.1	0.0	0.0	OK
STUB3-bfl 1	10.2	LE1	355.4	0.2	0.0	OK
STUB3-tfl 1	10.2	LE1	355.3	0.1	0.0	OK
STUB3-w 1	6.6	LE1	338.4	0.0	0.0	OK
PP1a	5.0	LE1	238.5	0.0	115.4	OK
PP1b	5.0	LE1	159.8	0.0	115.4	OK
EP1a	15.0	LE1	355.7	0.3	72.0	OK
EP1b	15.0	LE1	359.8	2.3	165.4	OK
EP2	10.0	LE1	359.7	2.2	347.4	OK
WID1a	5.9	LE1	294.3	0.0	0.0	OK
WID1b	9.2	LE1	359.0	1.9	0.0	OK
STUB2-EPa	6.0	LE1	249.9	0.0	50.6	OK
STUB2-EPb	6.0	LE1	276.7	0.0	50.6	OK
SP1	10.0	LE1	355.2	0.1	125.6	OK
STUB3-EPa	12.0	LE1	358.5	1.6	312.7	OK
STUB3-EPb	12.0	LE1	360.0	2.4	312.5	OK
SP4	6.6	LE1	355.5	0.3	0.0	OK
SP12	5.0	LE1	358.1	1.5	0.0	OK
WID2a	6.6	LE1	355.5	0.2	0.0	OK
WID2b	10.2	LE1	356.1	0.5	0.0	OK
SP14	10.2	LE1	357.2	1.1	0.0	OK

Na me	t_p [mm]	**Loads**	σ_{Ed} [MPa]	ε_{Pl} [%]	$\sigma_{c,Ed}$ [MPa]	**Status**
STIFF1a	5.0	LE1	355.4	0.2	0.0	OK
STIFF1b	5.0	LE1	357.1	1.0	0.0	OK

Design data

Material	f_y [MPa]	ε_{lim} [%]
S 355	355.0	5.0

Detailed result for Member 2-w 1

Design values used in the analysis

$f_{yd} = \frac{f_{yk}}{\gamma_{M0}} =$ 355.0 MPa

Where:

$f_{yk} = 355.0$ MPa – characteristic yield strength

$\gamma_{M0} = 1.00$ – partial safety factor for steel material EN 1993-1-1 – 6.1

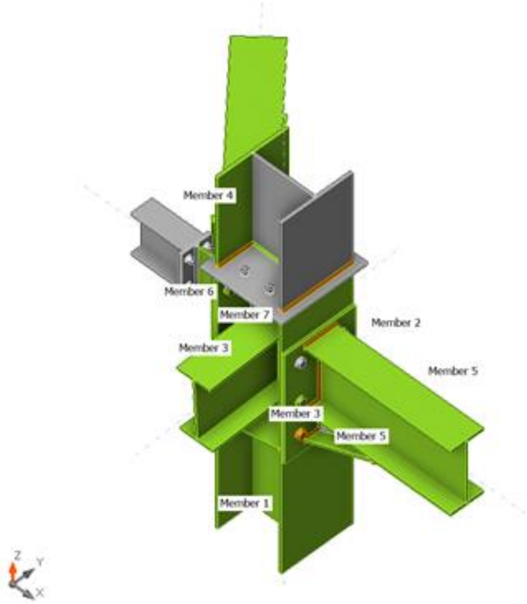

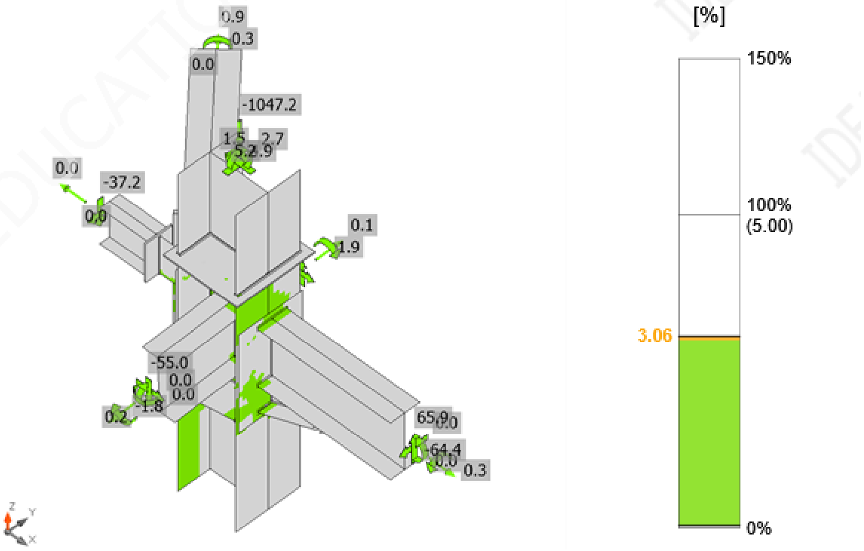

Strain check, LE1

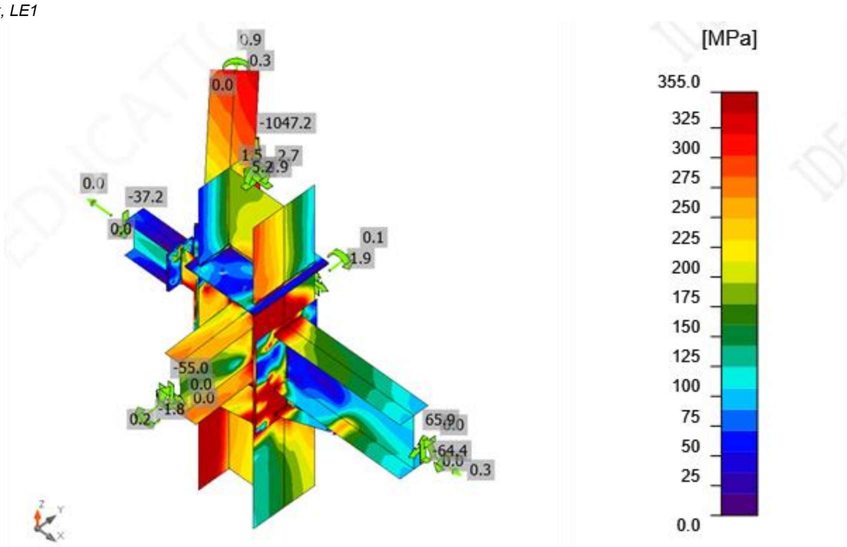

Equivalent stress, LE1

Bolts

Shape	Item	Grade	Loads	$F_{t,Ed}$ [kN]	$F_{v,Ed}$ [kN]	$F_{b,Rd}$ [kN]	Ut_t [%]	Ut_s [%]	Ut_{ts} [%]	Detailing	Status
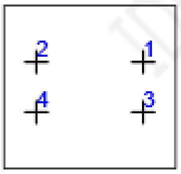	B1	M12 8.8 - 1	LE1	0.1	0.8	58.8	0.3	2.6	2.8	OK	OK
	B2	M12 8.8 - 1	LE1	0.3	0.1	58.8	0.6	0.3	0.7	OK	OK
	B3	M12 8.8 - 1	LE1	0.3	1.5	58.8	0.5	4.6	5.0	OK	OK
	B4	M12 8.8 - 1	LE1	0.1	1.3	58.8	0.2	4.1	4.3	OK	OK
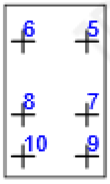	B5	M12 10.9 - 2	LE1	37.9	14.4	76.4	62.5	42.7	87.3	OK	OK
	B6	M12 10.9 - 2	LE1	26.5	14.9	76.4	43.7	44.3	75.5	OK	OK
	B7	M12 10.9 - 2	LE1	39.3	8.6	76.4	64.8	25.5	71.8	OK	OK
	B8	M12 10.9 - 2	LE1	41.6	14.6	76.4	68.6	43.2	92.2	OK	OK
	B9	M12 10.9 - 2	LE1	56.5	5.2	76.4	93.2	15.4	82.0	OK	OK
	B10	M12 10.9 - 2	LE1	54.7	10.0	76.4	90.2	29.6	94.0	OK	OK
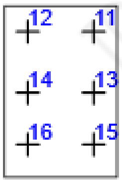	B11	M16 10.9 - 3	LE1	8.0	14.5	141.1	7.1	23.1	28.1	OK	OK
	B12	M16 10.9 - 3	LE1	11.4	18.9	141.1	10.1	30.0	37.2	OK	OK
	B13	M16 10.9 - 3	LE1	79.4	9.3	141.1	70.3	14.9	65.0	OK	OK
	B14	M16 10.9 - 3	LE1	73.1	12.2	141.1	64.7	19.4	65.6	OK	OK
	B15	M16 10.9 - 3	LE1	110.2	5.0	141.1	97.5	8.0	77.6	OK	OK
	B16	M16 10.9 - 3	LE1	112.9	7.4	141.1	99.8	11.7	83.1	OK	OK
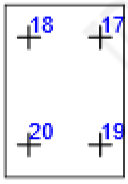	B17	M12 8.8 - 4	LE1	13.0	9.1	48.8	26.9	28.1	47.3	OK	OK
	B18	M12 8.8 - 4	LE1	11.1	9.5	48.8	22.8	29.4	45.7	OK	OK
	B19	M12 8.8 - 4	LE1	1.9	9.2	48.8	3.9	28.3	31.1	OK	OK
	B20	M12 8.8 - 4	LE1	0.3	9.4	48.8	0.5	29.1	29.5	OK	OK
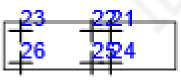	B21	M18 10.9 - 5	LE1	75.4	42.7	119.1	54.5	55.6	94.5	OK	OK
	B22	M18 10.9 - 5	LE1	57.2	21.8	119.1	41.3	28.3	57.9	OK	OK
	B23	M18 10.9 - 5	LE1	2.2	67.4	132.3	1.6	87.7	88.9	OK	OK
	B24	M18 10.9 - 5	LE1	54.9	52.9	109.3	39.7	68.9	97.3	OK	OK
	B25	M18 10.9 - 5	LE1	55.5	50.7	124.3	40.2	66.0	94.7	OK	OK
	B26	M18 10.9 - 5	LE1	7.3	63.9	92.6	5.3	83.3	87.0	OK	OK
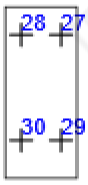	B27	M20 10.9 - 6	LE1	39.5	22.4	235.2	22.4	22.9	38.9	OK	OK
	B28	M20 10.9 - 6	LE1	55.8	17.7	235.2	31.7	18.0	40.7	OK	OK
	B29	M20 10.9 - 6	LE1	168.9	9.9	197.2	95.7	10.1	78.5	OK	OK
	B30	M20 10.9 - 6	LE1	173.0	5.7	235.2	98.1	5.8	75.9	OK	OK

Design data

Grade	$F_{t,Rd}$ [kN]	$B_{p,Rd}$ [kN]	$F_{v,Rd}$ [kN]
M12 8.8 - 1	48.6	70.3	32.4
M12 10.9 - 2	60.7	210.8	33.7

M16 10.9 - 3	113.0	168.7	62.8
M12 8.8 - 4	48.6	84.3	32.4
M18 10.9 - 5	138.2	190.0	76.8
M20 10.9 - 6	176.4	281.7	98.0

Detailed result for B16

Tension resistance check (EN 1993-1-8 – Table 3.4)

$$F_{t,Rd} = \frac{k_2\, f_{ub}\, A_s}{\gamma_{M2}} = 113.0 \text{ kN} \geq F_{t,Ed} = 112.9 \text{ kN}$$

Where:

$k_2 = 0.90$ – Factor

$f_{ub} = 1000.0$ MPa – Ultimate tensile strength of the bolt

$A_s = 157$ mm^2 – Tensile stress area of the bolt

$\gamma_{M2} = 1.25$ – Safety factor

Punching resistance check (EN 1993-1-8 – Table 3.4)

$$B_{p,Rd} = \frac{0.6\, \pi\, d_m\, t_p\, f_u}{\gamma_{M2}} = 168.7 \text{ kN} \geq F_{t,Ed} = 112.9 \text{ kN}$$

Where:

$d_m = 25$ mm – The mean of the across points and across flats dimensions of the bolt head or the nut, whichever is smaller

$t_p = 9$ mm – Plate thickness

$f_u = 490.0$ MPa – Ultimate strength

$\gamma_{M2} = 1.25$ – Safety factor

Shear resistance check (EN 1993-1-8 – Table 3.4)

$$F_{v,Rd} = \frac{\beta_p\ \alpha_v f_{ub} A}{\gamma_{M2}} = 62.8 \text{ kN} \geq F_{v,Ed} = 7.4 \text{ kN}$$

Where:

$\beta_p = 1.00$ – Reduction factor for packing

$\alpha_v = 0.50$ – Reduction factor for shear stress

$f_{ub} = 1000.0$ MPa – Ultimate tensile strength of the bolt

$A = 157$ mm^2 – Tensile stress area of the bolt

$\gamma_{M2} = 1.25$ – Safety factor

Bearing resistance check (EN 1993-1-8 – Table 3.4)

$$F_{b,Rd} = \frac{k_1\, \alpha_b\, f_u\, d t}{\gamma_{M2}} = 141.1 \text{ kN} \geq F_{b,Ed} = 7.4 \text{ kN}$$

Where:

$k_1 = \min(2.8\frac{e_2}{d_0} - 1.7, 1.4\frac{p_2}{d_0} - 1.7, 2.5) = 2.50$ – Factor for edge distance and bolt spacing perpendicular to the direction of load transfer

$\alpha_b = \min(\frac{e_1}{3d_0}, \frac{p_1}{3d_0} - \frac{1}{4}, \frac{f_{ub}}{f_u}, 1) = 1.00$ – Factor for end distance and bolt spacing in direction of load transfer

$e_2 = 53$ mm – Distance to the plate edge perpendicular to the shear force

$p_2 = \infty$ mm – Distance between bolts perpendicular to the shear force

$d_0 = 18$ mm – Bolt hole diameter

$e_1 = \infty$ mm – Distance to the plate edge in the direction of the shear force

$p_1 = \infty$ mm – Distance between bolts in the direction of the shear force

$f_{ub} = 1000.0$ MPa – Ultimate tensile strength of the bolt

$f_u = 490.0$ MPa – Ultimate strength of the plate

$d = 16$ mm – Nominal diameter of the fastener

$t = 9$ mm – Thickness of the plate

$\gamma_{M2} = 1.25$ – Safety factor

Utilization in tension

$$\frac{F_{t,Ed}}{\min(F_{t,Rd};\, B_{p,Rd})} = 1.00 \leq 1.0$$

Where:

$F_{t,Ed} = 112.9$ kN – Tensile force

$F_{t,Rd} = 113.0$ kN – Tension resistance

$B_{p,Rd} = 168.7$ kN – Punching resistance

Utilization in shear

$$\max\left(\frac{F_{v,Ed}}{F_{v,Rd}}; \frac{F_{b,Ed}}{F_{b,Rd}}\right) = 0.12 \leq 1.0$$

Where:

$F_{v,Ed} = 7.4$ kN – Shear force (in decisive shear plane)

$F_{v,Rd} = 62.8$ kN – Shear resistance

$F_{b,Ed} = 7.4$ kN – Bearing force (for decisive plate)

$F_{b,Rd} = 141.1$ kN – Bearing resistance

Interaction of tension and shear (EN 1993-1-8 – Table 3.4)

$$\frac{F_{v,Ed}}{F_{v,Rd}} + \frac{F_{t,Ed}}{1.4\,F_{t,Rd}} = 0.83 \leq 1.0$$

Where:

$F_{v,Ed} = 7.4$ kN – Shear force (in decisive shear plane)

$F_{v,Rd} = 62.8$ kN – Shear resistance

$F_{t,Ed} = 112.9$ kN – Tensile force

$F_{t,Rd} = 113.0$ kN – Tension resistance

Welds

Item	Edge	T_w [mm]	L [mm]	Loads	$\sigma_{w,Ed}$ [MPa]	ε_{Pl} [%]	$\sigma_{\perp}$ [MPa]	$\tau_{\perp}$ [MPa]	$\tau_{\parallel}$ [MPa]	Ut [%]	Ut_c [%]	Detailing	Status
PP1a	Member 1-bfl 1	◢ 4.5 L	238	LE1	429.2	1.4	-224.0	-211.4	1.7	98.5	78.1	OK	OK
		◢ 4.5 L	238	LE1	427.2	0.2	-177.1	224.3	-8.0	98.1	69.0	OK	OK
PP1a	Member 1-tfl 1	◢ 4.5 L	238	LE1	427.0	0.1	-150.5	-230.7	-3.1	98.0	66.7	OK	OK
		◢ 4.5 L	238	LE1	431.8	2.8	-217.4	214.7	-17.5	99.1	99.1	OK	OK
PP1a	Member 1-w 1	◢ 4.0 L	214	LE1	357.8	0.0	-180.7	-174.0	39.1	82.2	59.6	OK	OK
		◢ 4.0 L	214	LE1	209.1	0.0	-90.1	107.7	16.2	48.0	43.2	OK	OK
PP1b	Member 7-bfl 1	◢ 4.5 L	238	LE1	413.8	0.0	-209.6	-205.6	-12.8	95.0	64.6	OK	OK
		◢ 4.5 L	239	LE1	426.8	0.0	-205.4	198.1	-86.3	98.0	67.0	OK	OK
PP1b	Member 7-tfl 1	◢ 4.5 L	238	LE1	427.0	0.1	-209.6	-200.9	-76.1	98.0	64.8	OK	OK
		◢ 4.5 L	238	LE1	426.9	0.1	-209.6	214.2	-15.5	98.0	69.0	OK	OK
PP1b	Member 7-w 1	◢ 4.0 L	214	LE1	278.7	0.0	-134.1	-134.8	41.6	64.0	52.8	OK	OK
		◢ 4.0 L	214	LE1	258.8	0.0	-124.1	126.1	35.9	59.4	51.7	OK	OK
EP1a	Member 2-w 1	◢ 4.0 L	133	LE1	435.3	4.9	195.7	-131.1	182.3	99.9	98.9	OK	OK
		◢ 4.0 L	133	LE1	434.5	4.4	-215.3	-144.9	162.7	99.8	99.0	OK	OK
EP1b	Member 3-w 1	◢ 4.0 L	210	LE1	370.1	0.0	-10.1	-20.0	-212.7	85.0	49.4	OK	OK

		◢ 4.0 L	210	LE1	316.9	0.0	-142.1	162.9	14.3	72.8	59.3	OK	OK
EP2	Member 5-bfl 1	◢ 4.5 L	110	LE1	430.7	2.2	159.7	179.8	-145.0	98.9	96.9	OK	OK
		◢ 4.5 L	109	LE1	432.1	3.0	189.9	-174.6	140.5	99.2	99.2	OK	OK
EP2	Member 5-tfl 1	◢ 4.5 L	109	LE1	432.0	3.0	-257.3	-200.3	3.6	99.2	99.2	OK	OK
		◢ 4.5 L	109	LE1	429.3	1.4	-123.3	234.8	-34.8	98.6	78.7	OK	OK
EP2	Member 5-w 1	◢ 4.0 L	210	LE1	428.5	1.0	-211.0	-197.2	86.5	98.4	65.5	OK	OK
		◢ 4.0 L	210	LE1	428.5	1.0	-185.8	199.8	-99.0	98.4	68.0	OK	OK
SP1	SP4	◢ 4.0 L	104	LE1	269.2	0.0	30.2	125.2	90.5	61.8	30.3	OK	OK

Item	Edge	T_w [mm]	L [mm]	Loads	$\sigma_{w,Ed}$ [MPa]	ε_{Pl} [%]	$\sigma_{\perp}$ [MPa]	$\tau_{\perp}$ [MPa]	$\tau_{\parallel}$ [MPa]	Ut [%]	Ut_c [%]	Detailing	Status
		◢ 4.0 L	104	LE1	251.1	0.0	-26.9	32.1	140.5	57.7	25.4	OK	OK
Member 5-bfl 1	WID1a	◢ 4.5 L	218	LE1	99.4	0.0	15.5	15.2	54.6	22.8	13.7	OK	OK
		◢ 4.5 L	218	LE1	99.4	0.0	14.2	-14.6	-54.9	22.8	13.5	OK	OK
WID1b	WID1a	◢ 4.5 L	235	LE1	173.5	0.0	-79.6	-74.0	-49.6	39.8	25.4	OK	OK
		◢ 4.5 L	235	LE1	167.6	0.0	-64.5	70.1	55.3	38.5	28.1	OK	OK
STUB3-EPb	SP4	◢ 5.0 L	104	LE1	426.9	0.0	106.1	115.1	-209.1	98.0	53.5	OK	OK
		◢ 5.0 L	104	LE1	427.1	0.2	191.2	-176.2	-132.6	98.1	50.4	OK	OK
Member 5-bfl 1	WID1b	◢ 4.5 L	109	LE1	427.0	0.1	74.1	242.8	-0.2	98.0	48.0	OK	OK
		◢ 4.5 L	109	LE1	154.7	0.0	64.4	-81.2	1.5	35.5	16.1	OK	OK
STUB2-EPa	Member 6-w 1	◢ 4.0 L	132	LE1	179.6	0.0	74.1	94.5	-0.5	41.2	27.1	OK	OK
		◢ 4.0 L	132	LE1	381.3	0.0	-158.5	187.7	69.8	87.5	73.8	OK	OK
EP2	WID1a	◢ 4.0 L	89	LE1	338.2	0.0	71.5	69.4	-177.8	77.6	53.7	OK	OK
		◢ 4.0 L	89	LE1	334.2	0.0	150.7	-172.0	9.1	76.7	51.5	OK	OK
EP2	WID1b	◢ 6.0 L	109	LE1	430.6	2.2	186.5	136.5	-177.8	98.9	98.9	OK	OK
		◢ 6.0 L	109	LE1	427.4	0.3	120.6	-225.3	-72.9	98.1	95.6	OK	OK

STUB3-EPa	Member 4-bfl 1	◢ 5.0 L	135	LE1	414.3	0.0	-81.3	224.0	-69.6	95.1	75.7	OK	OK
		◢ 5.0 L	135	LE1	429.0	1.2	218.7	-175.0	121.5	98.5	94.2	OK	OK
STUB3-EPa	Member 4-tfl 1	◢ 5.0 L	134	LE1	427.5	0.4	-223.4	-210.4	1.4	98.1	87.6	OK	OK
		◢ 5.0 L	134	LE1	407.5	0.0	-174.9	210.6	28.6	93.6	71.4	OK	OK
STUB3-EPa	Member 4-w 1	◢ 4.0 L	259	LE1	234.7	0.0	-80.2	-100.5	78.1	53.9	47.9	OK	OK
		◢ 4.0 L	259	LE1	272.5	0.0	-114.2	93.9	-107.7	62.6	46.2	OK	OK
STUB3-EPb	STUB3-bfl1	◢ 5.0 L	134	LE1	427.1	0.2	34.8	236.0	68.5	98.1	77.3	OK	OK
		◢ 5.0 L	135	LE1	429.5	1.5	208.6	-166.6	-138.7	98.6	92.3	OK	OK
STUB3-EPb	STUB3-tfl 1	◢ 5.0 L	134	LE1	427.0	0.1	-221.9	-210.4	11.0	98.0	90.7	OK	OK

Item	Edge	T_w [mm]	L [mm]	Loads	$\sigma_{w,Ed}$ [MPa]	ε_{Pl} [%]	$\sigma_{\perp}$ [MPa]	$\tau_{\perp}$ [MPa]	$\tau_{\|\|}$ [MPa]	Ut [%]	Ut_c [%]	Detailing	Status
		◢ 5.0 L	135	LE1	427.2	0.2	-225.8	201.8	56.0	98.1	73.8	OK	OK
STUB3-EPb	STUB3-w 1	◢ 4.0 L	259	LE1	341.0	0.0	-101.2	-96.4	-161.4	78.3	58.8	OK	OK
		◢ 4.0 L	259	LE1	288.6	0.0	-86.9	91.7	129.7	66.3	49.7	OK	OK
STUB3-bfl1	SP4	◢ 4.0 L	168	LE1	97.4	0.0	-33.5	-26.0	45.9	22.4	15.0	OK	OK
		◢ 4.0 L	168	LE1	314.1	0.0	10.4	-16.7	180.5	72.1	25.0	OK	OK
STUB3-w 1	SP12	◢ 4.0 L	139	LE1	427.2	0.2	-252.9	-53.1	-191.5	98.1	93.5	OK	OK
		◢ 4.0 L	139	LE1	428.9	1.2	-71.6	244.0	6.8	98.5	98.5	OK	OK
STUB2-EPb	SP12	◢ 4.0 L	139	LE1	113.7	0.0	-53.4	-52.5	24.5	26.1	22.1	OK	OK
		◢ 4.0 L	139	LE1	190.4	0.0	-87.5	88.2	-41.8	43.7	34.5	OK	OK
STUB3-EPa	WID2a	◢ 5.0 L	99	LE1	427.0	0.1	200.3	190.3	105.7	98.0	47.5	OK	OK
		◢ 5.0 L	99	LE1	396.2	0.0	194.2	-198.1	-22.6	91.0	48.7	OK	OK
Member 4-bfl 1	WID2a	◢ 5.0 L	278	LE1	134.2	0.0	-21.3	-15.8	74.9	30.8	21.0	OK	OK
		◢ 5.0 L	278	LE1	140.2	0.0	2.2	3.3	-80.8	32.2	21.6	OK	OK
WID2b	WID2a	◢ 5.0 L	295	LE1	257.4	0.0	-60.7	-51.9	-134.8	59.1	28.0	OK	OK
		◢ 5.0 L	295	LE1	255.1	0.0	8.3	3.5	147.1	58.6	27.7	OK	OK

STUB3-EPa	WID2b	◢ 5.0 L	135	LE1	429.6	1.6	240.0	167.2	-119.9	98.6	94.4	OK	OK
		◢ 5.0 L	134	LE1	427.0	0.1	-118.5	111.8	-208.8	98.0	47.9	OK	OK
Member 4-bfl 1	WID2b	◢ 5.0 L	134	LE1	427.7	0.5	80.9	242.3	7.8	98.2	60.4	OK	OK
		◢ 5.0 L	134	LE1	188.1	0.0	51.1	-5.5	104.4	43.2	22.1	OK	OK
SP1	SP14	◢ 5.0 L	186	LE1	283.5	0.0	120.7	114.5	93.9	65.1	61.3	OK	OK
		◢ 5.0 L	186	LE1	427.7	0.5	273.8	-188.8	-18.5	98.2	84.8	OK	OK
SP14	SP4	◢ 4.0 L	168	LE1	426.9	0.1	-62.9	-53.4	237.9	98.0	46.1	OK	OK
		◢ 4.0 L	168	LE1	324.0	0.0	-59.9	106.5	-149.8	74.4	32.5	OK	OK
STUB3-EPb	SP14	◢ 5.0 L	132	LE1	433.7	3.9	218.5	202.8	75.1	99.6	96.3	OK	OK

Item	Edge	T_w [mm]	L [mm]	Loads	$\sigma_{w,Ed}$ [MPa]	ε_{Pl} [%]	$\sigma_{\perp}$ [MPa]	$\tau_{\perp}$ [MPa]	$\tau_{\parallel}$ [MPa]	Ut [%]	Ut_c [%]	Detailing	Status
		◢ 5.0 L	131	LE1	427.2	0.2	-173.7	116.6	192.8	98.1	69.2	OK	OK
SP1	STUB3-bfl1	◢ 5.0 L	197	LE1	199.5	0.0	65.4	10.1	108.4	45.8	32.5	OK	OK
		◢ 5.0 L	197	LE1	340.9	0.0	239.6	-138.4	-21.5	78.3	46.9	OK	OK
SP1	STUB3-w 1	◢ 4.0 L	259	LE1	418.7	0.0	-68.9	122.0	-204.9	96.1	50.9	OK	OK
		◢ 4.0 L	259	LE1	427.6	0.4	-47.9	-32.2	-243.2	98.2	66.2	OK	OK
SP1	STUB3-tfl 1	◢ 5.0 L	197	LE1	427.0	0.1	-259.2	-155.6	-119.1	98.0	74.4	OK	OK
		◢ 5.0 L	197	LE1	397.8	0.0	-125.7	134.8	171.2	91.3	70.8	OK	OK
EP1b	Member 3-tfl 1	◢ 6.0 L	109	LE1	432.8	3.4	-165.2	-135.7	186.9	99.4	96.4	OK	OK
		◢ 6.0 L	109	LE1	433.3	3.7	-146.2	158.9	173.8	99.5	99.5	OK	OK
EP1b	Member 3-bfl 1	◢ 5.0 L	109	LE1	432.1	3.0	204.1	174.1	134.3	99.2	99.2	OK	OK
		◢ 5.0 L	109	LE1	434.6	4.4	177.3	-198.9	-113.5	99.8	99.8	OK	OK
Member 1-bfl 1	STIFF1a	◢ 4.0 L	116	LE1	196.6	0.0	119.8	89.8	6.3	45.1	21.4	OK	OK
		◢ 4.0 L	116	LE1	351.0	0.0	95.3	-140.7	135.1	80.6	32.6	OK	OK
Member 1-w 1	STIFF1a	◢ 4.0 L	208	LE1	158.6	0.0	70.6	62.4	53.2	36.4	19.5	OK	OK
		◢ 4.0 L	208	LE1	271.8	0.0	41.8	-49.9	146.8	62.4	30.3	OK	OK

Member 1-tfl 1	STIFF1a	◢ 4.0 L	116	LE1	427.5	0.4	79.0	240.1	-34.4	98.1	56.6	OK	OK
		◢ 4.0 L	116	LE1	427.4	0.3	83.3	-94.0	-223.0	98.1	64.9	OK	OK
Member 1-bfl 1	STIFF1b	◢ 4.0 L	116	LE1	156.4	0.0	58.8	81.8	17.4	35.9	20.6	OK	OK
		◢ 4.0 L	116	LE1	151.3	0.0	77.9	-64.3	38.4	34.7	27.6	OK	OK
Member 1-w 1	STIFF1b	◢ 4.0 L	208	LE1	183.9	0.0	-85.4	-83.2	43.7	42.2	21.3	OK	OK
		◢ 4.0 L	208	LE1	304.7	0.0	88.1	-85.9	144.9	70.0	30.7	OK	OK
Member 1-tfl 1	STIFF1b	◢ 4.0 L	116	LE1	428.3	0.8	128.4	123.3	201.1	98.3	71.1	OK	OK
		◢ 4.0 L	116	LE1	427.8	0.5	49.5	-241.9	40.9	98.2	63.9	OK	OK

Design data

Material	f_u [MPa]	β_w [-]	$\sigma_{w,Rd}$ [MPa]	0.9 σ [MPa]
S 355	490.0	0.90	435.6	352.8

Detailed result for EP1a / Member 2-w 1

Weld resistance check (EN 1993-1-8 – Cl. 4.5.3.2)

$\sigma_{w,Rd} = f_u/(\beta_w \gamma_{M2}) =$ 435.6 MPa $\geq$ $\sigma_{w,Ed} = [\sigma_\perp^2 + 3(\tau_\perp^2 + \tau_\parallel^2)]^{0.5} =$ 435.3 MPa

$\sigma_{\perp,Rd} = 0.9\, f_u \,/\, \gamma_{M2}$ = 352.8 MPa $\geq$ $|\sigma_\perp| =$ 341.8 MPa

where:

$f_u = 490.0$ MPa – Ultimate strength

$\beta_w = 0.90$ – Correlation factor EN 1993-1-8 – Tab. 4.1

$\gamma_{M2} = 1.25$ – Safety factor

Stress utilization

$U_t = \max(\frac{\sigma_{w,Ed}}{\sigma_{w,Rd}} ; \frac{|\sigma_\perp|}{\sigma_{\perp,Rd}}) =$ 1.00 $\leq$ 1.0

Where:

$\sigma_{w,Ed} = 435.3$ MPa – Maximum normal stress transverse to the axis of the weld

$\sigma_{w,Rd} = 435.6$ MPa – Equivalent stress resistance

$\sigma_\perp = -341.8$ MPa – Normal stress perpendicular to the throat

$\sigma_{\perp,Rd} = 352.8$ MPa – Perpendicular stress resistance

Buckling

Loads	Shape	Factor [-]
LE1	1	3.07
	2	3.61
	3	4.17
	4	4.59
	5	4.83
	6	5.39

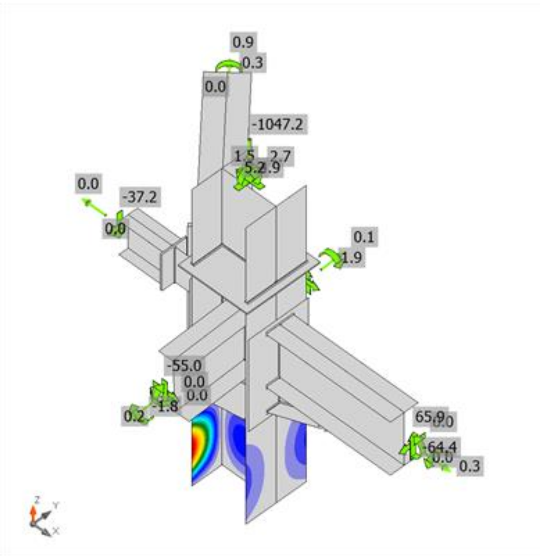

Cost estimation

Steel

Steel grade	Total weight [kg]	Unit cost [€/kg]	Cost [€]
S 355	66.29	2.00	132.57

Bolts

Bolt assembly	Total weight [kg]	Unit cost [€/kg]	Cost [€]
M12 8.8	0.56	5.00	2.78
M12 10.9	0.56	5.00	2.81
M16 10.9	1.07	5.00	5.35
M18 10.9	1.42	5.00	7.08
M20 10.9	1.32	5.00	6.62

Welds

Weld type	Throat thickness [mm]	Leg size [mm]	Total weight [kg]	Unit cost [€/kg]	Cost [€]
Double fillet	4.5	6.4	0.49	40.00	19.43
Double fillet	4.0	5.7	0.90	40.00	36.14
Double fillet	4.5	6.4	0.07	40.00	2.80
Double fillet	5.0	7.1	0.04	40.00	1.65
Double fillet	6.0	8.5	0.06	40.00	2.49
Double fillet	5.0	7.1	0.29	40.00	11.41
Double fillet	5.0	7.1	0.62	40.00	24.89
Double fillet	6.0	8.5	0.06	40.00	2.49

Hole drilling

Bolt assembly cost [€]	Percentage of bolt assembly cost [%]	Cost [€]
24.64	30.0	7.39

Cost summary

Cost estimation summary	Cost [€]
Total estimated cost	265.89

Bill of Material

Manufacturing Operations

Name	Plate s [mm]	Shape	Nr.	Welds Throat thickness [mm]	Length [mm]	Bolts	Nr.
PP1	P5.0x290.0-274.0 (S 355)	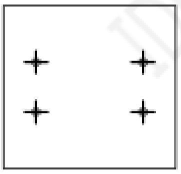	1	Double fillet: 4.5 Double fillet: 4.0	960.0 430.0	M12 8.8	4
	P5.0x290.0-274.0 (S 355)	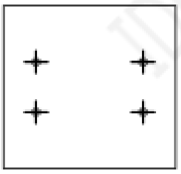	1				
EP1	P15.0x193.0-330.2 (S 355)	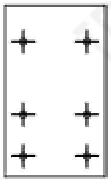	1	Double fillet: 4.0	344.4	M12 10.9	6
	P15.0x193.0-330.2 (S 355)	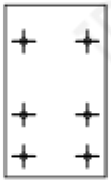	1				
EP2	P10.0x240.0-365.0 (S 355)	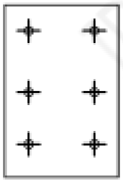	1	Double fillet: 4.5 Double fillet: 4.0	220.0 210.8	M16 10.9	6
WID1	P5.9x90.0-220.0 (S 355)	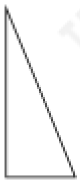	1	Double fillet: 4.5	567.7		
	P9.2x110.0-237.7 (S 355)	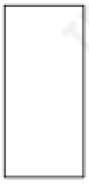	1				

STUB2	P6.0x100.0-144.0 (S 355)	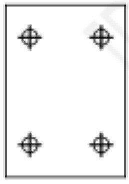	1	Double fillet: 4.0	133.1	M12 8.8	4

Name	Plate s [mm]	Shape	Nr.	Welds Throat thickness [mm]	Length [mm]	Bolts	Nr.
	P6.0x100.0-144.0 (S 355)	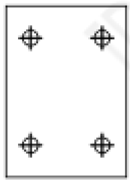	1				
SP1	P10.0x515.0-240.0 (S 355)	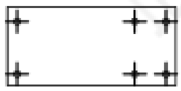	1			M18 10.9	6
STUB3	P12.0x180.0-430.0 (S 355)	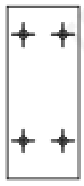	1	Double fillet: 5.0 Double fillet: 4.0	540.0 519.6	M20 10.9	4
	P12.0x180.0-430.0 (S 355)	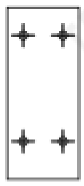	1				
SP4	P6.6x169.6-104.9 (S 355)		1				
SP12	P5.0x163.7-140.0 (S 355)		1				
WID2	P6.6x100.0-280.0 (S 355)	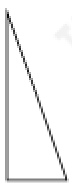	1	Double fillet: 5.0	947.3		

	P10.2x135.0-297.3 (S 355)	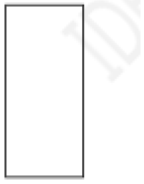	1				

Name	Plates [mm]	Shape	Nr.	Welds Throat thickness [mm]	Length [mm]	Bolts	Nr.
SP14	P10.2x231.0-132.0 (S 355)	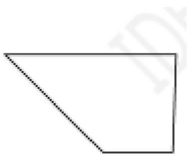	1				
STIFF1	P5.0x116.7-208.9 (S 355)	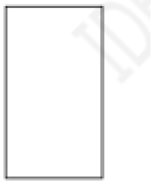	2	Double fillet: 4.0	884.8		

Welds

Type	Material	Throat thickness [mm]	Leg size [mm]	Length [mm]
Double fillet	S 355	4.5	6.4	1747.7
Double fillet	S 355	4.0	5.7	3596.5
Double fillet	S 355	5.0	7.1	2416.9
Double fillet	S 355	6.0	8.5	220.0

Bolts

Name	Grip length [mm]	Count
M12 8.8	10	4
M12 10.9	36	6
M16 10.9	19	6
M12 8.8	12	4
M18 10.9	19	6
M20 10.9	24	4

8.6.3 7 Member Diagrid Connection

Members

Geometry

Name	Cross-section	β – Direction [°]	γ - Pitch [°]	α - Rotation [°]	Offset ex [mm]	Offset ey [mm]	Offset ez [mm]
Member 1	14 - IPE180	0.0	0.0	0.0	200	0	0
Member 2	14 - IPE180	180.0	0.0	0.0	200	0	0
Member 3	15 - CHS159,4	0.0	60.0	0.0	0	0	0
Member 4	15 - CHS159,4	0.0	-60.0	0.0	0	0	0
Member 5	15 - CHS159,4	180.0	60.0	0.0	0	0	0
Member 6	15 - CHS159,4	180.0	-60.0	0.0	0	0	0
Member 7	13 - IPE140	90.0	0.0	0.0	250	0	0

Supports and forces

Name	Support	Forces in	X [mm]
Member 1 / end	N-Vy-Vz-Mx-My-Mz	Position	0
Member 2 / end		Position	0
Member 3 / end		Position	0
Member 4 / end		Position	0
Member 5 / end		Position	0
Member 6 / end		Position	0
Member 7 / end		Position	0

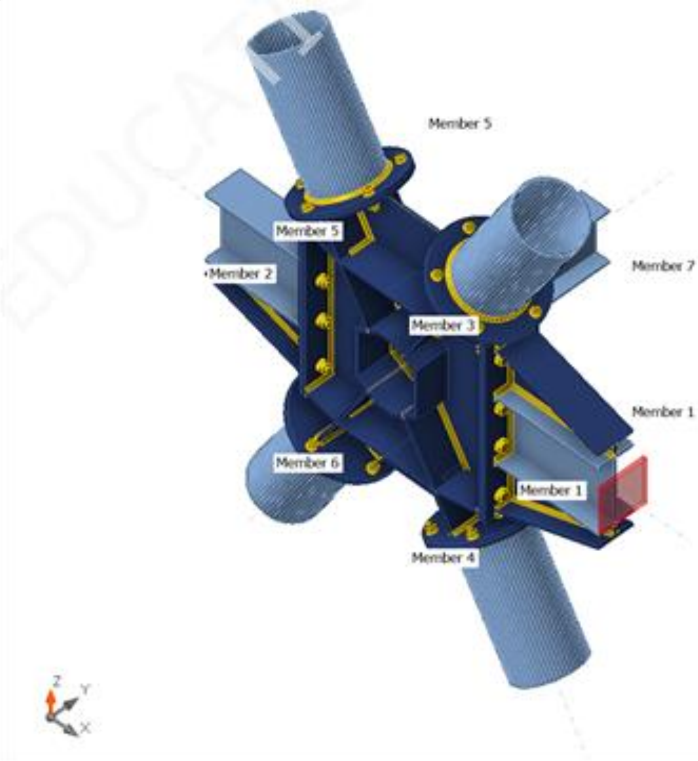

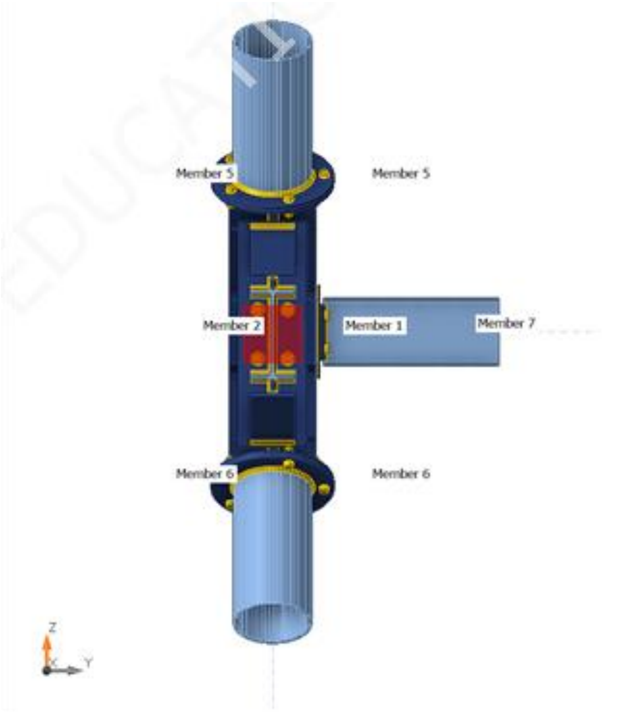

Cross-sections

Name	Material
14 - IPE180	S 355
15 - CHS159,4	S 355
13 - IPE140	S 355

Bolts

Name	Diameter [mm]	f_y [MPa]	f_u [MPa]	Gross area [mm^2]
M12 8.8	12	640.0	800.0	113
M14 8.8	14	640.0	800.0	154
M16 8.8	16	640.0	800.0	201

Load effects (forces in equilibrium)

Name	Member	N [kN]	Vy [kN]	Vz [kN]	Mx [kNm]	My [kNm]	Mz [kNm]
LE1	Member 1 / End	-0.1	0.0	-38.2	-0.7	-40.6	0.0
	Member 2 / End	1.0	0.0	38.4	0.7	-40.6	0.0
	Member 3 / End	-236.5	0.0	-0.5	-3.3	0.0	0.0
	Member 4 / End	-304.3	0.0	0.5	5.3	0.0	0.0
	Member 5 / End	-244.8	0.0	-0.5	4.2	0.0	0.0
	Member 6 / End	-304.0	0.0	0.5	-5.3	0.0	0.0
	Member 7 / End	-0.2	0.0	-33.2	0.0	0.0	0.0

Unbalanced forces

Name	X [kN]	Y [kN]	Z [kN]	Mx [kNm]	My [kNm]	Mz [kNm]
LE1	2.9	-0.2	77.0	-8.2	15.7	0.7

Check

Summary

Name	Value	Check status
Analysis	100.0%	OK
Plates	3.9 < 5.0%	OK
Loc. deformation	0.1 < 3%	OK
Bolts	99.1 < 100%	OK
Welds	99.8 < 100%	OK
Buckling	6.93	

Plates

Name	Material	t_p [mm]	Loads	σ_{Ed} [MPa]	ε_{Pl} [%]	$\sigma_{c,Ed}$ [MPa]	Status
Member 1-bfl 1	S 355	8.0	LE1	356.9	0.9	0.0	OK
Member 1-tfl 1	S 355	8.0	LE1	355.6	0.3	0.0	OK
Member 1-w 1	S 355	5.3	LE1	358.2	1.5	0.0	OK
Member 2-bfl 1	S 355	8.0	LE1	284.3	0.0	0.0	OK
Member 2-tfl 1	S 355	8.0	LE1	355.3	0.1	0.0	OK
Member 2-w 1	S 355	5.3	LE1	304.0	0.0	0.0	OK
Member 3	S 355	4.0	LE1	350.2	0.0	0.0	OK
Member 4	S 355	4.0	LE1	355.2	0.1	0.0	OK
Member 5	S 355	4.0	LE1	355.1	0.0	0.0	OK
Member 6	S 355	4.0	LE1	355.0	0.0	0.0	OK
Member 7-bfl 1	S 355	6.9	LE1	89.1	0.0	0.0	OK
Member 7-tfl 1	S 355	6.9	LE1	89.3	0.0	0.0	OK
Member 7-w 1	S 355	4.7	LE1	359.1	2.0	0.0	OK
Operation 5	S 355	8.0	LE1	355.2	0.1	0.0	OK
Operation 6a	S 355	8.0	LE1	355.1	0.1	67.0	OK
Operation 6b	S 355	8.0	LE1	322.4	0.2	0.0	OK
Operation 9	S 355	8.0	LE1	355.2	0.1	0.0	OK
Operation 10a	S 355	8.0	LE1	355.2	0.1	76.7	OK
Operation 10b	S 355	8.0	LE1	331.8	0.3	0.0	OK
Operation 13	S 355	8.0	LE1	357.1	1.0	0.0	OK
Operation 14a	S 355	10.0	LE1	355.2	0.1	62.3	OK
Operation 14b	S 355	8.0	LE1	356.4	0.7	0.0	OK
Operation 17	S 355	8.0	LE1	127.3	0.0	0.0	OK
Operation 18a	S 355	8.0	LE1	356.1	0.5	74.7	OK
Operation 18b	S 355	8.0	LE1	363.2	3.9	0.0	OK
Operation 21	S 355	8.0	LE1	355.8	0.4	0.0	OK

Operation 24	S 355	8.0	LE1	356.1	0.5	0.0	OK
Operation 28	S 355	8.0	LE1	210.2	0.0	0.0	OK
Operation 31	S 355	8.0	LE1	356.8	0.8	0.0	OK
Operation 34	S 355	8.0	LE1	356.3	0.6	0.0	OK
Operation 37	S 355	8.0	LE1	356.8	0.9	0.0	OK
Operation 44	S 355	10.0	LE1	317.8	0.0	66.6	OK
Operation 45	S 355	8.0	LE1	355.0	0.0	79.0	OK
Operation 46	S 355	8.0	LE1	355.4	0.2	72.7	OK
Operation 47	S 355	10.0	LE1	355.0	0.0	56.7	OK
Operation 16	S 355	8.0	LE1	87.1	0.0	0.0	OK
Operation 20a	S 355	10.0	LE1	355.1	0.0	194.3	OK
Operation 20b	S 355	8.0	LE1	355.1	0.0	0.0	OK
Operation 25	S 355	6.0	LE1	359.6	2.2	194.3	OK
Operation 8	S 355	8.0	LE1	245.1	0.0	0.0	OK
Operation 12a	S 355	10.0	LE1	183.7	0.0	0.0	OK
Operation 12b	S 355	8.0	LE1	164.9	0.0	0.0	OK
Operation 4a	S 355	10.0	LE1	355.3	0.2	149.8	OK

Name	Material	t_p [mm]	Loads	σ_{Ed} [MPa]	ε_{Pl} [%]	$\sigma_{c,Ed}$ [MPa]	Status
Operation 4b	S 355	8.0	LE1	276.5	0.0	0.0	OK
Operation 3a	S 355	10.0	LE1	272.9	0.0	0.0	OK
Operation 3b	S 355	8.0	LE1	91.8	0.0	0.0	OK
Operation 2	S 355	8.0	LE1	362.9	3.8	149.8	OK
SP13	S 355	8.0	LE1	355.3	0.1	88.1	OK
EP7	S 355	8.0	LE1	360.7	2.7	211.3	OK
WID1a	S 355	5.3	LE1	358.0	1.4	0.0	OK
WID1b	S 355	8.0	LE1	359.9	2.3	0.0	OK
WID1c	S 355	5.3	LE1	357.6	1.3	0.0	OK
WID1d	S 355	8.0	LE1	359.5	2.1	0.0	OK
WID2a	S 355	5.3	LE1	355.7	0.4	0.0	OK
WID2b	S 355	8.0	LE1	355.6	0.3	0.0	OK
SP14	S 355 - 1	175.0	LE1	161.7	0.0	0.0	OK

Design data

Material	f_y [MPa]	ε_{lim} [%]
S 355	355.0	5.0
S 355 - 1	335.0	5.0

Symbol explanation

t_p	Plate thickness
σ_{Ed}	Equivalent stress
ε_{Pl}	Plastic strain
$\sigma_{c,Ed}$	Contact stress
f_y	Yield strength
ε_{lim}	Limit of plastic strain

Detailed result for Operation 18b

Design values used in the analysis

$f_{yd} = \frac{f_{yk}}{\gamma_{M0}} =$ 355.0 MPa

Where:

$f_{yk} = 355.0$ MPa – characteristic yield strength

$\gamma_{M0} = 1.00$ – partial safety factor for steel material EN 1993-1-1 – 6.1

Loc. deformation

Name	d_0 [mm]	Loads	δ [mm]	δ_{lim} [mm]	δ/d_0 [%]	Check status
Member 3	159	LE1	0	5	0.1	OK
Member 4	159	LE1	0	5	0.1	OK
Member 5	159	LE1	0	5	0.1	OK
Member 6	159	LE1	0	5	0.1	OK

Symbol explanation

d_0	Cross-section size
δ	Local cross-section deformation
δ_{lim}	Allowed deformation

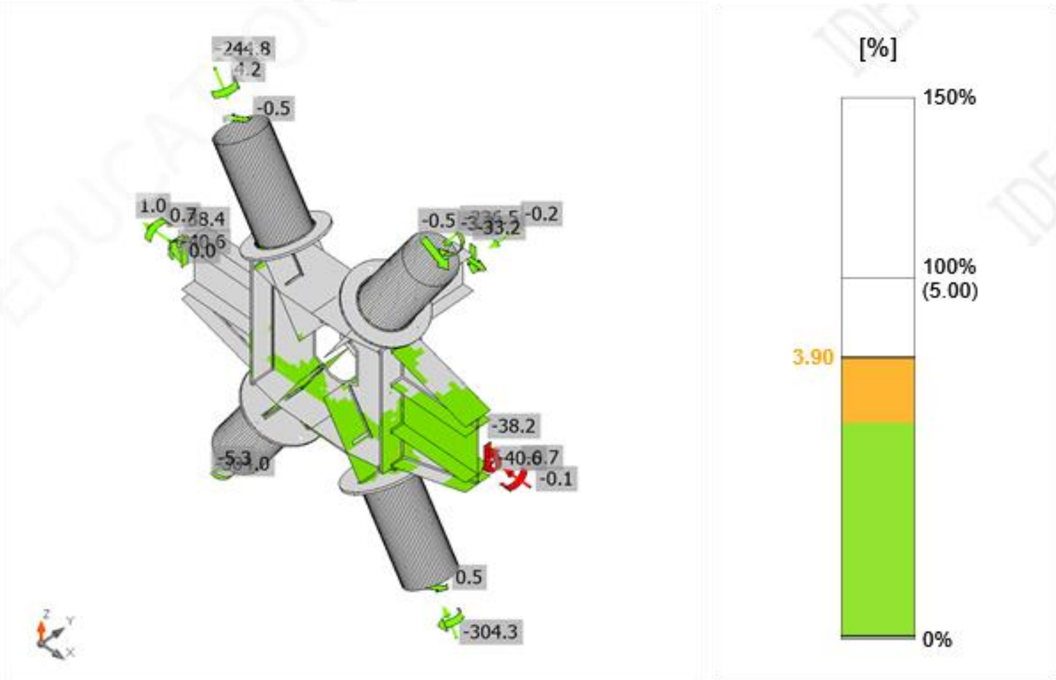

Strain check, LE1

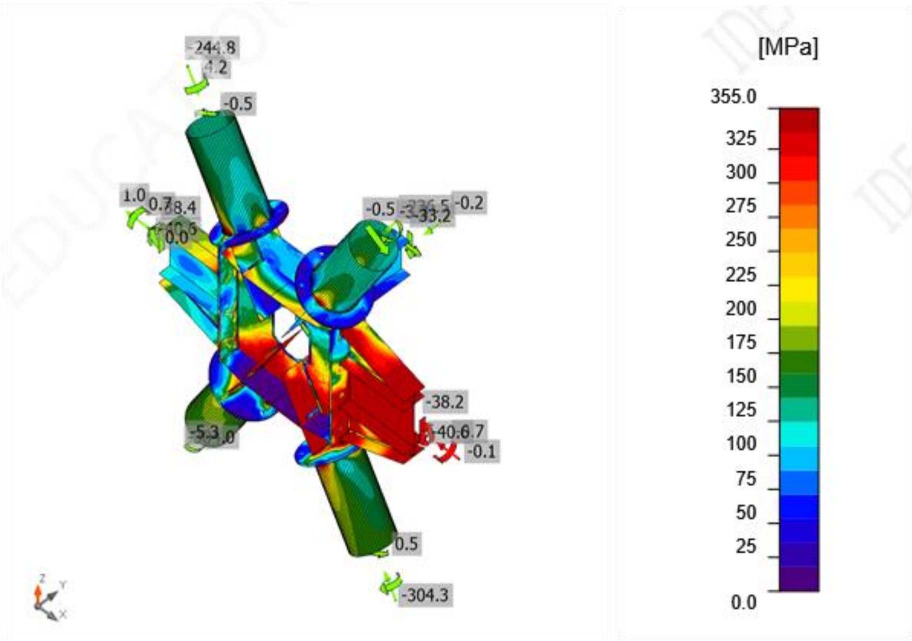

Equivalent stress, LE1

Bolts

Shape	Item	Grade	Loads	$F_{t,Ed}$ [kN]	$F_{v,Ed}$ [kN]	$F_{b,Rd}$ [kN]	Ut_t [%]	Ut_s [%]	Ut_{ts} [%]	Detailing	Status
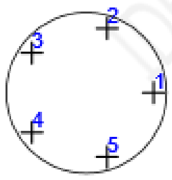	B1	M12 8.8 - 1	LE1	0.5	6.8	87.9	0.9	20.9	21.6	OK	OK
	B2	M12 8.8 - 1	LE1	0.5	6.4	86.5	1.0	19.7	20.4	OK	OK
	B3	M12 8.8 - 1	LE1	0.7	6.1	82.4	1.5	18.7	19.8	OK	OK
	B4	M12 8.8 - 1	LE1	0.4	6.5	85.5	0.9	20.0	20.6	OK	OK
	B5	M12 8.8 - 1	LE1	0.3	6.5	83.8	0.7	19.9	20.4	OK	OK
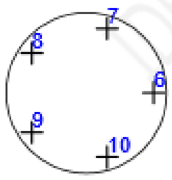	B6	M12 8.8 - 1	LE1	0.7	7.3	69.7	1.4	22.7	23.7	OK	OK
	B7	M12 8.8 - 1	LE1	0.2	8.1	71.4	0.5	25.1	25.4	OK	OK
	B8	M12 8.8 - 1	LE1	0.2	8.7	68.9	0.5	26.7	27.1	OK	OK
	B9	M12 8.8 - 1	LE1	0.2	8.0	68.2	0.4	24.6	25.0	OK	OK
	B10	M12 8.8 - 1	LE1	0.1	8.2	67.6	0.3	25.5	25.6	OK	OK
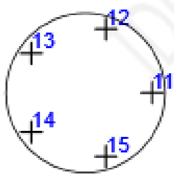	B11	M12 8.8 - 1	LE1	0.7	10.9	69.4	1.4	33.7	34.7	OK	OK
	B12	M12 8.8 - 1	LE1	0.3	10.4	63.6	0.6	32.1	32.5	OK	OK
	B13	M12 8.8 - 1	LE1	0.3	10.3	67.5	0.6	31.8	32.2	OK	OK
	B14	M12 8.8 - 1	LE1	0.3	9.7	65.0	0.5	30.1	30.5	OK	OK
	B15	M12 8.8 - 1	LE1	0.7	10.3	67.9	1.5	31.8	32.9	OK	OK
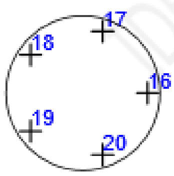	B16	M12 8.8 - 2	LE1	0.5	9.5	87.5	1.1	29.3	30.1	OK	OK
	B17	M12 8.8 - 2	LE1	0.2	10.3	84.5	0.5	31.7	32.0	OK	OK
	B18	M12 8.8 - 2	LE1	0.3	10.1	84.9	0.7	31.3	31.8	OK	OK
	B19	M12 8.8 - 2	LE1	0.4	10.9	85.1	0.8	33.6	34.1	OK	OK
	B20	M12 8.8 - 2	LE1	0.1	10.4	89.2	0.2	32.1	32.3	OK	OK
	B21	M14 8.8 - 3	LE1	1.9	9.0	82.3	2.9	20.4	22.4	OK	OK
	B22	M14 8.8 - 3	LE1	1.4	6.2	82.3	2.2	13.9	15.5	OK	OK
	B23	M14 8.8 - 3	LE1	12.1	7.7	82.3	18.3	17.3	30.3	OK	OK

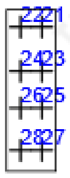	B24	M14 8.8 - 3	LE1	11.3	4.9	82.3	17.1	11.1	23.2	OK	OK
	B25	M14 8.8 - 3	LE1	56.2	4.3	82.3	84.6	9.6	70.0	OK	OK
	B26	M14 8.8 - 3	LE1	56.1	2.6	82.3	84.4	5.8	66.1	OK	OK
	B27	M14 8.8 - 3	LE1	61.5	2.7	82.3	92.6	6.1	72.2	OK	OK
	B28	M14 8.8 - 3	LE1	60.4	2.7	68.9	90.9	6.1	71.1	OK	OK
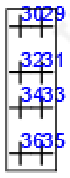	B29	M16 8.8 - 4	LE1	15.7	16.0	98.1	17.3	26.6	38.9	OK	OK
	B30	M16 8.8 - 4	LE1	0.0	21.0	116.2	0.0	34.9	34.9	OK	OK
	B31	M16 8.8 - 4	LE1	18.9	13.6	125.4	20.9	22.6	37.6	OK	OK
	B32	M16 8.8 - 4	LE1	14.4	23.7	125.4	15.9	39.3	50.7	OK	OK
	B33	M16 8.8 - 4	LE1	72.7	14.5	125.4	80.4	24.1	81.5	OK	OK
	B34	M16 8.8 - 4	LE1	81.5	16.4	125.4	90.1	27.2	91.6	OK	OK
	B35	M16 8.8 - 4	LE1	80.1	10.9	120.6	88.5	18.1	81.4	OK	OK
	B36	M16 8.8 - 4	LE1	89.6	12.3	99.9	99.1	20.4	91.2	OK	OK
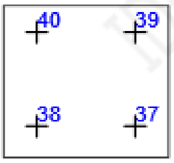	B37	M12 8.8 - 1	LE1	10.6	9.8	94.1	21.8	30.2	45.7	OK	OK
	B38	M12 8.8 - 1	LE1	10.3	10.3	94.1	21.2	31.9	47.0	OK	OK
	B39	M12 8.8 - 1	LE1	41.2	7.0	48.2	84.9	21.7	82.4	OK	OK
	B40	M12 8.8 - 1	LE1	41.2	7.5	48.2	84.9	23.1	83.8	OK	OK

Design data

Grade	$F_{t,Rd}$ [kN]	$B_{p,Rd}$ [kN]	$F_{v,Rd}$ [kN]
M12 8.8 - 1	48.6	112.4	32.4
M12 8.8 - 2	48.6	140.5	32.4
M14 8.8 - 3	66.5	98.3	44.3
M16 8.8 - 4	90.4	150.0	60.3

Symbol explanation

$F_{t,Ed}$	Tension force
$F_{v,Ed}$	Resultant of bolt shear forces Vy and Vz in shear planes
$F_{b,Rd}$	Plate bearing resistance EN 1993-1-8 – Tab. 3.4
Ut_t	Utilization in tension
Ut_s	Utilization in shear
Ut_{ts}	Interaction of tension and shear EN 1993-1-8 – Tab. 3.4
$F_{t,Rd}$	Bolt tension resistance EN 1993-1-8 – Tab. 3.4
$B_{p,Rd}$	Punching shear resistance EN 1993-1-8 – Tab. 3.4
$F_{v,Rd}$	Bolt shear resistance EN 1993-1-8 – Tab. 3.4

Detailed result for B36

Tension resistance check (EN 1993-1-8 – Table 3.4)

$$F_{t,Rd} = \frac{k_2 f_{ub} A_s}{\gamma_{M2}} = 90.4 \text{ kN} \geq F_{t,Ed} = 89.6 \text{ kN}$$

Where:

$k_2 = 0.90$ – Factor

$f_{ub} = 800.0$ MPa – Ultimate tensile strength of the bolt

$A_s = 157$ mm^2 – Tensile stress area of the bolt

$\gamma_{M2} = 1.25$ – Safety factor

Punching resistance check (EN 1993-1-8 – Table 3.4)

$$B_{p,Rd} = \frac{0.6\,\pi\, d_m\, t_p\, f_u}{\gamma_{M2}} = 150.0 \text{ kN} \geq F_{t,Ed} = 89.6 \text{ kN}$$

Where:

$d_m = 25$ mm – The mean of the across points and across flats dimensions of the bolt head or the nut, whichever is smaller

$t_p = 8$ mm – Plate thickness

$f_u = 490.0$ MPa – Ultimate strength

$\gamma_{M2} = 1.25$ – Safety factor

Shear resistance check (EN 1993-1-8 – Table 3.4)

$F_{v,Rd} = \frac{\beta_p \ \alpha_v f_{ub} A}{\gamma_{M2}} =$ 60.3 kN ≥ $F_{v,Ed} =$ 12.3 kN

Where:

$\beta_p = 1.00$	– Reduction factor for packing
$\alpha_v = 0.60$	– Reduction factor for shear stress
$f_{ub} = 800.0$ MPa	– Ultimate tensile strength of the bolt
$A = 157$ mm^2	– Tensile stress area of the bolt
$\gamma_{M2} = 1.25$	– Safety factor

Bearing resistance check (EN 1993-1-8 – Table 3.4)

$F_{b,Rd} = \frac{k_1 \ \alpha_b \ f_u \ dt}{\gamma_{M2}} =$ 99.9 kN ≥ $F_{b,Ed} =$ 12.3 kN

Where:

$k_1 = \min(2.8\frac{e_2}{d_0} - 1.7, 1.4\frac{p_2}{d_0} - 1.7, 2.5) = 2.50$	– Factor for edge distance and bolt spacing perpendicular to the direction of load transfer
$\alpha_b = \min(\frac{e_1}{3d_0}, \frac{p_1}{3d_0} - \frac{1}{4}, \frac{f_{ub}}{f_u}, 1) = 0.80$	– Factor for end distance and bolt spacing in direction of load transfer
$e_2 = 40$ mm	– Distance to the plate edge perpendicular to the shear force
$p_2 = \infty$ mm	– Distance between bolts perpendicular to the shear force
$d_0 = 18$ mm	– Bolt hole diameter
$e_1 = 43$ mm	– Distance to the plate edge in the direction of the shear force
$p_1 = \infty$ mm	– Distance between bolts in the direction of the shear force
$f_{ub} = 800.0$ MPa	– Ultimate tensile strength of the bolt
$f_u = 490.0$ MPa	– Ultimate strength of the plate
$d = 16$ mm	– Nominal diameter of the fastener
$t = 8$ mm	– Thickness of the plate
$\gamma_{M2} = 1.25$	– Safety factor

Utilization in tension

$\frac{F_{t,Ed}}{\min(F_{t,Rd}; B_{p,Rd})} =$ 0.99 ≤ 1.0

Where:

$F_{t,Ed} = 89.6$ kN	– Tensile force
$F_{t,Rd} = 90.4$ kN	– Tension resistance
$B_{p,Rd} = 150.0$ kN	– Punching resistance

Utilization in shear

$\max(\frac{F_{v,Ed}}{F_{v,Rd}}; \frac{F_{b,Ed}}{F_{b,Rd}}) =$ 0.20 ≤ 1.0

Where:

$F_{v,Ed} = 12.3$ kN	– Shear force (in decisive shear plane)
$F_{v,Rd} = 60.3$ kN	– Shear resistance
$F_{b,Ed} = 12.3$ kN	– Bearing force (for decisive plate)
$F_{b,Rd} = 99.9$ kN	– Bearing resistance

Interaction of tension and shear (EN 1993-1-8 – Table 3.4)

$\frac{F_{v,Ed}}{F_{v,Rd}} + \frac{F_{t,Ed}}{1.4 \ F_{t,Rd}} =$ 0.91 ≤ 1.0

Where:

$F_{v,Ed} = 12.3$ kN	– Shear force (in decisive shear plane)
$F_{v,Rd} = 60.3$ kN	– Shear resistance
$F_{t,Ed} = 89.6$ kN	– Tensile force
$F_{t,Rd} = 90.4$ kN	– Tension resistance

Welds

Item	Edge	Material	T_w [mm]	L [mm]	Loads	$\sigma_{w,Ed}$ [MPa]	ε_{Pl} [%]	$\sigma_\perp$ [MPa]	$\tau_\perp$ [MPa]	$\tau_{\parallel}$ [MPa]	Ut [%]	Ut_c [%]	Detailing	Status
Operation 6a	Operation 6b	S 355	◢ 7.5 L	174	LE1	322.2	0.0	-179.7	-154.4	0.9	74.0	54.1	OK	OK
		S 355	◢ 7.5 L	174	LE1	427.1	0.1	-230.6	204.4	36.1	98.0	63.5	OK	OK
Operation 6b	Operation 5	Steel4	-	120	-	-	-	-	-	-	-	-	OK	OK

Item	Edge	Material	T_w [mm]	L [mm]	Loads	$\sigma_{w,Ed}$ [MPa]	ε_{Pl} [%]	$\sigma_{\perp}$ [MPa]	$\tau_{\perp}$ [MPa]	$\tau_{\|\|}$ [MPa]	Ut [%]	Ut_c [%]	Detailing	Status
Operation 10b	Operation 9	Steel4	-	120	-	-	-	-	-	-	-	-	OK	OK
Operation 14b	Operation 13	Steel4	-	120	-	-	-	-	-	-	-	-	OK	OK
Operation 18b	Operation 17	S 355	-	120	-	-	-	-	-	-	-	-	OK	OK
Operation 10b	Operation 21	S 355	◢ 5.0 L	253	LE1	164.0	0.0	-99.3	35.7	-66.3	37.6	32.4	OK	OK
		S 355	◢ 5.0 L	252	LE1	197.0	0.0	-122.4	-57.4	68.3	45.2	24.7	OK	OK
Operation 6b	Operation 24	S 355	◢ 5.0 L	253	LE1	149.3	0.0	-87.7	21.7	66.3	34.3	24.2	OK	OK
		S 355	◢ 5.0 L	252	LE1	192.4	0.0	-106.5	-65.7	-65.1	44.2	30.6	OK	OK
Operation 6b	Operation 28	S 355	◢ 5.0 L	252	LE1	133.4	0.0	-24.3	9.4	-75.2	30.6	17.3	OK	OK
		S 355	◢ 5.0 L	252	LE1	98.8	0.0	-61.3	-43.9	-8.8	22.7	16.1	OK	OK
Operation 10b	Operation 28	S 355	◢ 5.0 L	252	LE1	94.7	0.0	-30.8	-14.7	49.6	21.8	13.8	OK	OK
		S 355	◢ 5.0 L	253	LE1	97.5	0.0	-5.4	-50.9	23.8	22.4	15.1	OK	OK
Operation 14b	Operation 31	S 355	◢ 5.0 L	252	LE1	338.8	0.0	9.5	-65.8	-184.1	77.8	37.9	OK	OK
		S 355	◢ 5.0 L	253	LE1	427.1	0.1	-1.0	-9.8	-246.4	98.1	72.8	OK	OK
Operation 18b	Operation 34	S 355	◢ 5.0 L	252	LE1	303.2	0.0	51.3	-56.4	163.1	69.6	35.8	OK	OK
		S 355	◢ 5.0 L	252	LE1	426.9	0.0	-57.0	-61.4	236.4	98.0	65.6	OK	OK
Operation 18b	Operation 37	S 355	◢ 5.0 L	252	LE1	414.6	0.0	13.1	7.2	239.2	95.2	43.3	OK	OK
		S 355	◢ 5.0 L	252	LE1	346.5	0.0	-19.1	1.2	199.7	79.6	37.7	OK	OK
Operation 14b	Operation 37	S 355	◢ 5.0 L	252	LE1	426.9	0.0	40.4	-16.3	-244.8	98.0	51.8	OK	OK

		S 355	◢ 5.0 ∟	252	LE1	427.0	0.1	-0.8	16.6	-246.0	98.0	49.4	OK	OK
Operation 20a	Operation 20b	S 355	◢ 4.0 ∟	140	LE1	176.1	0.0	20.8	-10.7	100.4	40.4	21.9	OK	OK
		S 355	◢ 4.0 ∟	140	LE1	227.5	0.0	-149.9	-98.7	5.5	52.2	43.9	OK	OK
Operation 12a	Operation 12b	S 355	◢ 5.0 ∟	140	LE1	171.5	0.0	-37.6	23.7	93.6	39.4	23.9	OK	OK
		S 355	◢ 5.0 ∟	140	LE1	154.0	0.0	-18.6	-32.5	82.0	35.4	15.6	OK	OK
Operation 4a	Operation 4b	S 355	◢ 4.0 ∟	140	LE1	354.9	0.0	-178.2	172.0	-42.5	81.5	36.3	OK	OK
		S 355	◢ 4.0 ∟	140	LE1	324.8	0.0	-157.4	-163.6	12.6	74.6	33.2	OK	OK
Operation 3a	Operation 3b	S 355	◢ 4.0 ∟	140	LE1	159.3	0.0	-56.8	42.4	-74.8	36.6	24.4	OK	OK
		S 355	◢ 4.0 ∟	140	LE1	130.6	0.0	-29.7	-44.1	-58.7	30.0	20.5	OK	OK
EP7	Member 7-w 1	S 355	◢ 5.0 ∟	112	LE1	434.7	4.5	-209.1	-208.5	-70.4	99.8	99.8	OK	OK
		S 355	◢ 5.0 ∟	112	LE1	434.8	4.5	-208.0	208.6	71.4	99.8	99.8	OK	OK
Operation 5	Operation 24	S 355	◢ 4.0 ∟	10	LE1	189.8	0.0	123.1	77.1	-31.9	43.6	42.9	OK	OK
		S 355	◢ 4.0 ∟	10	LE1	216.4	0.0	-115.9	84.3	-63.5	49.7	48.9	OK	OK
Operation 5	Operation 31	S 355	◢ 4.0 ∟	10	LE1	288.5	0.0	52.5	158.7	-40.2	66.2	63.4	OK	OK
		S 355	◢ 4.0 ∟	10	LE1	190.9	0.0	-181.2	30.0	-17.4	51.4	43.2	OK	OK
Operation 6b	Operation 31	S 355	◢ 4.0 ∟	252	LE1	156.3	0.0	-31.5	11.9	-87.6	35.9	18.2	OK	OK

Item	Edge	Material	T_w [mm]	L [mm]	Loads	$\sigma_{w,Ed}$ [MPa]	ε_{Pl} [%]	$\sigma_{\perp}$ [MPa]	$\tau_{\perp}$ [MPa]	$\tau_{\parallel}$ [MPa]	Ut [%]	Ut_c [%]	Detailing	Status
		S 355	◢ 4.0 ∟	252	LE1	138.6	0.0	-79.0	-48.1	-44.9	31.8	20.3	OK	OK

Operation 9	Operation 21	S 355	◢ 4.0 L	10	LE1	417.5	0.0	-121.5	228.7	29.9	95.9	87.4	OK	OK
		S 355	◢ 4.0 L	10	LE1	179.0	0.0	-140.4	-33.1	-54.9	41.1	40.5	OK	OK
Operation 9	Operation 34	S 355	◢ 4.0 L	10	LE1	169.7	0.0	164.2	8.2	-23.3	46.6	38.4	OK	OK
		S 355	◢ 4.0 L	10	LE1	205.1	0.0	-60.1	112.3	14.5	47.1	46.3	OK	OK
Operation 10b	Operation 34	S 355	◢ 4.0 L	252	LE1	114.9	0.0	-40.1	-18.4	59.3	26.4	16.6	OK	OK
		S 355	◢ 4.0 L	253	LE1	119.8	0.0	-5.1	-63.7	26.7	27.5	17.9	OK	OK
Operation 13	Operation 24	S 355	◢ 4.0 L	10	LE1	422.9	1.4	-346.4	122.3	-68.1	98.2	87.8	OK	OK
		S 355	◢ 4.0 L	10	LE1	377.3	1.1	346.0	73.8	-45.9	98.1	79.4	OK	OK
Operation 13	Operation 31	S 355	◢ 4.0 L	10	LE1	362.8	2.3	348.1	53.6	-24.9	98.7	77.5	OK	OK
		S 355	◢ 4.0 L	10	LE1	402.2	2.0	-347.6	103.1	-54.8	98.5	84.2	OK	OK
Operation 14b	Operation 24	S 355	◢ 4.0 L	252	LE1	427.1	0.1	-24.7	32.8	-244.0	98.1	67.6	OK	OK
		S 355	◢ 4.0 L	252	LE1	427.2	0.2	7.0	7.6	-246.5	98.1	57.0	OK	OK
Operation 18b	Operation 21	S 355	◢ 4.0 L	252	LE1	426.9	0.0	13.5	7.9	246.2	98.0	50.3	OK	OK
		S 355	◢ 4.0 L	252	LE1	404.4	0.0	-2.3	22.3	232.4	92.8	44.8	OK	OK
Operation 24	Operation 21	Steel4	-	188	-	-	-	-	-	-	-	-	OK	OK
Operation 31	Operation 21	Steel4	-	548	-	-	-	-	-	-	-	-	OK	OK
Operation 37	Operation 21	Steel4	-	188	-	-	-	-	-	-	-	-	OK	OK
Operation 37	Operation 21	Steel4	-	253	-	-	-	-	-	-	-	-	OK	OK

Item	Edge	Material	T_w [mm]	L [mm]	Loads	$\sigma_{w,Ed}$ [MPa]	ε_{Pl} [%]	$\sigma_{\perp}$ [MPa]	$\tau_{\perp}$ [MPa]	$\tau_{\parallel}$ [MPa]	Ut [%]	Ut_c [%]	Detailing	Status
Operation 20a	Operation 21	S 355	◢ 4.0 ∟	458	LE1	398.3	0.0	-154.1	-146.3	153.4	91.4	58.7	OK	OK
		S 355	◢ 4.0 ∟	458	LE1	376.3	0.0	-150.9	163.8	113.0	86.4	63.3	OK	OK
Operation 12a	Operation 21	S 355	◢ 4.0 ∟	459	LE1	336.1	0.0	-65.6	-73.2	175.7	77.2	70.3	OK	OK
		S 355	◢ 4.0 ∟	459	LE1	247.2	0.0	-114.4	111.5	59.7	56.8	44.8	OK	OK
Operation 34	Operation 24	Steel4	-	548	-	-	-	-	-	-	-	-	OK	OK
Operation 37	Operation 24	Steel4	-	188	-	-	-	-	-	-	-	-	OK	OK
Operation 37	Operation 24	Steel4	-	253	-	-	-	-	-	-	-	-	OK	OK
Operation 4a	Operation 24	S 355	◢ 4.0 ∟	459	LE1	427.2	0.2	119.8	163.4	171.3	98.1	75.8	OK	OK
		S 355	◢ 4.0 ∟	459	LE1	388.3	0.0	-92.2	179.7	123.0	89.1	67.6	OK	OK
Operation 3a	Operation 24	S 355	◢ 4.0 ∟	459	LE1	427.2	0.2	168.4	146.0	173.4	98.1	87.2	OK	OK
		S 355	◢ 4.0 ∟	459	LE1	357.1	0.0	-141.4	95.4	163.6	82.0	67.8	OK	OK
Operation 31	Operation 28	Steel4	-	253	-	-	-	-	-	-	-	-	OK	OK
Operation 31	Operation 28	Steel4	-	188	-	-	-	-	-	-	-	-	OK	OK
Operation 34	Operation 28	Steel4	-	188	-	-	-	-	-	-	-	-	OK	OK
Operation 34	Operation 28	Steel4	-	253	-	-	-	-	-	-	-	-	OK	OK
Operation 34	Operation 31	Steel4	-	188	-	-	-	-	-	-	-	-	OK	OK
Operation 20a	Operation 31	S 355	◢ 4.0 ∟	458	LE1	398.3	0.0	-154.1	-146.3	153.4	91.4	58.7	OK	OK
		S 355	◢ 4.0 ∟	458	LE1	376.3	0.0	-150.9	163.8	113.0	86.4	63.3	OK	OK
Operation 12a	Operation 31	S 355	◢ 4.0 ∟	459	LE1	336.1	0.0	-65.6	-73.2	175.7	77.2	70.3	OK	OK
		S 355	◢ 4.0 ∟	459	LE1	247.2	0.0	-114.4	111.5	59.7	56.8	44.8	OK	OK
Operation 4a	Operation 34	S 355	◢ 4.0 ∟	459	LE1	427.2	0.2	119.8	163.4	171.3	98.1	75.8	OK	OK

Item	Edge	Material	T_w [mm]	L [mm]	Loads	$\sigma_{w,Ed}$ [MPa]	ε_{Pl} [%]	$\sigma_{\perp}$ [MPa]	$\tau_{\perp}$ [MPa]	$\tau_{\parallel}$ [MPa]	Ut [%]	Ut_c [%]	Detailing	Status
		S 355	◢ 4.0 L	459	LE1	388.3	0.0	-92.2	179.7	123.0	89.1	67.6	OK	OK
Operation 3a	Operation 34	S 355	◢ 4.0 L	459	LE1	427.2	0.2	168.4	146.0	173.4	98.1	87.2	OK	OK
		S 355	◢ 4.0 L	459	LE1	357.1	0.0	-141.4	95.4	163.6	82.0	67.8	OK	OK
Operation 12a	Operation 20a	Steel4	-	141	-	-	-	-	-	-	-	-	OK	OK
Operation 12a	Operation 20a	Steel4	-	460	-	-	-	-	-	-	-	-	OK	OK
Operation 12a	Operation 20a	Steel4	-	141	-	-	-	-	-	-	-	-	OK	OK
Operation 12a	Operation 20a	Steel4	-	460	-	-	-	-	-	-	-	-	OK	OK
Operation 3a	Operation 4a	Steel4	-	141	-	-	-	-	-	-	-	-	OK	OK
Operation 3a	Operation 4a	Steel4	-	460	-	-	-	-	-	-	-	-	OK	OK
Operation 3a	Operation 4a	Steel4	-	141	-	-	-	-	-	-	-	-	OK	OK
Operation 3a	Operation 4a	Steel4	-	460	-	-	-	-	-	-	-	-	OK	OK
SP14	Operation 31	S 355	-	33	-	-	-	-	-	-	-	-	OK	OK
SP14	Operation 31	S 355	-	70	-	-	-	-	-	-	-	-	OK	OK
SP14	Operation 31	S 355	-	40	-	-	-	-	-	-	-	-	OK	OK
SP14	Operation 31	S 355	-	28	-	-	-	-	-	-	-	-	OK	OK
SP14	Operation 24	S 355	-	130	-	-	-	-	-	-	-	-	OK	OK
SP14	Operation 24	S 355	-	70	-	-	-	-	-	-	-	-	OK	OK
SP14	Operation 24	S 355	-	40	-	-	-	-	-	-	-	-	OK	OK
SP14	Operation 24	S 355	-	28	-	-	-	-	-	-	-	-	OK	OK
SP14	Operation 21	S 355	-	28	-	-	-	-	-	-	-	-	OK	OK
Operation 10a	Operation 10b	S 355	◢ 7.5 L	174	LE1	336.1	0.0	-170.4	-142.0	-88.5	77.2	68.8	OK	OK
		S 355	◢ 7.5 L	174	LE1	427.2	0.2	-230.6	204.2	-37.3	98.1	85.6	OK	OK
SP14	Operation 21	S 355	-	70	-	-	-	-	-	-	-	-	OK	OK
SP14	Operation 28	S 355	-	29	-	-	-	-	-	-	-	-	OK	OK

Item	Edge	Material	T_w [mm]	L [mm]	Loads	$\sigma_{w,Ed}$ [MPa]	ε_{Pl} [%]	$\sigma_{\perp}$ [MPa]	$\tau_{\perp}$ [MPa]	$\tau_{\parallel}$ [MPa]	Ut [%]	Ut_c [%]	Detailing	Status
SP14	Operation 28	S 355	-	29	-	-	-	-	-	-	-	-	OK	OK
SP14	Operation 37	S 355	-	28	-	-	-	-	-	-	-	-	OK	OK
SP14	Operation 37	S 355	-	40	-	-	-	-	-	-	-	-	OK	OK
SP14	Operation 37	S 355	-	29	-	-	-	-	-	-	-	-	OK	OK
SP14	Operation 34	S 355	-	70	-	-	-	-	-	-	-	-	OK	OK
SP14	Operation 34	S 355	-	34	-	-	-	-	-	-	-	-	OK	OK
Operation 4b	Operation 20b	S 355	-	175	-	-	-	-	-	-	-	-	OK	OK
Operation 5	Operation 28	S 355	◢ 4.0 L	10	LE1	289.5	0.0	52.3	159.2	-40.9	66.5	63.6	OK	OK
		S 355	◢ 4.0 L	10	LE1	189.4	0.0	-181.6	29.9	-8.5	51.5	42.9	OK	OK
Operation 9	Operation 28	S 355	◢ 4.0 L	10	LE1	169.7	0.0	164.2	8.2	-23.3	46.5	38.4	OK	OK
		S 355	◢ 4.0 L	10	LE1	205.1	0.0	-60.1	112.3	14.4	47.1	46.3	OK	OK
Operation 13	Operation 37	S 355	◢ 4.0 L	10	LE1	429.4	1.5	-312.9	161.5	-52.5	98.6	89.1	OK	OK
		S 355	◢ 4.0 L	10	LE1	417.8	0.8	345.5	131.8	-31.9	97.9	87.8	OK	OK
Operation 14a	Operation 14b	S 355	◢ 5.0 L	174	LE1	428.4	0.9	-210.5	-199.7	80.7	98.4	92.0	OK	OK
		S 355	◢ 5.0 L	174	LE1	427.7	0.5	-206.1	194.0	95.8	98.2	89.0	OK	OK
Operation 18a	Operation 18b	S 355	◢ 5.0 L	174	LE1	428.9	1.2	-206.6	-191.3	-102.5	98.5	97.3	OK	OK
		S 355	◢ 5.0 L	174	LE1	428.3	0.8	-196.8	191.2	-108.0	98.3	98.3	OK	OK
Operation 10a	Operation 21	S 355	◢ 5.0 L	53	LE1	428.8	1.1	-4.3	-171.0	179.0	98.4	93.5	OK	OK
		S 355	◢ 5.0 L	53	LE1	430.4	2.0	-281.2	181.2	-50.5	98.8	89.4	OK	OK
Operation 6a	Operation 24	S 355	◢ 5.0 L	53	LE1	428.2	0.8	-101.3	-186.6	-151.3	98.3	80.3	OK	OK

Item	Edge	Material	T_w [mm]	L [mm]	Loads	$\sigma_{w,Ed}$ [MPa]	ε_{Pl} [%]	$\sigma_{\perp}$ [MPa]	$\tau_{\perp}$ [MPa]	$\tau_{\parallel}$ [MPa]	Ut [%]	Ut_c [%]	Detailing	Status
		S 355	5.0	53	LE1	429.4	1.4	-242.8	192.8	68.1	98.6	87.0	OK	OK
Operation 14a	Operation 31	S 355	7.0	53	LE1	428.0	0.7	-13.3	-162.6	-185.9	98.3	80.9	OK	OK
		S 355	7.0	53	LE1	430.3	2.0	-252.6	192.5	58.2	98.8	91.5	OK	OK
Operation 18a	Operation 34	S 355	7.0	54	LE1	429.4	1.5	95.5	-142.5	195.3	98.6	92.9	OK	OK
		S 355	7.0	54	LE1	432.4	3.2	-297.6	177.9	-33.9	99.3	92.6	OK	OK
Operation 14a	Operation 37	S 355	5.0	90	LE1	427.1	0.2	-241.5	-200.4	-34.6	98.1	64.3	OK	OK
		S 355	5.0	90	LE1	301.2	0.0	201.8	-127.0	-23.1	69.1	47.0	OK	OK
Operation 18a	Operation 37	S 355	4.0	89	LE1	427.5	0.4	-234.6	-204.4	28.2	98.2	72.9	OK	OK
		S 355	4.0	89	LE1	394.6	0.0	259.4	-170.9	15.6	90.6	70.9	OK	OK
Operation 10a	Operation 28	S 355	4.0	90	LE1	342.5	0.0	-176.2	-161.9	50.5	78.6	64.9	OK	OK
		S 355	4.0	90	LE1	104.6	0.0	56.4	-42.2	28.4	24.0	20.8	OK	OK
Operation 6a	Operation 28	S 355	4.0	90	LE1	314.8	0.0	-157.0	-150.7	-46.0	72.3	45.1	OK	OK
		S 355	4.0	90	LE1	80.8	0.0	42.1	-35.8	17.5	18.5	15.8	OK	OK
Operation 25	Member 2-bfl 1	S 355	5.0	91	LE1	295.6	0.0	157.1	94.3	-109.6	67.9	44.0	OK	OK
		S 355	5.0	91	LE1	184.7	0.0	57.3	-90.5	-45.6	42.4	35.8	OK	OK
Operation 25	Member 2-tfl 1	S 355	5.0	91	LE1	427.5	0.4	-255.9	-197.1	-15.9	98.2	67.2	OK	OK
		S 355	5.0	91	LE1	427.3	0.3	-147.4	221.8	-66.6	98.1	65.1	OK	OK
Operation 25	Member 2-w 1	S 355	4.0	171	LE1	428.3	0.9	206.3	195.9	-92.8	98.3	61.0	OK	OK

Item	Edge	Material	T_w [mm]	L [mm]	Loads	$\sigma_{w,Ed}$ [MPa]	ε_{Pl} [%]	$\sigma_{\perp}$ [MPa]	$\tau_{\perp}$ [MPa]	$\tau_{\parallel}$ [MPa]	Ut [%]	Ut_c [%]	Detailing	Status
		S 355	4.0	171	LE1	428.4	0.9	187.2	-196.9	103.7	98.4	62.2	OK	OK
Operation 2	Member 1-bfl 1	S 355	6.0	91	LE1	428.2	0.8	208.5	114.6	-183.0	98.3	80.8	OK	OK
		S 355	6.0	91	LE1	427.1	0.2	100.2	-96.4	-219.5	98.1	75.0	OK	OK
Operation 2	Member 1-tfl 1	S 355	6.0	91	LE1	174.2	0.0	-45.3	-92.3	30.2	40.0	32.9	OK	OK
		S 355	6.0	91	LE1	290.2	0.0	-166.4	119.3	-67.9	66.6	47.5	OK	OK
Operation 2	Member 1-w 1	S 355	4.0	171	LE1	428.2	0.8	103.4	190.1	-146.4	98.3	75.4	OK	OK
		S 355	4.0	171	LE1	430.0	1.8	172.4	-128.8	187.4	98.7	88.5	OK	OK
Operation 14b	Operation 8	S 355	4.0	119	LE1	427.6	0.4	11.2	3.2	246.7	98.2	92.0	OK	OK
		S 355	4.0	119	LE1	426.9	0.0	-5.4	-1.1	246.4	98.0	54.1	OK	OK
Operation 2	WID1a	S 355	5.5	119	LE1	165.1	0.0	-68.2	-86.2	10.3	37.9	22.4	OK	OK
		S 355	5.5	120	LE1	207.6	0.0	-97.8	103.3	22.4	47.7	34.9	OK	OK
Member 1-tfl 1	WID1a	S 355	5.5	269	LE1	246.7	0.0	-20.2	-34.7	-137.6	56.6	34.6	OK	OK
		S 355	5.5	269	LE1	427.0	0.1	36.8	-18.5	-244.9	98.0	72.7	OK	OK
WID1b	WID1a	S 355	5.5	285	LE1	377.4	0.0	-113.5	-176.9	109.0	86.6	61.5	OK	OK
		S 355	5.5	285	LE1	427.6	0.4	-102.6	82.4	-225.0	98.2	70.9	OK	OK
Operation 2	WID1b	S 355	5.5	90	LE1	428.6	1.0	-171.7	-219.0	-58.7	98.4	85.7	OK	OK
		S 355	5.5	90	LE1	427.5	0.4	-219.8	147.3	152.1	98.2	76.7	OK	OK
Operation 2	WID1c	S 355	5.5	120	LE1	427.3	0.2	152.6	141.0	182.2	98.1	80.2	OK	OK

Item	Edge	Material	T_w [mm]	L [mm]	Loads	$\sigma_{w,Ed}$ [MPa]	ε_{Pl} [%]	$\sigma_{\perp}$ [MPa]	$\tau_{\perp}$ [MPa]	$\tau_{\parallel}$ [MPa]	Ut [%]	Ut_c [%]	Detailing	Status
		S 355	5.5	120	LE1	427.1	0.2	197.2	-211.8	-54.5	98.1	76.0	OK	OK
Member 1-bfl 1	WID1c	S 355	5.5	269	LE1	427.0	0.1	-52.7	-39.9	-241.4	98.0	81.3	OK	OK
		S 355	5.5	269	LE1	258.0	0.0	5.7	-29.2	146.0	59.2	49.7	OK	OK
WID1d	WID1c	S 355	5.5	285	LE1	427.5	0.4	85.7	78.4	-228.8	98.2	73.1	OK	OK
		S 355	5.5	285	LE1	324.1	0.0	109.7	-131.0	117.7	74.4	56.2	OK	OK
Operation 2	WID1d	S 355	5.5	90	LE1	432.9	3.5	225.9	135.4	-164.7	99.4	94.4	OK	OK
		S 355	5.5	90	LE1	427.4	0.3	-67.2	142.1	-197.9	98.1	77.1	OK	OK
Operation 25	WID2a	S 355	5.0	119	LE1	429.9	1.8	131.9	157.2	-176.3	98.7	85.7	OK	OK
		S 355	5.0	119	LE1	430.2	1.9	166.8	-142.9	178.9	98.8	88.9	OK	OK
Member 2-bfl 1	WID2a	S 355	5.0	268	LE1	69.6	0.0	30.9	23.3	-27.5	16.0	13.7	OK	OK
		S 355	5.0	269	LE1	67.3	0.0	28.5	-16.2	-31.2	15.5	13.3	OK	OK
WID2b	WID2a	S 355	5.0	285	LE1	155.2	0.0	4.9	-5.0	-89.4	35.6	26.8	OK	OK
		S 355	5.0	285	LE1	167.8	0.0	-60.9	86.8	-25.0	38.5	29.3	OK	OK
Operation 25	WID2b	S 355	5.0	90	LE1	427.2	0.2	242.5	29.6	200.9	98.1	94.2	OK	OK
		S 355	5.0	90	LE1	426.9	0.1	-18.6	60.5	238.7	98.0	52.7	OK	OK
Operation 6a	Operation 34	S 355	4.0	151	LE1	429.7	1.6	-165.6	-215.7	-76.7	98.7	83.8	OK	OK
Operation 6a	Operation 31	S 355	4.0	89	LE1	159.9	0.0	-77.0	-70.3	-40.0	36.7	31.6	OK	OK
Operation 10a	Operation 34	S 355	4.0	90	LE1	161.7	0.0	-99.7	-52.8	51.2	37.1	29.5	OK	OK
Operation 10a	Operation 31	S 355	4.0	151	LE1	431.0	2.4	-123.9	-225.1	78.4	99.0	90.2	OK	OK
Operation 14a	Operation 21	S 355	4.0	151	LE1	431.3	2.6	-173.9	-216.2	-72.1	99.0	94.5	OK	OK

Item	Edge	Material	T_w [mm]	L [mm]	Loads	$\sigma_{w,Ed}$ [MPa]	ε_{Pl} [%]	$\sigma_{\perp}$ [MPa]	$\tau_{\perp}$ [MPa]	$\tau_{\parallel}$ [MPa]	Ut [%]	Ut_c [%]	Detailing	Status
Operation 14a	Operation 24	S 355	◢ 4.0	89	LE1	306.7	0.0	-306.4	6.4	-5.1	86.8	59.2	OK	OK
Operation 18a	Operation 21	S 355	◢ 4.0	89	LE1	293.1	0.0	-146.3	-146.4	8.5	67.3	57.2	OK	OK
Operation 18a	Operation 24	S 355	◢ 5.0	151	LE1	433.4	3.8	-108.2	-232.2	69.4	99.5	98.8	OK	OK
SP14	Operation 6b	S 355	-	10	-	-	-	-	-	-	-	-	OK	OK
SP14	Operation 6b	S 355	-	10	-	-	-	-	-	-	-	-	OK	OK
SP14	Operation 31	S 355	-	130	-	-	-	-	-	-	-	-	OK	OK
SP14	Operation 24	S 355	-	33	-	-	-	-	-	-	-	-	OK	OK
SP14	Operation 21	S 355	-	33	-	-	-	-	-	-	-	-	OK	OK
SP14	Operation 14b	S 355	-	10	-	-	-	-	-	-	-	-	OK	OK
SP14	Operation 14b	S 355	-	10	-	-	-	-	-	-	-	-	OK	OK
SP14	Operation 10b	S 355	-	10	-	-	-	-	-	-	-	-	OK	OK
SP14	Operation 10b	S 355	-	10	-	-	-	-	-	-	-	-	OK	OK
SP14	Operation 18b	S 355	-	10	-	-	-	-	-	-	-	-	OK	OK
SP14	Operation 18b	S 355	-	10	-	-	-	-	-	-	-	-	OK	OK
SP14	SP13	S 355	-	58	-	-	-	-	-	-	-	-	OK	OK
SP14	SP13	S 355	-	50	-	-	-	-	-	-	-	-	OK	OK
SP14	SP13	S 355	-	58	-	-	-	-	-	-	-	-	OK	OK
SP14	SP13	S 355	-	130	-	-	-	-	-	-	-	-	OK	OK
SP14	SP13	S 355	-	58	-	-	-	-	-	-	-	-	OK	OK
SP14	SP13	S 355	-	50	-	-	-	-	-	-	-	-	OK	OK
SP14	SP13	S 355	-	58	-	-	-	-	-	-	-	-	OK	OK
SP14	SP13	S 355	-	130	-	-	-	-	-	-	-	-	OK	OK
SP13	SP14	S 355	-	63	-	-	-	-	-	-	-	-	OK	OK
SP13	SP14	S 355	-	117	-	-	-	-	-	-	-	-	OK	OK
SP13	SP14	S 355	-	63	-	-	-	-	-	-	-	-	OK	OK
SP13	SP14	S 355	-	36	-	-	-	-	-	-	-	-	OK	OK
SP13	SP14	S 355	-	63	-	-	-	-	-	-	-	-	OK	OK
SP13	SP14	S 355	-	117	-	-	-	-	-	-	-	-	OK	OK
SP13	SP14	S 355	-	63	-	-	-	-	-	-	-	-	OK	OK
SP13	SP14	S 355	-	36	-	-	-	-	-	-	-	-	OK	OK
Operation 4b	Operation 5	S 355	◢ 4.0 L	119	LE1	427.3	0.2	-171.2	-41.5	222.2	98.1	85.8	OK	OK
		S 355	◢ 4.0 L	119	LE1	428.2	0.8	199.9	-71.7	206.6	98.3	88.6	OK	OK

Item	Edge	Material	T_w [mm]	L [mm]	Loads	$\sigma_{w,Ed}$ [MPa]	ε_{Pl} [%]	$\sigma_\perp$ [MPa]	$\tau_\perp$ [MPa]	$\tau_{\parallel}$ [MPa]	Ut [%]	Ut_c [%]	Detailing	Status
Operation 4b	Operation 5	S 355	◢ 4.0 L	119	LE1	204.2	0.0	-8.2	-112.0	-36.5	46.9	34.5	OK	OK
		S 355	◢ 4.0 L	119	LE1	252.5	0.0	-13.9	15.6	144.7	58.0	27.4	OK	OK
Operation 16	Operation 9	S 355	◢ 4.0 L	119	LE1	47.5	0.0	33.0	17.5	9.1	10.9	9.1	OK	OK
		S 355	◢ 4.0 L	119	LE1	31.8	0.0	-4.6	-6.6	-16.9	7.3	7.3	OK	OK
Operation 20b	Operation 9	S 355	◢ 4.0 L	119	LE1	342.5	0.0	-52.7	-195.3	4.0	78.6	58.8	OK	OK
		S 355	◢ 4.0 L	119	LE1	222.0	0.0	12.6	-39.6	-121.7	51.0	31.1	OK	OK
Operation 20b	Operation 9	S 355	◢ 4.0 L	119	LE1	427.4	0.3	-130.5	-78.6	-221.4	98.1	89.2	OK	OK
		S 355	◢ 4.0 L	119	LE1	428.7	1.0	62.1	-119.3	-213.8	98.4	98.0	OK	OK
Operation 44	Member 3	S 235	◢ 5.0	487	LE1	352.9	0.1	-153.8	167.9	73.7	98.0	90.0	OK	OK
Operation 45	Member 5	S 235	◢ 5.0	487	LE1	353.4	0.4	-165.1	178.1	-28.7	98.2	91.5	OK	OK
Operation 46	Member 4	S 235	◢ 5.0	487	LE1	354.1	0.9	-163.9	181.0	8.5	98.3	94.7	OK	OK
Operation 47	Member 6	S 235	◢ 5.0	487	LE1	352.9	0.1	-156.0	167.2	-73.8	98.0	96.4	OK	OK

Design data

Material	f_u [MPa]	β_w [-]	$\sigma_{w,Rd}$ [MPa]	0.9 σ [MPa]
S 355	490.0	0.90	435.6	352.8
S 235	360.0	0.80	360.0	259.2

Symbol explanation

T_w	Throat thickness a
L	Length
$\sigma_{w,Ed}$	Equivalent stress
ε_{Pl}	Strain
$\sigma_\perp$	Perpendicular stress
$\tau_\perp$	Shear stress perpendicular to weld axis
$\tau_{\parallel}$	Shear stress parallel to weld axis
Ut	Utilization
Ut_c	Weld capacity estimation
◢	Fillet weld
f_u	Ultimate strength of weld
β_w	Correlation factor EN 1993-1-8 – Tab. 4.1
$\sigma_{w,Rd}$	Equivalent stress resistance
0.9 σ	Perpendicular stress resistance: 0.9*fu/γM2

Detailed result for EP7 / Member 7-w 1

Weld resistance check (EN 1993-1-8 – Cl. 4.5.3.2)

$$\sigma_{w,Rd} = f_u/(\beta_w \gamma_{M2}) = 435.6 \text{ MPa} \geq \sigma_{w,Ed} = [\sigma_\perp^2 + 3(\tau_\perp^2 + \tau_\parallel^2)]^{0.5} = 434.8 \text{ MPa}$$

$$\sigma_{\perp,Rd} = 0.9\, f_u \,/\, \gamma_{M2} = 352.8 \text{ MPa} \geq |\sigma_\perp| = 216.1 \text{ MPa}$$

where:

$f_u = 490.0$ MPa – Ultimate strength

$\beta_w = 0.90$ – Correlation factor EN 1993-1-8 – Tab. 4.1

$\gamma_{M2} = 1.25$ – Safety factor

Stress utilization

$U_t = \max(\frac{\sigma_{w,Ed}}{\sigma_{w,Rd}} ; \frac{|\sigma_\perp|}{\sigma_{\perp,Rd}}) =$ 1.00 ≤ 1.0

Where:

$\sigma_{w,Ed} =$ 434.8 MPa – Maximum normal stress transverse to the axis of the weld

$\sigma_{w,Rd} =$ 435.6 MPa – Equivalent stress resistance

$\sigma_\perp =$ -216.1 MPa – Normal stress perpendicular to the throat

$\sigma_{\perp,Rd} =$ 352.8 MPa – Perpendicular stress resistance

Buckling

Loads	Shape	Factor [-]
LE1	1	6.93
	2	9.19
	3	9.50
	4	11.74
	5	12.84
	6	14.68

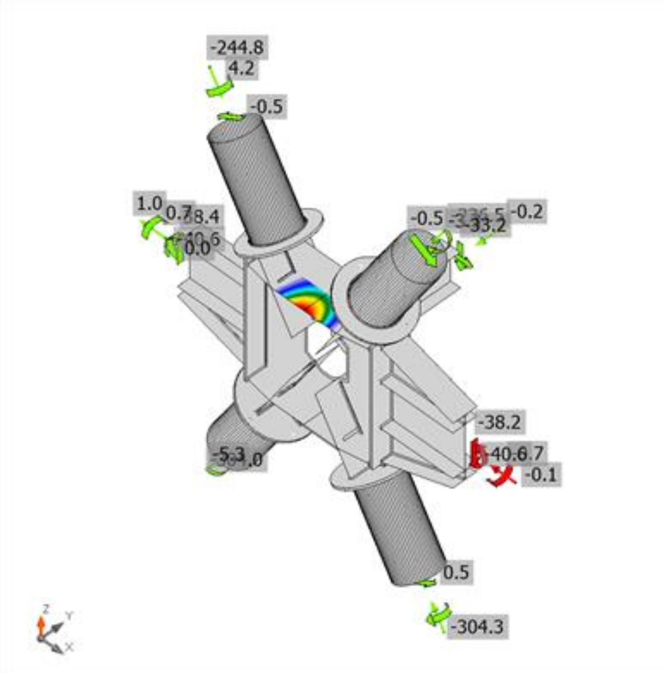

First buckling mode shape, LE1

Cost estimation

Steel

Steel grade	Total weight [kg]	Unit cost [€/kg]	Cost [€]
S 355	159.60	2.00	319.21

Bolts

Bolt assembly	Total weight [kg]	Unit cost [€/kg]	Cost [€]
M12 8.8	1.86	5.00	9.31
M14 8.8	0.91	5.00	4.55
M16 8.8	1.43	5.00	7.13

Welds

Weld type	Throat thickness [mm]	Leg size [mm]	Plate thickness [mm]	Total weight [kg]	Unit cost [€/kg]	Cost [€]
Double fillet	7.5	10.6	-	0.31	40.00	12.36
Double fillet	5.0	7.1	-	1.72	40.00	68.94
Double fillet	4.0	5.7	-	1.75	40.00	69.80
Double fillet	5.0	7.1	-	0.17	40.00	6.78
Double fillet	7.0	9.9	-	0.08	40.00	3.31
Double fillet	6.0	8.5	-	0.10	40.00	4.11
Double fillet	5.5	7.8	-	0.73	40.00	29.03
Bevel	-	-	8.0	1.88	50.00	93.99
Bevel	-	-	10.0	1.13	50.00	56.61

Hole drilling

Bolt assembly cost [€]	Percentage of bolt assembly cost [%]	Cost [€]
20.99	30.0	6.30

Cost summary

Cost estimation summary	Cost [€]
Total estimated cost	691.44

Bill of Material

Manufacturing Operations

Name	Plates [mm]	Shape	Nr.	Welds Throat thickness [mm]	Length [mm]	Bolts	Nr.
Operation 5	P8.0x10.0-120.0 (S 355)		1				
Operation 6	P8.0x249.0-0.0 (S 355)	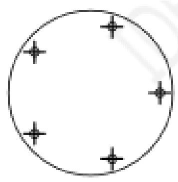	1	Double fillet: 7.5	175.0	M12 8.8	5
	P8.0x263.0-175.0 (S 355)	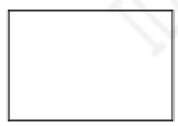	1				

Operation 9	P8.0x10.0-120.0 (S 355)		1				
Operation 10	P8.0x249.0-0.0 (S 355)	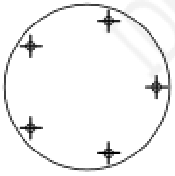	1	Double fillet: 7.5	175.0	M12 8.8	5
	P8.0x263.0-175.0 (S 355)	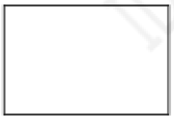	1				
Operation 13	P8.0x10.0-120.0 (S 355)		1				
Operation 14	P10.0x249.0-0.0 (S 355)	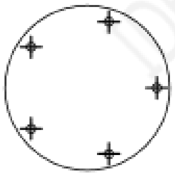	1	Double fillet: 5.0	175.0	M12 8.8	5

Name	Plates [mm]	Shape	Nr.	Welds Throat thickness [mm]	Length [mm]	Bolts	Nr.
	P8.0x263.0-175.0 (S 355)	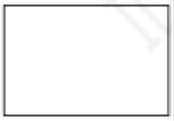	1				
Operation 17	P8.0x10.0-120.0 (S 355)		1				
Operation 18	P8.0x249.0-0.0 (S 355)	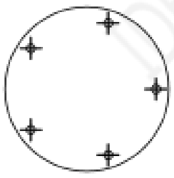	1	Double fillet: 5.0	175.0	M12 8.8	5

	P8.0x263.0-175.0 (S 355)	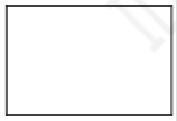	1				
Operation 21	P8.0x396.1-650.8 (S 355)	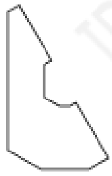	1				
Operation 24	P8.0x396.1-650.8 (S 355)	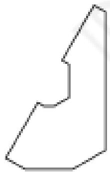	1				
Operation 28	P8.0x344.0-264.6 (S 355)	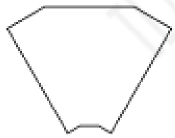	1				
Operation 31	P8.0x396.1-650.8 (S 355)	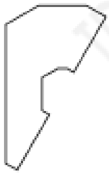	1				
Name	**Plates [mm]**		**Nr.**	Welds Throat thickness [mm]	Length [mm]	Bolts	Nr.
Operation 34	**P8.0x397.0-651.4 (S 355)**	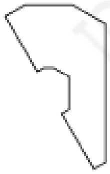	**1**				
Operation 37	**P8.0x343.1-264.6 (S 355)**	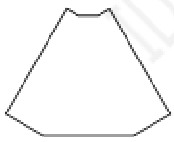	**1**				
Operation 44	**P10.0x250.0-0.0 (S 355)**	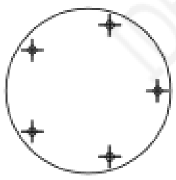	**1**	Fillet: 5.0	486.8	M12 8.8	5

Operation 45	**P8.0x250.0-0.0 (S 355)**	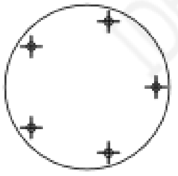	**1**	Fillet: 5.0	486.8	M12 8.8	5
Operation 46	**P8.0x250.0-0.0 (S 355)**	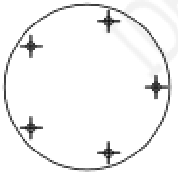	**1**	Fillet: 5.0	486.8	M12 8.8	5
Operation 47	**P10.0x250.0-0.0 (S 355)**	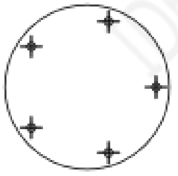	**1**	Fillet: 5.0	486.8	M12 8.8	5
Operation 16	**P8.0x10.0-120.0 (S 355)**		**1**				
Operation 20	**P10.0x141.0-460.0 (S 355)**	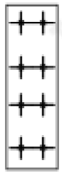	**1**	Double fillet: 4.0	141.0	M14 8.8	8

Name	Plates [mm]	Shape	Nr.	Welds Throat thickness [mm]	Length [mm]	Bolts	Nr.
Operation 34	P8.0x397.0-651.4 (S 355)	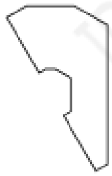	1				
Operation 37	P8.0x343.1-264.6 (S 355)	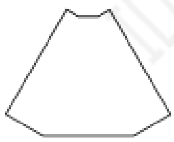	1				
Operation 44	P10.0x250.0-0.0 (S 355)	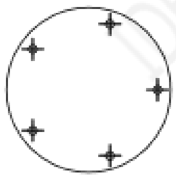	1	Fillet: 5.0	486.8	M12 8.8	5

Operation 45	P8.0x250.0-0.0 (S 355)	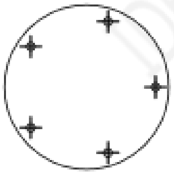	1	Fillet: 5.0	486.8	M12 8.8	5
Operation 46	P8.0x250.0-0.0 (S 355)	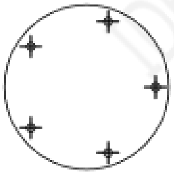	1	Fillet: 5.0	486.8	M12 8.8	5
Operation 47	P10.0x250.0-0.0 (S 355)	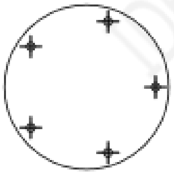	1	Fillet: 5.0	486.8	M12 8.8	5
Operation 16	P8.0x10.0-120.0 (S 355)		1				
Operation 20	P10.0x141.0-460.0 (S 355)	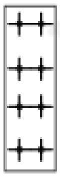	1	Double fillet: 4.0	141.0	M14 8.8	8
Name	**Plates [mm]**		**Nr.**	**Welds** **Throat thickness [mm]**	**Length [mm]**	**Bolts**	**Nr.**
	P8.0x225.0-175.0 (S 355)	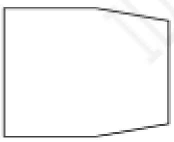	**1**				
Operation 25	**P6.0x141.0-460.0 (S 355)**	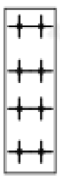	**1**	**Double fillet: 5.0** **Double fillet: 4.0**	**182.0** **172.0**	**M14 8.8**	**8**

Operation 8	**P8.0x10.0-120.0 (S 355)**		**1**				
Operation 12	**P10.0x141.0-460.0 (S 355)**	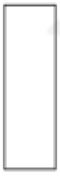	**1**	**Double fillet: 5.0**	**141.0**		
	P8.0x225.0-175.0 (S 355)	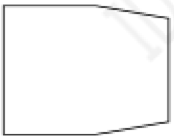	**1**				
Operation 4	**P10.0x141.0-460.0 (S 355)**	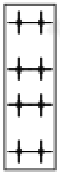	**1**	**Double fillet: 4.0**	**141.0**	**M16 8.8**	**8**
	P8.0x225.0-175.0 (S 355)	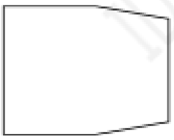	**1**				
Operation 3	**P10.0x141.0-460.0 (S 355)**	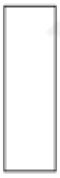	**1**	**Double fillet: 4.0**	**141.0**		

Name	Plates [mm]	Shape	Nr.	Welds Throat thickness [mm]	Length [mm]	Bolts	Nr.
	P8.0x225.0-175.0 (S 355)	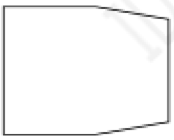	1				
Operation 25	P6.0x141.0-460.0 (S 355)	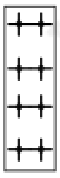	1	Double fillet: 5.0 Double fillet: 4.0	182.0 172.0	M14 8.8	8

Name	Plates [mm]	Shape	Nr.	Welds Throat thickness [mm]	Length [mm]	Bolts	Nr.
Operation 8	P8.0x10.0-120.0 (S 355)		1				
Operation 12	P10.0x141.0-460.0 (S 355)	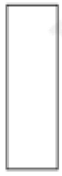	1	Double fillet: 5.0	141.0		
	P8.0x225.0-175.0 (S 355)	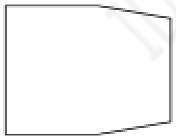	1				
Operation 4	P10.0x141.0-460.0 (S 355)	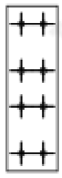	1	Double fillet: 4.0	141.0	M16 8.8	8
	P8.0x225.0-175.0 (S 355)	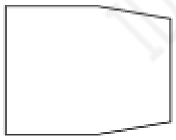	1				
Operation 3	P10.0x141.0-460.0 (S 355)	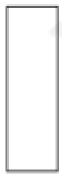	1	Double fillet: 4.0	141.0		
	P8.0x225.0-175.0 (S 355)	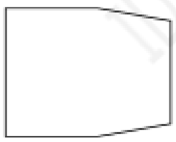	1				
Operation 2	P8.0x141.0-460.0 (S 355)	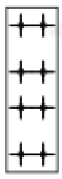	1	Double fillet: 6.0 Double fillet: 4.0	182.0 172.0	M16 8.8	8

SP13	P8.0x150.0-190.0 (S 355)	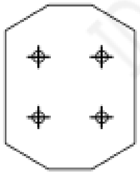	1			M12 8.8	4
EP7	P8.0x123.0-113.0 (S 355)	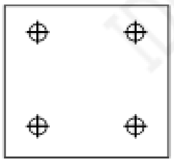	1	Double fillet: 5.0	113.0	M12 8.8	4
WID1	P5.3x120.0-270.0 (S 355)	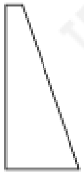	2	Double fillet: 5.5	1528.1		
	P8.0x90.0-284.1 (S 355)	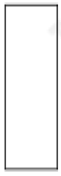	2				
WID2	P5.3x120.0-270.0 (S 355)	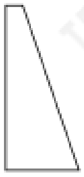	1	Double fillet: 5.0	764.1		
	P8.0x90.0-284.1 (S 355)	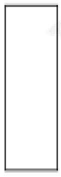	1				

Name	Plates [mm]	Shape	Nr.	Welds Throat thickness [mm]	Length [mm]	Bolts	Nr.
SP14	P175.0x161.2-200.0 (S 355)	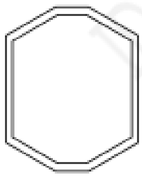	1				
NVOL1							

Welds

Type	Material	Throat thickness [mm]	Leg size [mm]	Length [mm]
Double fillet	S 355	7.5	10.6	350.0
Butt	Steel4	-	-	360.0
Butt	S 355	-	-	120.0
Double fillet	S 355	5.0	7.1	3773.9
Double fillet	S 355	4.0	5.7	2126.9
Double fillet	Steel4	4.0	5.7	4413.6
Butt	Steel4	-	-	5639.9
Butt	S 355	-	-	1837.4
Double fillet	S 355	7.0	9.9	107.5
Fillet	S 235	5.0	7.1	1947.0
Double fillet	S 355	6.0	8.5	182.0
Double fillet	S 355	5.5	7.8	1528.1
Fillet	S 355	4.0	5.7	812.6
Fillet	S 355	5.0	7.1	151.5
Butt	S 355	-	-	558.0

Bolts

Name	Grip length [mm]	Count
M12 8.8	18	5
M12 8.8	16	14
M12 8.8	20	5
M14 8.8	16	8
M16 8.8	18	8

8.7 Appendix G: ECI Cost Calculations and Detailing

https://www.ecocostsvalue.com/ecocosts/eco-costs-concept/																
calculated			Steel Beam/ Column					Steel Pipe (CHS)					Steel Rod (Bracing)				
1.30E+00	inflation		Production Stage	End of life stage				Production Sta	End of life stage				Productior	End of life stage			
Impact Category	Unit	Cost (€)	A1-A3	C1	C2	C3	C4	A1-A3	C1	C2	C3	C4	A1-A3	C1	C2	C3	C4
GWP total	kg CO2e	1.33E-01	7.19E-01	3.30E-03	8.27E-03	2.21E-02	2.64E-04	5.61E-01	3.30E-03	8.34E-03	2.21E-02	2.64E-04	1.10E+00	2.06E-02	6.84E-03	1.13E-02	2.50E-04
GWP fossil	kg CO2e	1.33E-01	7.12E-01	3.30E-03	8.26E-03	2.34E-02	2.63E-04	5.38E-01	3.30E-03	8.33E-03	2.34E-02	2.63E-04	1.10E+00	2.06E-02	6.84E-03	1.11E-02	2.50E-04
GWP Biogenic	kg CO2e	1.33E-01	6.01E-03	9.17E-07	4.44E-06	-1.34E-03	5.22E-07	1.87E-02	9.17E-07	4.45E-06	-1.34E-03	5.22E-07	3.83E-03	1.00E-05	0.00E+00	1.20E-04	0.00E+00
GWP LULUC	kg CO2e	1.33E-01	8.09E-04	2.79E-07	2.96E-06	2.66E-05	7.82E-08	4.17E-03	2.79E-07	2.96E-06	2.66E-05	7.82E-08	3.70E-04	0.00E+00	0.00E+00	1.00E-05	0.00E+00
Ozone depletion pot	kg CFC11	3.00E+01	8.68E-08	7.12E-10	1.89E-09	3.37E-09	1.08E-10	7.79E-08	7.12E-10	1.89E-09	3.37E-09	1.08E-10	6.28E-08	4.60E-09	1.64E-09	1.90E-09	5.24E-11
Acidification pot	mol H+e	7.65E+00	3.81E-03	3.45E-05	4.20E-05	2.84E-04	2.50E-06	1.33E-03	3.45E-05	3.40E-05	2.84E-04	2.50E-06	4.79E-03	2.20E-04	3.00E-05	1.00E-05	0.00E+00
EP-freshwater	kg Pe	1.65E+01	4.08E-05	1.33E-08	6.97E-08	1.62E-06	3.18E-09	9.89E-06	1.33E-08	6.97E-08	1.62E-06	3.18E-09	8.13E-08	1.45E-08	3.53E-09	3.73E-07	8.96E-10
EP-marine	kg Ne	2.00E+01	8.16E-04	1.52E-05	1.43E-05	6.27E-05	8.61E-07	2.85E-04	1.52E-05	1.01E-05	6.27E-05	8.61E-07	1.10E-03	1.00E-04	1.00E-05	4.00E-05	0.00E+00
EP-terrestrial	mol Ne	3.11E+01	9.38E-03	1.67E-04	1.58E-04	7.28E-04	9.48E-06	3.17E-03	1.67E-04	1.12E-04	7.28E-04	9.48E-06	1.23E-02	1.09E-03	1.30E-04	4.40E-04	1.00E-05
POCP ("smog")	kg NMVOC	1.55E+00	3.26E-03	4.59E-05	4.50E-05	1.99E-04	2.75E-06	1.24E-03	4.59E-05	3.42E-05	1.99E-04	2.75E-06	3.94E-03	3.00E-04	3.00E-05	1.20E-04	0.00E+00
ADP- minerals & metals	kg Sbe	2.13E+00	1.33E-06	5.03E-09	2.25E-07	1.30E-06	2.41E-09	9.84E-07	5.03E-09	2.25E-07	1.30E-06	2.41E-09	4.57E-06	1.06E-09	3.00E-10	5.86E-10	1.22E-11
ADP- fossil resources	MJ	1.69E-02	1.16E+01	4.54E-02	1.26E-01	3.25E-01	7.36E-03	1.12E+01	4.54E-02	1.26E-01	3.25E-01	7.36E-03	1.42E+01	2.84E-01	9.78E-02	1.80E-01	3.36E-03
Water use	m3e depr.	6.50E-02	1.29E+00	8.46E-05	4.05E-04	4.61E-03	3.40E-04	1.69E-01	8.46E-05	4.05E-04	4.61E-03	3.40E-04	1.22E-01	7.00E-05	-2.00E-05	8.20E-04	0.00E+00

IPE/HE/UPE			CHS tube			Steel Rod Bracing		
Production	EOL	Demountable	Productior	EOL	Demountat	Production	EOL	Demountable
9.56E-02	4.51E-03	9.56E-02	7.46E-02	4.52E-03	7.46E-02	1.46E-01	5.17E-03	1.46E-01
9.47E-02	4.68E-03	9.47E-02	7.16E-02	4.69E-03	7.16E-02	1.46E-01	5.16E-03	1.46E-01
7.99E-04	-1.77E-04	7.99E-04	2.49E-03	-1.77E-04	2.49E-03	5.09E-04	1.73E-05	5.09E-04
1.08E-04	3.98E-06	1.08E-04	5.55E-04	3.98E-06	5.55E-04	4.92E-05	1.33E-06	4.92E-05
2.60E-06	1.82E-07	2.60E-06	2.34E-06	1.82E-07	2.34E-06	1.88E-06	2.46E-07	1.88E-06
2.91E-02	2.78E-03	2.91E-02	1.02E-02	2.72E-03	1.02E-02	3.66E-02	1.99E-03	3.66E-02
6.72E-04	2.81E-05	6.72E-04	1.63E-04	2.81E-05	1.63E-04	1.34E-06	6.45E-06	1.34E-06
1.63E-02	1.86E-03	1.63E-02	5.70E-03	1.78E-03	5.70E-03	2.20E-02	3.00E-03	2.20E-02
2.91E-01	3.30E-02	2.91E-01	9.84E-02	3.16E-02	9.84E-02	3.82E-01	5.19E-02	3.82E-01
5.04E-03	4.53E-04	5.04E-03	1.92E-03	4.36E-04	1.92E-03	6.10E-03	6.96E-04	6.10E-03
2.84E-06	3.27E-06	2.84E-06	2.10E-06	3.27E-06	2.10E-06	9.74E-06	4.17E-09	9.74E-06
1.96E-01	8.51E-03	1.96E-01	1.89E-01	8.51E-03	1.89E-01	2.39E-01	9.56E-03	2.39E-01
8.39E-02	3.54E-04	8.39E-02	1.10E-02	3.54E-04	1.10E-02	7.90E-03	5.66E-05	7.90E-03
Total and de	1.57E+00	1.48E+00	Total ECI	1.07E+00	9.88E-01	Total ECI	2.12E+00	2.01E+00

<u>5 meter Column Spacing:</u>

5 m spacing

Diagrid 60 Final Design						Diagrid 65						Diagrid 70					
Production Stage			End of Life Stage			Production Stage			End of Life Stage			Production Stage			End of Life Stage		
Beam	Braces (Diagrid)	Column	Beam	Braces (Diagrid)	Column	Beam	Braces (Diagrid)	Column	Beam	Braces (Diagrid	Column	Beam	Braces (Diagrid)	Column	Beam	Braces (Diagrid	Column
A1-A3	A1-A3	A1-A3	C1-C4	C1-C4	C1-C4	A1-A3	A1-A3	A1-A3	C1-C4	C1-C4	C1-C4	A1-A3	A1-A3	A1-A3	C1-C4	C1-C4	C1-C4
5.91E+03	1.41E+03	3.46E+03	2.79E+02	8.54E+01	1.63E+02	6.21E+03	1.48E+03	3.46E+03	2.93E+02	8.94E+01	1.63E+02	5.60E+03	2.97E+03	3.46E+03	2.64E+02	1.80E+02	1.63E+02
5.85E+03	1.35E+03	3.42E+03	2.89E+02	8.87E+01	1.69E+02	6.15E+03	1.41E+03	3.42E+03	3.04E+02	9.28E+01	1.69E+02	5.55E+03	2.85E+03	3.42E+03	2.74E+02	1.87E+02	1.69E+02
4.94E+01	4.70E+01	2.89E+01	-1.10E+01	-3.35E+00	-6.42E+00	5.19E+01	4.92E+01	2.89E+01	########	-3.51E+00	########	4.68E+01	9.91E+01	2.89E+01	-1.04E+01	-7.07E+00	-6.42E+00
6.65E+00	1.05E+01	3.89E+00	2.46E-01	7.52E-02	1.44E-01	6.98E+00	1.10E+01	3.89E+00	2.58E-01	7.87E-02	1.44E-01	6.30E+00	2.21E+01	3.89E+00	2.33E-01	1.59E-01	1.44E-01
1.61E-01	4.41E-02	9.42E-02	1.13E-02	3.45E-03	6.60E-03	1.69E-01	4.62E-02	9.42E-02	1.18E-02	3.61E-03	6.60E-03	1.53E-01	9.31E-02	9.42E-02	1.07E-02	7.27E-03	6.60E-03
1.80E+03	1.92E+02	1.05E+03	1.72E+02	5.13E+01	1.00E+02	1.89E+03	2.01E+02	1.05E+03	1.80E+02	5.37E+01	1.00E+02	1.71E+03	4.05E+02	1.05E+03	1.63E+02	1.08E+02	1.00E+02
4.15E+01	3.08E+00	2.43E+01	1.74E+00	5.31E-01	1.02E+00	4.36E+01	3.22E+00	2.43E+01	1.82E+00	5.55E-01	1.02E+00	3.93E+01	6.49E+00	2.43E+01	1.65E+00	1.12E+00	1.02E+00
1.01E+03	1.08E+02	5.90E+02	1.15E+02	3.36E+01	6.73E+01	1.06E+03	1.13E+02	5.90E+02	1.21E+02	3.51E+01	6.73E+01	9.56E+02	2.27E+02	5.90E+02	1.09E+02	7.08E+01	6.73E+01
1.80E+04	1.86E+03	1.05E+04	2.04E+03	5.96E+02	1.19E+03	1.89E+04	1.95E+03	1.05E+04	2.14E+03	6.24E+02	1.19E+03	1.71E+04	3.92E+03	1.05E+04	1.93E+03	1.26E+03	1.19E+03
3.12E+02	3.62E+01	1.82E+02	2.80E+01	8.24E+00	1.64E+01	3.27E+02	3.79E+01	1.82E+02	2.94E+01	8.62E+00	1.64E+01	2.96E+02	7.64E+01	1.82E+02	2.65E+01	1.74E+01	1.64E+01
1.75E-01	3.96E-02	1.03E-01	2.02E-01	6.17E-02	1.18E-01	1.84E-01	4.15E-02	1.03E-01	2.12E-01	6.46E-02	1.18E-01	1.66E-01	8.36E-02	1.03E-01	1.91E-01	1.30E-01	1.18E-01
1.21E+04	3.58E+03	7.09E+03	5.26E+02	1.61E+02	3.08E+02	1.27E+04	3.74E+03	7.09E+03	5.53E+02	1.68E+02	3.08E+02	1.15E+04	7.54E+03	7.09E+03	4.99E+02	3.39E+02	3.08E+02
5.18E+03	2.08E+02	3.03E+03	2.18E+01	6.68E+00	1.28E+01	5.44E+03	2.17E+02	3.03E+03	2.30E+01	6.99E+00	1.28E+01	4.91E+03	4.38E+02	3.03E+03	2.07E+01	1.41E+01	1.28E+01
9.16E+04	1.87E+04	5.36E+04	5.41E+03	1.63E+03	3.17E+03	9.63E+04	1.95E+04	5.36E+04	5.69E+03	1.70E+03	3.17E+03	8.69E+04	3.94E+04	5.36E+04	5.13E+03	3.43E+03	3.17E+03
	1.64E+05		Tot eol	1.02E+04			1.69E+05		Tot eol	1.06E+04			1.80E+05		Tot eol	1.17E+04	
Total ECI	1.74E+05	Demountable cos	1.64E+05	-1.02E+04		Total ECI	1.80E+05	Demount cos	1.69E+05	-1.06E+04		Total ECI	1.92E+05	Demount cos	1.80E+05	-1.17E+04	

Diagrid 75						G+Diagrid 60						Conventional (Conservative) (2.5 m secondary spacing)					
Production Stage			End of Life Stage			Production Stage			End of Life Stage			Production Stage			End of Life Stage		
Beam	Braces (Diagrid	Column	Beam	Braces (Diagrid	Column	Beam	Braces (Diagrid)	Column	Beam	Braces (Diagrid	Column	Beam	Braces	Column	Beam	Braces	Column
A1-A3	A1-A3	A1-A3	C1-C4	C1-C4	C1-C4	A1-A3	A1-A3	A1-A3	C1-C4	C1-C4	C1-C4	A1-A3	A1-A3	A1-A3	C1-C4	C1-C4	C1-C4
7.59E+03	1.91E+03	3.46E+03	3.58E+02	1.16E+02	1.63E+02	5.90E+03	1.08E+03	4.08E+03	2.79E+02	6.54E+01	1.93E+02	6.52E+03	4.28E+01	5.67E+03	3.08E+02	1.51E+00	2.67E+02
7.52E+03	1.83E+03	3.42E+03	3.72E+02	1.20E+02	1.69E+02	5.85E+03	1.04E+03	4.04E+03	2.89E+02	6.79E+01	2.00E+02	6.46E+03	4.27E+01	5.61E+03	3.19E+02	1.51E+00	2.78E+02
6.35E+01	6.38E+01	2.89E+01	-1.41E+01	-4.55E+00	-6.42E+00	4.93E+01	3.60E+01	3.41E+01	-1.10E+01	-2.57E+00	-7.57E+00	5.45E+01	1.49E-01	4.74E+01	-1.21E+01	5.06E-03	-1.05E+01
8.54E+00	1.42E+01	3.89E+00	3.16E-01	1.02E-01	1.44E-01	6.64E+00	8.02E+00	4.59E+00	2.46E-01	5.76E-02	1.70E-01	7.33E+00	1.44E-02	6.38E+00	2.71E-01	3.89E-04	2.36E-01
2.07E-01	5.99E-02	9.42E-02	1.45E-02	4.68E-03	6.60E-03	1.61E-01	3.38E-02	1.11E-01	1.13E-02	2.64E-03	7.78E-03	1.78E-01	5.52E-04	1.54E-01	1.24E-02	7.20E-05	1.08E-02
2.31E+03	2.61E+02	1.05E+03	2.20E+02	6.96E+01	1.00E+02	1.80E+03	1.47E+02	1.24E+03	1.71E+02	3.93E+01	1.18E+02	1.99E+03	1.07E+01	1.73E+03	1.89E+02	5.82E-01	1.65E+02
5.33E+01	4.17E+00	2.43E+01	2.23E+00	7.20E-01	1.02E+00	4.15E+01	2.36E+00	2.87E+01	1.73E+00	4.06E-01	1.20E+00	4.58E+01	3.92E-04	3.98E+01	1.91E+00	1.89E-03	1.66E+00
1.30E+03	1.46E+02	5.90E+02	1.48E+02	4.56E+01	6.73E+01	1.01E+03	8.25E+01	6.96E+02	1.15E+02	2.57E+01	7.94E+01	1.11E+03	6.44E+00	9.67E+02	1.27E+02	8.78E-01	1.10E+02
2.31E+04	2.52E+03	1.05E+04	2.62E+03	8.09E+02	1.19E+03	1.80E+04	1.42E+03	1.24E+04	2.04E+03	4.57E+02	1.41E+03	1.99E+04	1.12E+02	1.73E+04	2.25E+03	1.52E+01	1.96E+03
4.00E+02	4.92E+01	1.82E+02	3.59E+01	1.12E+01	1.64E+01	3.11E+02	2.78E+01	2.15E+02	2.79E+01	6.31E+00	1.93E+01	3.44E+02	1.78E+00	2.99E+02	3.09E+01	2.04E-01	2.68E+01
2.25E-01	5.38E-02	1.03E-01	2.59E-01	8.38E-02	1.18E-01	1.75E-01	3.04E-02	1.21E-01	2.02E-01	4.73E-02	1.39E-01	1.93E-01	2.85E-03	1.68E-01	2.23E-01	1.22E-06	1.94E-01
1.56E+04	4.85E+03	7.09E+03	6.76E+02	2.18E+02	3.08E+02	1.21E+04	2.74E+03	8.36E+03	5.26E+02	1.23E+02	3.63E+02	1.34E+04	7.01E+01	1.16E+04	5.80E+02	2.80E+00	5.05E+02
6.66E+03	2.82E+02	3.03E+03	2.81E+01	9.07E+00	1.28E+01	5.18E+03	1.59E+02	3.58E+03	2.18E+01	5.12E+00	1.51E+01	5.72E+03	2.31E+00	4.97E+03	2.41E+01	1.66E-02	2.10E+01
1.18E+05	2.53E+04	5.36E+04	6.95E+03	2.21E+03	3.17E+03	9.15E+04	1.43E+04	6.33E+04	5.41E+03	1.25E+03	3.74E+03	1.01E+05	5.89E+02	8.79E+04	5.97E+03	3.33E+01	5.19E+03
	1.97E+05		Tot eol	1.23E+04			1.69E+05		Tot eol	1.04E+04			1.90E+05		Tot eol	1.12E+04	
Total ECI	2.09E+05	Demount cos	1.97E+05	-1.23E+04		Total ECI	1.80E+05	Demount cos	1.69E+05	-1.04E+04		Total ECI	2.01E+05	Demount cos	1.90E+05	-1.12E+04	

X Braced Frame						V Braced Frame					
Production Stage			End of Life Stage			Production Stage			End of Life Stage		
Beam	Braces (Rod)	Column	Beam	Braces (Rod)	Column	Beam	Braces (Rod)	Column	Beam	Braces (Rod)	Column
A1-A3	A1-A3	A1-A3	C1-C4	C1-C4	C1-C4	A1-A3	A1-A3	A1-A3	C1-C4	C1-C4	C1-C4
6.52E+03	4.85E+01	5.58E+03	3.08E+02	1.72E+00	2.63E+02	6.52E+03	3.71E+01	5.58E+03	3.08E+02	1.31E+00	2.63E+02
6.46E+03	4.83E+01	5.52E+03	3.19E+02	1.71E+00	2.73E+02	6.46E+03	3.70E+01	5.52E+03	3.19E+02	1.31E+00	2.73E+02
5.45E+01	1.69E-01	4.66E+01	-1.21E+01	5.74E-03	-1.03E+01	5.45E+01	1.29E-01	4.66E+01	-1.21E+01	4.39E-03	-1.03E+01
7.34E+00	1.63E-02	6.27E+00	2.71E-01	4.41E-04	2.32E-01	7.34E+00	1.25E-02	6.27E+00	2.71E-01	3.38E-04	2.32E-01
1.78E-01	6.25E-04	1.52E-01	1.24E-02	8.15E-05	1.06E-02	1.78E-01	4.78E-04	1.52E-01	1.24E-02	6.24E-05	1.06E-02
1.99E+03	1.22E+01	1.70E+03	1.89E+02	6.60E-01	1.62E+02	1.99E+03	9.30E+00	1.70E+03	1.89E+02	5.05E-01	1.62E+02
4.58E+01	4.44E-04	3.92E+01	1.91E+00	2.14E-03	1.64E+00	4.58E+01	3.40E-04	3.92E+01	1.91E+00	1.64E-03	1.64E+00
1.11E+03	7.30E+00	9.52E+02	1.27E+02	9.95E-01	1.09E+02	1.11E+03	5.59E+00	9.52E+02	1.27E+02	7.62E-01	1.09E+02
1.99E+04	1.27E+02	1.70E+04	2.25E+03	1.72E+01	1.92E+03	1.99E+04	9.71E+01	1.70E+04	2.25E+03	1.32E+01	1.92E+03
3.44E+02	2.02E+00	2.94E+02	3.09E+01	2.31E-01	2.64E+01	3.44E+02	1.55E+00	2.94E+02	3.09E+01	1.77E-01	2.64E+01
1.93E-01	3.23E-03	1.65E-01	2.23E-01	1.38E-06	1.90E-01	1.93E-01	2.47E-03	1.65E-01	2.23E-01	1.06E-06	1.90E-01
1.34E+04	7.94E+01	1.14E+04	5.80E+02	3.17E+00	4.96E+02	1.34E+04	6.08E+01	1.14E+04	5.80E+02	2.43E+00	4.96E+02
5.72E+03	2.62E+00	4.89E+03	2.41E+01	1.88E-02	2.06E+01	5.72E+03	2.01E+00	4.89E+03	2.41E+01	1.44E-02	2.06E+01
1.01E+05	6.67E+02	8.65E+04	5.97E+03	3.77E+01	5.11E+03	1.01E+05	5.10E+02	8.65E+04	5.97E+03	2.89E+01	5.11E+03
	1.88E+05		Tot eol	1.11E+04			1.88E+05		Tot eol	1.11E+04	
Total ECI	1.99E+05	Demount cos	1.88E+05	-1.11E+04		Total ECI	1.99E+05	Demount c	1.88E+05	-1.11E+04	

6 meter Column Spacing:

	Diagrid 60					
	Production Stage			End of Life Stage		
	Beam	Braces (Diagrid)	Column	Beam	Braces (Diagrid)	Column
C4	A1-A3	A1-A3	A1-A3	C1-C4	C1-C4	C1-C4
2.50E-04	7.46E+03	1.41E+03	3.63E+03	3.52E+02	8.54E+01	1.71E+02
2.50E-04	7.39E+03	1.35E+03	3.60E+03	3.65E+02	8.87E+01	1.78E+02
########	6.24E+01	4.70E+01	3.04E+01	-1.38E+01	-3.35E+00	-6.74E+00
########	8.39E+00	1.05E+01	4.09E+00	3.10E-01	7.52E-02	1.51E-01
5.24E-11	2.03E-01	4.41E-02	9.89E-02	1.42E-02	3.45E-03	6.93E-03
########	2.27E+03	1.92E+02	1.11E+03	2.17E+02	5.13E+01	1.05E+02
8.96E-10	5.24E+01	3.08E+00	2.55E+01	2.19E+00	5.31E-01	1.07E+00
########	1.27E+03	1.08E+02	6.20E+02	1.45E+02	3.36E+01	7.07E+01
1.00E-05	2.27E+04	1.86E+03	1.11E+04	2.57E+03	5.96E+02	1.25E+03
########	3.93E+02	3.62E+01	1.92E+02	3.53E+01	8.24E+00	1.72E+01
1.22E-11	2.21E-01	3.96E-02	1.08E-01	2.55E-01	6.17E-02	1.24E-01
3.36E-03	1.53E+04	3.58E+03	7.45E+03	6.64E+02	1.61E+02	3.23E+02
########	6.54E+03	2.08E+02	3.19E+03	2.76E+01	6.68E+00	1.34E+01
total	1.16E+05	1.87E+04	5.63E+04	6.83E+03	1.63E+03	3.33E+03
total production		1.91E+05		Tot eol	1.18E+04	
	Total ECI	2.02E+05	Demountab	1.91E+05	-1.18E+04	

Diagrid 65					
Production Stage			End of Life Stage		
Beam	Braces (Diagrid)	Column	Beam	Braces (Diagrid)	Column
A1-A3	A1-A3	A1-A3	C1-C4	C1-C4	C1-C4
6.95E+03	1.61E+03	2.96E+03	3.28E+02	9.78E+01	1.40E+02
6.88E+03	1.55E+03	2.94E+03	3.41E+02	1.02E+02	1.45E+02
5.81E+01	5.38E+01	2.48E+01	-1.29E+01	-3.84E+00	-5.50E+00
7.82E+00	1.20E+01	3.34E+00	2.89E-01	8.60E-02	1.23E-01
1.89E-01	5.05E-02	8.07E-02	1.33E-02	3.94E-03	5.66E-03
2.12E+03	2.20E+02	9.04E+02	2.02E+02	5.87E+01	8.61E+01
4.88E+01	3.52E+00	2.08E+01	2.04E+00	6.07E-01	8.71E-01
1.19E+03	1.23E+02	5.06E+02	1.35E+02	3.84E+01	5.77E+01
2.12E+04	2.13E+03	9.03E+03	2.40E+03	6.83E+02	1.02E+03
3.67E+02	4.15E+01	1.56E+02	3.29E+01	9.43E+00	1.40E+01
2.06E-01	4.54E-02	8.79E-02	2.38E-01	7.07E-02	1.01E-01
1.43E+04	4.09E+03	6.08E+03	6.19E+02	1.84E+02	2.64E+02
6.10E+03	2.38E+02	2.60E+03	2.57E+01	7.65E+00	1.10E+01
1.08E+05	2.14E+04	4.60E+04	6.37E+03	1.86E+03	2.72E+03
	1.75E+05		Tot eol	1.09E+04	
Total ECI	1.86E+05	Demountable c	1.75E+05	-1.09E+04	

Diagrid 70					
Production Stage			End of Life Stage		
Beam	Braces (Diagrid)	Column	Beam	Braces (Diagr	Column
A1-A3	A1-A3	A1-A3	C1-C4	C1-C4	C1-C4
6.85E+03	1.72E+03	3.00E+03	3.23E+02	1.04E+02	1.42E+02
6.78E+03	1.65E+03	2.97E+03	3.36E+02	1.08E+02	1.47E+02
5.73E+01	5.73E+01	2.51E+01	-1.27E+01	-4.09E+00	-5.56E+00
7.71E+00	1.28E+01	3.37E+00	2.85E-01	9.16E-02	1.25E-01
1.87E-01	5.38E-02	8.17E-02	1.31E-02	4.20E-03	5.72E-03
2.09E+03	2.34E+02	9.14E+02	1.99E+02	6.25E+01	8.71E+01
4.81E+01	3.75E+00	2.11E+01	2.01E+00	6.47E-01	8.81E-01
1.17E+03	1.31E+02	5.12E+02	1.33E+02	4.09E+01	5.84E+01
2.09E+04	2.27E+03	9.13E+03	2.36E+03	7.27E+02	1.03E+03
3.61E+02	4.42E+01	1.58E+02	3.24E+01	1.00E+01	1.42E+01
2.03E-01	4.83E-02	8.89E-02	2.34E-01	7.52E-02	1.02E-01
1.40E+04	4.36E+03	6.15E+03	6.10E+02	1.96E+02	2.67E+02
6.01E+03	2.53E+02	2.63E+03	2.53E+01	8.14E+00	1.11E+01
1.06E+05	2.28E+04	4.65E+04	6.28E+03	1.98E+03	2.75E+03
	1.76E+05		Tot eol	1.10E+04	
Total ECI	1.87E+05	Demountable cost	1.76E+05	-1.10E+04	

Diagrid 75					
Production Stage			End of Life Stage		
Beam	Braces (Diagrid)	Column	Beam	Braces (Diagrid)	Column
A1-A3	A1-A3	A1-A3	C1-C4	C1-C4	C1-C4
6.77E+03	2.03E+03	3.02E+03	3.19E+02	1.23E+02	1.42E+02
6.70E+03	1.94E+03	2.99E+03	3.31E+02	1.28E+02	1.48E+02
5.66E+01	6.76E+01	2.52E+01	-1.26E+01	-4.82E+00	-5.60E+00
7.61E+00	1.51E+01	3.40E+00	2.82E-01	1.08E-01	1.26E-01
1.84E-01	6.35E-02	8.22E-02	1.29E-02	4.96E-03	5.76E-03
2.06E+03	2.77E+02	9.20E+02	1.96E+02	7.38E+01	8.77E+01
4.75E+01	4.42E+00	2.12E+01	1.99E+00	7.63E-01	8.87E-01
1.15E+03	1.55E+02	5.15E+02	1.32E+02	4.83E+01	5.88E+01
2.06E+04	2.68E+03	9.20E+03	2.33E+03	8.58E+02	1.04E+03
3.57E+02	5.21E+01	1.59E+02	3.20E+01	1.19E+01	1.43E+01
2.01E-01	5.70E-02	8.95E-02	2.31E-01	8.88E-02	1.03E-01
1.39E+04	5.14E+03	6.19E+03	6.02E+02	2.31E+02	2.69E+02
5.93E+03	2.99E+02	2.65E+03	2.50E+01	9.61E+00	1.12E+01
1.05E+05	2.69E+04	4.68E+04	6.20E+03	2.34E+03	2.77E+03
	1.79E+05		Tot eol	1.13E+04	
Total ECI	1.90E+05	Demountable cost	1.79E+05	-1.13E+04	

Conventional (Conservative) (2 m secondary spacing)					
Production Stage			End of Life Stage		
Beam	Braces	Column	Beam	Braces	Column
A1-A3	A1-A3	A1-A3	C1-C4	C1-C4	C1-C4
7.91E+03	4.38E+01	5.64E+03	3.73E+02	2.37E+00	2.66E+02
7.83E+03	4.34E+01	5.59E+03	3.87E+02	2.36E+00	2.76E+02
6.61E+01	3.66E-01	4.72E+01	-1.47E+01	7.92E-03	-1.05E+01
8.89E+00	4.93E-02	6.35E+00	3.29E-01	6.10E-04	2.35E-01
2.15E-01	1.19E-03	1.54E-01	1.51E-02	1.13E-04	1.08E-02
2.41E+03	1.34E+01	1.72E+03	2.30E+02	9.12E-01	1.64E+02
5.55E+01	3.08E-01	3.96E+01	2.32E+00	2.96E-03	1.66E+00
1.35E+03	7.48E+00	9.63E+02	1.54E+02	1.38E+00	1.10E+02
2.41E+04	1.34E+02	1.72E+04	2.73E+03	2.38E+01	1.95E+03
4.17E+02	2.31E+00	2.98E+02	3.74E+01	3.19E-01	2.67E+01
2.34E-01	1.30E-03	1.67E-01	2.70E-01	1.91E-06	1.93E-01
1.62E+04	8.99E+01	1.16E+04	7.04E+02	4.38E+00	5.02E+02
6.93E+03	3.84E+01	4.95E+03	2.92E+01	2.59E-02	2.09E+01
1.23E+05	6.80E+02	8.75E+04	7.24E+03	5.21E+01	5.17E+03
	2.11E+05		Tot eol	1.25E+04	
Total ECI	2.23E+05	Demounta	2.11E+05	-1.25E+04	

Conventional (Conservative) (3 m secondary spacing)					
Production Stage			End of Life Stage		
Beam	Braces	Column	Beam	Braces	Column
A1-A3	A1-A3	A1-A3	C1-C4	C1-C4	C1-C4
7.59E+03	2.43E+01	5.59E+03	3.58E+02	1.31E+00	2.64E+02
7.52E+03	2.40E+01	5.54E+03	3.72E+02	1.31E+00	2.74E+02
6.35E+01	2.03E-01	4.67E+01	-1.41E+01	4.39E-03	-1.04E+01
8.54E+00	2.73E-02	6.29E+00	3.16E-01	3.38E-04	2.33E-01
2.07E-01	6.61E-04	1.52E-01	1.45E-02	6.24E-05	1.07E-02
2.31E+03	7.40E+00	1.70E+03	2.21E+02	5.05E-01	1.62E+02
5.33E+01	1.70E-01	3.93E+01	2.23E+00	1.64E-03	1.64E+00
1.30E+03	4.14E+00	9.54E+02	1.48E+02	7.62E-01	1.09E+02
2.31E+04	7.40E+01	1.70E+04	2.62E+03	1.32E+01	1.93E+03
4.00E+02	1.28E+00	2.95E+02	3.60E+01	1.77E-01	2.65E+01
2.25E-01	7.20E-04	1.66E-01	2.59E-01	1.06E-06	1.91E-01
1.56E+04	4.98E+01	1.15E+04	6.76E+02	2.43E+00	4.98E+02
6.66E+03	2.13E+01	4.90E+03	2.81E+01	1.44E-02	2.07E+01
1.18E+05	3.77E+02	8.67E+04	6.96E+03	2.89E+01	5.12E+03
	2.05E+05		Tot eol	1.21E+04	
Total ECI	2.17E+05	Demountable c	2.05E+05	-1.21E+04	

Cross Section Trials:

Diagrid 60: CHS to SHS					
Production Stage			End of Life Stage		
Beam	Braces (Diagri	Column	Beam	Braces (Diag	Column
A1-A3	A1-A3	A1-A3	C1-C4	C1-C4	C1-C4
5.91E+03	2.32E+03	3.46E+03	2.79E+02	1.41E+02	1.63E+02
5.85E+03	2.22E+03	3.42E+03	2.89E+02	1.46E+02	1.69E+02
4.94E+01	7.73E+01	2.89E+01	-1.10E+01	-5.52E+00	-6.42E+00
6.65E+00	1.72E+01	3.89E+00	2.46E-01	1.24E-01	1.44E-01
1.61E-01	7.27E-02	9.42E-02	1.13E-02	5.67E-03	6.60E-03
1.80E+03	3.16E+02	1.05E+03	1.72E+02	8.44E+01	1.00E+02
4.15E+01	5.06E+00	2.43E+01	1.74E+00	8.73E-01	1.02E+00
1.01E+03	1.77E+02	5.90E+02	1.15E+02	5.53E+01	6.73E+01
1.80E+04	3.06E+03	1.05E+04	2.04E+03	9.81E+02	1.19E+03
3.12E+02	5.96E+01	1.82E+02	2.80E+01	1.36E+01	1.64E+01
1.75E-01	6.52E-02	1.03E-01	2.02E-01	1.02E-01	1.18E-01
1.21E+04	5.88E+03	7.09E+03	5.26E+02	2.65E+02	3.08E+02
5.18E+03	3.42E+02	3.03E+03	2.18E+01	1.10E+01	1.28E+01
9.16E+04	3.07E+04	5.36E+04	5.41E+03	2.68E+03	3.17E+03
	1.76E+05		Tot eol	1.13E+04	
Total ECI	1.87E+05	Demountable cos	1.76E+05	-1.13E+04	

Diagrid 60: HEA col - IPE col					
Production Stage			End of Life Stage		
Beam	Braces (Diagri	Column	Beam	Braces (Diag	Column
A1-A3	A1-A3	A1-A3	C1-C4	C1-C4	C1-C4
5.91E+03	1.41E+03	5.11E+03	2.79E+02	8.54E+01	2.41E+02
5.85E+03	1.35E+03	5.06E+03	2.89E+02	8.87E+01	2.50E+02
4.94E+01	4.70E+01	4.27E+01	-1.10E+01	-3.35E+00	-9.47E+00
6.65E+00	1.05E+01	5.75E+00	2.46E-01	7.52E-02	2.12E-01
1.61E-01	4.41E-02	1.39E-01	1.13E-02	3.45E-03	9.74E-03
1.80E+03	1.92E+02	1.56E+03	1.72E+02	5.13E+01	1.48E+02
4.15E+01	3.08E+00	3.59E+01	1.74E+00	5.31E-01	1.50E+00
1.01E+03	1.08E+02	8.71E+02	1.15E+02	3.36E+01	9.94E+01
1.80E+04	1.86E+03	1.56E+04	2.04E+03	5.96E+02	1.76E+03
3.12E+02	3.62E+01	2.69E+02	2.80E+01	8.24E+00	2.42E+01
1.75E-01	3.96E-02	1.51E-01	2.02E-01	6.17E-02	1.74E-01
1.21E+04	3.58E+03	1.05E+04	5.26E+02	1.61E+02	4.55E+02
5.18E+03	2.08E+02	4.48E+03	2.18E+01	6.68E+00	1.89E+01
9.16E+04	1.87E+04	7.92E+04	5.41E+03	1.63E+03	4.68E+03
	1.89E+05		Tot eol	1.17E+04	
Total ECI	2.01E+05	Demountable cos	1.89E+05	-1.17E+04	

Diagrid 60: CHS to RHS					
Production Stage			End of Life Stage		
Beam	Braces (Diagri	Column	Beam	Braces (Diag	Column
A1-A3	A1-A3	A1-A3	C1-C4	C1-C4	C1-C4
5.91E+03	2.30E+03	3.46E+03	2.79E+02	1.39E+02	1.63E+02
5.85E+03	2.21E+03	3.42E+03	2.89E+02	1.45E+02	1.69E+02
4.94E+01	7.66E+01	2.89E+01	-1.10E+01	-5.47E+00	-6.42E+00
6.65E+00	1.71E+01	3.89E+00	2.46E-01	1.23E-01	1.44E-01
1.61E-01	7.20E-02	9.42E-02	1.13E-02	5.62E-03	6.60E-03
1.80E+03	3.14E+02	1.05E+03	1.72E+02	8.37E+01	1.00E+02
4.15E+01	5.02E+00	2.43E+01	1.74E+00	8.65E-01	1.02E+00
1.01E+03	1.76E+02	5.90E+02	1.15E+02	5.48E+01	6.73E+01
1.80E+04	3.03E+03	1.05E+04	2.04E+03	9.73E+02	1.19E+03
3.12E+02	5.91E+01	1.82E+02	2.80E+01	1.34E+01	1.64E+01
1.75E-01	6.47E-02	1.03E-01	2.02E-01	1.01E-01	1.18E-01
1.21E+04	5.83E+03	7.09E+03	5.26E+02	2.62E+02	3.08E+02
5.18E+03	3.39E+02	3.03E+03	2.18E+01	1.09E+01	1.28E+01
9.16E+04	3.05E+04	5.36E+04	5.41E+03	2.65E+03	3.17E+03
	1.76E+05		Tot eol	1.12E+04	
Total ECI	1.87E+05	Demountable cos	1.76E+05	-1.12E+04	

Diagrid 60: IPE beam - HEB Beam					
Production Stage			End of Life Stage		
Beam	Braces (Diagri	Column	Beam	Braces (Diag	Column
A1-A3	A1-A3	A1-A3	C1-C4	C1-C4	C1-C4
7.13E+03	1.41E+03	3.46E+03	2.81E+02	8.54E+01	1.63E+02
7.06E+03	1.35E+03	3.42E+03	2.80E+02	8.87E+01	1.69E+02
5.96E+01	4.70E+01	2.89E+01	1.71E-04	-3.35E+00	-6.42E+00
8.02E+00	1.05E+01	3.89E+00	8.25E-06	7.52E-02	1.44E-01
1.94E-01	4.41E-02	9.42E-02	3.76E-12	3.45E-03	6.60E-03
2.17E+03	1.92E+02	1.05E+03	1.36E-02	5.13E+01	1.00E+02
5.00E+01	3.08E+00	2.43E+01	1.70E-09	5.31E-01	1.02E+00
1.22E+03	1.08E+02	5.90E+02	1.43E-03	3.36E+01	6.73E+01
2.17E+04	1.86E+03	1.05E+04	1.76E-01	5.96E+02	1.19E+03
3.76E+02	3.62E+01	1.82E+02	1.52E-02	8.24E+00	1.64E+01
2.11E-01	3.96E-02	1.03E-01	2.20E-09	6.17E-02	1.18E-01
1.46E+04	3.58E+03	7.09E+03	5.00E+04	1.61E+02	3.08E+02
6.25E+03	2.08E+02	3.03E+03	7.98E-01	6.68E+00	1.28E+01
1.11E+05	1.87E+04	5.36E+04	5.26E+04	1.63E+03	3.17E+03
	1.83E+05		Tot eol	5.73E+04	
Total ECI	2.40E+05	Demountable cos	1.83E+05	-5.73E+04	

Diagrid 60: HEA col - HEB col					
Production Stage			End of Life Stage		
Beam	Braces (Diagri	Column	Beam	Braces (Diagri	Column
A1-A3	A1-A3	A1-A3	C1-C4	C1-C4	C1-C4
5.91E+03	1.41E+03	4.06E+03	2.79E+02	8.54E+01	1.91E+02
5.85E+03	1.35E+03	4.02E+03	2.89E+02	8.87E+01	1.99E+02
4.94E+01	4.70E+01	3.39E+01	-1.10E+01	-3.35E+00	-7.53E+00
6.65E+00	1.05E+01	4.57E+00	2.46E-01	7.52E-02	1.69E-01
1.61E-01	4.41E-02	1.10E-01	1.13E-02	3.45E-03	7.74E-03
1.80E+03	1.92E+02	1.24E+03	1.72E+02	5.13E+01	1.18E+02
4.15E+01	3.08E+00	2.85E+01	1.74E+00	5.31E-01	1.19E+00
1.01E+03	1.08E+02	6.92E+02	1.15E+02	3.36E+01	7.90E+01
1.80E+04	1.86E+03	1.24E+04	2.04E+03	5.96E+02	1.40E+03
3.12E+02	3.62E+01	2.14E+02	2.80E+01	8.24E+00	1.92E+01
1.75E-01	3.96E-02	1.20E-01	2.02E-01	6.17E-02	1.39E-01
1.21E+04	3.58E+03	8.32E+03	5.26E+02	1.61E+02	3.61E+02
5.18E+03	2.08E+02	3.56E+03	2.18E+01	6.68E+00	1.50E+01
9.16E+04	1.87E+04	6.29E+04	5.41E+03	1.63E+03	3.72E+03
	1.73E+05		Tot eol	1.08E+04	
Total ECI	1.84E+05	Demountable co:	1.73E+05	-1.08E+04	

Diagrid 60: IPE beam - HEA Beam					
Production Stage			End of Life Stage		
Beam	Braces (Diagri	Column	Beam	Braces (Diagri	Column
A1-A3	A1-A3	A1-A3	C1-C4	C1-C4	C1-C4
6.62E+03	1.41E+03	3.46E+03	2.61E+02	8.54E+01	1.63E+02
6.56E+03	1.35E+03	3.42E+03	2.60E+02	8.87E+01	1.69E+02
5.53E+01	4.70E+01	2.89E+01	1.59E-04	-3.35E+00	-6.42E+00
7.45E+00	1.05E+01	3.89E+00	7.66E-06	7.52E-02	1.44E-01
1.80E-01	4.41E-02	9.42E-02	3.49E-12	3.45E-03	6.60E-03
2.02E+03	1.92E+02	1.05E+03	1.27E-02	5.13E+01	1.00E+02
4.65E+01	3.08E+00	2.43E+01	1.58E-09	5.31E-01	1.02E+00
1.13E+03	1.08E+02	5.90E+02	1.33E-03	3.36E+01	6.73E+01
2.02E+04	1.86E+03	1.05E+04	1.63E-01	5.96E+02	1.19E+03
3.49E+02	3.62E+01	1.82E+02	1.41E-02	8.24E+00	1.64E+01
1.96E-01	3.96E-02	1.03E-01	2.05E-09	6.17E-02	1.18E-01
1.36E+04	3.58E+03	7.09E+03	4.65E+04	1.61E+02	3.08E+02
5.81E+03	2.08E+02	3.03E+03	7.41E-01	6.68E+00	1.28E+01
1.03E+05	1.87E+04	5.36E+04	4.88E+04	1.63E+03	3.17E+03
	1.75E+05		Tot eol	5.36E+04	
Total ECI	2.29E+05	Demountable co:	1.75E+05	-5.36E+04	

Tall Structures:

Diagrid 60						Diagrid 60 + Core						Ground + Diagrid 60					
Production Stage			End of Life Stage			Production Stage			End of Life Stage			Production Stage			End of Life Stage		
Beam	Braces (Diagrid)	Column	Beam	Braces (Diagri	Column	Beam	Braces (Di	Column	Beam	Braces (Diagrid)	Column	Beam	Braces (Di	Column	Beam	Braces (Diagi	Column
A1-A3	A1-A3	A1-A3	C1-C4	C1-C4	C1-C4	A1-A3	A1-A3	A1-A3	C1-C4	C1-C4	C1-C4	A1-A3	A1-A3	A1-A3	C1-C4	C1-C4	C1-C4
1.75E+04	1.18E+04	2.14E+04	8.27E+02	7.13E+02	1.01E+03	1.75E+04	1.41E+04	2.31E+04	8.26E+02	7.56E+02	1.09E+03	2.62E+04	9.53E+03	2.54E+04	1.24E+03	5.78E+02	1.20E+03
1.73E+04	1.13E+04	2.12E+04	8.58E+02	7.41E+02	1.05E+03	1.73E+04	1.37E+04	2.29E+04	8.58E+02	7.79E+02	1.13E+03	2.60E+04	9.14E+03	2.51E+04	1.28E+03	6.00E+02	1.24E+03
1.46E+02	3.92E+02	1.79E+02	-3.25E+01	-2.80E+01	-3.97E+01	1.46E+02	3.54E+02	1.93E+02	-3.25E+01	-2.38E+01	-4.29E+01	2.19E+02	3.18E+02	2.12E+02	-4.86E+01	-2.27E+01	-4.70E+01
1.97E+01	8.75E+01	2.41E+01	7.29E-01	6.28E-01	8.90E-01	1.97E+01	7.72E+01	2.60E+01	7.29E-01	5.80E-01	9.62E-01	2.95E+01	7.08E+01	2.85E+01	1.09E+00	5.08E-01	1.06E+00
4.77E-01	3.69E-01	5.83E-01	3.34E-02	2.88E-02	4.08E-02	4.77E-01	3.70E-01	6.29E-01	3.34E-02	3.15E-02	4.41E-02	7.14E-01	2.98E-01	6.90E-01	5.00E-02	2.33E-02	4.84E-02
5.34E+03	1.61E+03	6.52E+03	5.09E+02	4.28E+02	6.21E+02	5.34E+03	2.37E+03	7.05E+03	5.08E+02	4.24E+02	6.71E+02	7.99E+03	1.30E+03	7.73E+03	7.61E+02	3.47E+02	7.36E+02
1.23E+02	2.57E+01	1.50E+02	5.15E+00	4.43E+00	6.28E+00	1.23E+02	2.23E+01	1.62E+02	5.14E+00	4.01E+00	6.79E+00	1.84E+02	2.08E+01	1.78E+02	7.70E+00	3.59E+00	7.45E+00
2.99E+03	8.99E+02	3.65E+03	3.41E+02	2.80E+02	4.16E+02	2.99E+03	1.36E+03	3.94E+03	3.41E+02	3.23E+02	4.50E+02	4.47E+03	7.28E+02	4.33E+03	5.10E+02	2.27E+02	4.94E+02
5.34E+04	1.55E+04	6.52E+04	6.05E+03	4.98E+03	7.38E+03	5.33E+04	2.36E+04	7.04E+04	6.04E+03	5.70E+03	7.98E+03	7.99E+04	1.26E+04	7.72E+04	9.05E+03	4.03E+03	8.75E+03
9.24E+02	3.03E+02	1.13E+03	8.29E+01	6.88E+01	1.01E+02	9.23E+02	4.24E+02	1.22E+03	8.29E+01	7.82E+01	1.09E+02	1.38E+03	2.45E+02	1.34E+03	1.24E+02	5.57E+01	1.20E+02
5.20E-01	3.31E-01	6.34E-01	5.99E-01	5.15E-01	7.31E-01	5.19E-01	5.46E-01	6.85E-01	5.98E-01	4.47E-01	7.90E-01	7.77E-01	2.68E-01	7.52E-01	8.96E-01	4.17E-01	8.66E-01
3.59E+04	2.99E+04	4.39E+04	1.56E+03	1.34E+03	1.90E+03	3.59E+04	3.23E+04	4.74E+04	1.56E+03	1.42E+03	2.06E+03	5.37E+04	2.42E+04	5.20E+04	2.33E+03	1.09E+03	2.26E+03
1.54E+04	1.73E+03	1.88E+04	6.48E+01	5.58E+01	7.91E+01	1.54E+04	1.71E+03	2.03E+04	6.47E+01	4.99E+01	8.55E+01	2.30E+04	1.40E+03	2.22E+04	9.69E+01	4.52E+01	9.38E+01
2.72E+05	1.56E+05	3.32E+05	1.61E+04	1.36E+04	1.96E+04	2.72E+05	1.89E+05	3.58E+05	1.60E+04	1.48E+04	2.12E+04	4.07E+05	1.26E+05	3.93E+05	2.40E+04	1.10E+04	2.32E+04
	7.59E+05		Tot eol	4.92E+04			8.19E+05		Tot eol	5.20E+04			9.26E+05		Tot eol	5.82E+04	
Total ECI	8.09E+05	Demounta	7.59E+05	-4.92E+04		Total ECI	8.71E+05	Demount (	8.19E+05	-5.20E+04		Total ECI	9.84E+05	Demount (	9.26E+05	-5.82E+04	

Ground + Diagrid 60 + Core						V (Chevron) Bracing Sides and Middle						V (Chevron) Bracing + Core					
Production Stage			End of Life Stage			Production Stage			End of Life Stage			Production Stage			End of Life Stage		
Beam	Braces (Diagri	Column	Beam	Braces (Diagri	Column	Beam	Braces	Column	Beam	Braces	Column	Beam	Braces	Column	Beam	Braces	Column
A1-A3	A1-A3	A1-A3	C1-C4	C1-C4	C1-C4	A1-A3	A1-A3	A1-A3	C1-C4	C1-C4	C1-C4	A1-A3	A1-A3	A1-A3	C1-C4	C1-C4	C1-C4
1.75E+04	1.58E+04	2.44E+04	8.25E+02	8.00E+02	1.15E+03	3.67E+04	8.02E+03	4.28E+04	1.73E+03	2.84E+02	2.02E+03	3.22E+04	7.22E+03	4.28E+04	1.52E+03	2.55E+02	2.02E+03
1.73E+04	1.54E+04	2.42E+04	8.57E+02	8.21E+02	1.20E+03	3.64E+04	7.99E+03	4.24E+04	1.80E+03	2.83E+02	2.10E+03	3.19E+04	7.19E+03	4.24E+04	1.58E+03	2.55E+02	2.10E+03
1.46E+02	3.40E+02	2.04E+02	-3.24E+01	-2.19E+01	-4.53E+01	3.07E+02	2.79E+01	3.58E+02	-6.82E+01	9.48E-01	-7.94E+01	2.69E+02	2.52E+01	3.58E+02	-5.98E+01	8.54E-01	-7.94E+01
1.97E+01	7.30E+01	2.75E+01	7.28E-01	5.65E-01	1.02E+00	4.13E+01	2.70E+00	4.82E+01	1.53E+00	7.29E-02	1.78E+00	3.63E+01	2.43E+00	4.82E+01	1.34E+00	6.57E-02	1.78E+00
4.76E-01	3.80E-01	6.65E-01	3.34E-02	3.39E-02	4.65E-02	1.00E+00	1.03E-01	1.17E+00	7.01E-02	1.35E-02	8.17E-02	8.77E-01	9.30E-02	1.17E+00	6.15E-02	1.21E-02	8.17E-02
5.33E+03	2.88E+03	7.44E+03	5.08E+02	4.32E+02	7.09E+02	1.12E+04	2.01E+03	1.30E+04	1.07E+03	1.09E+02	1.24E+03	9.82E+03	1.81E+03	1.30E+04	9.36E+02	9.82E+01	1.24E+03
1.23E+02	2.08E+01	1.71E+02	5.14E+00	3.86E+00	7.17E+00	2.58E+02	7.34E-02	3.01E+02	1.08E+01	3.54E-01	1.26E+01	2.26E+02	6.61E-02	3.01E+02	9.46E+00	3.19E-01	1.26E+01
2.98E+03	1.67E+03	4.16E+03	3.40E+02	3.56E+02	4.75E+02	6.27E+03	1.21E+03	7.31E+03	7.15E+02	1.65E+02	8.33E+02	5.50E+03	1.09E+03	7.31E+03	6.27E+02	1.48E+02	8.33E+02
5.33E+04	2.90E+04	7.43E+04	6.03E+03	6.26E+03	8.42E+03	1.12E+05	2.10E+04	1.30E+05	1.27E+04	2.84E+03	1.48E+04	9.82E+04	1.89E+04	1.30E+05	1.11E+04	2.56E+03	1.48E+04
9.22E+02	5.07E+02	1.29E+03	8.28E+01	8.57E+01	1.16E+02	1.94E+03	3.34E+02	2.26E+03	1.74E+02	3.82E+01	2.03E+02	1.70E+03	3.01E+02	2.26E+03	1.53E+02	3.44E+01	2.03E+02
5.19E-01	6.87E-01	7.24E-01	5.97E-01	4.17E-01	8.34E-01	1.09E+00	5.34E-01	1.27E+00	1.26E+00	2.29E-04	1.46E+00	9.56E-01	4.81E-01	1.27E+00	1.10E+00	2.06E-04	1.46E+00
3.58E+04	3.45E+04	5.00E+04	1.56E+03	1.50E+03	2.17E+03	7.53E+04	1.31E+04	8.78E+04	3.27E+03	5.24E+02	3.81E+03	6.61E+04	1.18E+04	8.78E+04	2.87E+03	4.72E+02	3.81E+03
1.53E+04	1.74E+03	2.14E+04	6.47E+01	4.76E+01	9.02E+01	3.22E+04	4.33E+02	3.75E+04	1.36E+02	3.10E+00	1.58E+02	2.83E+04	3.90E+02	3.75E+04	1.19E+02	2.79E+00	1.58E+02
2.71E+05	2.13E+05	3.78E+05	1.60E+04	1.59E+04	2.24E+04	5.70E+05	1.10E+05	6.64E+05	3.37E+04	6.24E+03	3.92E+04	5.00E+05	9.93E+04	6.64E+05	2.95E+04	5.62E+03	3.92E+04
	8.62E+05		Tot eol	5.43E+04			1.34E+06		Tot eol	7.91E+04			1.26E+06		Tot eol	7.44E+04	
Total ECI	9.17E+05	Demount (	8.62E+05	-5.43E+04		Total ECI	1.42E+06	Demount (	1.34E+06	-7.91E+04		Total ECI	1.34E+06	Demount (	1.26E+06	-7.44E+04	

X Bracing Sides + Middle						X Bracing + Core						Conservative with Core					
Production Stage			End of Life Stage			Production Stage			End of Life Stage			Production Stage			End of Life Stage		
Beam	Braces (Rc	Column	Beam	Braces (Rod)	Column	Beam	Braces (Rc	Column	Beam	Braces (Ro	Column	Beam	Braces (Rc	Column	Beam	Braces (Rod	Column
A1-A3	A1-A3	A1-A3	C1-C4	C1-C4	C1-C4	A1-A3	A1-A3	A1-A3	C1-C4	C1-C4	C1-C4	A1-A3	A1-A3	A1-A3	C1-C4	C1-C4	C1-C4
3.66E+04	7.28E+03	4.78E+04	1.73E+03	2.57E+02	2.26E+03	3.22E+04	6.16E+03	4.28E+04	1.52E+03	2.18E+02	2.02E+03	3.66E+04	7.22E+03	4.78E+04	1.73E+03	2.56E+02	2.26E+03
3.62E+04	7.25E+03	4.73E+04	1.79E+03	2.57E+02	2.34E+03	3.19E+04	6.13E+03	4.24E+04	1.58E+03	2.17E+02	2.10E+03	3.62E+04	7.20E+03	4.73E+04	1.79E+03	2.55E+02	2.34E+03
3.06E+02	2.53E+01	4.00E+02	-6.79E+01	8.60E-01	-8.87E+01	2.69E+02	2.15E+01	3.58E+02	-5.98E+01	7.28E-01	-7.94E+01	3.06E+02	2.52E+01	4.00E+02	-6.79E+01	8.54E-01	-8.87E+01
4.11E+01	2.45E+00	5.38E+01	1.52E+00	6.62E-02	1.99E+00	3.63E+01	2.07E+00	4.82E+01	1.34E+00	5.60E-02	1.78E+00	4.11E+01	2.43E+00	5.38E+01	1.52E+00	6.57E-02	1.99E+00
9.96E-01	9.38E-02	1.30E+00	6.97E-02	1.22E-02	9.12E-02	8.77E-01	7.93E-02	1.17E+00	6.15E-02	1.04E-02	8.17E-02	9.96E-01	9.31E-02	1.30E+00	6.97E-02	1.21E-02	9.12E-02
1.11E+04	1.82E+03	1.46E+04	1.06E+03	9.90E+01	1.39E+03	9.82E+03	1.54E+03	1.30E+04	9.36E+02	8.38E+01	1.24E+03	1.11E+04	1.81E+03	1.46E+04	1.06E+03	9.83E+01	1.39E+03
2.57E+02	6.66E-02	3.36E+02	1.07E+01	3.21E-01	1.40E+01	2.26E+02	5.64E-02	3.01E+02	9.46E+00	2.72E-01	1.26E+01	2.57E+02	6.61E-02	3.36E+02	1.07E+01	3.19E-01	1.40E+01
6.24E+03	1.09E+03	8.16E+03	7.12E+02	1.49E+02	9.31E+02	5.50E+03	9.27E+02	7.31E+03	6.27E+02	1.26E+02	8.33E+02	6.24E+03	1.09E+03	8.16E+03	7.12E+02	1.48E+02	9.31E+02
1.11E+05	1.90E+04	1.46E+05	1.26E+04	2.58E+03	1.65E+04	9.82E+04	1.61E+04	1.30E+05	1.11E+04	2.18E+03	1.48E+04	1.11E+05	1.89E+04	1.46E+05	1.26E+04	2.56E+03	1.65E+04
1.93E+03	3.03E+02	2.52E+03	1.73E+02	3.46E+01	2.26E+02	1.70E+03	2.57E+02	2.26E+03	1.53E+02	2.93E+01	2.03E+02	1.93E+03	3.01E+02	2.52E+03	1.73E+02	3.44E+01	2.26E+02
1.08E+00	4.85E-01	1.42E+00	1.25E+00	2.08E-04	1.63E+00	9.56E-01	4.10E-01	1.27E+00	1.10E+00	1.76E-04	1.46E+00	1.08E+00	4.81E-01	1.42E+00	1.25E+00	2.06E-04	1.63E+00
7.50E+04	1.19E+04	9.80E+04	3.26E+03	4.76E+02	4.26E+03	6.61E+04	1.01E+04	8.78E+04	2.87E+03	4.03E+02	3.81E+03	7.50E+04	1.18E+04	9.80E+04	3.26E+03	4.72E+02	4.26E+03
3.21E+04	3.93E+02	4.19E+04	1.35E+02	2.81E+00	1.77E+02	2.83E+04	3.33E+02	3.75E+04	1.19E+02	2.38E+00	1.58E+02	3.21E+04	3.90E+02	4.19E+04	1.35E+02	2.79E+00	1.77E+02
5.67E+05	1.00E+05	7.41E+05	3.35E+04	5.66E+03	4.38E+04	5.00E+05	8.47E+04	6.64E+05	2.95E+04	4.79E+03	3.92E+04	5.67E+05	9.93E+04	7.41E+05	3.35E+04	5.62E+03	4.38E+04
	1.41E+06		Tot eol	8.30E+04			1.25E+06		Tot eol	7.35E+04			1.41E+06		Tot eol	8.29E+04	
Total ECI	1.49E+06	Demount (	1.41E+06	-8.30E+04		Total ECI	1.32E+06	Demount (	1.25E+06	-7.35E+04		Total ECI	1.49E+06	Demount (	1.41E+06	-8.29E+04	